

Unit 3 - Chapter 10

Two-State Evolution, Coupled Oscillators, and Spin

W. G. Harter

Schrodinger time evolution is analogous to the motion of coupled oscillators or pendulums. This analogy is valuable for theoretical insight, visualization, and for developing computer simulations. Particularly valuable is the insight into the use of Hamilton-Pauli algebra of reflection-symmetry operators σ_A , σ_B , and σ_C , which are known as *spinor* or *quaternion* operators and generate the $U(2)$ group. Hamiltonians made of the σ_μ apply to many 2-state phenomena including the NH_3 maser, spin resonance, and optical polarization introduced in Chapter 1. We have said that in quantum dynamics, “It takes two to tango.” Now we begin to see how the pros do it!

CHAPTER 10. TWO-STATE EVOLUTION AND ANALOGIES4

10.1 Mechanical Analogies to Schrodinger Dynamics4
 (a). ABCD Symmetry operator analysis6

10.2 The ABCD's of 2-State Dynamics8
 (a) Asymmetric-Diagonal or C2A symmetry8
 (b) Bilateral or C2B symmetry10
 C2B projectors and eigenstates: Normal modes11
 Understanding C2B eigenstates: Tunneling splitting12
 Understanding C2B dynamics: Beats and transition frequency13
 (c) Circular or C2C symmetry17
 $R(2)=C\infty$ projectors and C2C eigenstates18
 Understanding C2C eigenstates: Zeeman-like splitting and coriolis or cyclotron motion19
 Understanding C2C dynamics: Faraday rotation22

10.3 Mixed A and B Symmetry25
 (a) Asymmetric bilateral C2AB symmetry: Stark-like-splitting25
 High field splitting: Strong C2A or weak C2B symmetry26
 Low field splitting: Strong C2B or weak C2A symmetry and $A \rightarrow B$ basis change29
 (b) Ammonia (NH3) maser29
 C2AB Symmetry : Weyl reflections31
 Unitary U(2) versus Special Unitary SU(2)33
 Complete sets of commuting operators33

10.4 Mixed ABCD Symmetry: U(2) quantum systems34
 (a) ABC Symmetry catalog: Standing, moving, or galloping waves35
 A, B, and AB-Archetypes are standing waves (Linear polarization)35
 C-Archetypes are moving waves (Circular polarization)35
 ...All others are galloping waves (Elliptical polarization)35
 (b) General HABCD eigenvalues36

10.5 Spin-Vector Pictures for Two-State Quantum Systems38
 (a) Density operators and Pauli σ -operators40
 (b) Hamiltonian operators and Pauli-Jordan spin operators ($J=S$)43
 (c) Bloch equations and spin precession44
 Magnetic spin precession (ESR, NMR,...)45
 (d) Visualizing quantum dynamics as S-precession46
 Crank Ω polar angles (φ, ϑ) versus Spin S polar angles (α, β)49
 Hamilton's generalization of $\exp(-i\omega t)=\cos\omega t-i\sin\omega t : \exp(-i \sigma t)=\text{What?}$ 51
 Why the 1/2?52

Problems for Chapter 10.53

REVIEW TOPICS & FORMULAS FOR UNIT 357
 U(2)-R(3) Two-State and Spin-Vector Summary60

Appendix 10.A. U(2) Angles and Spin Rotation Operators2
 (a) Equivalence transformations of rotations5
 (b) Euler equivalence transformations of 3-vectors5
 (c) Euler angle goniometer: Double valued position6
 (d) Axis angle rotation: Double valued operation11
 (1) Combining rotations: U(2) group products13
 (2) Mirror reflections and Hamilton's turns13
 (3) Similarity transformation and Hamilton's turns15
 (e) Quaternion and spinor algebra (again)16
 Why rotations are such a big deal17

Appendix 10.B Spin control and ellipsometry	1
(a). Polarization ellipsometry coordinate angles	6
(1) Type-A ellipsometry Euler angles	7
(2) Type-C ellipsometry Euler angles	9
(b) Beam evolution of polarization.....	13
Problems for Appendix 10.A and B	14

Chapter 10. Two-State Evolution and Analogies

10.1 Mechanical Analogies to Schrodinger Dynamics

The quantum Schrodinger time evolution equations (9.2.5) are similar to the classical Newtonian equations of motion for coupled pendulums. This analogy may help to understand quantum dynamics in this and later chapters. Indeed, for certain constant \mathbf{H} Hamiltonian operators, the classical and quantum equations are mathematically and dynamically identical. Also, the concept of *spin* will be introduced.

We begin with the simplest non-trivial quantum systems having just two-states ($N=2$) such as optical polarization and electron spin-polarization introduced in Chapter 1. This $U(2)$ system is such an experimentally important system that we will devote several units to its technology. This chapter will provide an introduction to $U(2)$ systems and their symmetry by using classical mechanical analogies.

The simplest non-trivial quantum system is the *two-level atom* or a spin-1/2 particle. The Schrodinger equation (9.2.5) for these systems has the general form:

$$i\hbar \frac{\partial}{\partial t} |\Psi(t)\rangle = \mathbf{H} |\Psi(t)\rangle \quad (10.1.1a)$$

where \mathbf{H} is a two-by-two Hermitian ($\mathbf{H}^\dagger = \mathbf{H}$) matrix operator

$$\mathbf{H} = \begin{pmatrix} A & B - iC \\ B + iC & D \end{pmatrix}. \quad (10.1.1b)$$

and ket $|\Psi\rangle$ is a two-dimensional complex *phasor vector* $x_j + ip_j$

$$|\Psi\rangle = \begin{pmatrix} \Psi_1 \\ \Psi_2 \end{pmatrix} = \begin{pmatrix} x_1 + ip_1 \\ x_2 + ip_2 \end{pmatrix}. \quad (10.1.1c)$$

Separating real x_j and imaginary p_j parts of the amplitudes (10.1.1c) lets us convert the complex Schrodinger equation (10.1.1a) into twice as many real differential equations. The results are as follows.

$$\begin{aligned} \dot{x}_1 &= Ap_1 + Bp_2 - Cx_2 & \dot{p}_1 &= -Ax_1 - Bx_2 - Cp_2 \\ \dot{x}_2 &= Bp_1 + Dp_2 + Cx_1 & \dot{p}_2 &= -Bx_1 - Dx_2 + Cp_1 \end{aligned} \quad (10.1.2a) \quad (10.1.2b)$$

The same equations arise from the following classical coupled oscillator Hamiltonian in which x_j and p_j are canonical coordinates and momenta, respectively.

$$H_c = \frac{A}{2}(p_1^2 + x_1^2) + B(x_1x_2 + p_1p_2) + C(x_1p_2 - x_2p_1) + \frac{D}{2}(p_2^2 + x_2^2) \quad (10.1.3a)$$

Hamilton's classical canonical equations of motion are the following:

$$\begin{aligned} \dot{x}_1 &= \frac{\partial H_c}{\partial p_1} = Ap_1 + Bp_2 - Cx_2 & \dot{p}_1 &= -\frac{\partial H_c}{\partial x_1} = -(Ax_1 + Bx_2 + Cp_2) \\ \dot{x}_2 &= \frac{\partial H_c}{\partial p_2} = Bp_1 + Dp_2 + Cx_1 & \dot{p}_2 &= -\frac{\partial H_c}{\partial x_2} = -(Bx_1 + Dx_2 - Cp_1) \end{aligned} \quad (10.1.3b) \quad (10.1.3c)$$

Note that these are identical to Schrodinger's equations (10.1.2).

To see a connection with conventional second order coupled oscillator equations, we differentiate the \dot{x}_j equations (10.1.3b) and substitute the \dot{p}_j expressions (10.1.3c). (Note: Canonical momentum here is not the usual $p_j = m\dot{x}_j$. See exercises at the end of the chapter.)

$$\begin{aligned} \ddot{x}_1 &= A\dot{p}_1 + B\dot{p}_2 - C\dot{x}_2 \\ &= -A(Ax_1 + Bx_2 + Cp_2) - B(Bx_1 + Dx_2 - Cp_1) - C(Bp_1 + Dp_2 + Cx_1) \\ &= -(A^2 + B^2 + C^2)x_1 - (AB + BD)x_2 - (A + D)Cp_2 \end{aligned} \tag{10.1.4a}$$

$$\begin{aligned} \ddot{x}_2 &= B\dot{p}_1 + D\dot{p}_2 + C\dot{x}_1 \\ &= -B(Ax_1 + Bx_2 + Cp_2) - D(Bx_1 + Dx_2 - Cp_1) + C(Ap_1 + Bp_2 - Cx_2) \\ &= -(AB + BD)x_1 - (B^2 + D^2 + C^2)x_2 + (A + D)Cp_1 \end{aligned} \tag{10.1.4b}$$

If the complex parameter C is zero this reduces to classical coupled oscillator equations

$$-\ddot{x}_1 = K_{11}x_1 + K_{12}x_2, \tag{10.1.5a} \quad -\ddot{x}_2 = K_{21}x_1 + K_{22}x_2, \tag{10.1.5b}$$

where the force or *acceleration* or *spring matrix* K_{ij} depends on masses and spring constants in Fig. 10.1.1a and is related as follows to the Schrodinger H -matrix parameters $A, B,$ and D .

$$m_1K_{11} = A^2 + B^2 = k_1 + k_{12}, \tag{10.1.5c} \quad m_1K_{12} = AB + BD = -k_{12},$$

$$m_2K_{21} = AB + BD = -k_{12}, \tag{10.1.5d} \quad m_2K_{22} = B^2 + D^2 = k_2 + k_{12}.$$

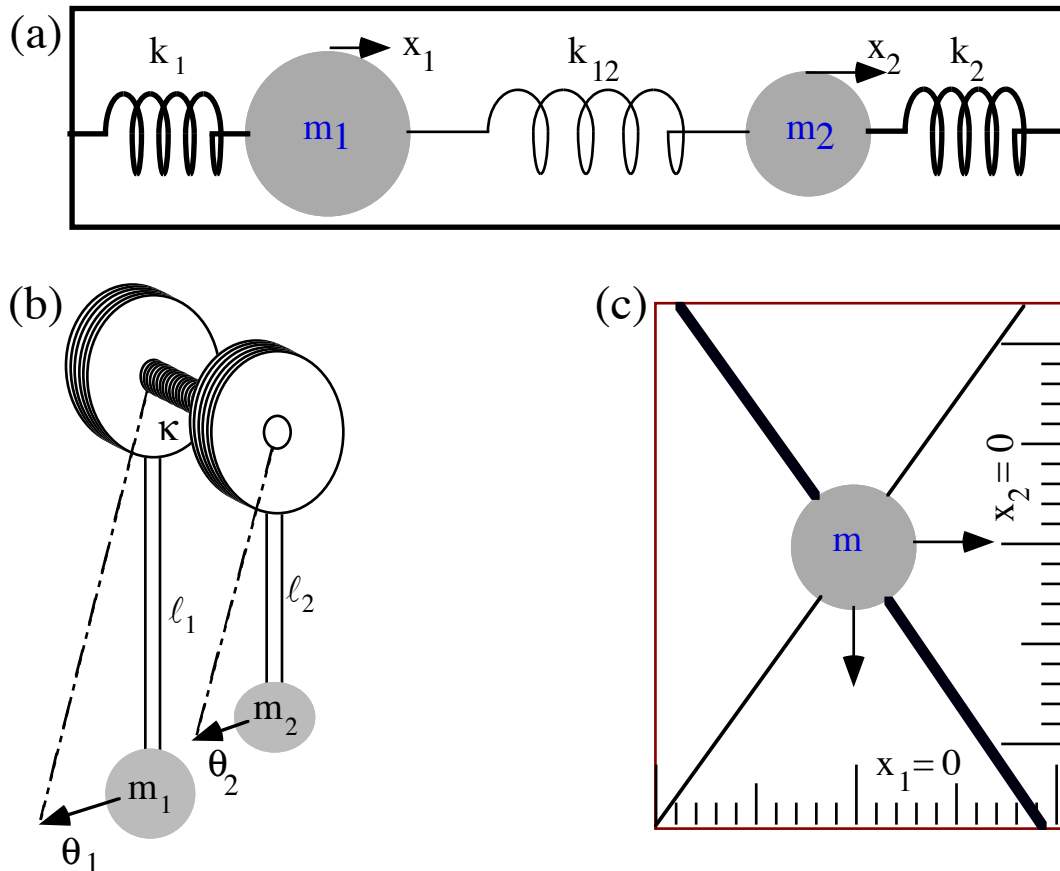


Fig.10.1.1 Classical analogs for spatially asymmetric $U(2)$ quantum system.

Fig. 10.1.1 shows (a) two masses, (b) two pendulums, and (c) a single mass m hung by diagonal springs. Each has an isotropic kinetic energy T (m is divided out) and an anisotropic potential V .

$$T = \frac{1}{2}\dot{x}_1^2 + \frac{1}{2}\dot{x}_2^2 = \frac{1}{2}\dot{\mathbf{x}} \cdot \dot{\mathbf{x}} \tag{10.1.6a}$$

$$V = \frac{1}{2}K_{11}x_1^2 + \frac{1}{2}(K_{12} + K_{21})x_1x_2 + \frac{1}{2}K_{22}x_2^2 = \frac{1}{2}\mathbf{x} \cdot \mathbf{K} \cdot \mathbf{x} \tag{10.1.6b}$$

Constant- V curves (equipotentials) are ellipses as shown in Fig. 10.1.2 below. The parameters A , B , and D in the \mathbf{K} -matrix (10.1.5) or \mathbf{H} -matrix (10.1.1b) determine the shape of the ellipses and inclination of their major axes which correspond to different \mathbf{K} -matrix eigenvalues and eigenvectors, that is, different frequencies and normal modes in the classical models and different energy states in the original quantum $U(2)$ model. We now study different cases and see how they correspond to different *symmetries*.

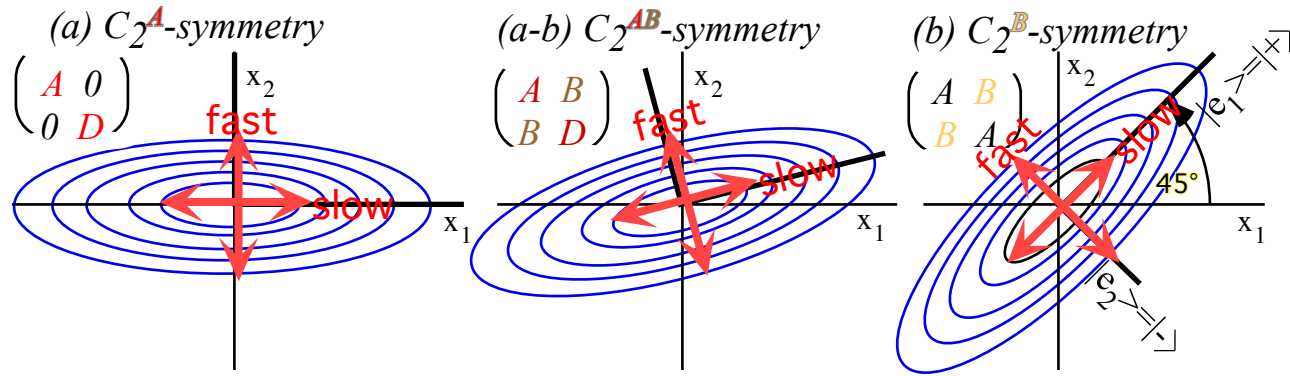


Fig. 10.1.2 Potentials for (a) C_2^A -asymmetric-diagonal, (ab) C_2^{AB} -mixed, (b) C_2^B -bilateral $U(2)$ system.

(a). ABCD Symmetry operator analysis

Following the lead of Chapters 8 and 9, we decompose the Hamiltonian (10.1.1b) into four $ABCD$ symmetry operators that are so labeled to provide helpful mnemonics in sections following.

$$\begin{aligned} \begin{pmatrix} A & B-iC \\ B+iC & D \end{pmatrix} &= A \begin{pmatrix} 1 & 0 \\ 0 & 0 \end{pmatrix} + B \begin{pmatrix} 0 & 1 \\ 1 & 0 \end{pmatrix} + C \begin{pmatrix} 0 & -i \\ i & 0 \end{pmatrix} + D \begin{pmatrix} 0 & 0 \\ 0 & 1 \end{pmatrix} = A\mathbf{e}_{11} + B\sigma_B + C\sigma_C + D\mathbf{e}_{22} \\ &= \frac{A+D}{2} \begin{pmatrix} 1 & 0 \\ 0 & 1 \end{pmatrix} + B \begin{pmatrix} 0 & 1 \\ 1 & 0 \end{pmatrix} + C \begin{pmatrix} 0 & -i \\ i & 0 \end{pmatrix} + \frac{A-D}{2} \begin{pmatrix} 1 & 0 \\ 0 & -1 \end{pmatrix} \\ \mathbf{H} &= \frac{A+D}{2} \sigma_1 + B \sigma_B + C \sigma_C + \frac{A-D}{2} \sigma_A \end{aligned} \tag{10.1.7}$$

The $\{\sigma_I, \sigma_A, \sigma_B, \sigma_C\}$ are best known as *Pauli-spin operators* $\{\sigma_I = \sigma_0, \sigma_B = \sigma_X, \sigma_C = \sigma_Y, \sigma_A = \sigma_Z\}$ but they (or ones quite like them) were discovered almost a century earlier by Hamilton. (He carved them into a bridge in Dublin in 1843.) Hamilton was looking for a consistent generalization of complex numbers to 3-dimensional space. One day he hit upon the idea of a four-dimensional set of operators which he labeled $\{\mathbf{1}, \mathbf{i}, \mathbf{j}, \mathbf{k}\}$.

Hamilton's *quaternions* are related as follows to the $ABCD$ or $ZXYO$ operators.

$$\{\sigma_I = \mathbf{1} = \sigma_0, i\sigma_B = \mathbf{i} = i\sigma_X, i\sigma_C = \mathbf{j} = i\sigma_Y, i\sigma_A = \mathbf{k} = i\sigma_Z\} \tag{10.1.8}$$

Note: $\mathbf{i}^2 = \mathbf{j}^2 = \mathbf{k}^2 = -\mathbf{1}$. They square to *negative-1* like imaginary number $i^2 = -1$. Pauli's form removes the imaginary i so the σ_μ all square to *positive 1* ($\sigma_X^2 = \sigma_Y^2 = \sigma_Z^2 = +\mathbf{1}$) and each belongs to a C_2 group. Note that

our first operator σ_A (or Pauli's third σ_Z) is a difference $\sigma_A = e_{11} - e_{22}$ of elementary operators e_{11} and e_{22} . σ_A is a group operator but e_{kk} are not since they are projectors and do not have inverses.

Now each C_2 group $C_2^A = \{1, \sigma_A\}$, $C_2^B = \{1, \sigma_B\}$, and $C_2^C = \{1, \sigma_C\}$ is considered in turn. They are labeled *A (asymmetric-diagonal)*, *B (bilateral balanced beat)*, and *C (circular)* symmetry for reasons that will become clear. Each of them represents a different physical archetype and a different kind of dynamics. Mnemonic alliteration is used for pedagogical enhancement, particularly the *C (circular)* symmetry for which the following *C*-adjectives apply: *complex, circular, chiral, cyclotron, Coriolis, centrifugal, curly, and circulating-current*.

The last symmetry adjective explains its important distinction and the coloring scheme used in formulae and illustrations. The *A* and *B* designations are colored the yellow, orange or red color of traffic signals for **CAUTION**, or **STOP** since these symmetries refer to real-*standing* waves. The green or blue-green **GO** signal color applies to the *C (current-like)* symmetry of imaginary or complex *moving* or *galloping* waves.

10.2 The ABCD's of 2-State Dynamics

Operators σ_A , σ_B , any σ_C within each C_2 group $C_2^A = \{1, \sigma_A\}$, $C_2^B = \{1, \sigma_B\}$, and $C_2^C = \{1, \sigma_C\}$ do not commute with each other. Therefore they are first considered separately as is done in the following sections labeled, appropriately, (a), (b), and (c). Then follows a discussion of how they intermix.

(a) Asymmetric-Diagonal or C_2^A symmetry

The first case involves an **H**-matrix that is *asymmetric-diagonal*, that is ($B=0=C$) and ($A < D$)

$$\mathbf{H} = \begin{pmatrix} A & 0 \\ 0 & D \end{pmatrix}, \text{ or: } \mathbf{K} = \begin{pmatrix} A^2 & 0 \\ 0 & D^2 \end{pmatrix}. \quad (10.2.1a)$$

The **A**-matrix gives *uncoupled* oscillators in (10.1.5) or a single mass in a diagonal potential (10.1.6).

$$V = \frac{1}{2}K_{11}x_1^2 + \frac{1}{2}K_{22}x_2^2 \quad \text{where: } K_{11} = A^2 = \frac{k_1}{m}, \text{ and: } K_{22} = D^2 = \frac{k_2}{m} \quad (10.2.1b)$$

Such an elliptical potential is plotted in Fig. 10.1.2a. Here cross coupling is zero ($k_{12}=0$), so each mass or pendulum in Fig. 10.1.1a-b is disconnected and independent of the other one. Motion that is purely along one of the Cartesian axes in Fig. 10.1.2a, say purely along the x or x_1 -axis, or else purely along the y or x_2 -axis, will be simple harmonic motion whose frequency is a "slow" $A = \sqrt{k_1/m}$ or else a "fast" $D = \sqrt{k_2/m}$, respectively. This is because the force or gradient for any mass on the x -axis is also along the x or x_1 -axis driving it directly back to the origin. The same holds for the x_2 -axis but the force constant k_2 is presumed stronger than k_1 making the x_2 -axis gradient steeper so x_2 -axial motion is faster than x_1 -axial motion.

Arrows in Fig. 10.1.2a indicate elementary normal modes of the uncoupled x -and y -dimensions. The modes are plotted (using the program *Color U(2)*) as separate functions of time in Fig. 10.2.1a and b.

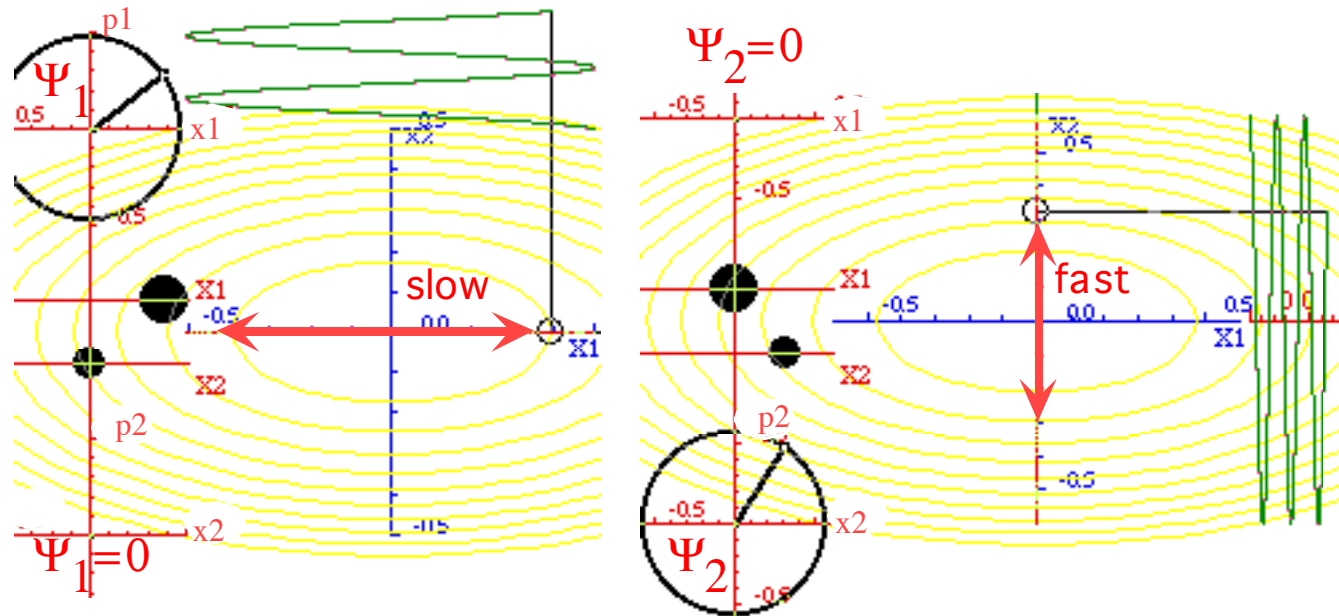


Fig. 10.2.1 Pure normal modes for C_2^A -asymmetric-diagonal potential (a) Slow x -mode (b) Fast y -mode

By setting both the x -and- y -modes in motion at once we get a plot like the one shown below in Fig. 10.2.2. In this *mixed mode* the two motions go about their business as though the companion oscillator was not even present. Note that the x vs. y plot of coordinates $x_1 = \text{Re}\Psi_1$ and $x_2 = \text{Re}\Psi_2$ shows the beginning of a

Lissajous pattern caused by the unequal frequencies of the Ψ_1 and Ψ_2 phasors, but the phasors themselves are each unfazed, so to speak, by the motion of their companion. The x vs. y trajectory curves due to the potential gradient whose direction varies continuously for points not following x or y axes.

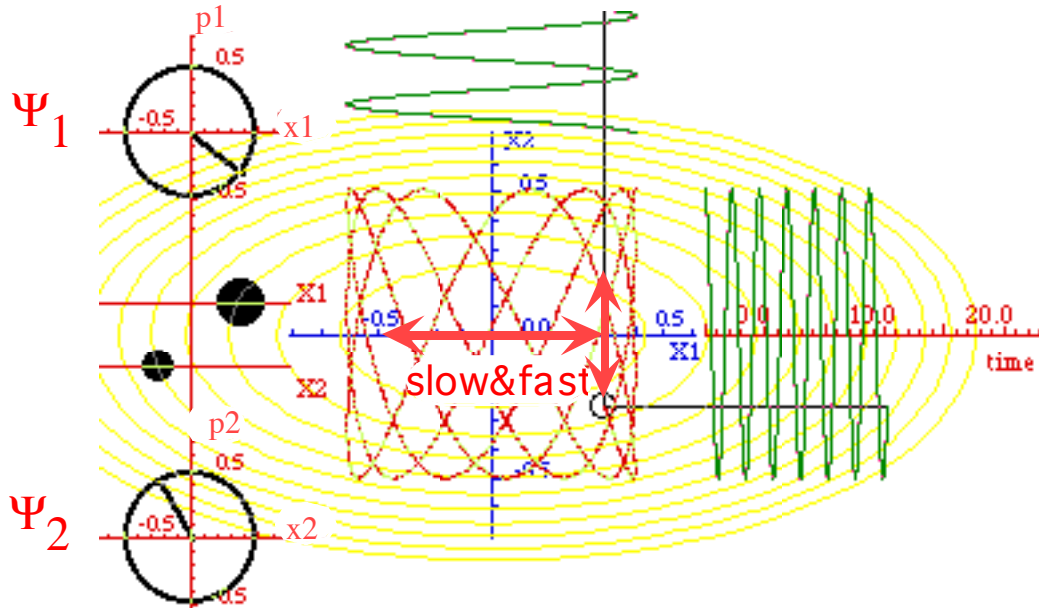


Fig. 10.2.2 Mixed modes for C_2^A -symmetric-diagonal potential

This \mathbf{H} -matrix Hamiltonian or \mathbf{K} -matrix potential in Fig. 10.2.2 above has a most elementary example of symmetry, namely *axial-reflection symmetry* C_2^A or *Cartesian mirror-plane symmetry*. The potential ellipse is invariant to reflecting the y or x_2 -axis ($x_2 \rightarrow -x_2$). We define an x -plane-reflection operator σ_A accordingly to reflect the y -base ket $|2\rangle$ but leave the x -base ket $|1\rangle$ alone.

$$\sigma_A |1\rangle = |1\rangle, \quad \sigma_A |2\rangle = -|2\rangle \tag{10.2.2a}$$

Operator σ_A and unit operator $\mathbf{1}$ make the following C_2^A group multiplication table and representation.

C_2	$\mathbf{1}$	σ_A
$\mathbf{1}$	$\mathbf{1}$	σ_A
σ_A	σ_A	$\mathbf{1}$

$$\left(\begin{array}{cc} \langle 1|\mathbf{1}|1\rangle & \langle 1|\mathbf{1}|2\rangle \\ \langle 2|\mathbf{1}|1\rangle & \langle 2|\mathbf{1}|2\rangle \end{array} \right) = \begin{pmatrix} 1 & 0 \\ 0 & 1 \end{pmatrix}, \quad \left(\begin{array}{cc} \langle 1|\sigma_A|1\rangle & \langle 1|\sigma_A|2\rangle \\ \langle 2|\sigma_A|1\rangle & \langle 2|\sigma_A|2\rangle \end{array} \right) = \begin{pmatrix} 1 & 0 \\ 0 & -1 \end{pmatrix} \tag{10.2.2b}$$

And, as required of symmetry \mathbf{g} -operators ($\mathbf{H}=\mathbf{g}\mathbf{H}\mathbf{g}^\dagger$ or $\mathbf{g}\mathbf{H}=\mathbf{H}\mathbf{g}$), σ_A must commute with \mathbf{H} and \mathbf{K} .

$$\sigma_A \mathbf{H} = \mathbf{H} \sigma_A, \text{ or: } \begin{pmatrix} 1 & 0 \\ 0 & -1 \end{pmatrix} \begin{pmatrix} A & 0 \\ 0 & D \end{pmatrix} = \begin{pmatrix} A & 0 \\ 0 & D \end{pmatrix} \begin{pmatrix} 1 & 0 \\ 0 & -1 \end{pmatrix} \tag{10.2.2c}$$

So, also, must the negative $-\sigma_A$ operator which is a y -plane-reflection operator σ_{-A} defined as follows to reflect the x -base ket $|1\rangle$ but leave the y -base ket $|2\rangle$ alone.

$$-\sigma_A |1\rangle = -|1\rangle, \quad -\sigma_A |2\rangle = |2\rangle \tag{10.2.2d}$$

Operator $-\sigma_A$ and the unit operator $\mathbf{1}$ make a similar C_2^A group multiplication table and representation.

C_2	$\mathbf{1}$	$-\sigma_A$
$\mathbf{1}$	$\mathbf{1}$	$-\sigma_A$
$-\sigma_A$	$-\sigma_A$	$\mathbf{1}$

$$\left(\begin{array}{cc} \langle 1|-\sigma_A|1\rangle & \langle 1|-\sigma_A|2\rangle \\ \langle 2|-\sigma_A|1\rangle & \langle 2|-\sigma_A|2\rangle \end{array} \right) = \begin{pmatrix} -1 & 0 \\ 0 & 1 \end{pmatrix} \tag{10.2.2e}$$

Furthermore, the product of the two reflection operators is a symmetry, too, since if two operators commute with \mathbf{H} then so do their group products. The product $(-\sigma_A)(\sigma_A)$ is a 180° rotation matrix \mathbf{R} .

$$-\sigma_A \sigma_A = \begin{pmatrix} 1 & 0 \\ 0 & -1 \end{pmatrix} \begin{pmatrix} -1 & 0 \\ 0 & 1 \end{pmatrix} = \begin{pmatrix} -1 & 0 \\ 0 & -1 \end{pmatrix} = \mathbf{R}(180^\circ) \quad (10.2.2f)$$

Together, all four operators $\{\mathbf{1}, \sigma_A, -\sigma_A, \mathbf{R}\}$ form a famous group called the *four-group* D_2^A or C_{2v}^A with the group multiplication table shown below. It is like the group D_2 in (8.3.5) and will be used later.

C_{2v}	$\mathbf{1}$	σ_A	$-\sigma_A$	\mathbf{R}	(10.2.2g)
$\mathbf{1}$	$\mathbf{1}$	σ_A	$-\sigma_A$	\mathbf{R}	
σ_A	σ_A	$\mathbf{1}$	\mathbf{R}	$-\sigma_A$	
$-\sigma_A$	$-\sigma_A$	\mathbf{R}	$\mathbf{1}$	σ_A	
\mathbf{R}	\mathbf{R}	$-\sigma_A$	σ_A	$\mathbf{1}$	

Here, σ_A and $\mathbf{1}$ are sufficient to describe the \mathbf{H} -matrix which, as in Sec. 9.3 (Recall especially (9.3.5).), is a linear combination of its own symmetry operators. This is the A -case of expansion (10.1.7).

$$\begin{pmatrix} A & 0 \\ 0 & D \end{pmatrix} = \frac{A+D}{2} \begin{pmatrix} 1 & 0 \\ 0 & 1 \end{pmatrix} + \frac{A-D}{2} \begin{pmatrix} 1 & 0 \\ 0 & -1 \end{pmatrix}, \text{ or: } \mathbf{H} = \frac{A+D}{2} \mathbf{1} + \frac{A-D}{2} \sigma_A \quad (10.2.2h)$$

(b) Bilateral or C_2^B symmetry

The next case- B involves identical *coupled* oscillators such are shown in Fig. 10.2.3 below. These have a symmetry called *bilateral* or C_2^B *symmetry*. We should be very familiar with this symmetry since it is the only one that our human bodies approximate. A *diagonal-reflection* operator σ_B is defined which simply reflects left and right sides of Fig. 10.2.3a-b or trades the x or x_1 -axis with the y or x_2 -axis.

In terms of base kets we define such a reflection as follows.

$$\sigma_B |1\rangle = |2\rangle, \quad \sigma_B |2\rangle = |1\rangle \quad (10.2.3a)$$

Operator σ_B and the unit operator $\mathbf{1}$ make a C_2^B group multiplication table and representation.

C_2	$\mathbf{1}$	σ_B	(10.2.3b)
$\mathbf{1}$	$\mathbf{1}$	σ_B	
σ_B	σ_B	$\mathbf{1}$	

$$\begin{pmatrix} \langle 1|\mathbf{H}|1\rangle & \langle 1|\mathbf{H}|2\rangle \\ \langle 2|\mathbf{H}|1\rangle & \langle 2|\mathbf{H}|2\rangle \end{pmatrix} = \begin{pmatrix} 1 & 0 \\ 0 & 1 \end{pmatrix}, \quad \begin{pmatrix} \langle 1|\sigma_B|1\rangle & \langle 1|\sigma_B|2\rangle \\ \langle 2|\sigma_B|1\rangle & \langle 2|\sigma_B|2\rangle \end{pmatrix} = \begin{pmatrix} 0 & 1 \\ 1 & 0 \end{pmatrix}$$

The Hamiltonian matrix \mathbf{H} in (10.1.1b) must be invariant to σ_B operator if \mathbf{H} is to have C_2^B symmetry.

$$\mathbf{H} = \sigma_B \mathbf{H} \sigma_B^\dagger = \sigma_B \mathbf{H} \sigma_B \quad (10.2.4a)$$

Stated another way: \mathbf{H} must commute with σ_B . $\mathbf{H} \sigma_B^\dagger = \sigma_B \mathbf{H}$

$$\begin{pmatrix} \langle 1|\mathbf{H}|1\rangle & \langle 1|\mathbf{H}|2\rangle \\ \langle 2|\mathbf{H}|1\rangle & \langle 2|\mathbf{H}|2\rangle \end{pmatrix} \begin{pmatrix} 0 & 1 \\ 1 & 0 \end{pmatrix} = \begin{pmatrix} 0 & 1 \\ 1 & 0 \end{pmatrix} \begin{pmatrix} \langle 1|\mathbf{H}|1\rangle & \langle 1|\mathbf{H}|2\rangle \\ \langle 2|\mathbf{H}|1\rangle & \langle 2|\mathbf{H}|2\rangle \end{pmatrix} \text{ or } \begin{pmatrix} \langle 1|\mathbf{H}|2\rangle & \langle 1|\mathbf{H}|1\rangle \\ \langle 2|\mathbf{H}|2\rangle & \langle 2|\mathbf{H}|1\rangle \end{pmatrix} = \begin{pmatrix} \langle 2|\mathbf{H}|1\rangle & \langle 2|\mathbf{H}|2\rangle \\ \langle 1|\mathbf{H}|1\rangle & \langle 1|\mathbf{H}|2\rangle \end{pmatrix}$$

The last result demands equality of the following \mathbf{H} -matrix component pairs.

$$\langle 1|\mathbf{H}|1\rangle = \langle 2|\mathbf{H}|2\rangle \quad (10.2.4b), \quad \langle 1|\mathbf{H}|2\rangle = \langle 2|\mathbf{H}|1\rangle \quad (10.2.4c)$$

This reduces the number of free parameters in the \mathbf{H} -matrix (10.1.1) and \mathbf{A} -matrix components (10.1.5b-c).

$$A = D, \quad B - iC = B + iC \quad (10.2.4b)$$

$$\begin{pmatrix} \langle 1|\mathbf{H}|1\rangle & \langle 1|\mathbf{H}|2\rangle \\ \langle 2|\mathbf{H}|1\rangle & \langle 2|\mathbf{H}|2\rangle \end{pmatrix} = \begin{pmatrix} A & B \\ B & A \end{pmatrix} \quad \text{or:} \quad \begin{pmatrix} \langle 1|\mathbf{K}|1\rangle & \langle 1|\mathbf{K}|2\rangle \\ \langle 2|\mathbf{K}|1\rangle & \langle 2|\mathbf{K}|2\rangle \end{pmatrix} = \begin{pmatrix} A^2 + B^2 & 2AB \\ 2AB & A^2 + B^2 \end{pmatrix} \quad (10.2.4c)$$

The complex parameter C must be zero to have C_2^B symmetry. (We also needed $C=0$ to get (10.1.5a) but the extra symmetry $A=D$ was not required there. Now we demand $A=D$, as well.)

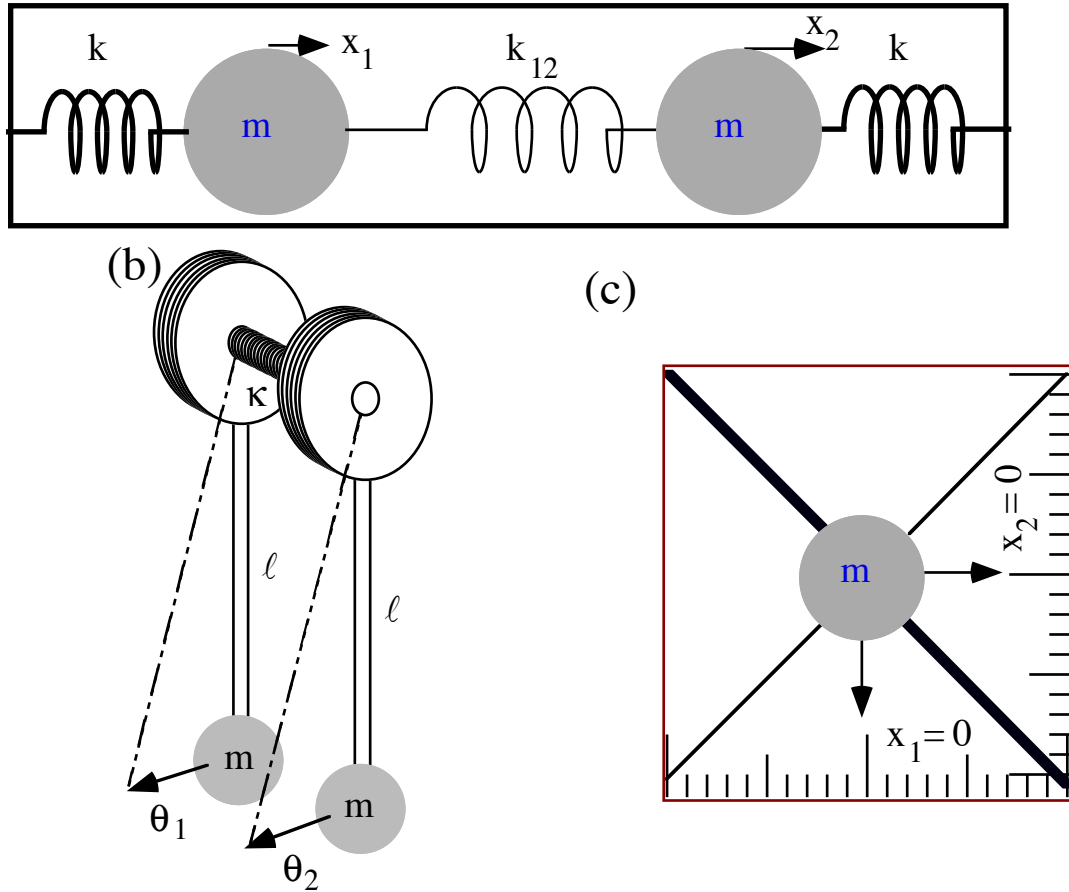


Fig. 10.2.3 Classical analogs for C_2 -symmetric $U(2)$ quantum system.

C_2^B projectors and eigenstates: Normal modes

The C_2^B projectors follow from the minimal equation for C_2^B operator σ_B that is simply

$$\sigma_B^2 = \mathbf{1} \quad , \quad \text{or} \quad \sigma_B^2 - \mathbf{1} = \mathbf{0} = (\sigma_B - \mathbf{1}) \cdot (\sigma_B + \mathbf{1})$$

We put the roots $\{\epsilon_+ = 1, \epsilon_- = -1\}$ in the general projection formula (3.1.15a) which is repeated below.

$$\mathbf{P}_k = \frac{\prod_{j \neq k} (\mathbf{M} - \epsilon_j \mathbf{1})}{\prod_{j \neq k} (\epsilon_k - \epsilon_j)} \quad , \quad (3.1.15a) \text{ repeated}$$

With $\mathbf{M} = \sigma_B$ this gives two normalized *symmetric* (+) and *anti-symmetric* (-) projectors

$$\mathbf{P}^{(+)} = (\mathbf{1} + \sigma_B)/2 \quad , \quad \mathbf{P}^{(-)} = (\mathbf{1} - \sigma_B)/2 \quad , \quad (10.2.5)$$

giving two normalized eigenstates of σ_B and the C_2^B -symmetric \mathbf{H} and \mathbf{K} operators in (10.2.4c)

$$|+\rangle = \mathbf{P}^{(+)} |1\rangle \sqrt{2} = (|1\rangle + |2\rangle)/\sqrt{2} \quad , \quad |-\rangle = \mathbf{P}^{(-)} |1\rangle \sqrt{2} = (|1\rangle - |2\rangle)/\sqrt{2} \quad , \quad (10.2.6a)$$

This yields a σ_B - or \mathbf{H} -diagonalizing transformation (d-tran).

$$\begin{pmatrix} \langle 1|+ \rangle & \langle 1|- \rangle \\ \langle 2|+ \rangle & \langle 2|- \rangle \end{pmatrix} = \begin{pmatrix} 1/\sqrt{2} & 1/\sqrt{2} \\ 1/\sqrt{2} & -1/\sqrt{2} \end{pmatrix}. \quad (10.2.6b)$$

This C_2^B -d-tran is actually a rare example of a d-tran matrix that is Hermitian ($\mathbf{T}^\dagger = \mathbf{T}$) as well as unitary ($\mathbf{T}^\dagger = \mathbf{T}^{-1}$). More about this later. The columns are eigenvectors of any matrix that commutes with C_2^B -operator σ_B . This includes the \mathbf{H} -matrix (10.2.4c) that is diagonalized as follows.

$$\begin{pmatrix} \langle +|1 \rangle & \langle +|2 \rangle \\ \langle -|1 \rangle & \langle -|2 \rangle \end{pmatrix} \begin{pmatrix} A & B \\ B & A \end{pmatrix} \begin{pmatrix} \langle 1|+ \rangle & \langle 1|- \rangle \\ \langle 2|+ \rangle & \langle 2|- \rangle \end{pmatrix} = \begin{pmatrix} A+B & 0 \\ 0 & A-B \end{pmatrix} \quad (10.2.6c)$$

The \mathbf{H} eigenvalues are

$$\langle +|\mathbf{H}|+ \rangle = A+B, \quad \langle -|\mathbf{H}|- \rangle = A-B. \quad (10.2.7a)$$

The \mathbf{K} eigenvalues are

$$\langle +|\mathbf{K}|+ \rangle = A^2 + 2AB + A^2 = (A+B)^2, \quad \langle -|\mathbf{K}|- \rangle = A^2 - 2AB + A^2 = (A-B)^2. \quad (10.2.7b)$$

The physical meaning of eigenvalues is different for quantum mechanics than for the classical analogies. For quantum mechanics, \mathbf{H} eigenvalues are eigenstate energies or \hbar times eigenfrequencies.

$$\varepsilon^+ = \hbar\omega^+ = A+B, \quad \varepsilon^- = \hbar\omega^- = A-B. \quad (10.2.8)$$

Classical \mathbf{K} -eigenvalues are squares of *normal mode frequencies*. (Classical energy is $m\omega^2/2$.)

$$\omega^2_{(+)\text{mode}} = (A+B)^2 = k/m, \quad \omega^2_{(-)\text{mode}} = (A-B)^2 = (k+2k_{12})/m. \quad (10.2.9)$$

Understanding C_2^B eigenstates: Tunneling splitting

C_2^B eigenstates (10.2.6a) point at $\pm 45^\circ$ angle to the base states $|1\rangle$ and $|2\rangle$ as shown in Fig. 10.1.2c and in Fig. 10.2.4 below. Why exactly $\pm 45^\circ$? It's because the $\pm 45^\circ$ directions are the $\pm\sigma_B$ mirror planes halfway between coordinate axes $|1\rangle$ and $|2\rangle$ that are C_2^B -equivalent or "indistinguishable."

The $+45^\circ$ mode $|+\rangle$ corresponds to two masses moving perfectly in phase with each other as in Fig. 10.2.4a. It is the $(0)_2$ "wave" in the C_2 table in Fig. 9.4.1a. The -45° mode $|-\rangle$ corresponds to two masses moving π out of phase with each other as in Fig. 10.2.4b, or a $(1)_2$ wave in the C_2 table.

The -45° mode has a higher frequency than the $+45^\circ$ mode since it stretches the connecting k_{12} spring. The $+45^\circ$ mode would behave the same if the k_{12} spring was gone. The $|+\rangle$ -mode direction is a major or "slow" axes of equipotential ellipses in Fig. 10.1.2c or Fig. 10.2.4; the $|-\rangle$ -mode use minor or "fast" axes. The steepest slope is found along the -45° "fast" mode line, and the gentlest slopes are found along the $+45^\circ$ "slow" mode line. Along these eigen-axes the motion is simple harmonic oscillation just as it was along x -or y -axes for the uncoupled oscillators in Fig. 10.2.1.

The preceding pictures apply as well to polarization oscillation inside optical analyzers which have "slow" or "fast" optical axes like the X or Y charge axes in the model given in Chapter 1 by Fig. 1.2.2 or the two-spring axes of the single-mass oscillator in Fig. 10.2.1c. Photons initially polarized along a "slow" or "fast" eigenvector direction pass unchanged except for overall phase that undergoes "slow" or "fast" harmonic oscillation, respectively. However, other polarizations are combinations of X and Y, and they undergo multi-harmonic "beating" that changes polarization as will be shown next.

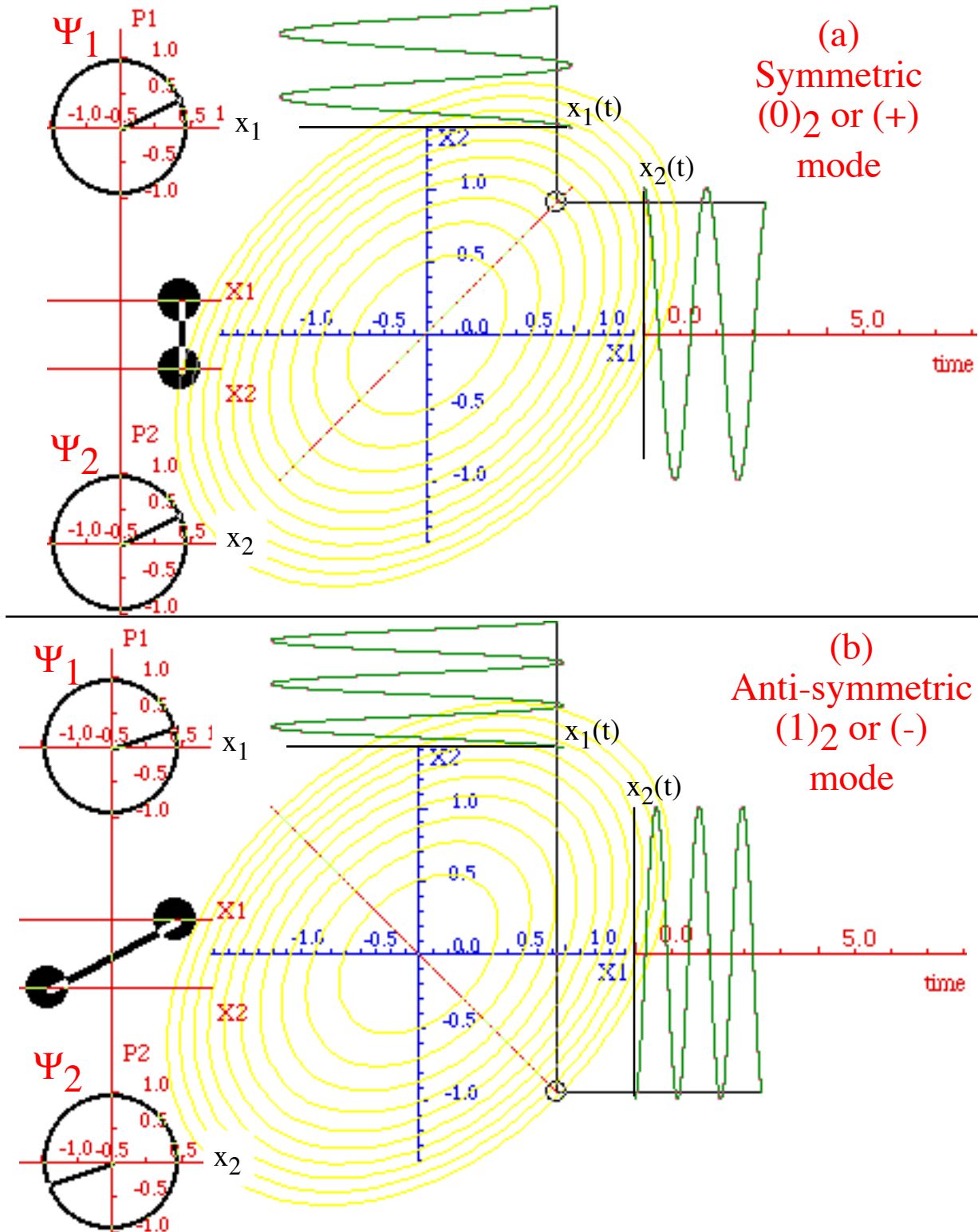


Fig. 10.2.4 Classical analog modes for C_2^B -symmetric $U(2)$ quantum system. ($m=1, k=13, k_{12}=7$)

Understanding C_2^B dynamics: Beats and transition frequency

We noted that quantum eigenstates are motionless except for their unobservable phase oscillation. Of course, phase oscillation is the motion for the classical analog normal modes in Fig. 10.2.4; we can see that easily. But, note that the phasor clocks Ψ_1 or Ψ_2 do not change in size or norm. ($\Psi_m^* \Psi_m = const.$) The norm is all we can see in a quantum system. Pure energy states are motionless blobs of probability.

However, *mixed energy states* or combinations of eigenstates will oscillate at a rate equal to the beat frequency or *transition frequency* that is the difference between their eigenfrequencies. (Recall Sec. 4.4.a and Fig. 9.4.1b.) In the example of Fig. 10.2.4 the eigenfrequencies are (from (10.2.9))

$$\omega_{(+)\text{mode}} = (A+B) = \sqrt{k} = \sqrt{13} = 3.6 \quad \omega_{(-)\text{mode}} = (A-B) = \sqrt{(k+2k_{12})} = \sqrt{27} = 5.2 \quad (10.2.10)$$

and the transition frequency is the beat frequency $|2B|$ (Actually, B is **negative** here.)

$$\omega_{(+)\text{transition}} = \omega_{\text{beat}} = |\omega_{(+)\text{mode}} - \omega_{(-)\text{mode}}| = |2B| = 5.2 - 3.6 = 1.6 \quad (10.2.11a)$$

which has the beat period shown in Fig. 10.2.5.

$$\tau_{\text{beat}} = 2\pi / \omega_{\text{beat}} = 3.9 \text{ s} \quad (10.2.11b)$$

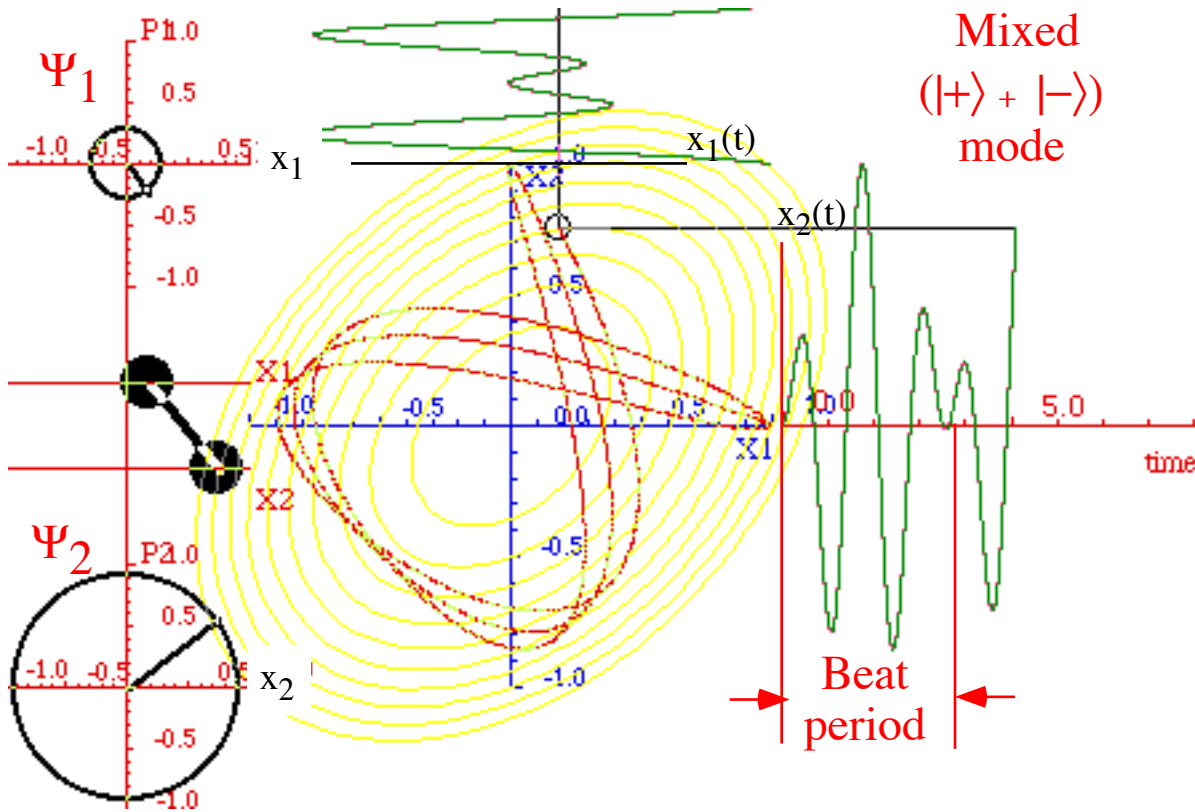


Fig. 10.2.5 Analog mixed modes for C_2^B -symmetric $U(2)$ quantum system. ($m=1, k=13, k_{12}=7$)

The mixed state in Fig. 10.2.5 was made by initially giving all the amplitude to the first coordinate ($x_1 = \Psi_1(0) = 1$) but none to the second ($\Psi_2(0) = 0$). This equivalent to having initial normal coordinates of

$$\langle + | \Psi(0) \rangle = 1/\sqrt{2}, \quad \langle - | \Psi(0) \rangle = 1/\sqrt{2}. \quad (10.2.12)$$

The time behavior of the state is then predetermined by the normal modes each oscillating at their eigenfrequencies according to a general diagonal evolution equation, a 2-D case of (9.2.1).

$$\begin{pmatrix} \langle + | \Psi(t) \rangle \\ \langle - | \Psi(t) \rangle \end{pmatrix} = \begin{pmatrix} e^{-i\omega_+ t} & 0 \\ 0 & e^{-i\omega_- t} \end{pmatrix} \begin{pmatrix} \langle + | \Psi(0) \rangle \\ \langle - | \Psi(0) \rangle \end{pmatrix} \quad (10.2.13a)$$

$$|\Psi(t)\rangle = e^{-i\omega_+ t} |+\rangle \langle + | \Psi(0) \rangle + e^{-i\omega_- t} |-\rangle \langle - | \Psi(0) \rangle \quad (10.2.13b)$$

This has the following coordinate phasor representation (Replacing abstract kets with representations.)

$$\begin{aligned}
 |\Psi(t)\rangle &= e^{-i\omega_+ t} |+\rangle \langle +|\Psi(0)\rangle + e^{-i\omega_- t} |-\rangle \langle -|\Psi(0)\rangle \\
 \begin{pmatrix} \Psi_1(t) \\ \Psi_2(t) \end{pmatrix} &= \begin{pmatrix} \langle 1|\Psi(t)\rangle \\ \langle 2|\Psi(t)\rangle \end{pmatrix} = e^{-i\omega_+ t} \begin{pmatrix} \langle 1|+\rangle \\ \langle 2|+\rangle \end{pmatrix} \langle +|\Psi(0)\rangle + e^{-i\omega_- t} \begin{pmatrix} \langle 1|-\rangle \\ \langle 2|-\rangle \end{pmatrix} \langle -|\Psi(0)\rangle \quad (10.2.14a) \\
 &= e^{-i\omega_+ t} \begin{pmatrix} 1/\sqrt{2} \\ 1/\sqrt{2} \end{pmatrix} 1/\sqrt{2} + e^{-i\omega_- t} \begin{pmatrix} 1/\sqrt{2} \\ -1/\sqrt{2} \end{pmatrix} 1/\sqrt{2}
 \end{aligned}$$

This reduces to the following. (Recall the use of the expo-sine identity in (4.4.3c).)

$$\begin{aligned}
 \begin{pmatrix} \Psi_1(t) \\ \Psi_2(t) \end{pmatrix} &= \frac{1}{2} \begin{pmatrix} e^{-i\omega_+ t} + e^{-i\omega_- t} \\ e^{-i\omega_+ t} - e^{-i\omega_- t} \end{pmatrix} = \frac{e^{-i(\omega_+ + \omega_-)t/2}}{2} \begin{pmatrix} e^{-i(\omega_+ - \omega_-)t/2} + e^{i(\omega_+ - \omega_-)t/2} \\ e^{-i(\omega_+ - \omega_-)t/2} - e^{i(\omega_+ - \omega_-)t/2} \end{pmatrix} \quad (10.2.14b) \\
 &= e^{-i(\omega_+ + \omega_-)t/2} \begin{pmatrix} \cos[(\omega_+ - \omega_-)t/2] \\ i \sin[(\omega_+ - \omega_-)t/2] \end{pmatrix}
 \end{aligned}$$

According to this, the bottom $\Psi_2(t)$ phasor amplitude grows sinusoidally from zero to its maximum with a rate that is half the beat frequency.

$$\omega_{\text{half-beat}} = \omega_{\text{beat}}/2 = |\omega_{(+)\text{mode}} - \omega_{(-)\text{mode}}|/2 \quad (10.2.15)$$

As seen in Fig. 10.2.5, the bottom $\Psi_2(t)$ phasor goes around 90° behind the top $\Psi_1(t)$ phasor. That is the i factor in the $\Psi_2(t)$ part of (10.2.14b). The overall phase rotates at an average rate

$$\omega_{\text{average}} = (\omega_{(+)\text{mode}} + \omega_{(-)\text{mode}})/2. \quad (10.2.16)$$

Then, just as the bottom $\Psi_2(t)$ phasor passes its maximum, it moves 90° ahead of the top $\Psi_1(t)$ phasor that has just gone through zero and starts to grow. The bottom $\Psi_2(t)$ phasor returns to zero amplitude every beat period τ_{beat} given by (10.2.11b) just as the top $\Psi_1(t)$ phasor reaches its maximum amplitude.

The relative phase between the two phasors is important classically as well as in the quantum analog. Whichever phasor is ahead is the one feeding energy to the other that grows while its feeder shrinks. One should recall an important resonance theorem: (Prove this if it's new to you. See exercises.)

Power transfer between two isochronous linearly connected oscillators is proportional to the product of their amplitudes and the sine of their relative phase.

A relative phase of 90° gives the best possible work rate. This type of resonance transfer is important in quantum mechanics. A relative phase of 0° or 180° gives no transfer, as in a classical normal mode or a quantum stationary state; having no net energy gain or loss by individual parts makes them stationary.

Another way to visualize beats is by analogy to optical polarization-wave-plates introduced in Fig. 1.3.6b. One quarter of a beat corresponds to a *quarter wave plate*. The effect is to convert X-polarization into right circular polarization as shown below in Fig. 10.2.6a. A half-beat converts $X=x_1$ to $Y=x_2$ as in Fig. 10.2.6b and corresponds to a *half-wave plate* as shown below in Fig. 10.2.6b. For this example, the coupling constant $2B = \sqrt{k} - \sqrt{k+2k_{12}}$ is reduced from -1.6 in (10.2.11a) to -0.26 to slow the beat from 3 periods to about 18. Real wave-plate beats take millions of periods so 18 is still way too fast.

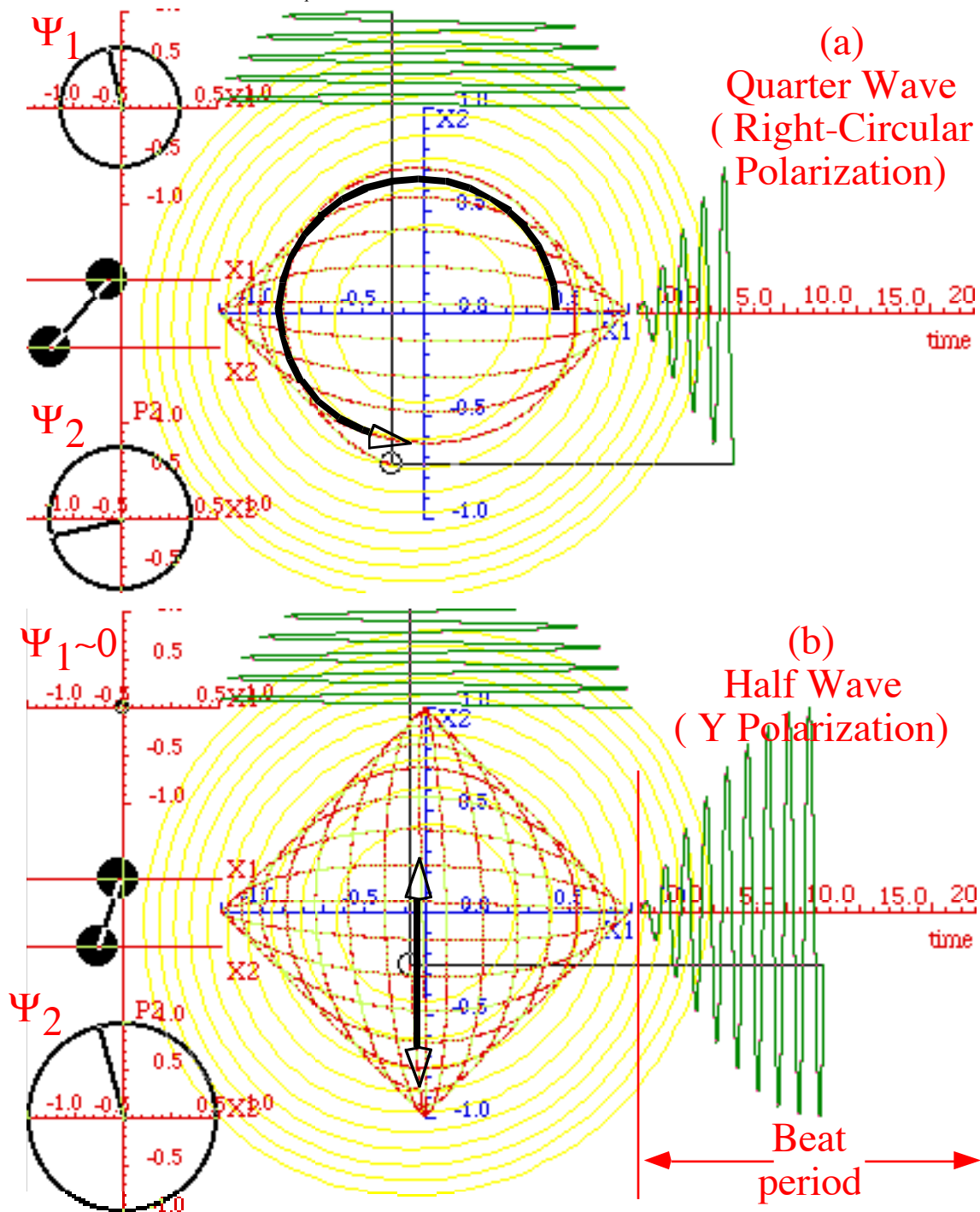


Fig. 10.2.6 Polarization evolution from X to (a) Circular, and (b) Y. ($m=1, k=19.1, k_1=1.17$)

(c) Circular or C_2^C symmetry

Now we consider the very different case in which all parameters are zero except C . Then a continuous circular rotational C_∞ symmetry or $R(2)$ symmetry is present. The reflection symmetry associated with the C -parameter is called C_2^C or $R(2)=C_\infty$. C_2^C -symmetry states are characterized by **circularity** and **chirality** or "handedness." Now the **circular** motion in Fig. 10.2.6a is an eigenstate.

C_∞ -symmetry means a two-by-two Hermitian Hamiltonian ($\mathbf{H}^\dagger = \mathbf{H}$) matrix operator

$$\mathbf{H} = \begin{pmatrix} \langle 1|\mathbf{H}|1\rangle & \langle 1|\mathbf{H}|2\rangle \\ \langle 2|\mathbf{H}|1\rangle & \langle 2|\mathbf{H}|2\rangle \end{pmatrix} = \begin{pmatrix} A & B-iC \\ B+iC & D \end{pmatrix}. \tag{10.1.1b} \textit{repeated}$$

commutes with any rotation operator $\mathbf{R}(\phi)$ defined as follows. (Recall (2.2.1) in Chapter 2.)

$$\mathbf{R}(\phi) |1\rangle = \cos \phi |1\rangle + \sin \phi |2\rangle, \quad \mathbf{R}(\phi) |2\rangle = -\sin \phi |1\rangle + \cos \phi |2\rangle \tag{10.2.18a}$$

Rotation $\mathbf{R}(\phi)$ has the following $R(2)=C_\infty$ group multiplication rule and C_∞ representation.

$$\mathbf{R}(\phi) \cdot \mathbf{R}(\phi') = \mathbf{R}(\phi + \phi'), \quad \begin{pmatrix} \langle 1|\mathbf{R}|1\rangle & \langle 1|\mathbf{R}|2\rangle \\ \langle 2|\mathbf{R}|1\rangle & \langle 2|\mathbf{R}|2\rangle \end{pmatrix} = \begin{pmatrix} \cos \phi & -\sin \phi \\ \sin \phi & \cos \phi \end{pmatrix} \tag{10.2.18b}$$

Since matrix \mathbf{H} must commute with $\mathbf{R}(\phi)$ for all ϕ , it must also commute with the derivative of $\mathbf{R}(\phi)$ at zero rotation ($\phi=0$ and $\mathbf{R}(0) = \mathbf{1}$). The derivative of a transformation operator near $\mathbf{1}$ is called the **generator \mathbf{G}** of the operator. The generator of the rotation $\mathbf{R}(\phi)$ is as follows.

$$\mathbf{G} = \left. \frac{\partial}{\partial \phi} \mathbf{R}(\phi) \right|_{\phi=0} = \begin{pmatrix} -\sin \phi & -\cos \phi \\ \cos \phi & -\sin \phi \end{pmatrix} \Bigg|_{\phi=0} = \begin{pmatrix} 0 & -1 \\ 1 & 0 \end{pmatrix}, \text{ or: } \mathbf{R}(\phi) = \mathbf{R}(0) e^{\phi \mathbf{G}} = e^{\phi \mathbf{G}} \tag{10.2.18c}$$

The set $R(2)=C_\infty$ of all $\mathbf{R}(\phi)$ operators is an example of continuous or **Lie group** symmetry. It is very much like the "empty time" symmetry made of all **time evolution operators** $\mathbf{U}(t) = e^{-i\mathbf{H}t}$. The generator of the evolution operators $\mathbf{U}(t)$ is the Hamiltonian \mathbf{H} itself.

Multiplying $\mathbf{R}(\phi)$ generator \mathbf{G} by i and gives a third **C_2^C -Hamilton-Pauli reflection operator σ_C** .

$$\sigma_C = \begin{pmatrix} 0 & -i \\ i & 0 \end{pmatrix} = i\mathbf{G}, \text{ where: } \sigma_C^\dagger \sigma_C = \sigma_C^2 = \mathbf{1} \tag{10.2.18d}$$

The i makes σ_C Hermitian-unitary like σ_A and σ_B , and gives it a (-1) determinant. ($\det|\sigma_C| = -1$) So σ_C has similar properties to a reflection operator, but it sure doesn't look like one!

Reflection operator σ_C for circular C_2^C -symmetry is imaginary unlike σ_A and σ_B that are real. However, the C_2^C rotation matrices $\mathbf{R}(\phi)$ are all real, but we will find imaginary rotations associated with C_2^A -symmetry or C_2^B -symmetry. Imaginary rotations are Lorentz transformations! More on this later.

The physical idea is that C_2^A or C_2^B -symmetries are associated with "static" or standing wave states that have a real (\pm)-reflection symmetry about their nodes or anti-nodes. For the classical analogies the nodes corresponded to normal modes or polarization planes. The nodes, modes, or planes sit in different places depending on whether it is C_2^A , C_2^{AB} , or C_2^B -symmetry, but they must sit still.

In contrast, states having C_2^C -symmetry are moving waves that have no fixed nodes or anti-nodes. Instead, they are characterized by a real (\pm)-direction of motion and a **chirality** of left or right handed motion.

This is why C_2^C -rotation operators are real while it is the reflection operators that are real for C_2^A , C_2^{AB} , or C_2^B -symmetries. The former has a constant momentum, the latter a constant position.

Commutation with reflection σ_C or generator G yields C_2^C -symmetry restrictions on H -matrices.

$$\begin{aligned} \mathbf{H} \cdot \mathbf{G} &= \mathbf{G} \cdot \mathbf{H} \\ \begin{pmatrix} \langle 1|\mathbf{H}|1\rangle & \langle 1|\mathbf{H}|2\rangle \\ \langle 2|\mathbf{H}|1\rangle & \langle 2|\mathbf{H}|2\rangle \end{pmatrix} \begin{pmatrix} 0 & -1 \\ 1 & 0 \end{pmatrix} &= \begin{pmatrix} 0 & -1 \\ 1 & 0 \end{pmatrix} \begin{pmatrix} \langle 1|\mathbf{H}|1\rangle & \langle 1|\mathbf{H}|2\rangle \\ \langle 2|\mathbf{H}|1\rangle & \langle 2|\mathbf{H}|2\rangle \end{pmatrix} \\ &= \begin{pmatrix} \langle 1|\mathbf{H}|2\rangle & -\langle 1|\mathbf{H}|1\rangle \\ \langle 2|\mathbf{H}|2\rangle & -\langle 2|\mathbf{H}|1\rangle \end{pmatrix} = \begin{pmatrix} -\langle 2|\mathbf{H}|1\rangle & -\langle 2|\mathbf{H}|2\rangle \\ \langle 1|\mathbf{H}|1\rangle & \langle 1|\mathbf{H}|2\rangle \end{pmatrix} \end{aligned} \quad (10.2.19a)$$

Thus, $R(2)=C_\infty$ or C_2^C -symmetry demands the following for H matrix components.

$$\langle 1|\mathbf{H}|1\rangle = \langle 2|\mathbf{H}|2\rangle, \quad \langle 1|\mathbf{H}|2\rangle = -\langle 2|\mathbf{H}|1\rangle \quad (10.2.19b)$$

For the H example (10.1.1b) we have

$$A = D, \quad B - iC = -(B + iC) \quad (10.2.19c)$$

so only two free parameters remain.
$$\begin{pmatrix} \langle 1|\mathbf{H}|1\rangle & \langle 1|\mathbf{H}|2\rangle \\ \langle 2|\mathbf{H}|1\rangle & \langle 2|\mathbf{H}|2\rangle \end{pmatrix} = \begin{pmatrix} A & -iC \\ iC & A \end{pmatrix} \quad (10.2.19d)$$

This H matrix is easy to diagonalize, but let's use symmetry projection just to get some more practice.

$R(2)=C_\infty$ projectors and C_2^C eigenstates

The $R(2)=C_\infty$ projectors follow from the secular equation for $R(2)=C_\infty$ operator $\mathbf{R}(\phi)$ which is

$$\varepsilon^2 - (\text{trace } \mathbf{R}(\phi)) \varepsilon + (\det \mathbf{R}(\phi)) = 0 = \varepsilon^2 - (2\cos \phi) \varepsilon + 1 \quad (10.2.20)$$

The \pm eigenvalues are labeled L and R for "Left" and "Right" for reasons that we'll see below.

$$\varepsilon_L = \cos \phi + \sqrt{\cos^2 \phi - 1} = \cos \phi + i \sin \phi = e^{i\phi} \quad (10.2.21a)$$

$$\varepsilon_R = \cos \phi - \sqrt{\cos^2 \phi - 1} = \cos \phi - i \sin \phi = e^{-i\phi} \quad (10.2.21b)$$

Substituting the roots $\{\varepsilon_L=e^{i\phi}, \varepsilon_R=e^{-i\phi}\}$ of $\mathbf{M}=\mathbf{R}(\phi)$ in the projection formula ((3.1.15) repeated below)

$$\mathbf{P}_k = \frac{\prod_{j \neq k} (\mathbf{M} - \varepsilon_j \mathbf{1})}{\prod_{j \neq k} (\varepsilon_k - \varepsilon_j)}, \quad (3.1.15a) \text{ repeated}$$

gives two normalized projectors

$$\begin{aligned} \mathbf{P}^{(L)} &= \frac{\begin{pmatrix} \cos \phi - e^{-i\phi} & -\sin \phi \\ \sin \phi & \cos \phi - e^{-i\phi} \end{pmatrix}}{e^{i\phi} - e^{-i\phi}}, & \mathbf{P}^{(R)} &= \frac{\begin{pmatrix} \cos \phi - e^{i\phi} & -\sin \phi \\ \sin \phi & \cos \phi - e^{i\phi} \end{pmatrix}}{e^{-i\phi} - e^{i\phi}}, \\ &= \frac{\begin{pmatrix} i \sin \phi & -\sin \phi \\ \sin \phi & i \sin \phi \end{pmatrix}}{2i \sin \phi} = \frac{\begin{pmatrix} 1 & i \\ -i & 1 \end{pmatrix}}{2}, & &= \frac{\begin{pmatrix} i \sin \phi & -\sin \phi \\ \sin \phi & i \sin \phi \end{pmatrix}}{-2i \sin \phi} = \frac{\begin{pmatrix} 1 & -i \\ i & 1 \end{pmatrix}}{2} \end{aligned} \quad (10.2.22)$$

which in turn, give two normalized eigenstates of the $R(2)$ -symmetric H operator in (10.2.19d)

$$|L\rangle = \mathbf{P}^{(L)} |1\rangle \sqrt{2} = (|1\rangle - i|2\rangle)/\sqrt{2}, \quad |R\rangle = \mathbf{P}^{(R)} |1\rangle \sqrt{2} = (|1\rangle + i|2\rangle)/\sqrt{2}, \quad (10.2.23a)$$

and a diagonalizing transformation

$$\begin{pmatrix} \langle 1|L\rangle & \langle 1|R\rangle \\ \langle 2|L\rangle & \langle 2|R\rangle \end{pmatrix} = \begin{pmatrix} 1/\sqrt{2} & 1/\sqrt{2} \\ -i/\sqrt{2} & i/\sqrt{2} \end{pmatrix} \quad (10.2.23b)$$

The columns are eigenvectors of any matrix that commutes with $R(2)=C_\infty$ operator $\mathbf{R}(\phi)$. This includes the \mathbf{H} -matrix (10.2.19d) that is diagonalized as follows.

$$\begin{pmatrix} \langle L|1\rangle & \langle L|2\rangle \\ \langle R|1\rangle & \langle R|2\rangle \end{pmatrix} \begin{pmatrix} A & -iC \\ iC & A \end{pmatrix} \begin{pmatrix} \langle 1|L\rangle & \langle 1|R\rangle \\ \langle 2|L\rangle & \langle 2|R\rangle \end{pmatrix} = \begin{pmatrix} A-C & 0 \\ 0 & A+C \end{pmatrix} \quad (10.2.23c)$$

The \mathbf{H} eigenvalues are (for $\hbar=1$) eigenfrequencies that determine the time evolution dynamics.

$$\epsilon_L = \langle L|\mathbf{H}|L\rangle = A-C = \hbar\omega_L, \quad \epsilon_R = \langle R|\mathbf{H}|R\rangle = A+C = \hbar\omega_R, \quad (10.2.24)$$

Understanding C_{2C} eigenstates: Zeeman-like splitting and coriolis or cyclotron motion

The eigenstate evolution is given below and represented in the original xy or $\{|1\rangle, |2\rangle\}$ basis.

$$|L(t)\rangle = |L\rangle e^{-i\omega_L t} = \begin{pmatrix} \langle 1|L\rangle \\ \langle 2|L\rangle \end{pmatrix} e^{-i\omega_L t}, \quad |R(t)\rangle = |R\rangle e^{-i\omega_R t} = \begin{pmatrix} \langle 1|R\rangle \\ \langle 2|R\rangle \end{pmatrix} e^{-i\omega_R t} \quad (10.2.25)$$

To help visualize the $R(2)$ base states $\{|L\rangle, |R\rangle\}$ we plot their real parts in the center parts of Fig. 10.2.7.

$$\text{Re} \begin{pmatrix} \langle 1|L(t)\rangle \\ \langle 2|L(t)\rangle \end{pmatrix} = \text{Re} \begin{pmatrix} e^{-i\omega_L t} / \sqrt{2} \\ -ie^{-i\omega_L t} / \sqrt{2} \end{pmatrix} = \begin{pmatrix} \cos \omega_L t \\ -\sin \omega_L t \end{pmatrix}, \quad \text{Re} \begin{pmatrix} \langle 1|R(t)\rangle \\ \langle 2|R(t)\rangle \end{pmatrix} = \text{Re} \begin{pmatrix} e^{-i\omega_R t} / \sqrt{2} \\ ie^{-i\omega_R t} / \sqrt{2} \end{pmatrix} = \begin{pmatrix} \cos \omega_R t \\ \sin \omega_R t \end{pmatrix} \quad (10.2.26)$$

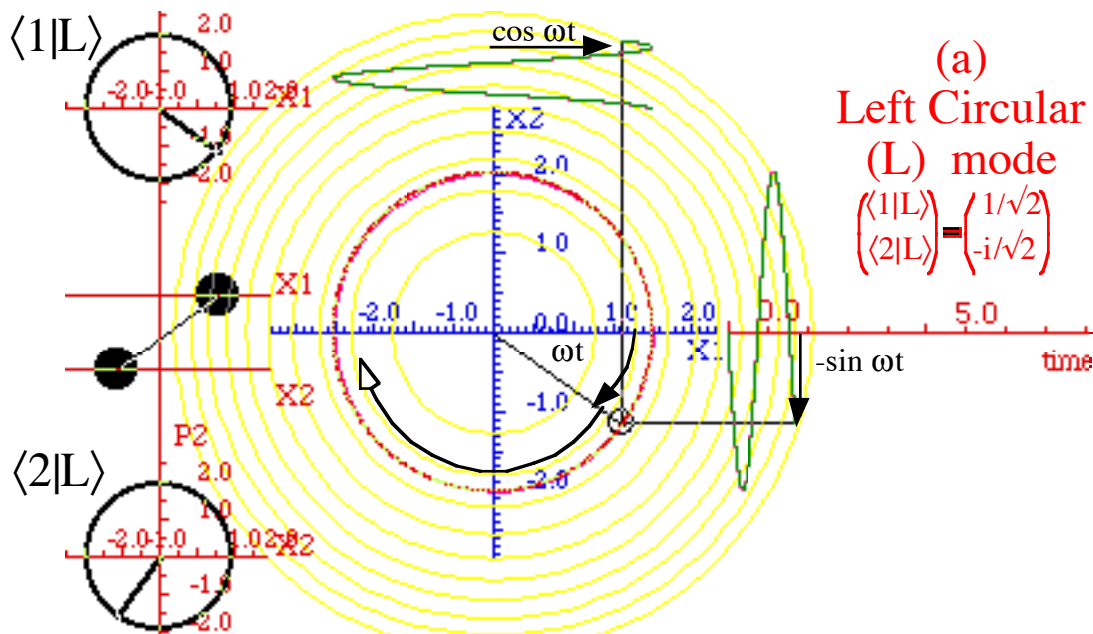


Fig. 10.2.7 $R(2)=C_\infty$ symmetry eigenstates (a) Left circular

From the Figures 10.2.7 a and b it seen how $|L\rangle$ and $|R\rangle$ stand for left and right handed *circular polarization* states. Previously, we have seen how to briefly achieve right circular polarization using a 1/4-beat of mixed C_2 -mode or a quarter wave plate in Fig. 10.2.6a. Here it's a pure $R(2)$ mode. Circular orbits are also known as *cyclotron modes*. They are the orbits that a positively charged particle in an isotropic 2-D oscillator

potential could have in the presence of a magnetic field normal to the orbit plane. They are also called *Coriolis modes* or *Foucault orbits* if the oscillator is on a rotating table.

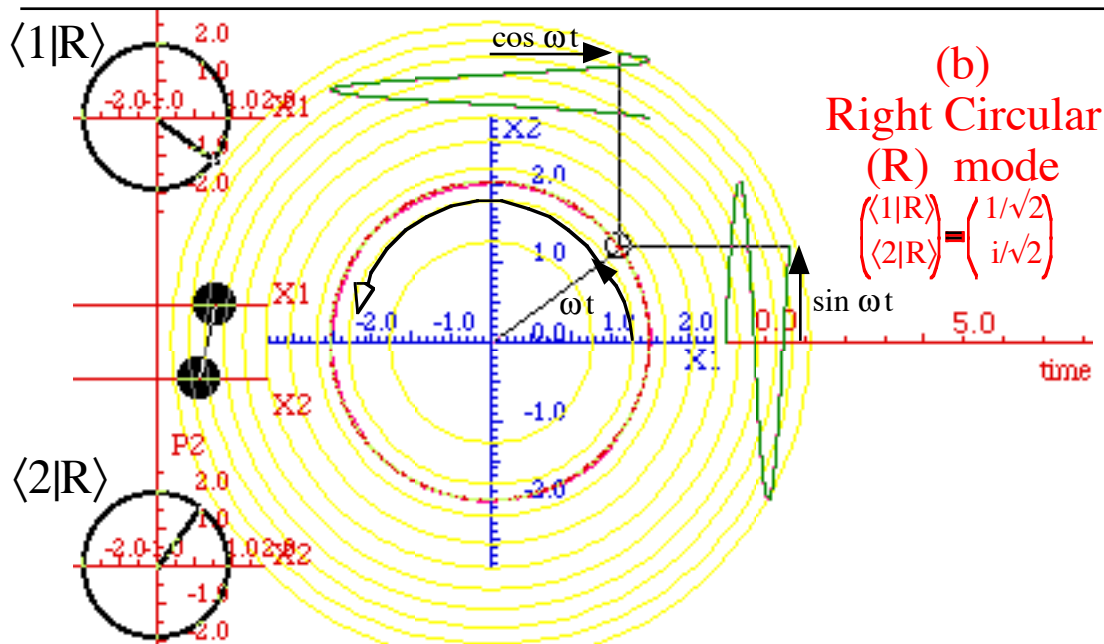


Fig. 10.2.7 $R(2)=C_\infty$ symmetry eigenstates (a) Left circular (b) Right circular polarization

With no magnetic field or rotation the particle orbits either way with the same orbit frequency as shown on the left-hand side of Fig. 10.2.8. It is only necessary that the centrifugal force $m\omega^2 r$ balance the attractive "spring" force $-kr$ of the oscillator. But, a magnetic field \mathbf{B} or rotation $\mathbf{\Omega}$ will either help to attract or else repel the particle depending on the particles direction of orbit. For left handed $|L\rangle$ -orbits the magnetic $\mathbf{F}=q\mathbf{v}\times\mathbf{B}$ force (or Coriolis force $\mathbf{F}=m\mathbf{v}\times\mathbf{\Omega}$) teams up with the attractive $\mathbf{F} = -kr$ of the oscillator. So, the centrifugal force must increase to balance these two and keep the particle at the same radius. That means faster orbit frequency ω as shown in the upper right hand side of Fig. 10.2.8. For right hand $|R\rangle$ -rotation the magnetic $q\mathbf{v}\times\mathbf{B}$ force or Coriolis $m\mathbf{v}\times\mathbf{\Omega}$ teams up with the centrifugal force $m\omega^2 r$ against the attractive $-kr$, so $m\omega^2 r$ must be reduced to maintain a given orbit radius, hence reduced orbit frequency ω .

This mechanics is also analogous to our prevailing weather phenomena. The Earth's counter clockwise rotation tends to create counterclockwise cyclones in the Northern hemisphere and the opposite ω in the Southern latitudes. Anti-cyclones are not impossible, just energetically disfavored.

The classical analogs for the rotational $R(2)$ -symmetric (Zeeman-like) quantum splitting are quite different from the corresponding analogs for bilateral AB -symmetric (Stark-like) splitting described later. The frequency equation resulting from cyclotron orbits in Fig. 10.2.8 is a force balance equation.

$$F_{centrifugal} + F_{B-field} + F_{oscillator} = 0 = m\omega^2 r + qBr\omega - kr \tag{10.2.27a}$$

It has quadratic solutions that are plotted in Fig. 10.2.9.

$$\omega = \frac{-qB \pm \sqrt{(qB)^2 + 4mk}}{2m} = \frac{-qB}{2m} \pm \sqrt{\left(\frac{qB}{2m}\right)^2 + \frac{k}{m}} = \frac{\omega_C}{2} \pm \sqrt{\left(\frac{\omega_C}{2}\right)^2 + (\omega_O)^2} \tag{10.2.27b}$$

The vacuum *cyclotron frequency* ω_C and zero-B-field *harmonic oscillator frequency* ω_O are labeled.

$$\omega_C = \frac{-qB}{m}, \quad \omega_O = \sqrt{\frac{k}{m}} \tag{10.2.27c}$$

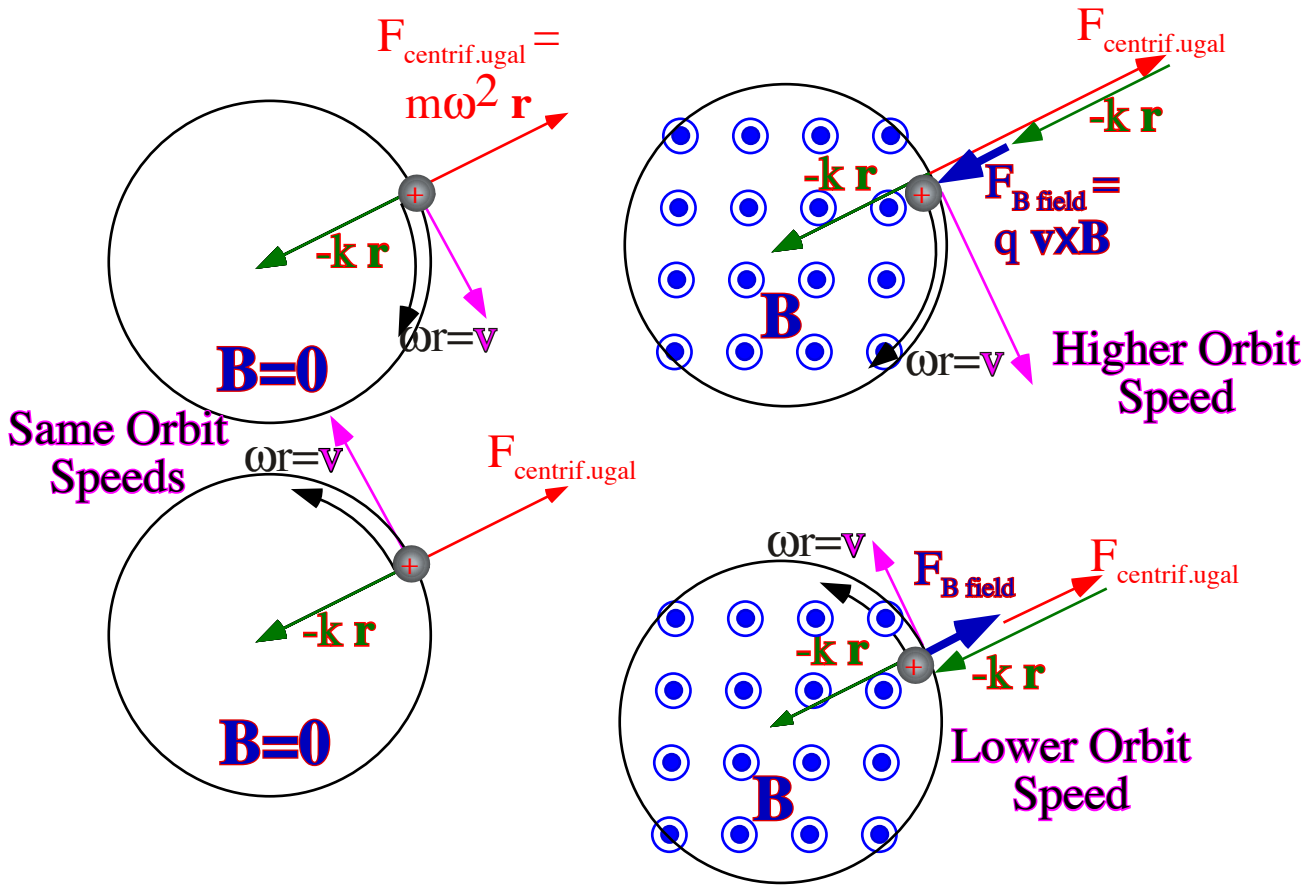


Fig. 10.2.8 Cyclotron or Coriolis orbit degeneracy lifted by **B**-field or rotation.

Note: the cyclotron frequency ω_C is minus the field parameter qB while ω_O is a positive (+)-root of parameter k/m . While ω_O is positive, orbit frequency or angular velocity ω or ω_C can each be positive or negative. In the vacuum case ($k=0$), positive qB means negative $\omega=\omega_C$ and clockwise or left L orbits only, as shown on the extreme upper right hand side of Fig. 10.2.9. Negative qB means positive $\omega=\omega_C$ and counter clockwise or R orbits only, as shown on the extreme upper left hand side of Fig. 10.2.9. The negative (-)-root in (10.2.10b) gives a zero frequency mode, that is, no motion at all, as indicated by dashed circles in Fig. 10.2.9. (A B -field does not affect effect a stationary charge.)

The plot in Fig. 10.2.9 is one of orbital speed $|\omega|$ which is quantum phasor velocity or energy $\hbar|\omega|$ rather than classical orbital velocity ω . An orbital velocity ω -plot would flip the ascending curve about the x -axis so it was below the axis and descending parallel to the other descending one. Classical kinetic energy is simply $1/2mr^2|\omega|^2$ and resembles Fig. 10.2.9, too.

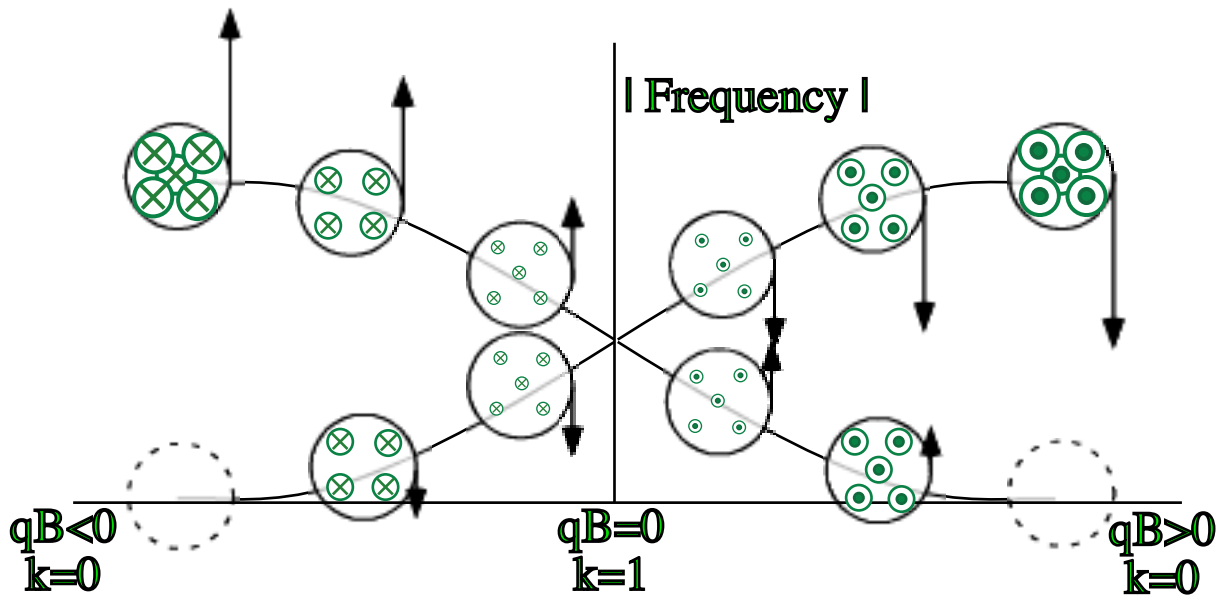


Fig. 10.2.9 Cyclotron orbital speed for varying **B**-field ($qB=x$) and oscillator spring constant $k=|1-x|$.

Consider the limiting cases. For weak oscillator potential ($\omega_O \ll |\omega_C|$) or strong qB -field, the approximate frequencies shift quadratically in ω_O .

$$\omega = \frac{-qB}{2m} \pm \sqrt{\left(\frac{qB}{2m}\right)^2 + \frac{k}{m}} = \frac{\omega_C}{2} \pm \sqrt{\left(\frac{\omega_C}{2}\right)^2 + (\omega_O)^2} \approx \frac{\omega_C}{2} \pm \left(\frac{\omega_C}{2} + \frac{(\omega_O)^2}{\omega_C} \dots\right) = \begin{cases} \omega_C + \frac{(\omega_O)^2}{\omega_C} \\ -\frac{(\omega_O)^2}{\omega_C} \end{cases} \quad (10.2.28a)$$

For strong potential ($\omega_O \gg |\omega_C|$) or weak qB -field, the approximate frequencies split linearly in ω_C .

$$\omega = \frac{-qB}{2m} \pm \sqrt{\left(\frac{qB}{2m}\right)^2 + \frac{k}{m}} = \frac{\omega_C}{2} \pm \sqrt{(\omega_O)^2 + \left(\frac{\omega_C}{2}\right)^2} \approx \frac{\omega_C}{2} \pm \left(\omega_O + \frac{\omega_C^2}{8\omega_O} \dots\right) = \begin{cases} \omega_O + \frac{\omega_C}{2} + \frac{\omega_C^2}{8\omega_O} \\ -\omega_O + \frac{\omega_C}{2} - \frac{\omega_C^2}{8\omega_O} \end{cases} \quad (10.2.28b)$$

Compare this to phasor frequencies (10.2.24) that, unlike the orbital velocities, are positive.

$$\hbar\omega_L = A - C \approx \hbar(\omega_O - \omega_C/2), \quad \hbar\omega_R = A + C \approx \hbar(\omega_O + \omega_C/2). \quad (10.2.29)$$

This connects the ω_C to the off-diagonal C -parameter in (10.2.19d) and ω_O to A , but only for weak qB .

Understanding C_2^C dynamics: Faraday rotation

The effect of mixing R and L modes in Fig. 10.2.7a-b is quite dramatic as shown in Fig. 10.2.10 where a 50-50 mixture gives perfect beats as were seen in Fig. 10.2.6 when x-polarization evolved into elliptic then circular then y-polarization. However, in Fig. 10.2.10 there is a rotation or precession of the plane of polarization directly from x to y. In the classical analogy this is a famous effect called *Foucault precession*

demonstrated in many science museums which trace the daily motion of a great pendulum due to Earth rotation. In optics, this is known as *Faraday rotation* of the plane of polarization.

A 50-50 mixture of *R* and *L* modes with the same frequency would just be plain old (or plane old) x-polarization. However, if, as in Fig. 10.2.10, *R* is a little faster in its counter-clockwise orbit than *L* is in going the other way then they will meet further and further to the right each period. The result is a nearly planar polarization ellipse that is slowly rotating to the right as shown in Fig. 10.2.10 where a half beat rotates x-into-y-polarization. Note that a whole beat will only be half a rotation, that is, x-polarization will only be rotated into minus-x-polarization. Later, we will see this is related to the spin-1/2 half-angle conundrum we encountered in Chapter 1. There in (1.2.12) a "whole" rotation by $\beta=2\pi$ of a spin vector only rotates spin-up $|\uparrow\rangle$ by $\beta/2=\pi$ and into minus spin-up $(-\uparrow)$. Same math, different physics!

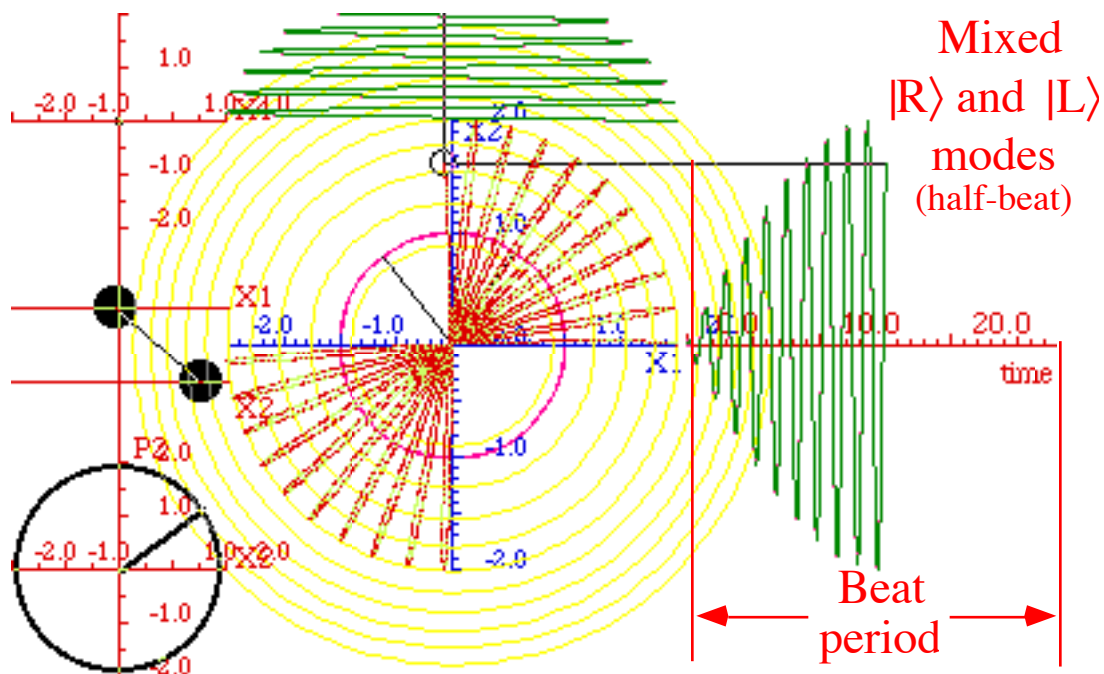


Fig. 10.2.10 Faraday rotation from X to Y. ($A=4.1=D$, $C=0.1$, $B=0$)

The picture changes radically if right handed rotation is much faster than the left handed orbit which would be zero in a purely negative $q\mathbf{B}$ -field cyclotron indicated on the left of Fig. 10.2.9. This sort of motion is shown in Fig. 10.2.11 where left-handed orbit is nearly zero and a cyclotron orbit circle is seen precessing around a circle of nearly the same radius.

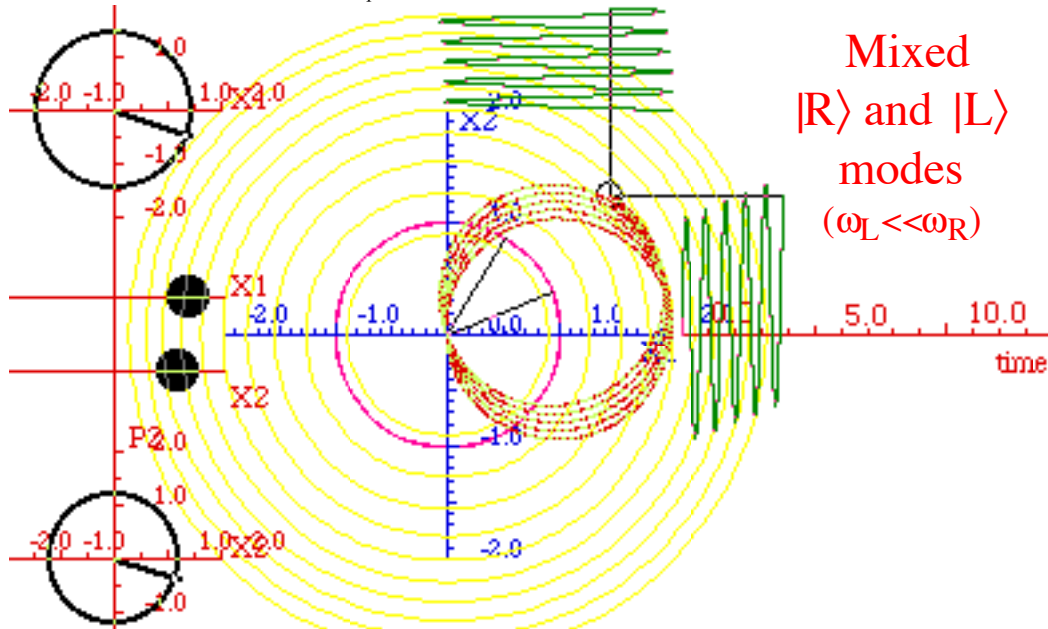


Fig. 10.2.11 Hyper-Faraday rotation. ($A=4.1=D$, $C=4.2$, $B=0$)

The analogy between Foucault precession and magnetic cyclotron orbiting, and Faraday rotation are profound and deep ones. The Foucault precession is due to an underlying rotation such as that of our Earth. The cyclotron orbit is due to an applied magnetic field as is, in some cases, the Faraday effect. The remarkable similarities of magnetism and rotation of space might lead one to speculate that magnetism *is*, in some sense, a rotation of space. Perhaps, we will have more to say about this later.

The magnetic or Zeeman like splitting seen in Fig. 10.2.9 starts out as a *first order* effect, that is, linear in the field, and then quadratic or *second order* effects show up at higher fields. The **B**-field splitting (*C*-type symmetry) is sketched below in Fig. 10.2.12b and mirrors behavior seen in Fig. 10.2.9.

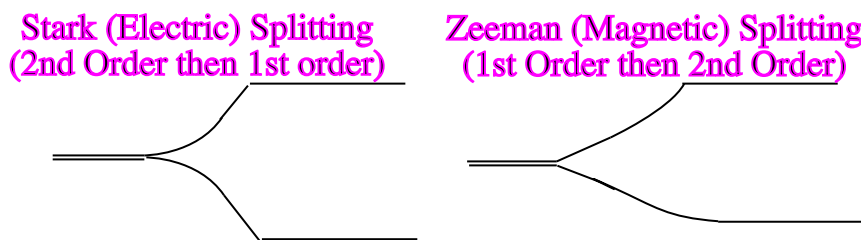


Fig. 10.2.12 Two archetypical splittings (a) Stark-like (*1st order*) (b) Zeeman-like (*2nd order*)

The next sections treat electric or Stark-like splitting which is quite the opposite. As sketched in Fig. 10.2.12a below, the electric or Stark-like splitting starts out as a second order effect and then becomes linear at higher **E**-fields. The symmetry differences between electric dipole or Stark effects (*A*-type symmetry) on one hand, and magnetic dipole or Zeeman effects (*C*-type symmetry) on the other, are important ones and are connected with quite different physics. Also, quadratic or *2nd* order variation of energy eigenvalues is a first sign that *eigenstates are changing*. Now we study some examples.

10.3 Mixed **A** and **B** Symmetry

So far our study of symmetry analysis has concentrated on its “easy” side. We found “easy” eigenvalue formulas that varied linearly with Hamiltonian parameters H, S, T , or A, B, C , and D , but the “easy” eigenstates remained *fixed*. This “easy” situation requires all the relevant symmetry operators commute with each other as do $\mathbf{r}, \mathbf{r}^2, \dots$ in Chapter 8 and 9. This is about to change because there is no such commutation between operators σ_A, σ_B , or σ_C . that make up a general $U(2)$ Hamiltonian,

$$\mathbf{H} = \frac{A+D}{2} \sigma_1 + B \sigma_B + C \sigma_C + \frac{A-D}{2} \sigma_A \tag{10.3.1}$$

The following non-commutation relations mean no *two* of σ_A, σ_B , and σ_C can be diagonalized *together*.

$$\sigma_A \sigma_B = -\sigma_B \sigma_A = \sigma_C, \quad \sigma_B \sigma_C = -\sigma_C \sigma_B = \sigma_A, \quad \sigma_C \sigma_A = -\sigma_A \sigma_C = \sigma_B, \tag{10.3.2}$$

So eigenvalues may vary *non-linearly* with parameters A, B, C , and D . Most important: *So do the eigenstates*. The study of mixed symmetries is not as “easy” but it’s quite interesting!

(a) Asymmetric bilateral C_2^{AB} symmetry: Stark-like-splitting

Consider the 2-state Hamiltonian with zero complex constant $C=0$ but nonzero A, B , and D .

$$\mathbf{H} = \begin{pmatrix} A & B \\ B & D \end{pmatrix} = \begin{pmatrix} H - pE & -S \\ -S & H + pE \end{pmatrix} \tag{10.3.3a}$$

$$\mathbf{H} = (A+D)/2 \sigma_1 + B \sigma_B + (A-D)/2 \sigma_A = H \sigma_1 - 2S \sigma_B - pE \sigma_A \tag{10.3.3a}$$

The presence of unequal diagonal energies ($A > D$) spoils bilateral C_2^B *symmetry* even if the complex constant vanishes ($C=0$). It makes the C_2^B projectors less useful. It appears one has to diagonalize the \mathbf{H} -matrix *brute force*. (Later, we will see how to elegantly "finesse" this C_2^{AB} case, too.)

Above it is imagined that a potential energy field $pE=(A-D)/2$ is turned on to make the $|1\rangle$ state lower in energy (or higher if pE is negative) than the $|2\rangle$ state. The coupling constant B has intentionally been set negative ($B=-S$) to match sign of the constant K_{12} in the coupled pendulum analogy (10.1.5a-c). The S -constant is a "sneak rate" or *tunneling amplitude* S like the S introduced in Fig. 9.3.5. (That was negative, as well, in (9.3.5g).) A positive field ($pE > 0$) corresponds to making the number-1 pendulum lower, slower, and longer than its number-2 neighbor as shown in Fig. 10.1.1b.

Now for the diagonalization. First the secular equation for \mathbf{H} in (10.3.3a) is (recalling (3.1.5))

$$\epsilon^2 - (\text{trace } \mathbf{H}) \epsilon + (\det \mathbf{H}) = 0 = \epsilon^2 - (2H) \epsilon + (H^2 - (pE)^2 - S^2). \tag{10.3.4}$$

The eigenvalues are hyperbolic conic sections plotted above a pE - S axes in Fig. 10.3.1a-b.

$$\epsilon_{hi} = H + \sqrt{(pE)^2 + S^2} \tag{10.3.5a}$$

$$\epsilon_{lo} = H - \sqrt{(pE)^2 + S^2} \tag{10.3.5b}$$

The high and low eigenvalues form two halves of an intersecting vertical cone in Fig. 10.3.1a. (Michael Berry calls the cone a *diablo* after a child's toy top. The intersection is called a *diabolical point* since it’s a devilish singularity, as we will see.) The corresponding eigenvector projectors are (using (3.1.15))

$$\mathbf{P}_{hi} = \frac{\begin{pmatrix} H - pE - \varepsilon_{lo} & -S \\ -S & H + pE - \varepsilon_{lo} \end{pmatrix}}{\varepsilon_{hi} - \varepsilon_{lo}} = \frac{\begin{pmatrix} -pE + \sqrt{(pE)^2 + S^2} & -S \\ -S & pE + \sqrt{(pE)^2 + S^2} \end{pmatrix}}{2\sqrt{(pE)^2 + S^2}} \quad (10.3.5c)$$

$$\mathbf{P}_{lo} = \frac{\begin{pmatrix} H - pE - \varepsilon_{hi} & -S \\ -S & H + pE - \varepsilon_{hi} \end{pmatrix}}{\varepsilon_{lo} - \varepsilon_{hi}} = \frac{\begin{pmatrix} pE + \sqrt{(pE)^2 + S^2} & S \\ S & -pE + \sqrt{(pE)^2 + S^2} \end{pmatrix}}{2\sqrt{(pE)^2 + S^2}} \quad (10.3.5d)$$

For constant $S > 0$ and varying pE the two eigenvalues trace *hyperbolic conic sections* or a *Wigner avoided level crossing* as shown in Fig. 10.3.1. Crossing happens only at one "diabolical" point where tunneling and field both vanish ($S=0=pE$). In Fig. 10.3.1b, relative amplitudes for the "up-field" or $|2\rangle=|y\rangle$ versus "dn-field" or $|1\rangle=|x\rangle$ states vary from 50-50 for $pE=0$ to 99up-1dn when pE field is up ($pE=+1$) or 1up-99dn for ($pE=-1$) for the "ground" states on the bottom hyperbola. Meanwhile, the "excited" states on the top curve go *against* the field. For smaller S , polarization shifts near the diabolical point become sharper, finally jumping from 100up-0dn to 0up-100dn right at $pE=0$. We now see how this works.

High field splitting: Strong C_2^A or weak C_2^B symmetry

For large $|pE|$ and small tunneling ($|pE| \gg S$) the approximate eigenvalues are growing up or down linearly with the applied field energy pE as the energy eigenvalues approach the hyperbolic asymptotes.

$$\varepsilon_{hi} = H + \sqrt{(pE)^2 + S^2} \approx H + pE + \frac{S^2}{2pE} + \dots \quad (10.3.6a)$$

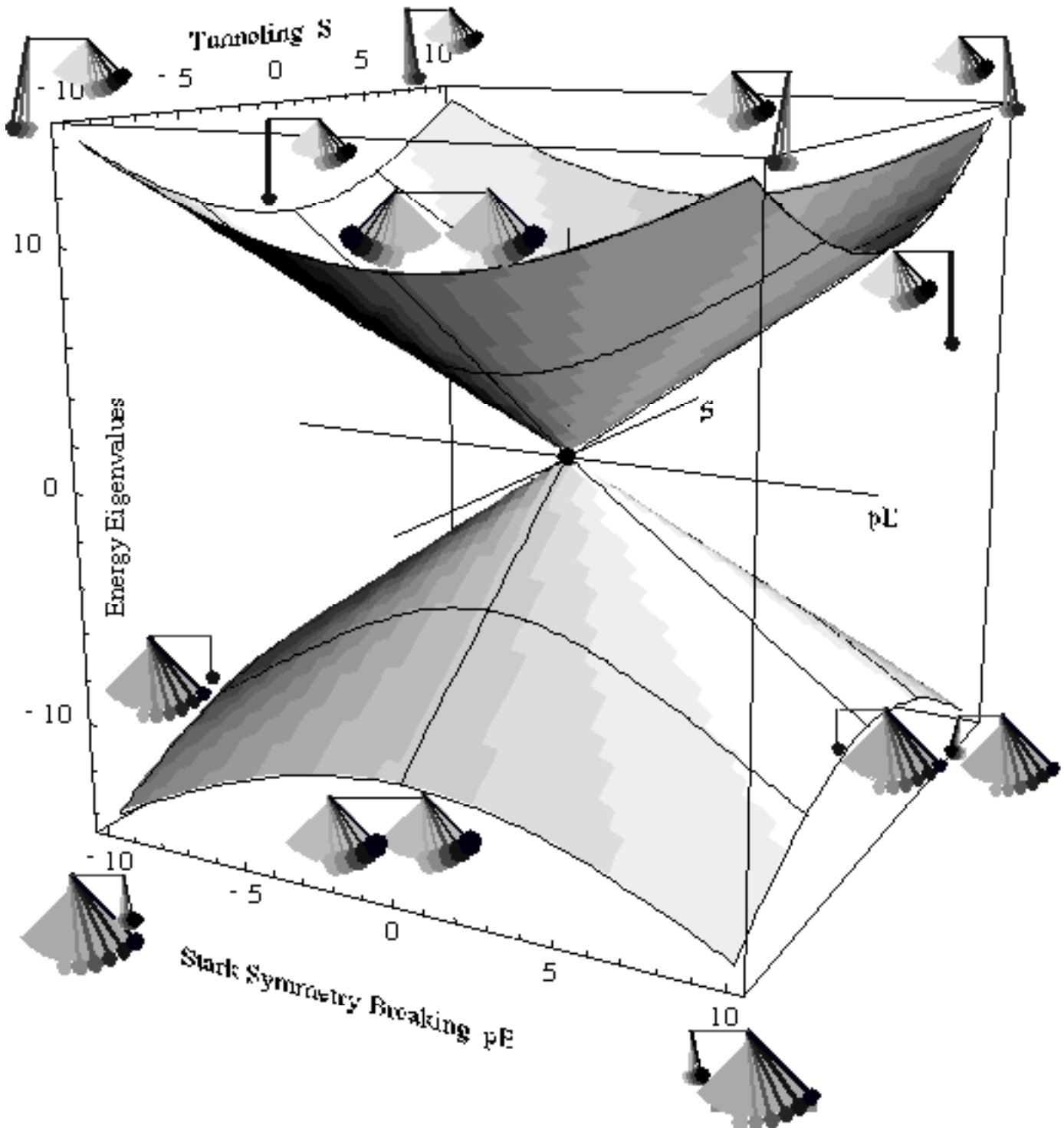
$$\varepsilon_{lo} = H - \sqrt{(pE)^2 + S^2} \approx H - pE - \frac{S^2}{2pE} + \dots \quad (\text{for } pE \gg S) \quad (10.3.6b)$$

In this limit, the eigenvectors get their symmetry broken, too. With zero field ($pE=0$) the lowest eigenstate $|+\rangle$ is a perfect 50-50 combination of the "down-field" state $|1\rangle$ and the "up-field" state $|2\rangle$ as in (10.2.6a). With a large field, the lowest state becomes nearly 100% "down-field" state $|1\rangle$ and negligible amplitude in the "up-field" direction of state $|2\rangle$, as seen in the following first column of (10.3.5d).

$$\begin{aligned} |\varepsilon_{lo}\rangle &= \begin{pmatrix} \langle 1|\varepsilon_{lo}\rangle \\ \langle 2|\varepsilon_{lo}\rangle \end{pmatrix} = \frac{1}{\sqrt{\text{norm.}}} \begin{pmatrix} pE + \sqrt{(pE)^2 + S^2} \\ S \end{pmatrix} \\ &\approx \frac{1}{\sqrt{\text{norm.}}} \begin{pmatrix} 2pE + S^2 / 2pE + \dots \\ S \end{pmatrix} \rightarrow \begin{pmatrix} 1 \\ 0 \end{pmatrix} = |1\rangle \quad (\text{for } pE \gg S) \end{aligned} \quad (10.3.7a)$$

Meanwhile, the highest eigenstate $|-\rangle$, also once a (minus) 50-50 combination, behaves in a contrary fashion and "fights" its way against the field toward almost 100% "up-field" direction of state $|2\rangle$.

$$\begin{aligned}
 |\varepsilon_{hi}\rangle &= \begin{pmatrix} \langle 1|\varepsilon_{hi}\rangle \\ \langle 2|\varepsilon_{hi}\rangle \end{pmatrix} = \frac{1}{\sqrt{\text{norm.}}} \begin{pmatrix} -S \\ pE + \sqrt{(pE)^2 + S^2} \end{pmatrix} \\
 &\approx \frac{1}{\sqrt{\text{norm.}}} \begin{pmatrix} -S \\ 2pE + S^2/2pE + \dots \end{pmatrix} \rightarrow \begin{pmatrix} 0 \\ 1 \end{pmatrix} = |2\rangle \quad (\text{for } pE \gg S)
 \end{aligned}
 \tag{10.3.7b}$$



10.3.1 (a) Two state eigenvalue "diablo" surfaces and conical intersection and pendulum eigenstates.

Fig.

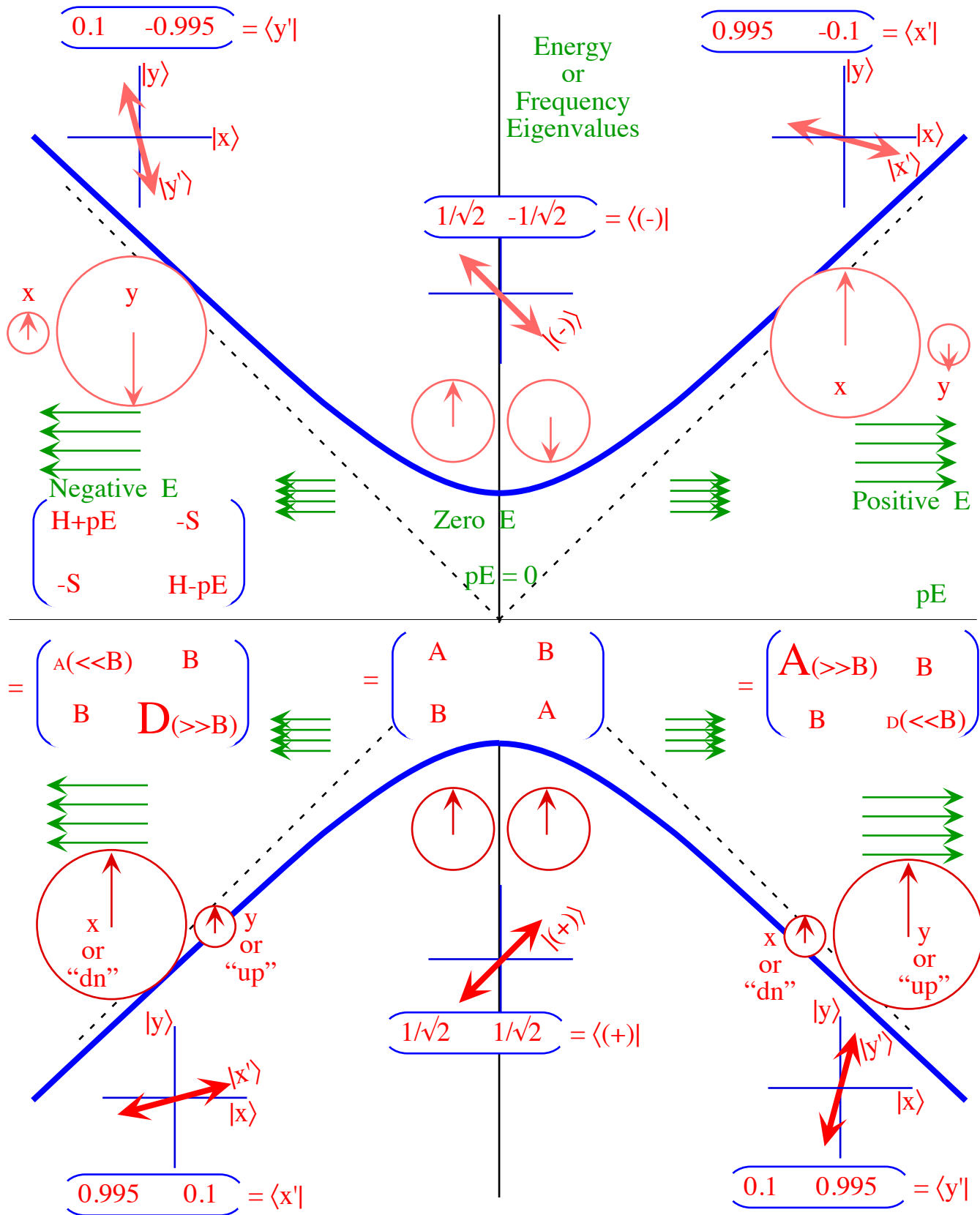


Fig. 10.3.1 (b) Wigner avoided level crossing. (Fixed tunneling S and variable pE field.)

The tendency for a ground state system to acquiesce or "polarize" in the direction of the applied field is quite natural. (Don't you feel like just "giving in" sometimes?) Most systems that we "push" in our classical world are in their ground states and respond accordingly. However, an excited quantum state can be a very different beast and will display a "passive aggressive" behavior, to use an anthropomorphic analogy. (That's right...fight the #%*@ system no matter what it takes!)

The pendulum analogy helps to understand this behavior in terms of resonance, or the lack thereof. If we reduce symmetry by making pendulum-1 longer and slower than pendulum-2 as in Fig. 10.1.1b then we spoil the resonance between them, particularly if the coupling is weak ($|k_{12}| \ll |k_2 - k_1|$). The response of faster pendulum-2 to the slower one drops off according to Lorentz's classical formula (Append. 1.B)

$$\text{response of 2 due to 1} \sim k_{12}/(\omega_2^2 - \omega_1^2) = k_{12}/(k_2 - k_1) = -\text{response of 1 due to 2.}$$

So the low-frequency mode is mostly the slow pendulum swinging. The fast pendulum swing is less by a factor ($\sim S/2pE$) in (10.3.7a). But, the high frequency mode is mostly the fast pendulum-2 swinging. The slow pendulum-1 response is down by about ($-S/2pE$) and π out of phase. (See (-) sign in (10.3.7b).)

For a geometric picture of the effect of reduced symmetry see Fig. 10.1.2(a) and (ab). For lower $S/|pE|$ the mode lines move away from mode axes $|+\rangle$ (low ω) or $|-\rangle$ (high ω) and toward the local axes $|x\rangle=|1\rangle$ (slow) or $|y\rangle=|2\rangle$ (fast) of individual pendulums. That is shown in Fig. 10.3.1b, too.

Low field splitting: Strong C_2^B or weak C_2^A symmetry and $A \rightarrow B$ basis change

For weak fields ($|pE| \ll S$) the symmetry breaking and energy splitting is much less severe. The eigenvalue splitting is approximately quadratic or 2nd order in the field pE near the hyperbolic minima.

$$\epsilon_{hi} = H + \sqrt{(pE)^2 + S^2} \approx H + S + \frac{(pE)^2}{2S} + \dots \quad (10.3.8a)$$

$$\epsilon_{lo} = H - \sqrt{(pE)^2 + S^2} \approx H - S - \frac{(pE)^2}{2S} + \dots \quad (\text{for: } S \gg pE) \quad (10.3.8b)$$

At first, as pE becomes non-zero, there is little change of eigenvalues or eigenvectors. Low pE favors B -symmetry eigenvectors $|+\rangle$ and $|-\rangle$ being the basis. The d-tran (10.2.6c) does the $A \rightarrow B$ change of basis.

$$\begin{pmatrix} \langle +|1\rangle & \langle +|2\rangle \\ \langle -|1\rangle & \langle -|2\rangle \end{pmatrix} \begin{pmatrix} \langle 1|\mathbf{H}|1\rangle & \langle 1|\mathbf{H}|2\rangle \\ \langle 2|\mathbf{H}|1\rangle & \langle 2|\mathbf{H}|2\rangle \end{pmatrix} \begin{pmatrix} \langle 1|+\rangle & \langle 1|-\rangle \\ \langle 2|+\rangle & \langle 2|-\rangle \end{pmatrix} = \begin{pmatrix} \langle +|\mathbf{H}|+\rangle & \langle +|\mathbf{H}|-\rangle \\ \langle -|\mathbf{H}|+\rangle & \langle -|\mathbf{H}|-\rangle \end{pmatrix} \quad (10.3.9a)$$

$$\begin{pmatrix} 1/\sqrt{2} & 1/\sqrt{2} \\ 1/\sqrt{2} & -1/\sqrt{2} \end{pmatrix} \begin{pmatrix} H - pE & -S \\ -S & H + pE \end{pmatrix} \begin{pmatrix} 1/\sqrt{2} & 1/\sqrt{2} \\ 1/\sqrt{2} & -1/\sqrt{2} \end{pmatrix} = \begin{pmatrix} H - S & -pE \\ -pE & H + S \end{pmatrix} \quad (10.3.9b)$$

Note that field energy pE and tunneling energy S switch places. Now (10.3.8) are perturbations of $H \pm S$ values due to an off-diagonal component $-pE$. In A -bases, tunneling energy $-S$ perturbs $H \pm pE$ values.

(b) Ammonia (NH₃) maser

If you imagine the ϵ vs. pE hyperbolas in Fig. 10.3.1 are effectively potential energy curves it is possible to understand how the first MASER (Microwave Amplification by Stimulated Excitation of Radiation) was made. To obtain a population of predominately excited ammonia (NH₃) molecules, Charles Townes and co-workers put a hot beam of NH₃ through a non-uniform electric field that acted as a sorter that distinguished which states belonged to one or the other of the two hyperbolic "potential" energies.

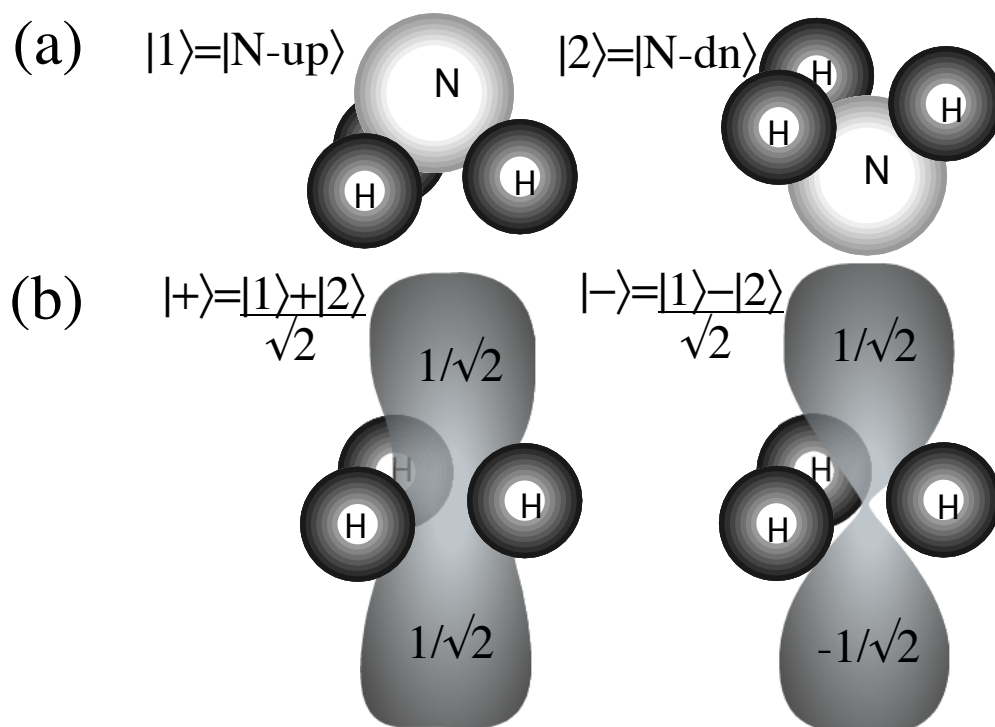


Fig. 10.3.2 Ammonia (NH_3) inversion states (a) Base states (b) C_2 -Eigenstates

The NH_3 molecule can be viewed as a C_2^B -symmetric two-state system in which the N-atom has two possible position base states $|1\rangle = |\text{N-up}\rangle$ and $|2\rangle = |\text{N-dn}\rangle$ wherein the N-atom resides on one or the other side of the H_3 plane as shown below in Fig. 10.3.2a. It is assumed that the system has a bilateral C_2^B -reflection symmetry about the H_3 plane.

Ammonia is a peculiar "fluxional" molecule that won't "stick" to one side or another, that is, it has states $|1\rangle = |\text{N-up}\rangle$ and $|2\rangle = |\text{N-dn}\rangle$ are not stationary states. In fact if NH_3 were to start out in state $|1\rangle = |\text{N-up}\rangle$ it would "beat" or "tunnel" up and down between state $|1\rangle$ and state $|2\rangle = |\text{N-down}\rangle$ with a beat or transition frequency of 24 GHz. This is analogous to the beat oscillations between $X=x_1$ and $Y=x_2$ in Fig. 10.2.6 and Fig. 9.4.1. It might oscillate like this forever. However, it is a tiny charged dipole coupled to the electromagnetic field as we'll study later. While oscillating its charge, it behaves like a tiny microwave antenna broadcasting at the transition frequency. After billions of cycles it finally must "damp out" to a stationary eigenstate $|\epsilon_{lo}\rangle = |+\rangle$, that is, it decays to its ground state emitting a 24 GHz photon.

For zero or low E -field the molecules start out in one of two inversion eigenstates $|\epsilon_{lo}\rangle = |+\rangle$ and $|\epsilon_{hi}\rangle = |-\rangle$ sketched in Fig. 10.3.2b. The temperature and statistical mechanics determine how many of each. The hotter the beam is, the more nearly the excited $|\epsilon_{hi}\rangle$ state population will become equal to unexcited ground $|\epsilon_{lo}\rangle$ state population.

Eigenstates are made of 50-50 (or $1/\sqrt{2}$, $\pm 1/\sqrt{2}$) combinations of $|1\rangle = |\text{N-up}\rangle$ and $|2\rangle = |\text{N-dn}\rangle$ exactly like the C_2^B prototypes in (10.2.6). In other words, the N-atom is "fuzzed-out" so it has the same probability of being found on either side of the H_3 plane, and the same or opposite quantum phase. These two states are analogous to the normal modes (+) and (-) in Fig. 10.2.4a and b, respectively.

As the beam of $|\epsilon_{lo}\rangle=|+\rangle$ and $|\epsilon_{hi}\rangle=|-\rangle$ molecules enters a non-uniform field the excited $|\epsilon_{hi}\rangle=|-\rangle$ state molecules fall away from the strong field because they are on the upper branch of the hyperbola in Fig. 10.3.1 and can get to lower energy by heading for the ($pE=0$) point. They become separated from ground state ($|\epsilon_{lo}\rangle=|+\rangle$)-molecules that gain kinetic energy by “gravitating” toward high field.

This makes it possible to cull out particles in the $|\epsilon_{hi}\rangle=|-\rangle$ state. The excited output is fed into a cavity tuned to the 24 GHz transition "broadcast" frequency which has a wavelength of 1.25 cm. , and it begins to resonate strongly and coherently. And so, the laser (and kitchen microwave) revolution began!

C_2^{AB} Symmetry : Weyl reflections

The symmetry of a Stark Hamiltonian matrix with $A \neq D$ might not be as obvious as the C_2^B symmetry of an \mathbf{H} -matrix with $A=D$. However, if you look again at the normal coordinate axes of the C_2^B modes in Fig. 10.1.2b you can see they are rotations of the original Cartesian xy -axes in Fig. 10.1.2a by an angle $\phi=45^\circ$. The normal coordinate axes of the "symmetry-broken" modes in Fig. 10.1.2ab are rotations of the original base states in Fig. 10.1.2a by some other angle $\phi=\beta/2$ that is less than 45° . In fact, each set of axes pictured in Figs. 10.1.2 (a), (ab), and (b) has its own reflection symmetry operator σ_A , σ_{AB} , and σ_B , respectively, and each is related to the other by rotational transformation.

We have used the bilateral reflection σ_B given by (10.2.3b) to switch x -axes with y -axes. The operation σ_B is a reflection through a 45° mirror plane lying on major axes of B -potential ellipses. ($V^B=const.$) As such, σ_B is a 45° rotation of the σ_A mirror reflection through an x -axial plane lying on major axes of A -potential ellipses ($V^A=const.$) in Fig. 10.1.2.

$$\sigma_A = \begin{pmatrix} 1 & 0 \\ 0 & -1 \end{pmatrix} \tag{10.3.9a}$$

$$\sigma_B = \mathbf{R}\left[\frac{\pi}{4}\right] \sigma_A \mathbf{R}^\dagger\left[\frac{\pi}{4}\right] = \mathbf{R}[45^\circ] \sigma_A \mathbf{R}[-45^\circ]$$

$$\begin{pmatrix} 0 & 1 \\ 1 & 0 \end{pmatrix} = \begin{pmatrix} \cos\frac{\pi}{4} & -\sin\frac{\pi}{4} \\ \sin\frac{\pi}{4} & \cos\frac{\pi}{4} \end{pmatrix} \begin{pmatrix} 1 & 0 \\ 0 & -1 \end{pmatrix} \begin{pmatrix} \cos\frac{\pi}{4} & \sin\frac{\pi}{4} \\ -\sin\frac{\pi}{4} & \cos\frac{\pi}{4} \end{pmatrix} = \begin{pmatrix} \frac{1}{\sqrt{2}} & \frac{-1}{\sqrt{2}} \\ \frac{1}{\sqrt{2}} & \frac{1}{\sqrt{2}} \end{pmatrix} \begin{pmatrix} 1 & 0 \\ 0 & -1 \end{pmatrix} \begin{pmatrix} \frac{1}{\sqrt{2}} & \frac{1}{\sqrt{2}} \\ \frac{-1}{\sqrt{2}} & \frac{1}{\sqrt{2}} \end{pmatrix} \tag{10.3.9b}$$

The matrices σ_A and σ_B are two real *Hamilton-Pauli-Jordan spinor operators*. (The third σ_C operator is the complex one.) The reflections σ_A and σ_B do so-called *Weyl reflections* after the famous theorist Hermann Weyl. Moving the rotations to the left side gives a diagonalization of σ_B and \mathbf{H}^B .

$$\begin{pmatrix} \frac{1}{\sqrt{2}} & \frac{1}{\sqrt{2}} \\ \frac{-1}{\sqrt{2}} & \frac{1}{\sqrt{2}} \end{pmatrix} \begin{pmatrix} 0 & 1 \\ 1 & 0 \end{pmatrix} \begin{pmatrix} \frac{1}{\sqrt{2}} & \frac{-1}{\sqrt{2}} \\ \frac{1}{\sqrt{2}} & \frac{1}{\sqrt{2}} \end{pmatrix} = \begin{pmatrix} 1 & 0 \\ 0 & -1 \end{pmatrix}, \text{ and: } \begin{pmatrix} \frac{1}{\sqrt{2}} & \frac{1}{\sqrt{2}} \\ \frac{-1}{\sqrt{2}} & \frac{1}{\sqrt{2}} \end{pmatrix} \begin{pmatrix} A & B \\ B & A \end{pmatrix} \begin{pmatrix} \frac{1}{\sqrt{2}} & \frac{-1}{\sqrt{2}} \\ \frac{1}{\sqrt{2}} & \frac{1}{\sqrt{2}} \end{pmatrix} = \begin{pmatrix} A+B & 0 \\ 0 & A-B \end{pmatrix} \tag{10.3.9c}$$

This is like d-tran (10.2.6c) except it is done here by a rotation $\mathbf{R}[-45^\circ]$ instead of a reflection through the 22.5° plane that is what we unknowingly wrote down in (10.2.6a). How can this be understood?

To understand this we need a couple of lessons from this elementary introduction of Weyl and Hamilton operations. First, as seen first in (10.1.7), all \mathbf{H} -matrices are made of "pieces" of their symmetry groups. (It's true whether or not we can easily see it!) Here, \mathbf{H}^B is made of C_2^B "pieces" $\mathbf{1}$ and σ_B .

$$\mathbf{H}^B = A \cdot \mathbf{1} + B \cdot \sigma_B, \text{ or: } \begin{pmatrix} A & B \\ B & A \end{pmatrix} = A \begin{pmatrix} 1 & 0 \\ 0 & 1 \end{pmatrix} + B \begin{pmatrix} 0 & 1 \\ 1 & 0 \end{pmatrix}$$

Rotation $\mathbf{R}[-45^\circ]$ diagonalizes σ_B and \mathbf{H}^B . A $\phi=22.5^\circ$ mirror reflection can do it, too, as in Fig. 10.3.3a.

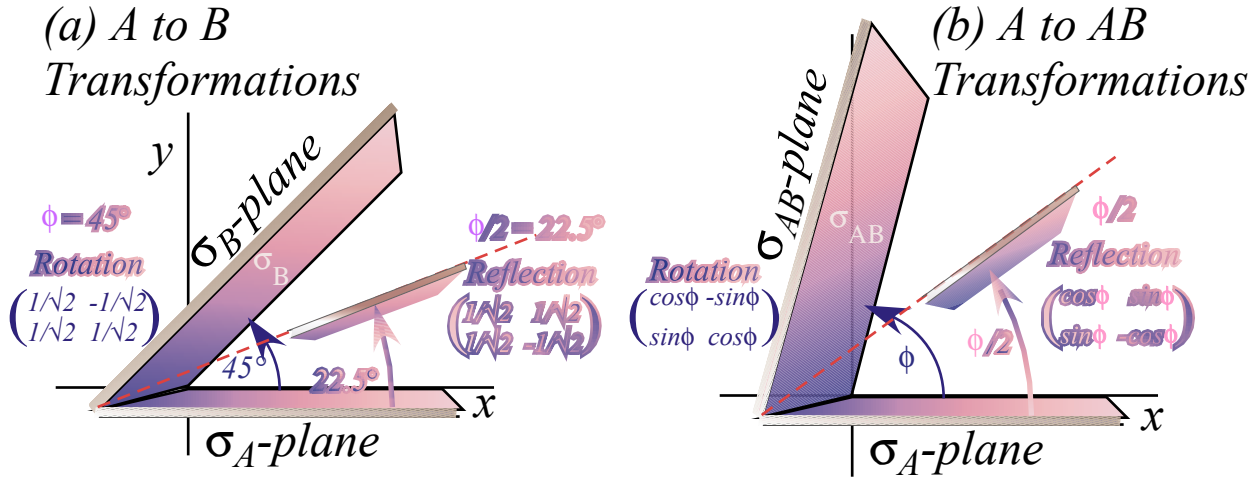


Fig. 10.3.3 Rotations and reflections that convert σ_A into (a) σ_B , (b) σ_{AB}

Generalizing (10.3.9c) for a rotation by angle $\phi=\beta/2$ yields a general ϕ -tipped σ_{AB} plane-reflection.

$$\mathbf{R}[\phi] \cdot \sigma_A \cdot \mathbf{R}^\dagger[\phi] = \sigma_{AB} = \sigma[\phi \text{ tipped plane}] \tag{10.3.10a}$$

$$\begin{pmatrix} \cos \phi & -\sin \phi \\ \sin \phi & \cos \phi \end{pmatrix} \begin{pmatrix} 1 & 0 \\ 0 & -1 \end{pmatrix} \begin{pmatrix} \cos \phi & \sin \phi \\ -\sin \phi & \cos \phi \end{pmatrix} = \begin{pmatrix} \cos^2 \phi - \sin^2 \phi & 2 \sin \phi \cos \phi \\ 2 \sin \phi \cos \phi & -\cos^2 \phi + \sin^2 \phi \end{pmatrix} = \begin{pmatrix} \cos 2\phi & \sin 2\phi \\ \sin 2\phi & -\cos 2\phi \end{pmatrix}$$

This shows we can bring a ϕ -tipped AB -plane parallel to the x -plane in two ways. We can do a rotation $\mathbf{R}[-\phi]$ that "untips" by angle $-\phi=-\beta/2$ or we can perform a reflection through a mirror plane that is tipped by $\phi/2=\beta/4$ half-way between the x -plane and the AB -plane. Here is the latter.

$$\sigma[\beta/4 \text{ tipped plane}] \cdot \sigma[\beta/2 \text{ tipped plane}] \cdot \sigma[\beta/4 \text{ tipped plane}] = \sigma_A \tag{10.3.10b}$$

$$\begin{pmatrix} \cos \beta/2 & \sin \beta/2 \\ \sin \beta/2 & -\cos \beta/2 \end{pmatrix} \cdot \begin{pmatrix} \cos \beta & \sin \beta \\ \sin \beta & -\cos \beta \end{pmatrix} \cdot \begin{pmatrix} \cos \beta/2 & \sin \beta/2 \\ \sin \beta/2 & -\cos \beta/2 \end{pmatrix} = \begin{pmatrix} 1 & 0 \\ 0 & -1 \end{pmatrix}$$

This transformation then also diagonalizes the general \mathbf{H}^{AB} matrix made of C_2^{AB} "pieces" $\mathbf{1}$ and σ_{AB} .

$$\mathbf{H}^{AB} = \frac{A+D}{2} \cdot \mathbf{1} + \frac{A-D}{2} \sigma_A + B \cdot \sigma_B, \begin{pmatrix} A & B \\ B & D \end{pmatrix} = \frac{A+D}{2} \begin{pmatrix} 1 & 0 \\ 0 & 1 \end{pmatrix} + \frac{A-D}{2} \begin{pmatrix} 1 & 0 \\ 0 & -1 \end{pmatrix} + B \begin{pmatrix} 0 & 1 \\ 1 & 0 \end{pmatrix} \tag{10.3.11a}$$

$$\mathbf{H}^{AB} = \frac{A+D}{2} \cdot \mathbf{1} + k_{ABD} \cdot \sigma_{AB}, \begin{pmatrix} A & B \\ B & D \end{pmatrix} = \frac{A+D}{2} \begin{pmatrix} 1 & 0 \\ 0 & 1 \end{pmatrix} + k_{ABD} \begin{pmatrix} \cos \beta & 0 \\ 0 & -\cos \beta \end{pmatrix} + k_{ABD} \begin{pmatrix} 0 & \sin \beta \\ \sin \beta & 0 \end{pmatrix}$$

$$k_{ABD} \cos \beta = \frac{A-D}{2}, \quad k_{ABD} \sin \beta = B, \quad \text{or: } \beta = \text{ATAN2}\left(B, \frac{A-D}{2}\right) \tag{10.3.11b}$$

Then tipping angle $\phi=\beta/2$ of the normal coordinate axes is found from the parameters A , B , and D .

This is a shortcut to solving \mathbf{H}^{AB} eigenvalues and eigenvectors. It generalizes to $U(2)$ "spin" in Section 10.5.

Unitary U(2) versus Special Unitary SU(2)

Before continuing, we should elaborate on some fine points and terminology. In Sec. 2.2 (d) and (e) we introduced the *unitary group* $U(n)$ of operators \mathbf{U} that satisfy *unitarity* ($\mathbf{U}^\dagger\mathbf{U}=\mathbf{1}$) and its subgroup called the *special unitary group* $SU(n)$ which had an additional requirement of *unimodularity*. ($\det|\mathbf{U}|=1$)

Note that rotational operators like $\mathbf{R}[-45^\circ]$ belong to $SU(2)$ while reflection operators like σ_{AB} belong to $U(2)$ ($\sigma^\dagger\sigma=\sigma\sigma=\mathbf{1}$) but not $SU(2)$ because σ 's have (-1) determinants. ($\det|\sigma|=-1$) Mirror reflections change left handed gloves into right handed ones. Since two reflections through the same mirror is an identity operation ($\sigma\sigma=\mathbf{1}$) it follows that reflections are both Hermitian ($\sigma^\dagger=\sigma$) and unitary ($\sigma^\dagger\sigma=\mathbf{1}$). In some sense they are the most "perfectly normal" operators.

If you multiply two members of $SU(2)$ the product has to be an $SU(2)$ member, too. (Closure axiom) So, products of rotations can never yield a reflection. However, the product of two reflections will have a positive unit determinant, in fact, it will be a rotation. This is easily see by an example that multiplies x-plane reflection σ_A in (10.2.13a) by an AB-plane or ϕ -tipped reflection σ_{AB} in (10.2.14a) .

$$\sigma[\phi \text{ tipped plane}] \cdot \sigma_A = \mathbf{R}[2\phi] \quad , \text{ or: } \sigma_A \cdot \sigma[\phi \text{ tipped plane}] = \mathbf{R}[-2\phi]$$

$$\begin{pmatrix} \cos 2\phi & \sin 2\phi \\ \sin 2\phi & -\cos 2\phi \end{pmatrix} \begin{pmatrix} 1 & 0 \\ 0 & -1 \end{pmatrix} = \begin{pmatrix} \cos 2\phi & -\sin 2\phi \\ \sin 2\phi & \cos 2\phi \end{pmatrix} \quad , \text{ or: } \begin{pmatrix} 1 & 0 \\ 0 & -1 \end{pmatrix} \begin{pmatrix} \cos 2\phi & \sin 2\phi \\ \sin 2\phi & -\cos 2\phi \end{pmatrix} = \begin{pmatrix} \cos 2\phi & \sin 2\phi \\ -\sin 2\phi & \cos 2\phi \end{pmatrix} \quad (10.3.12)$$

In other words, rotations are composed of reflections, and not vice-versa. The σ 's are more fundamental than the \mathbf{R} 's. In some sense reflections are "square roots" of rotations. One only needs half the angle $\phi=\beta/2$ to do the job that a full angle $2\phi=\beta$ rotation would need. As seen in (10.3.10) a pair of mirror planes separated by angle $\phi=\beta/2$ will perform a rotation by either β or $-\beta$, depending on the order of action.

Complete sets of commuting operators

One may turn the discussion of symmetry inside-out by asking what are all the operators \mathbf{Q} that commute with a given \mathbf{H} -matrix (or set of commuting \mathbf{H} -matrices). Spectral decomposition gives the answers to such questions, for if \mathbf{P}_k are the irreducible projectors of \mathbf{H} (or set of \mathbf{H} 's) then the answer is

$$\mathbf{Q} = \Sigma \alpha_k \mathbf{P}_k (= \alpha_1 \mathbf{P}_1 + \alpha_2 \mathbf{P}_2 \quad , \text{ for 2-by-2 } \mathbf{Q}) \quad (10.3.13a)$$

for arbitrary complex numbers α_k . If you further restrict \mathbf{Q} to be unitary (in $U(n)$) then the answer is

$$\mathbf{Q} = \Sigma e^{i\alpha_k} \mathbf{P}_k (= e^{i\alpha_1} \mathbf{P}_1 + e^{i\alpha_2} \mathbf{P}_2 \quad , \text{ for 2-by-2 } \mathbf{Q}) \quad (10.3.13b)$$

for arbitrary real numbers α_k . Finally, if you want \mathbf{Q} to be unimodular (in $SU(n)$), too, then the answer is

$$\mathbf{Q} = \Sigma e^{i\alpha_k} \mathbf{P}_k (= e^{-i\alpha} \mathbf{P}_1 + e^{i\alpha} \mathbf{P}_2 \quad \text{for 2-by-2 } \mathbf{Q}) \quad (10.3.13c)$$

where angles in exponents must sum to zero or multiples of 2π . ($\Sigma\alpha_k = 2\pi n$)

For example, the $SU(2)$ symmetry operators that commute with \mathbf{H}^B must be of the form

$$\mathbf{Q} = \frac{e^{-i\chi}}{2} \begin{pmatrix} 1 & 1 \\ 1 & 1 \end{pmatrix} + \frac{e^{i\chi}}{2} \begin{pmatrix} 1 & -1 \\ -1 & 1 \end{pmatrix} = \begin{pmatrix} \cos \chi & -i \sin \chi \\ -i \sin \chi & \cos \chi \end{pmatrix} = \mathbf{R}_B(\chi) \quad (10.3.14)$$

In other words, the only rotations that commute with \mathbf{H}^B are imaginary or complex. It turns out these are representations of Lorentz transformations that provide a relativistic theory of polarization.

10.4 Mixed ABCD Symmetry: U(2) quantum systems

With no symmetry restrictions the U(2) modes or eigenstates assume a general nondescript form of *conjugate elliptical polarization*. An example in Fig. 10.4.1 shows results of competition between all three archetypes of the *asymmetric (A)*, *bilateral (B)*, and *circular (C)* types of symmetry described previously.

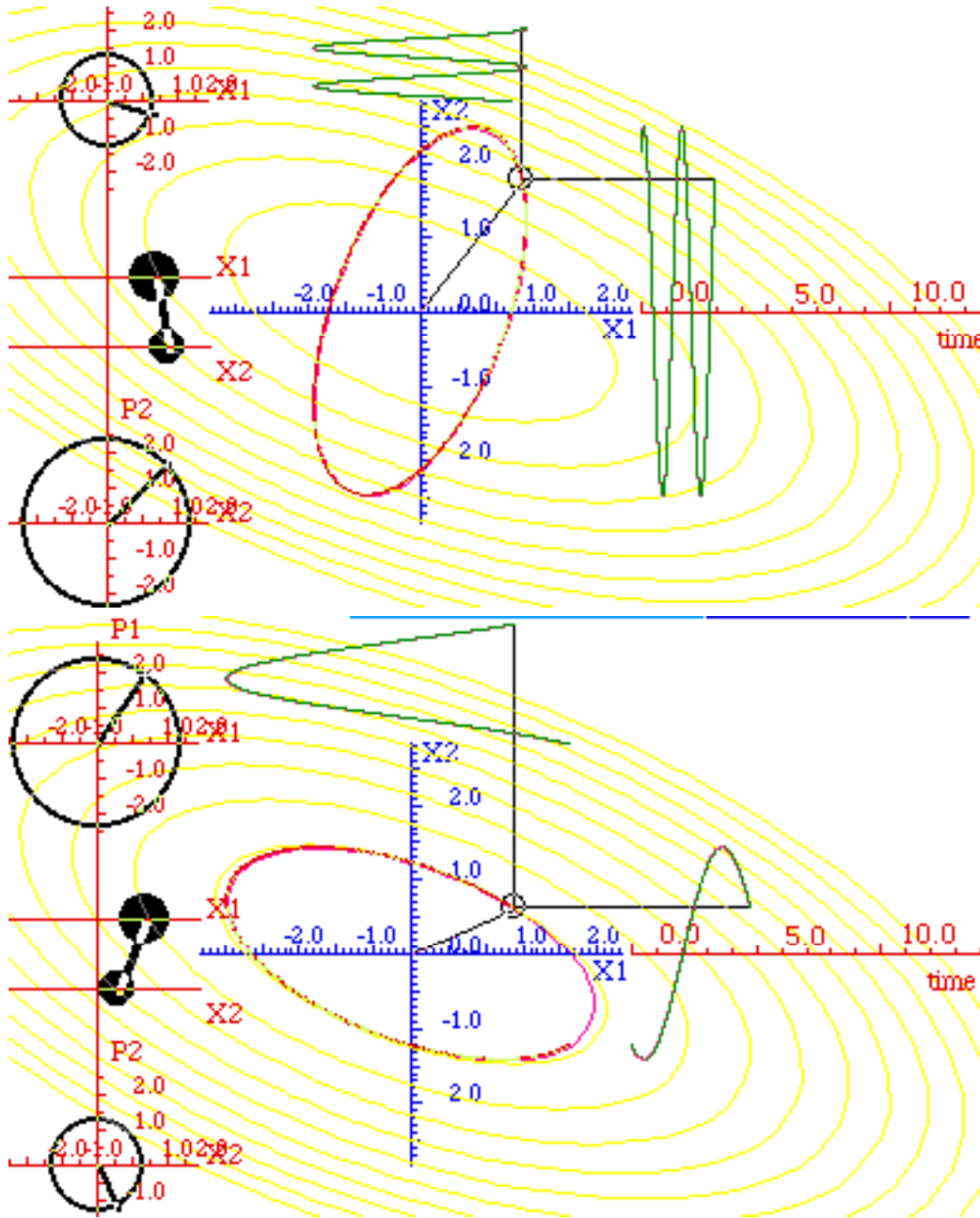


Fig.10.4.1 Typical asymmetric elliptical modes. ($A=4.1, B=0.67, C=1.16, D=3.3$)

The types of general 2-state Hamiltonian matrix 10.1.1b discussed so far have involved varying the parameters $A, B,$ and D while parameter C is set to zero. If $A=D$ then bilateral C_2^B -symmetry is present and parameter $B=-S$ determines *tunneling splitting*. If $pE=|A-D|>0$ then bilateral C_2^B -symmetry changes to C_2^{AB} -symmetry and *second order Stark splitting* occurs. If pE grows so $|A-D| \gg B$ then parameter B becomes

irrelevant and asymmetric-diagonal C_{2A} -symmetry takes effect. The parameter $pE=|A-D|$ for C_{2A} -symmetry determines *first order Stark splitting*. Adding the circular C_{2C} -symmetry makes ellipses.

(a) ABC Symmetry catalog: Standing, moving, or galloping waves

Let us review the archetypes C_{2A} , C_{2B} and $R(2) \supset C_{2C}$ symmetry using one-dimensional plane waves or Bohr orbitals (7.1.10) as the base states of a $U(2)$ two-state system, and compare that to the coupled-oscillator and optical polarization analogies. Various symmetries are summarized in Fig. 10.4.2.

A, B, and AB-Archetypes are standing waves (Linear polarization)

Asymmetric C_{2A} systems discussed in 10.2(a) have x -plane $|x_1\rangle$ and y -plane $|x_2\rangle$ modes. These are analogous to a pair of cosine and sine Bohr orbital $|c\rangle$ and $|s\rangle$ *standing waves*. The symmetry operation of reflection σ_A through $x=0$ (that is $x \rightarrow -x$) gives a positive eigenvalue (+1) for symmetric cosine function $\langle x|c\rangle$ and a negative (-1) value for anti symmetric sine wave $\langle x|s\rangle$.

$$\langle x|c\rangle = \cos mx = \cos -mx = + \langle -x|c\rangle, \quad \langle x|s\rangle = \sin mx = -\sin -mx = - \langle -x|s\rangle \quad (10.4.1a)$$

Taking $(\cos \phi, \sin \phi)$ combinations of (10.4.1a) gives states of C_{2AB} *systems* discussed in 10.2ab.

$$\begin{aligned} \langle x|+\rangle &= \cos \phi \cos mx + \sin \phi \sin mx & \langle x|-\rangle &= -\sin \phi \cos mx + \cos \phi \sin mx \\ &= \cos (mx - \phi) & &= \sin (mx - \phi) \end{aligned} \quad (10.4.1b)$$

These are *standing* waves, too. However, their nodes are shifted by angle ϕ to accommodate a new origin and symmetry plane at $x=\phi/m$. Weak D -field or strong B -coupling shifts angle toward $\phi = \pm 45^\circ$ of *bilateral symmetric C_{2B} system* coupled modes. The *decoupled* system is a C_{2A} *system* with $|x_1\rangle, |x_2\rangle$ bases. Decoupling is encouraged by applying a strong *polar vector field* like a Stark electric pE field.

C-Archetypes are moving waves (Circular polarization)

The opposite to the standing-wave systems is the *chiral or circularly symmetric $R^C(2)$ or C_∞^C system* with left handed and right handed modes $|R\rangle$ and $|L\rangle$. For the Bohr orbitals $|R\rangle$ and $|L\rangle$ correspond to positive and negative exponential *moving* waves, respectively. These involve complex combinations.

$$\langle x|R\rangle = e^{+imx} = \cos mx + i \sin mx \quad \langle x|L\rangle = e^{-imx} = \cos mx - i \sin mx \quad (10.4.2)$$

A symmetry reduction of $U(2)$ to $R^C(2)$ is caused by an *axial vector field* like a Zeeman magnetic \mathbf{B} field or a rotational velocity vector axis Ω . It is sometimes called "gauge symmetry" breaking.

....All others are galloping waves (Elliptical polarization)

The general Hamiltonian is labeled as a C_1 *system*, that is, *no symmetry*. It will have eigenstates that are general linear combination of the above, that is, elliptical polarized eigenstates like Fig. 10.4.1.

$$\langle x|\Psi\rangle = a_R \langle x|R\rangle + a_L \langle x|L\rangle = a_R e^{+imx} + a_L e^{-imx} \quad (10.4.3)$$

In other words, the vast majority of "nondescript" or asymmetric eigenstates are simply the *galloping waves* we introduced Chapter 4. (Fig. 4.2.6) The galloping phase velocity noticed there is related to the polar angle of the elliptic orbit. As the ellipse becomes more eccentric, that is, more like a standing wave states A, B , or AB , the polar angle has to gallop more and more rapidly at the passage of the minor axis. To conserve angular momentum it "gallops" faster at lesser radius and is faster at an orbital perigee than at an apogee. Newton and Kepler were first to note that Coulomb orbits sweep out equal area in equal time, but the same is true of any central force orbit including the isotropic harmonic oscillator which is a full $U(2)$ *symmetric system*. (Recall Fig. 4.2.6b and Fig. 4.2v8.)

Fighting rotational isotropy are the anisotropic (Stark-like) non-central " C_2^{AB} -symmetry-breaking forces. The A , B , or AB Hamiltonians do not conserve angular momentum and try to stretch orbits along certain directions and away from their circular $R(2)$ symmetric shape. The compromise is elliptical or galloping eigenstates such as are pictured in Fig. 10.4.1. Rotational $R(2) \supset C_2^C$ symmetry is the mortal enemy of "tensor" C_2^{AB} -symmetries, a yin-and-yang that live together as *subgroups* in the encompassing quantum operator group $U(2)$ of a 2-state system.

With isotropic $U(2)$ -symmetry all possible ellipses of any tipping or ratio or handedness are degenerate eigenstates. This is the case listed in the first column on the extreme lefthand side of Fig. 10.4.2. Then and only then do all four operators $\{\sigma_I, \sigma_A, \sigma_B, \sigma_C\}$ or all four quaternions $\{\mathbf{1}, \mathbf{i}, \mathbf{j}, \mathbf{k}\}$ or all four elementary operators $\{\mathbf{e}_{11}, \mathbf{e}_{12}, \mathbf{e}_{21}, \mathbf{e}_{22}\}$ commute with the Hamiltonian which is necessarily reduced to a constant H times a unit- $\mathbf{1}$ matrix. All vectors are eigenstates of such an operator.

$$\mathbf{H}^{U(2)} = H \mathbf{1} = H \sigma_I = H(\mathbf{e}_{11} + \mathbf{e}_{22}) \quad (10.4.4)$$

(b) General H_{ABCD} eigenvalues

The opposite extreme portrayed on the extreme right hand side of Fig. 10.4.2, is a Hamiltonian with no apparent symmetry in which all parameters A , B , C , and D are allowed.

$$\begin{aligned} \mathbf{H} &= \frac{A+D}{2} \begin{pmatrix} 1 & 0 \\ 0 & 1 \end{pmatrix} + B \begin{pmatrix} 0 & 1 \\ 1 & 0 \end{pmatrix} + C \begin{pmatrix} 0 & -i \\ i & 0 \end{pmatrix} + \frac{A-D}{2} \begin{pmatrix} 1 & 0 \\ 0 & -1 \end{pmatrix} \\ \mathbf{H} &= \frac{A+D}{2} \sigma_1 + B \sigma_B + C \sigma_C + \frac{A-D}{2} \sigma_A \end{aligned} \quad (10.4.5a)$$

Being made of all four $\{\sigma_I, \sigma_A, \sigma_B, \sigma_C\}$ guarantees \mathbf{H} will commute only with the unit operator itself. Eigenstates are determined by values of parameters A , B , C , and D . Any *single* operator of the form (10.4.5a) can be diagonalized and represented in its (own) eigen-basis as follows.

$$\begin{aligned} \mathbf{H} &= \frac{A+D}{2} \begin{pmatrix} 1 & 0 \\ 0 & 1 \end{pmatrix} + H_{ABCD} \begin{pmatrix} 1 & 0 \\ 0 & -1 \end{pmatrix} \\ \mathbf{H} &= \frac{A+D}{2} \sigma_1 + H_{ABCD} \sigma_{ABCD} \end{aligned} \quad (10.4.5b)$$

The constant H_{ABCD} is a Pythagorean sum and σ_{ABCD} is a reflection operator with (± 1) -eigenvalues.

$$\pm H_{ABCD} = \pm \sqrt{\left(\frac{A-D}{2}\right)^2 + B^2 + C^2} \quad (10.4.5c)$$

The combination operator σ_{ABCD} defined as follows

$$\sigma_{ABCD} = \frac{B}{H_{ABCD}} \sigma_B + \frac{C}{H_{ABCD}} \sigma_C + \frac{A-D}{2H_{ABCD}} \sigma_A \quad (10.4.5d)$$

is a reflection symmetry $(\sigma_{ABCD})^2 = \mathbf{1}$ because of the $\{\sigma_I, \sigma_A, \sigma_B, \sigma_C\}$ -multiplication rules.

$$\sigma_A \sigma_B = -\sigma_B \sigma_A = \sigma_C, \quad \sigma_B \sigma_C = -\sigma_C \sigma_B = \sigma_A, \quad \sigma_C \sigma_A = -\sigma_A \sigma_C = \sigma_B, \quad \sigma_A^2 = \sigma_B^2 = \sigma_C^2 = \mathbf{1} \quad (10.4.6)$$

A generalization of the AB solution (10.3.11) results. Eigenvectors are discussed in Sec. 10.5.

Catalog of Two - State Hamiltonians

$H = H^\dagger =$	$H_{U(2)} =$ $\begin{pmatrix} A & 0 \\ 0 & A \end{pmatrix}$	$H_{C_2^A} =$ $\begin{pmatrix} A & 0 \\ 0 & D \end{pmatrix}$	$H_{C_2^{AB}} =$ $\begin{pmatrix} A & B \\ B & D \end{pmatrix}$	$H_{C_2^B} =$ $\begin{pmatrix} A & B \\ B & A \end{pmatrix}$	$H_{C_2^C} =$ $\begin{pmatrix} A & -iC \\ iC & A \end{pmatrix}$	$H_{C_1} =$ $\begin{pmatrix} A & B - iC \\ B + iC & D \end{pmatrix}$
Commute with:	$U =$ $\begin{pmatrix} U_{11} & U_{12} \\ U_{21} & U_{22} \end{pmatrix}$	$R(\theta) =$ $\begin{pmatrix} e^{-i\theta} & 0 \\ 0 & e^{i\theta} \end{pmatrix}$	$R(\zeta) =$ $\begin{pmatrix} \cos \zeta & -i \sin \zeta \\ -i \sin \zeta & \cos \zeta \\ -i \sin \zeta & \cos \zeta \\ +i \sin \zeta & \cos \zeta \end{pmatrix}$	$R(\chi) =$ $\begin{pmatrix} \cos \chi & -i \sin \chi \\ -i \sin \chi & \cos \chi \end{pmatrix}$	$R(\varphi) =$ $\begin{pmatrix} \cos \varphi & -\sin \varphi \\ \sin \varphi & \cos \varphi \end{pmatrix}$	$1(\lambda) =$ $e^{i\lambda} \begin{pmatrix} 1 & 0 \\ 0 & 1 \end{pmatrix}$
Generated by:	$e_{11} = \begin{pmatrix} 1 & 0 \\ 0 & 0 \end{pmatrix}$ $e_{12} = \begin{pmatrix} 0 & 1 \\ 0 & 0 \end{pmatrix}$ $e_{21} = \begin{pmatrix} 0 & 0 \\ 1 & 0 \end{pmatrix}$ $e_{22} = \begin{pmatrix} 0 & 0 \\ 0 & 1 \end{pmatrix}$	$G_A =$ $\left. \frac{dR(\theta)}{d\theta} \right _0 =$ $\begin{pmatrix} -i & 0 \\ 0 & i \end{pmatrix}$	$G_{AB} =$ $\left. \frac{dR(\zeta)}{d\zeta} \right _0 =$ $\begin{pmatrix} -i c & -i s \\ -i s & i c \end{pmatrix}$	$G_B =$ $\left. \frac{dR(\chi)}{d\chi} \right _0 =$ $\begin{pmatrix} 0 & -i \\ -i & 0 \end{pmatrix}$	$G_C =$ $\left. \frac{dR(\varphi)}{d\varphi} \right _0 =$ $\begin{pmatrix} 0 & -1 \\ 1 & 0 \end{pmatrix}$	$G_1 =$ $\left. \frac{dR(\lambda)}{d\lambda} \right _0 =$ $\begin{pmatrix} 1 & 0 \\ 0 & 1 \end{pmatrix}$
Spin Operator:	(all)	$\sigma_A =$ $iG_A =$ $\begin{pmatrix} 1 & 0 \\ 0 & -1 \end{pmatrix}$	$\sigma_{AB} =$ $iG_{AB} =$ $\begin{pmatrix} c & s \\ s & -c \end{pmatrix}$	$\sigma_B =$ $iG_B =$ $\begin{pmatrix} 0 & 1 \\ 1 & 0 \end{pmatrix}$	$\sigma_C =$ $iG_C =$ $\begin{pmatrix} 0 & -i \\ i & 0 \end{pmatrix}$	$\sigma_0 =$ $\begin{pmatrix} 1 & 0 \\ 0 & 1 \end{pmatrix}$
Symmetry:	$U(2)$	$C_2^A \subset R^A(2)$	$C_2^{AB} \subset R^{AB}(2)$	$C_2^B \subset R^B(2)$	$C_\infty^C \subset R^C(2)$	C_1
H Eigenkets	(Any ket is an eigenvector)	$ x\rangle = \begin{pmatrix} 1 \\ 0 \end{pmatrix}, y\rangle = \begin{pmatrix} 0 \\ 1 \end{pmatrix}$	$ x'\rangle = \begin{pmatrix} \cos \frac{\beta}{2} \\ \sin \frac{\beta}{2} \end{pmatrix}, y'\rangle = \begin{pmatrix} -\sin \frac{\beta}{2} \\ \cos \frac{\beta}{2} \end{pmatrix}$	$ +\rangle = \frac{1}{\sqrt{2}} \begin{pmatrix} 1 \\ 1 \end{pmatrix}, -\rangle = \frac{1}{\sqrt{2}} \begin{pmatrix} 1 \\ -1 \end{pmatrix}$	$ L\rangle = \frac{1}{\sqrt{2}} \begin{pmatrix} 1 \\ -i \end{pmatrix}, R\rangle = \frac{1}{\sqrt{2}} \begin{pmatrix} 1 \\ i \end{pmatrix}$	$ \epsilon\rangle$ Depends on A, B, C, and D

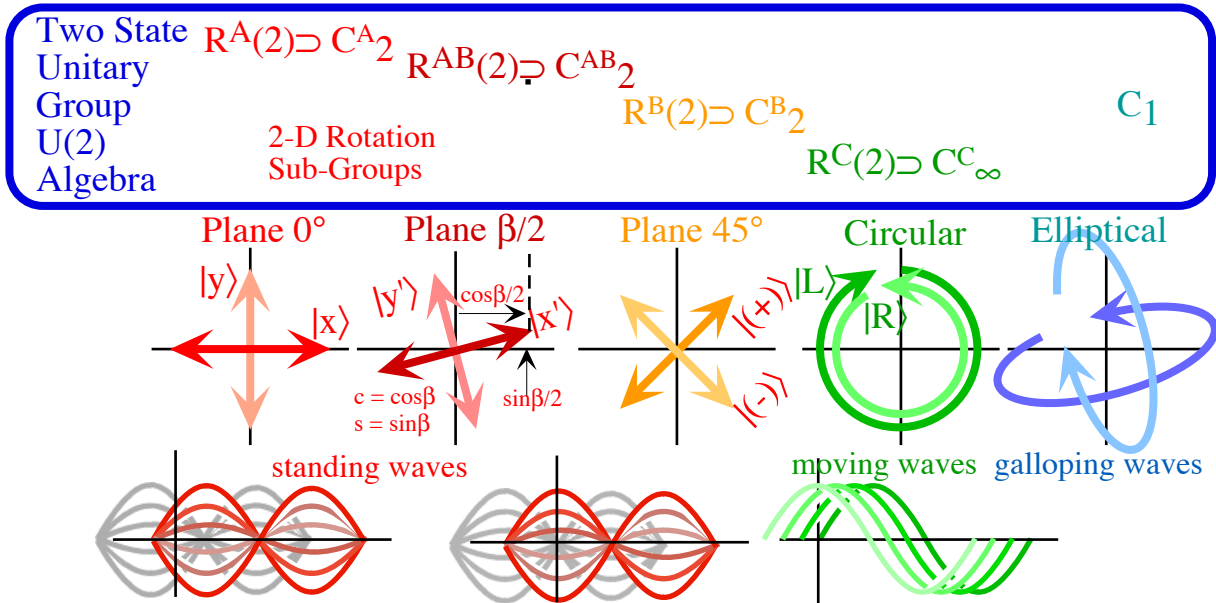
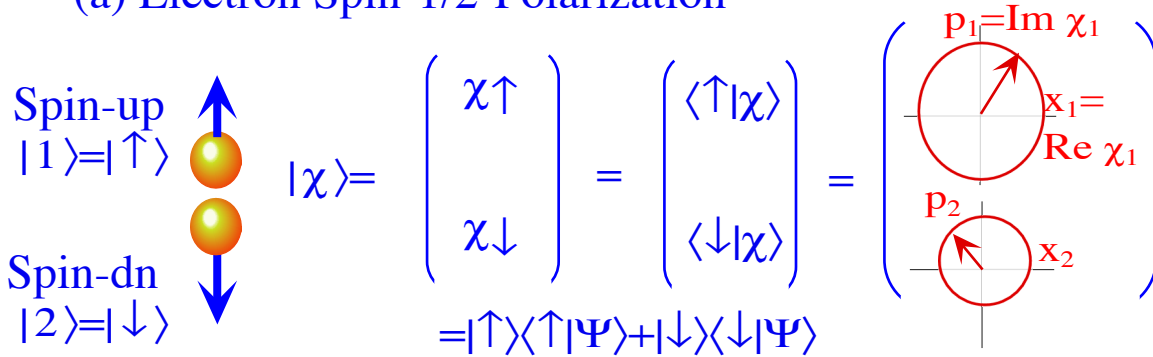


Fig. 10.4.2 Catalog of 2-state Hamiltonians, symmetry groups, eigenstates and analogs

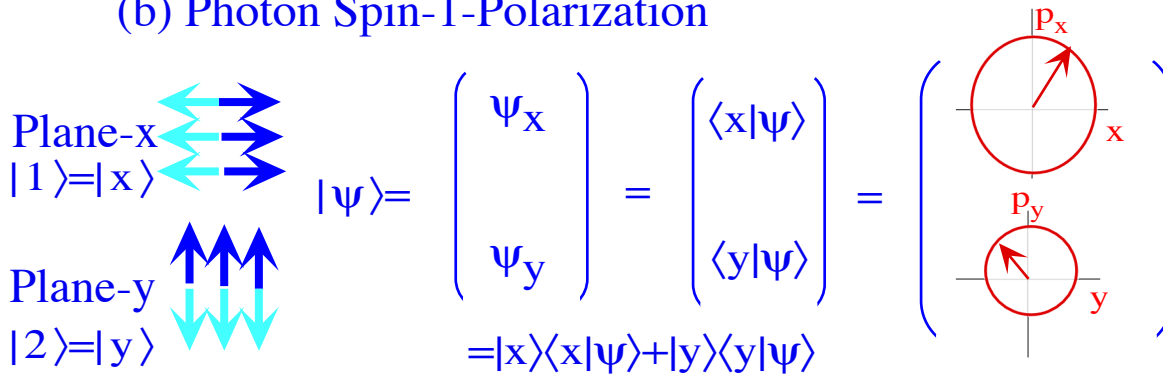
10.5 Spin-Vector Pictures for Two-State Quantum Systems

Our most common atomic "particles" are the electron with its 2-component (*up, dn*) spin- $\hbar/2$ and the photon with its two-component (*x, y*) polarization. Then there is the NH₃ inversion states (*UP, DN*) that gave us the laser revolution. These three are summarized in Fig. 10.5.1. Add to these the 2-component Bohr-waves or spins of neutrinos, neutrons, protons, quarks, etc.; it appears that our world is lousy with $U(2)$ objects! We need ways to picture them. Here we introduce another way called the *spin-vector*.

(a) Electron Spin-1/2-Polarization



(b) Photon Spin-1-Polarization



(c) Ammonia (NH₃) Inversion States

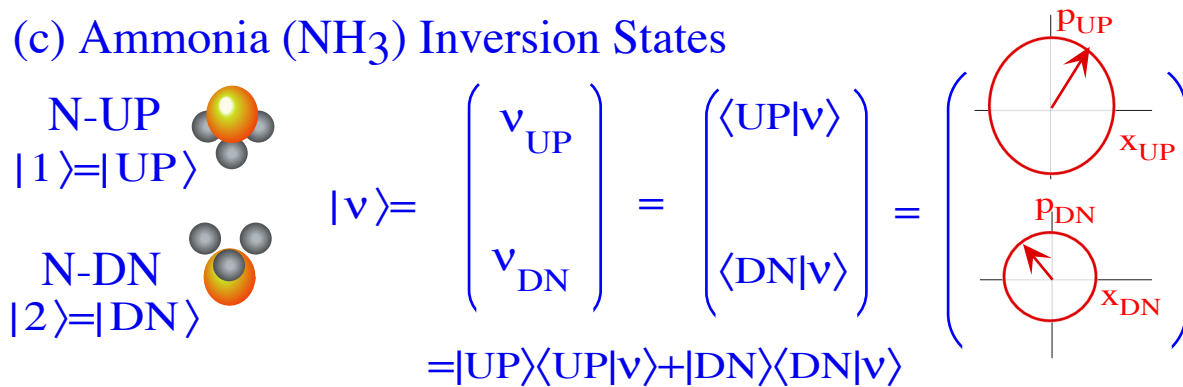


Fig. 10.5.1 Some of the most famous 2-state systems and their two-complex-component coordinates.

Ways to "picture" these $U(2)$ worlds begins with the $U(2)$ 2-phasor or spinor pictures shown in Fig. 10.5.2 (a-b). The full picture (b) is four dimensional but the polarization picture (a) takes only the real parts to make a 2D

orbit path. This was used earlier. If we can ignore overall phase, a three-dimensional $R(3)$ - $SU(2)$ spin-vector picture shown in Fig. 10.5.2(c) is sufficient and useful to define a $U(2)$ -state.

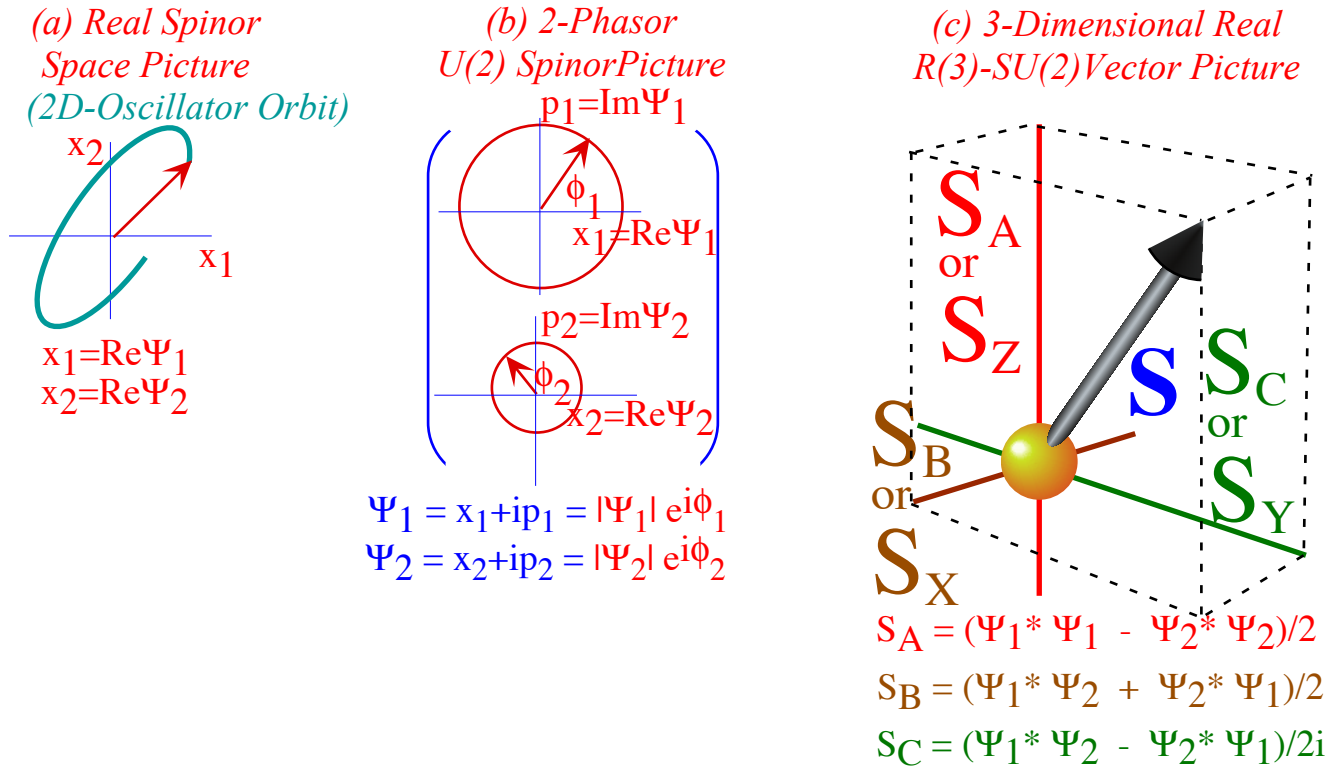


Fig. 10.5.2 Spinor, phasor, and vector descriptions of 2-state systems .

A set of four real coordinates of $U(2)$ states from (10.1.1) are listed here with phase angles (ϕ_1, ϕ_2) .

$$|\Psi\rangle = \begin{pmatrix} \Psi_1 \\ \Psi_2 \end{pmatrix} = \begin{pmatrix} \langle 1|\Psi\rangle \\ \langle 2|\Psi\rangle \end{pmatrix} = \begin{pmatrix} x_1 + ip_1 \\ x_2 + ip_2 \end{pmatrix} = \begin{pmatrix} |\Psi_1| e^{i\phi_1} \\ |\Psi_2| e^{i\phi_2} \end{pmatrix}, \text{ where: } \begin{matrix} x_1 = \text{Re}\Psi_1, \text{ and: } p_1 = \text{Im}\Psi_1 \\ x_2 = \text{Re}\Psi_2, \text{ and: } p_2 = \text{Im}\Psi_2 \end{matrix} \quad (10.5.1a)$$

Overall-phase-independent quantities $\Psi_m^* \Psi_n$ define the following three spin-vector coordinates.

$$\begin{aligned}
 S_Z = S_A &= \frac{1}{2}(\Psi_1^* \Psi_1 - \Psi_2^* \Psi_2) = \frac{1}{2}(|\Psi_1|^2 - |\Psi_2|^2) \\
 S_X = S_B &= \frac{1}{2}(\Psi_1^* \Psi_2 + \Psi_2^* \Psi_1) = \text{Re}\Psi_1^* \Psi_2 = |\Psi_1||\Psi_2| \cos(\phi_2 - \phi_1) \\
 S_Y = S_C &= \frac{1}{2i}(\Psi_1^* \Psi_2 - \Psi_2^* \Psi_1) = \text{Im}\Psi_1^* \Psi_2 = |\Psi_1||\Psi_2| \sin(\phi_2 - \phi_1)
 \end{aligned} \quad (10.5.1b)$$

(a) Density operators and Pauli σ -operators

The $\Psi_m^* \Psi_n$ quantities from which a spin-vector is built, are components of a very useful operator called the *density operator* $\rho = |\Psi\rangle\langle\Psi|$, first employed by U. Fano. ρ is defined as an outer (tensor \otimes) product of ket-bras as are projection operators in (2.1.19) but it's for a general state $|\Psi\rangle$, not just a base state $|1\rangle$ or $|2\rangle$.

$$\rho = |\Psi\rangle\langle\Psi| = \begin{pmatrix} \Psi_1 \\ \Psi_2 \end{pmatrix} \otimes \begin{pmatrix} \Psi_1^* & \Psi_2^* \end{pmatrix} = \begin{pmatrix} \Psi_1 \Psi_1^* & \Psi_1 \Psi_2^* \\ \Psi_2 \Psi_1^* & \Psi_2 \Psi_2^* \end{pmatrix} \quad (10.5.2)$$

We have three spin-vector components ($S_X = S_B$, $S_Y = S_C$, $S_Z = S_A$) and a fourth quantity, the norm N

$$N = \Psi_1^* \Psi_1 + \Psi_2^* \Psi_2 \quad (10.5.3)$$

(Norm or total probability must be unity ($N=1$) for base states but may be less than 1 for general states.) the density matrix components can be inverted from (10.5.1) to give

$$\begin{aligned} \rho_{11} &= \Psi_1^* \Psi_1 = \frac{1}{2}N + S_Z, & \rho_{12} &= \Psi_2^* \Psi_1 = S_X - iS_Y, \\ \rho_{21} &= \Psi_1^* \Psi_2 = S_X + iS_Y, & \rho_{22} &= \Psi_2^* \Psi_2 = \frac{1}{2}N - S_Z. \end{aligned} \quad (10.5.4)$$

Density operator $\rho = |\Psi\rangle\langle\Psi|$ becomes the following.

$$\begin{aligned} \begin{pmatrix} \rho_{11} & \rho_{12} \\ \rho_{21} & \rho_{22} \end{pmatrix} &= \begin{pmatrix} \Psi_1^* \Psi_1 & \Psi_2^* \Psi_1 \\ \Psi_1^* \Psi_2 & \Psi_2^* \Psi_2 \end{pmatrix} = \begin{pmatrix} \frac{1}{2}N + S_Z & S_X - iS_Y \\ S_X + iS_Y & \frac{1}{2}N - S_Z \end{pmatrix} \\ &= \frac{1}{2}N \begin{pmatrix} 1 & 0 \\ 0 & 1 \end{pmatrix} + S_X \begin{pmatrix} 0 & 1 \\ 1 & 0 \end{pmatrix} + S_Y \begin{pmatrix} 0 & -i \\ i & 0 \end{pmatrix} + S_Z \begin{pmatrix} 1 & 0 \\ 0 & -1 \end{pmatrix} \\ \rho &= \frac{1}{2}N \mathbf{1} + S_X \sigma_X + S_Y \sigma_Y + S_Z \sigma_Z \end{aligned} \quad (10.5.5a)$$

where the σ matrices are known as the *Pauli spin(or) operator matrices*.

$$\mathbf{1} = \begin{pmatrix} 1 & 0 \\ 0 & 1 \end{pmatrix}, \quad \sigma_X = \begin{pmatrix} 0 & 1 \\ 1 & 0 \end{pmatrix}, \quad \sigma_Y = \begin{pmatrix} 0 & -i \\ i & 0 \end{pmatrix}, \quad \sigma_Z = \begin{pmatrix} 1 & 0 \\ 0 & -1 \end{pmatrix}_A \quad (10.5.5b)$$

These are the spin generators σ_0 , σ_B , σ_C , and σ_A listed in Fig. 10.4.2 catalog of 2-state Hamiltonians and symmetry. This is no accident; these operators are all set up to do an elegant job of completely solving the 2-state Schrodinger problem and quite a bit more. We saw some of this in equation (10.4.5).

Furthermore, the ρ -operator lets us treat *statistical ensembles* of possibly dephased particles that suffer "peeking" or other randomizing effects as in Sec. 1.3b. For *pure-state* beams, each of N particles contributes a spin- $1/2$ so the total *expected spin magnitude* S exactly equals half-norm $N/2$ where

$$S = \sqrt{S_X^2 + S_Y^2 + S_Z^2} = \sqrt{S_B^2 + S_C^2 + S_A^2} \quad (10.5.6)$$

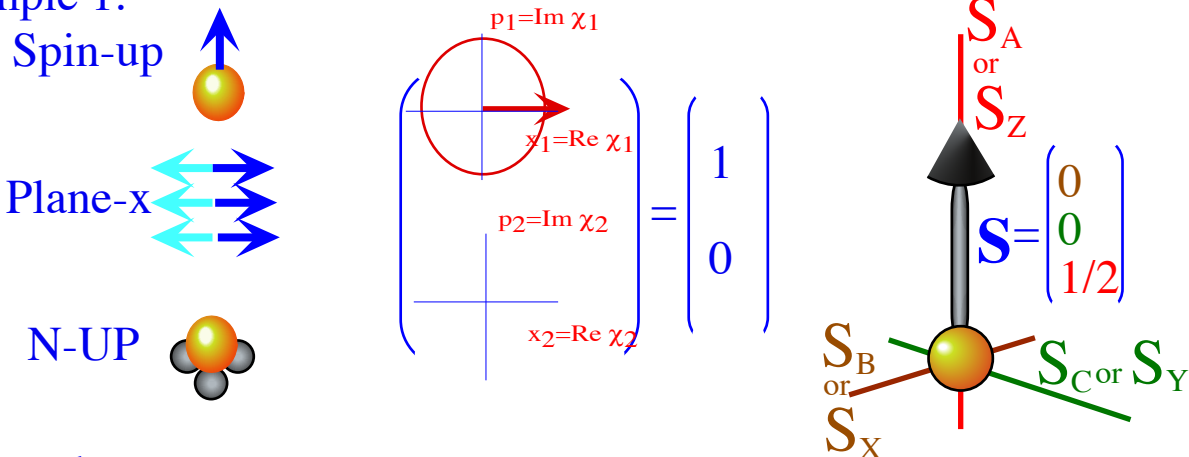
Beams with $S < N/2$ are known as *depolarized* or "dirty" beams, and $S=0$ corresponds to *completely depolarized* (or "filthy"-random) beams. Pure-state ($S=N/2$) beams are also called *100%-polarized*.

Before, beginning ρ -analysis, let us explore some of the possible states in various $U(2)$ worlds. Fig. 10.5.3 below shows the \mathbf{S} -vectors for our most commonly used base states. Examples 1 and 2 belong to the spin-up or dn ($|\uparrow\rangle$, $|\downarrow\rangle$), or x -or- y -polarization ($|x\rangle$, $|y\rangle$), or NH_3 base states ($|UP\rangle$, $|DN\rangle$). Spin vector \mathbf{S} is,

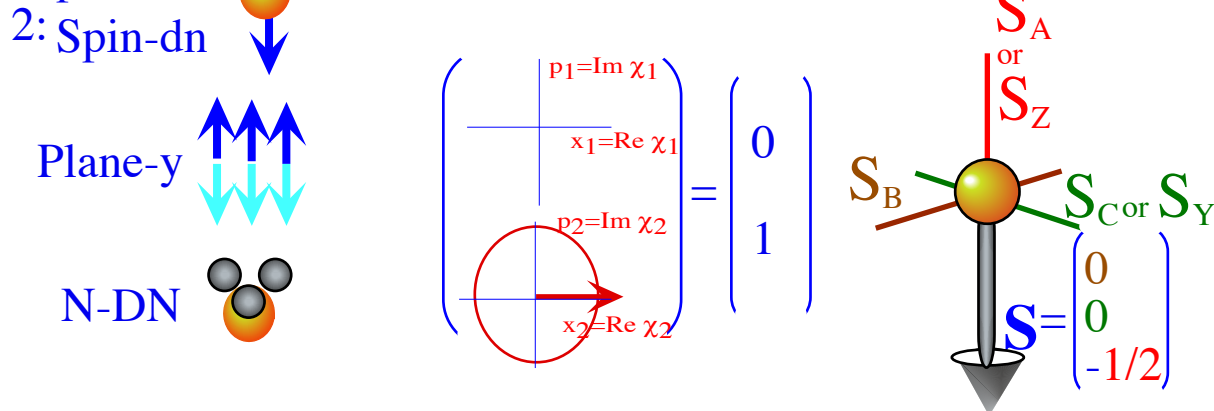
indeed, up or down, in Example 1 or 2, that is $\pm 180^\circ$, while in real spinor space $|\uparrow\rangle$ and $|\downarrow\rangle$ bases are 90° apart.

Recall 2:1 ratio between $R(3)$ and $U(2)$ angles first noted in (1.2.13).

Example 1:



Example 2:



Example 3:

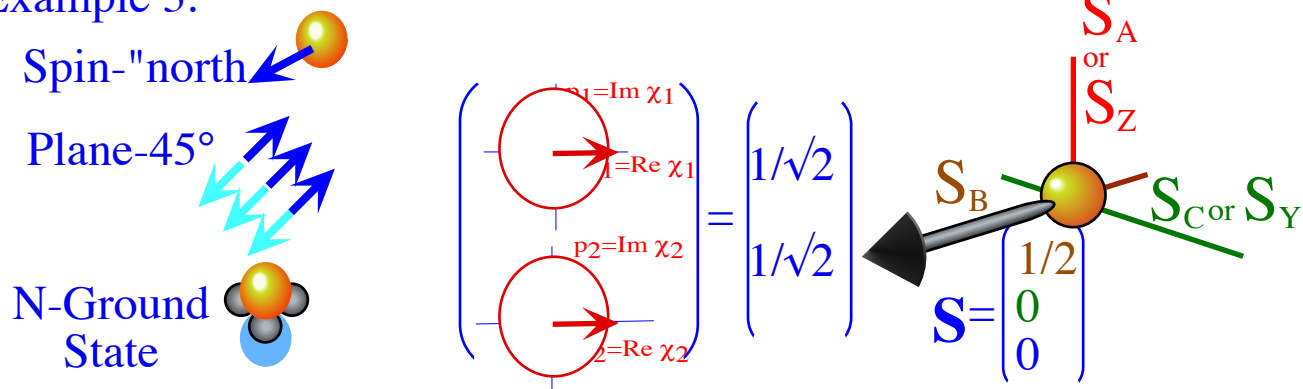


Fig. 10.5.3 Examples of spinor, phasor, and vector base states for electron, photon, or NH₃.

Example 3 is an eigenstate of bilateral C_2^B -symmetric Hamiltonian

$$\mathbf{H}_{C_2^B} = \begin{pmatrix} A & B \\ B & A \end{pmatrix} \tag{10.2.4a} \text{repeated}$$

such as the $\pm 45^\circ$ normal modes $|(+)\rangle$ and $|(-)\rangle$ shown previously in Fig. 10.2.4 or NH₃ ground and excited states shown in Fig. 10.3.2b. The C_2^B -type S-eigenvectors lie on the bilateral B-axis.

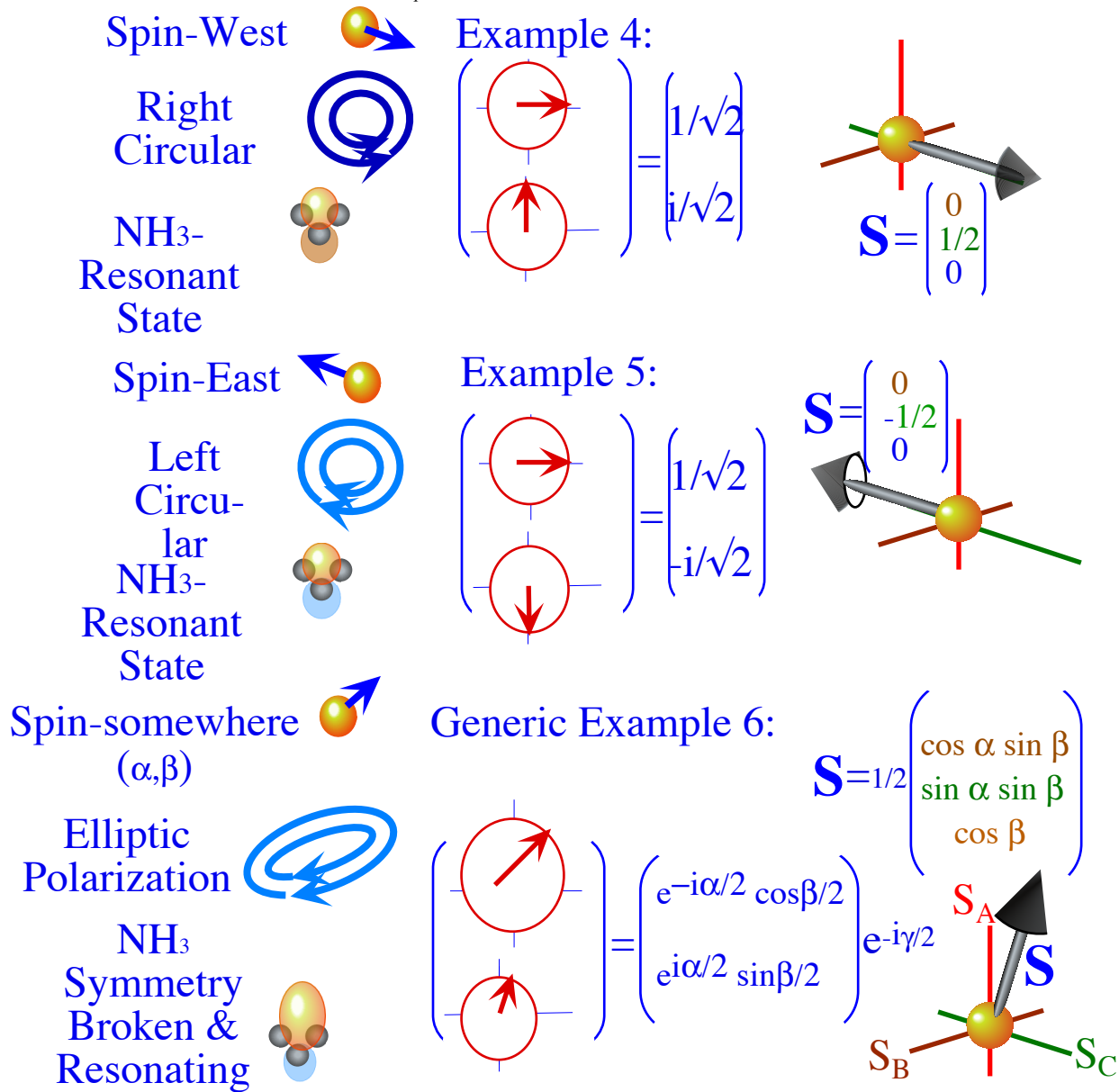


Fig. 10.5.4 Other spinor, phasor, and vector base states for electron, photon, or NH₃.

Examples 4 and 5 shown in Fig. 10.5.4 are eigenstates of circular C₂^C-symmetric Hamiltonians

$$H_{C_2^C} = \begin{pmatrix} A & -iC \\ iC & A \end{pmatrix} \quad (10.2.19d)_{repeated}$$

such as the left and right-circular-polarization eigenstates $|L\rangle$ and $|R\rangle$ shown in Fig. 10.2.7. The \mathbf{S} -vectors for the circular eigenbasis are "East" and "West" respectively, that is, along the circular C-axis. $|L\rangle$ and $|R\rangle$ are resonant "beat" modes or *transition states* for the NH₃ model. Recall how the beat in Fig. 10.2.6 briefly has two phasors; one "donor" phasor 90° ahead of a "receiver" phasor to give $|L\rangle$ -circular polarization like a 1/4-wave plate. State $|L\rangle$ corresponds to NH₃ actually undergoing an inversion. In example 4, the N-atom probability is moving down (because UP-phasor is ahead of DN), but in Example 5 the N-atom is moving up since the UP-phasor is behind that of DN. Recall phase principle stated after (10.2.16).

Finally, note that Examples 1 and 2 belong to *eigenbasis* of basic C₂^A-symmetric Hamiltonians

$$\mathbf{H}_{c_2^A} = \begin{pmatrix} A & 0 \\ 0 & D \end{pmatrix} \quad (10.2.2h) \text{repeated}$$

which have no off-diagonal coupling components of either the bilateral (*B*) or circular (*C*) types. Their **S**-vectors must lie "up" and "down" along the *A*-axis as shown in Fig. 10.5.3. At the other extreme are the vast majority of generic Hamiltonians with generic eigenstates like the one sketched in Example 6 of Fig. 10.5.4. For a generic state it is convenient to introduce *Euler phase-angle coordinates* (α, β, γ) along with a *norm* *N*.

$$|\Psi\rangle = \begin{pmatrix} \Psi_1 \\ \Psi_2 \end{pmatrix} = \begin{pmatrix} \langle 1|\Psi\rangle \\ \langle 2|\Psi\rangle \end{pmatrix} = \begin{pmatrix} x_1 + ip_1 \\ x_2 + ip_2 \end{pmatrix} = \sqrt{N} \begin{pmatrix} e^{-i\alpha/2} \cos \frac{\beta}{2} \\ e^{i\alpha/2} \sin \frac{\beta}{2} \end{pmatrix} e^{-i\gamma/2} \quad (10.5.8a)$$

From (10.5.1) this gives a length- $S=N/2$ spin **S**-vector with polar angles (α, β) in *ABC*-space!

$$\begin{aligned} S_Z = S_A &= \frac{1}{2} (|\Psi_1|^2 - |\Psi_2|^2) = \frac{N}{2} \left(\cos^2 \frac{\beta}{2} - \sin^2 \frac{\beta}{2} \right) = \frac{N}{2} \cos \beta \\ S_X = S_B &= \text{Re } \Psi_1^* \Psi_2 = N \cos \alpha \cos \frac{\beta}{2} \sin \frac{\beta}{2} = \frac{N}{2} \cos \alpha \sin \beta \\ S_Y = S_C &= \text{Im } \Psi_1^* \Psi_2 = N \sin \alpha \cos \frac{\beta}{2} \sin \frac{\beta}{2} = \frac{N}{2} \sin \alpha \sin \beta \end{aligned} \quad (10.5.8b)$$

Spin **S**-vector components are *one-half* the Pauli *spinor operator expectation values* $\langle \Psi | \sigma_{\mu} | \Psi \rangle$.

$$\begin{aligned} \langle \Psi | \sigma_Z | \Psi \rangle &= 2S_A = \begin{pmatrix} \Psi_1^* & \Psi_2^* \end{pmatrix} \begin{pmatrix} 1 & 0 \\ 0 & -1 \end{pmatrix} \begin{pmatrix} \Psi_1 \\ \Psi_2 \end{pmatrix} = N \cos \beta = N(p_1^2 + x_1^2 - p_2^2 - x_2^2) \\ \langle \Psi | \sigma_X | \Psi \rangle &= 2S_B = \begin{pmatrix} \Psi_1^* & \Psi_2^* \end{pmatrix} \begin{pmatrix} 0 & 1 \\ 1 & 0 \end{pmatrix} \begin{pmatrix} \Psi_1 \\ \Psi_2 \end{pmatrix} = N \cos \alpha \sin \beta = 2N(x_1 x_2 + p_1 p_2) \\ \langle \Psi | \sigma_Y | \Psi \rangle &= 2S_C = \begin{pmatrix} \Psi_1^* & \Psi_2^* \end{pmatrix} \begin{pmatrix} 0 & -i \\ i & 0 \end{pmatrix} \begin{pmatrix} \Psi_1 \\ \Psi_2 \end{pmatrix} = N \sin \alpha \sin \beta = 2N(x_1 p_2 - x_2 p_1) \end{aligned} \quad (10.5.8c)$$

For 2-state systems, like the electron or photon, which actually carry real-live-spin-angular momentum we need to introduce *Jordan spin operators* $\mathbf{J} = \mathbf{S} = (1/2)\sigma$ that are 1/2 of Pauli's "quasi-spin" σ -operators. Note that the *Y*-or *C*-component $J_C = S_C$ is precisely the angular momentum $xp_y - yp_x$ of an orbit in the mechanical analogy involving 2-dimensional oscillators.

$$\langle \Psi | \mathbf{J}_Y | \Psi \rangle = \langle \Psi | \mathbf{J}_C | \Psi \rangle = \langle \Psi | \mathbf{S}_C | \Psi \rangle = 2 \langle \Psi | \sigma_C | \Psi \rangle = N(xp_y - yp_x) \quad (10.5.9)$$

This is analogous to *photon-spin momentum*. Circularly polarized photons hitting make you twist!

(b) Hamiltonian operators and Pauli-Jordan spin operators ($\mathbf{J}=\mathbf{S}$)

Symmetry and operator analysis solves the generic asymmetric Hamiltonian (10.1.1). The trick is to expand **H** in terms of the spinor σ -operators as was done for the state density ρ -operator in (10.5.5a). Instead, we use Jordan's $\mathbf{J} = (1/2)\sigma$ operators so as to respect that spin-1/2 factor.

$$\mathbf{J}_B = \mathbf{S}_B = (1/2)\sigma_B = (1/2)\sigma_X, \quad \mathbf{J}_C = \mathbf{S}_C = (1/2)\sigma_C = (1/2)\sigma_Y, \quad \mathbf{J}_A = \mathbf{S}_A = (1/2)\sigma_A = (1/2)\sigma_Z$$

The resulting generic **H** Hamiltonian operator expansion is here.

$$\begin{pmatrix} H_{11} & H_{12} \\ H_{21} & H_{22} \end{pmatrix} = \begin{pmatrix} \langle 1|\mathbf{H}|1\rangle & \langle 1|\mathbf{H}|2\rangle \\ \langle 2|\mathbf{H}|1\rangle & \langle 2|\mathbf{H}|2\rangle \end{pmatrix} = \hbar \begin{pmatrix} A & B-iC \\ B+iC & D \end{pmatrix}$$

$$\mathbf{H}/\hbar = \frac{1}{2}(A+D) \begin{pmatrix} 1 & 0 \\ 0 & 1 \end{pmatrix} + 2B \begin{pmatrix} 0 & 1 \\ 1 & 0 \end{pmatrix} \frac{1}{2} + 2C \begin{pmatrix} 0 & -i \\ i & 0 \end{pmatrix} \frac{1}{2} + (A-D) \begin{pmatrix} 1 & 0 \\ 0 & -1 \end{pmatrix} \frac{1}{2} \quad (10.5.10a)$$

$$\mathbf{H}/\hbar = \frac{1}{2}(A+D) \mathbf{1} + 2B \mathbf{S}_X + 2C \mathbf{S}_Y + (A-D) \mathbf{S}_Z$$

$$\mathbf{H}/\hbar = \frac{1}{2}(A+D) \sigma_0 + 2B \mathbf{S}_B + 2C \mathbf{S}_C + (A-D) \mathbf{S}_A$$

The three constants (2B, 2C, A-D) multiplying the respective (σ_X, σ_Y, σ_Z) = (σ_B, σ_C, σ_A) operators are components of what is called the *Hamiltonian Ω-cranking vector*

$$\mathbf{\Omega} = (\Omega_X, \Omega_Y, \Omega_Z) = (2B, 2C, A-D) = (\Omega_B, \Omega_C, \Omega_A) \quad (10.5.10b)$$

while the coefficient (A+D)/2 of the unit operator σ₀ is just the average overall phase rate or energy ε/ħ.

$$\Omega_0 = (A+D)/2 \quad (10.5.10c)$$

The Hamiltonian expression involves an *operator scalar product* Ω•S = Ω•σ/2.

$$\mathbf{H} = \hbar\Omega_0 \mathbf{s}_0 + \hbar\mathbf{\Omega} \cdot \mathbf{\bar{S}} = \hbar\Omega_0 \mathbf{1} + \hbar\mathbf{\Omega} \cdot \mathbf{\bar{S}} \quad (10.5.10d)$$

Here Ω is an ordinary 3-vector made of three numerical components Ω_X, Ω_Y, and Ω_Z, but S is an *operator 3-vector* made of three Jordan-Pauli spin operators S_X = (1/2)σ_X, S_Y = (1/2)σ_Y, and S_Z = (1/2)σ_Z.

Each of the B, C, or A type H-matrices (10.5.7 A-C) has its Ω-vector pointing along the B, C, or A axis, respectively, precisely the direction of the S-vector for H-eigenstates in each case. This lining up of S and Ω is particularly useful since it's true for the generic H-matrices, too. S-vectors of all H-eigenstates must lie along (or against) its Hamiltonian Ω-vector.

Bingo! The Hamiltonian Ω-vector completely determines the observable dynamics of all states, not just H-eigenstates. The result is a closed-form analytic and pictorial solution of all possible eigenvectors and dynamics, that is, all possible states of all possible U(2) Hamiltonians! The first result is frequency

$$|\Omega| = \sqrt{\Omega_X^2 + \Omega_Y^2 + \Omega_Z^2} = \sqrt{(2B)^2 + (2C)^2 + (A-D)^2} \quad (10.5.10e)$$

which is the beat-transition frequency difference between ABCD eigenlevels of (10.4.5). (That factor of 1/2 in defining spin S is key to getting the right Ω-cranking rate or *beat frequency* Ω = ω_{hi} - ω_{lo}.)

(c) Bloch equations and spin precession

The notion of cranking or precession of a gyroscope is an old classical one. Here it is appearing in a purely quantum mechanical context and applies to all the Schrodinger 2-state dynamics described so far.

Precession arises from the density operator ρ by writing the Schrodinger equation backwards and forwards in time, that is, as a ket equation (forwards) and as a "dagged" bra-equation (backwards).

$$i\hbar|\dot{\Psi}\rangle = \mathbf{H}|\Psi\rangle, \quad \Leftarrow \text{Dagger} \Rightarrow -i\hbar\langle\dot{\Psi}| = \langle\Psi|\mathbf{H} \quad (10.5.11)$$

Note: H[†] = H. Combining these gives a time derivative of the density operator ρ = |Ψ⟩⟨Ψ|

$$i\hbar \frac{\partial}{\partial t} \rho = i\hbar \dot{\rho} = i\hbar|\dot{\Psi}\rangle\langle\Psi| + i\hbar|\Psi\rangle\langle\dot{\Psi}| = \mathbf{H}|\Psi\rangle\langle\Psi| - |\Psi\rangle\langle\Psi|\mathbf{H} \quad (10.5.12a)$$

The result is called a *Bloch equation*. This is the "professional" version of the Schrodinger equation.

$$i\hbar \frac{\partial}{\partial t} \mathbf{p} = i\hbar \dot{\mathbf{p}} = \mathbf{H}\mathbf{p} - \mathbf{p}\mathbf{H} = [\mathbf{H}, \mathbf{p}] \quad (10.5.12b)$$

Then we write \mathbf{p} and \mathbf{H} in terms spin \mathbf{S} -vector and crank $\mathbf{\Omega}$ -vector by (10.5.5) and (10.5.10), respectively.

$$\begin{aligned} \mathbf{H}\mathbf{p} &= \left(\hbar\Omega_0 \mathbf{1} + \frac{\hbar}{2} \mathbf{\Omega} \cdot \boldsymbol{\sigma} \right) \left(\frac{N}{2} \mathbf{1} + \mathbf{S} \cdot \boldsymbol{\sigma} \right) = \hbar\Omega_0 \frac{N}{2} \mathbf{1} + \frac{N}{4} \hbar \mathbf{\Omega} \cdot \boldsymbol{\sigma} + \hbar\Omega_0 \mathbf{S} \cdot \boldsymbol{\sigma} + \frac{\hbar}{2} (\mathbf{\Omega} \cdot \boldsymbol{\sigma})(\mathbf{S} \cdot \boldsymbol{\sigma}) \\ \mathbf{p}\mathbf{H} &= \left(\frac{N}{2} \mathbf{1} + \mathbf{S} \cdot \boldsymbol{\sigma} \right) \left(\hbar\Omega_0 \mathbf{1} + \frac{\hbar}{2} \mathbf{\Omega} \cdot \boldsymbol{\sigma} \right) = \hbar\Omega_0 \frac{N}{2} \mathbf{1} + \frac{N}{4} \hbar \mathbf{\Omega} \cdot \boldsymbol{\sigma} + \hbar\Omega_0 \mathbf{S} \cdot \boldsymbol{\sigma} + \frac{\hbar}{2} (\mathbf{S} \cdot \boldsymbol{\sigma})(\mathbf{\Omega} \cdot \boldsymbol{\sigma}) \end{aligned}$$

Only the last terms don't cancel, and then only if the spin \mathbf{S} and crank $\mathbf{\Omega}$ *point in different directions*.

$$\mathbf{H}\mathbf{p} - \mathbf{p}\mathbf{H} = \frac{\hbar}{2} (\mathbf{\Omega} \cdot \boldsymbol{\sigma})(\mathbf{S} \cdot \boldsymbol{\sigma}) - \frac{\hbar}{2} (\mathbf{S} \cdot \boldsymbol{\sigma})(\mathbf{\Omega} \cdot \boldsymbol{\sigma})$$

To finish this we need to derive the *Pauli-Hamilton identity*. This uses $\boldsymbol{\sigma}$ -multiplication rules (10.4.6).

$$\begin{aligned} (\mathbf{A} \cdot \boldsymbol{\sigma})(\mathbf{B} \cdot \boldsymbol{\sigma}) &= A_\alpha B_\beta \sigma_\alpha \sigma_\beta = A_\alpha B_\beta (\delta_{\alpha\beta} + i\varepsilon_{\alpha\beta\gamma} \sigma_\gamma) \\ &= A_\alpha B_\alpha + i\varepsilon_{\alpha\beta\gamma} A_\alpha B_\beta \sigma_\gamma \\ &= \mathbf{A} \cdot \mathbf{B} + i(\mathbf{A} \times \mathbf{B}) \cdot \boldsymbol{\sigma} \end{aligned} \quad (10.5.13)$$

So finally the time dynamics is reduced to the following.

$$\begin{aligned} i\hbar \frac{\partial}{\partial t} \mathbf{p} = i\hbar \dot{\mathbf{p}} &= \frac{i\hbar}{2} (\mathbf{\Omega} \times \mathbf{S}) \cdot \boldsymbol{\sigma} - \frac{i\hbar}{2} (\mathbf{S} \times \mathbf{\Omega}) \cdot \boldsymbol{\sigma} \\ i\hbar \frac{\partial}{\partial t} \left(\frac{N}{2} \mathbf{1} + \mathbf{S} \cdot \boldsymbol{\sigma} \right) &= i\hbar \dot{\mathbf{S}} \cdot \boldsymbol{\sigma} = i\hbar (\mathbf{\Omega} \times \mathbf{S}) \cdot \boldsymbol{\sigma} \end{aligned}$$

Factoring out $\boldsymbol{\sigma}$ gives a *gyroscopic precession equation*.

$$\frac{\partial \mathbf{S}}{\partial t} = \dot{\mathbf{S}} = \mathbf{\Omega} \times \mathbf{S} \quad (10.5.14)$$

Perhaps, the Fig. 1.2.4 sketch of “helicopter” electrons in Stern-Gerlach analyzers is not so silly after all!

Magnetic spin precession (ESR, NMR,..)

Indeed, the classical Hamiltonian for a magnetic moment \mathbf{m} in a magnetic \mathbf{B} -field is $H = -\mathbf{m} \cdot \mathbf{B}$. If the particle's magnetic moment is proportional to its spin angular momentum

$$\mathbf{m} = g \mathbf{S} \quad (10.5.15a)$$

where g is called a *gyromagnetic ratio* then the Hamiltonian can be written

$$H = -\mathbf{m} \cdot \mathbf{B} = -g \mathbf{S} \cdot \mathbf{B} = -g (B_x S_x + B_y S_y + B_z S_z) \quad (10.5.15b)$$

Replacing each classical spin component S_μ by a spin operator $\hbar \mathbf{S}_\mu$ gives the quantum Hamiltonian.

$$\mathbf{H} = -g \mathbf{S} \cdot \mathbf{B} = -g \hbar (B_x \mathbf{S}_x + B_y \mathbf{S}_y + B_z \mathbf{S}_z) \quad (10.5.15c)$$

The matrix representation of this has the $\mathbf{\Omega} \cdot \mathbf{S}$ form of the generic $U(2)$ Hamiltonian (10.5.10).

$$\begin{aligned} \mathbf{H} = -g\hbar \mathbf{B} \cdot \mathbf{S} &= \frac{g\hbar}{2} \left[B_x \begin{pmatrix} 0 & 1 \\ 1 & 0 \end{pmatrix} + B_y \begin{pmatrix} 0 & -i \\ i & 0 \end{pmatrix} + B_z \begin{pmatrix} 1 & 0 \\ 0 & -1 \end{pmatrix} \right] \\ &= \frac{g\hbar}{2} \begin{pmatrix} B_z & B_x - iB_y \\ B_x + iB_y & -B_z \end{pmatrix} \end{aligned} \quad (10.5.16a)$$

The $\mathbf{\Omega}$ -crank is the $g\hbar \mathbf{B}/2$ -field vector! It will make the spin \mathbf{S} -vector precess around $\mathbf{\Omega}$ at a rate given by the *magnetic resonance frequency* $\mathbf{\Omega}$.

$$\mathbf{\Omega} = g|\mathbf{B}|\hbar/2 \quad (10.5.16b)$$

In other words, if you have seen one $U(2)$ Hamiltonian, you have seen them all! They are basically all the same no matter whether it describes nuclear magnetic resonance (NMR), electron spin resonance (ESR), muon spin resonance (MSR), and so forth, as long there are just two base states. The difference lies in how we set the parameters $B_x, B_y,$ and B_z or, for our generic \mathbf{H} matrix, the parameters $2B, 2C,$ and $(A-D)$. Finally (and most important!) we need to understand how parameters may be varied with time to cause a desired resonance.

(d) Visualizing quantum dynamics as S-precession

Perhaps, the greatest advantage of the 3-space spin vector rotational formulation is its power of visualization. Let us return to the earlier 2-state models and analogies to see this. We begin with the bilateral B -type Hamiltonian (Sec. 10.2(b)) of NH_3 and our coupled pendulum analogy. This will then be compared with the C -type Zeeman-like Hamiltonians of Sec. 10.2(c). Then we see how this changes to the basic A -type problem via the "avoided-crossing" Stark-like AB -types discussed in Sec. 10.3(a). The B -type Hamiltonian

$$\begin{pmatrix} \langle 1|\mathbf{H}|1\rangle & \langle 1|\mathbf{H}|2\rangle \\ \langle 2|\mathbf{H}|1\rangle & \langle 2|\mathbf{H}|2\rangle \end{pmatrix} = \begin{pmatrix} A & B \\ B & A \end{pmatrix} \tag{10.2.4a} \text{repeated}$$

has a cranking Ω -vector on the X or B -axis of the spin 3-vector space according to (10.5.10b).

$$\Omega = (\Omega_X, \Omega_Y, \Omega_Z) = (2B, 0, 0) = (\Omega_B, \Omega_C, \Omega_A) \tag{10.5.17}$$

It has no effect, except for overall phase advance, on the $\pm 45^\circ$ or B -eigenvectors $|(+)\rangle$ or $|(-)\rangle$ whose spin vectors lie up and down the B -axis as shown in Examples 3 and 4, respectively, of Fig. 10.5.3. However, if the initial state is the first base state $|1\rangle = |x\rangle$ of x -polarization whose spin \mathbf{S} -vector lies on the A -axis then it begins to precess at the beat frequency of $\Omega=2B$. If $2B = -2S$ is negative (our choice in (10.3.3)), the precession is clockwise from A to the positive C -axis and then to $-A$ as shown in the Fig. 10.5.5 below. This is a "birds-eye" view of what happened in Fig. 10.2.6.

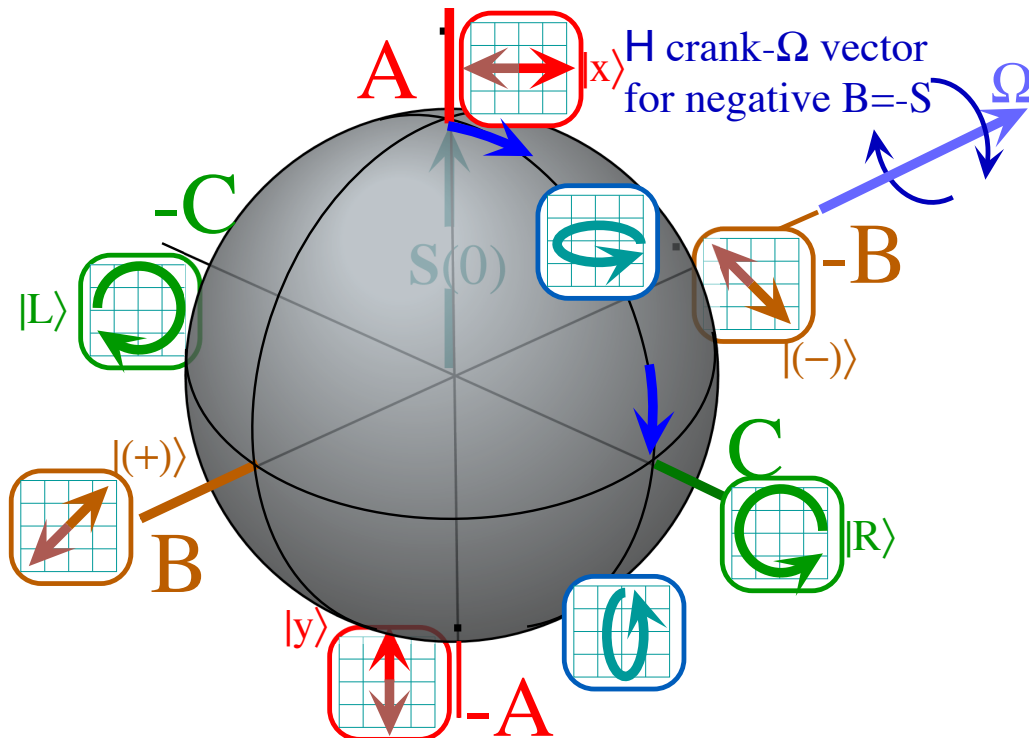


Fig. 10.5.5 Time evolution of a B -type beat. \mathbf{S} -vector rotates from A to C to $-A$ to $-C$ and back to A .

Contrast that to what happened in Fig. 10.2.10 with a circular C -type Zeeman-like Hamiltonian.

$$\begin{pmatrix} \langle 1|\mathbf{H}|1\rangle & \langle 1|\mathbf{H}|2\rangle \\ \langle 2|\mathbf{H}|1\rangle & \langle 2|\mathbf{H}|2\rangle \end{pmatrix} = \begin{pmatrix} A & -iC \\ iC & A \end{pmatrix} \quad (10.2.19d)_{repeated}$$

Its cranking Ω -vector is aligned with the C - or Y -axis.

$$\Omega = (\Omega_x, \Omega_y, \Omega_z) = (0, 2C, 0) = (\Omega_B, \Omega_C, \Omega_A) \quad (10.5.18)$$

The resulting rotation is shown in Fig. 10.5.6. It is a very simple *Faraday Rotation* of the initial x -plane of polarization. However, it is a funny kind of rotation since the plane only rotates at half the angle β of the precessing spin S -vector. When the spin is at $\beta=60^\circ$ the plane is only at $\beta/2=30^\circ$, as seen in the figure. This makes big trouble when the S -vector arrives back at A after going $\beta=360^\circ$, all the way around the globe. The polarization is back to being a level x -polarization, but it is exactly $\beta/2=180^\circ$ out of phase! That is, the plane has only gone half-way. Once again, there is a 2:1 ratio between what happens to spin *vectors* and *spinors*.

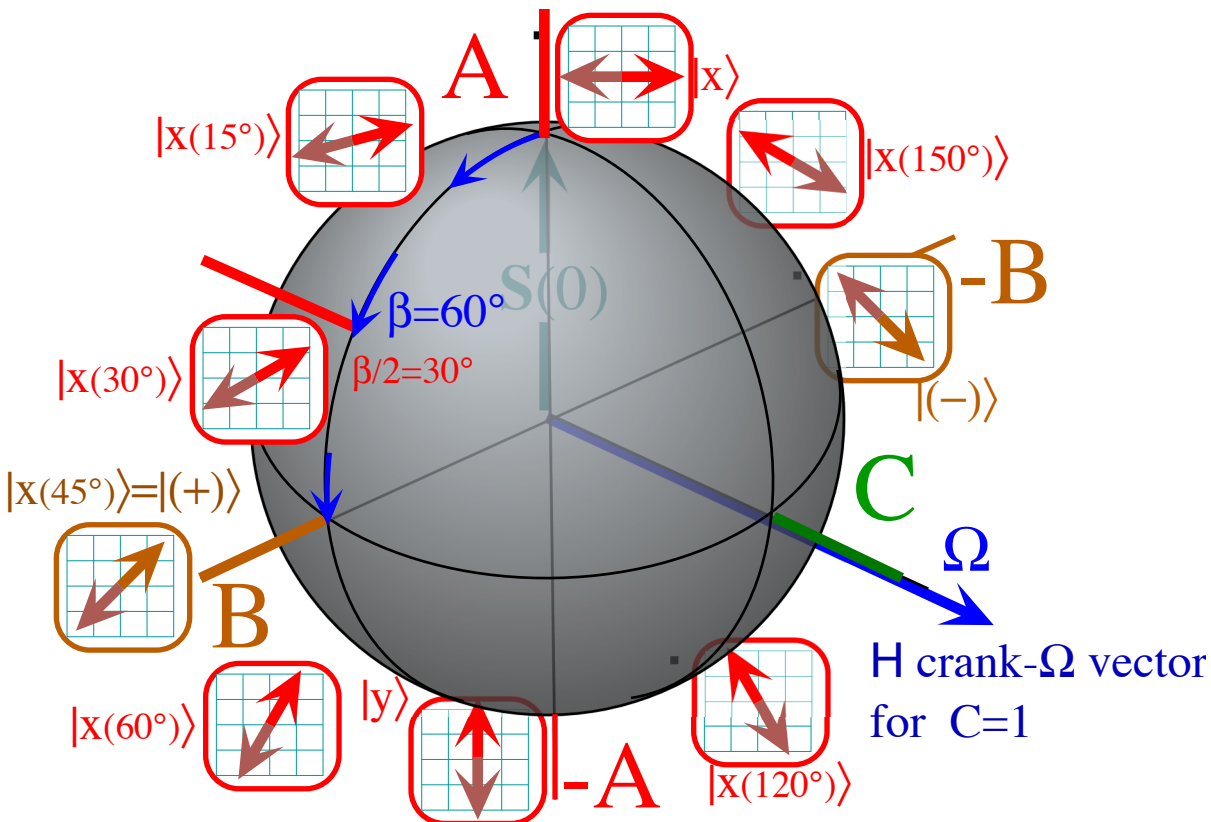


Fig. 10.5.6 Time evolution of a C -type beat. S -vector rotates from A to B to $-A$ to $-B$ and back to A .

If you follow carefully the evolution of the beat in the previous Fig. 10.5.5 you find that it, too, acquires a 180° phase shift upon one "complete" 360° rotation. So do electrons or any $U(2)$ object. It is a fundamental property of rotational space, and a quite mysterious one. This is studied in a later chapter.

By breaking the bilateral B -symmetry we make it more difficult for the initial A -spin state to resonate or rotate around the $R(3)$ globe. This is shown in Fig. 10.5.7 which diagrams the effect of a Stark-like ABD -type Hamiltonian

$$\begin{pmatrix} \langle 1|\mathbf{H}|1\rangle & \langle 1|\mathbf{H}|2\rangle \\ \langle 2|\mathbf{H}|1\rangle & \langle 2|\mathbf{H}|2\rangle \end{pmatrix} = \begin{pmatrix} A & B \\ B & D \end{pmatrix} = \begin{pmatrix} H - pE & -S \\ -S & H - pE \end{pmatrix} \quad (10.3.3a)_{repeated}$$

Its cranking Ω -vector is between the A - or Z -axis and the B - or X -axis..

$$\Omega = (\Omega_x, \Omega_y, \Omega_z) = (2B, 0, A-D) = (-2S, 0, -2pE) = (\Omega_B, \Omega_C, \Omega_A) \quad (10.5.19)$$

The chosen parameters are tunneling $S=1$, and symmetry breaking $pE=\sqrt{3}$. The resulting rotation goes along a much smaller circle that only "throws" the \mathbf{S} -vector out to $\beta=60^\circ$, twice as far as the polar angle $\vartheta=30^\circ$ of the Ω -vector. Along the way the polarization becomes elliptical briefly with its ellipse always contained in a box which is tipped by exactly the angle $\vartheta/2=15^\circ$. (Prove this!)

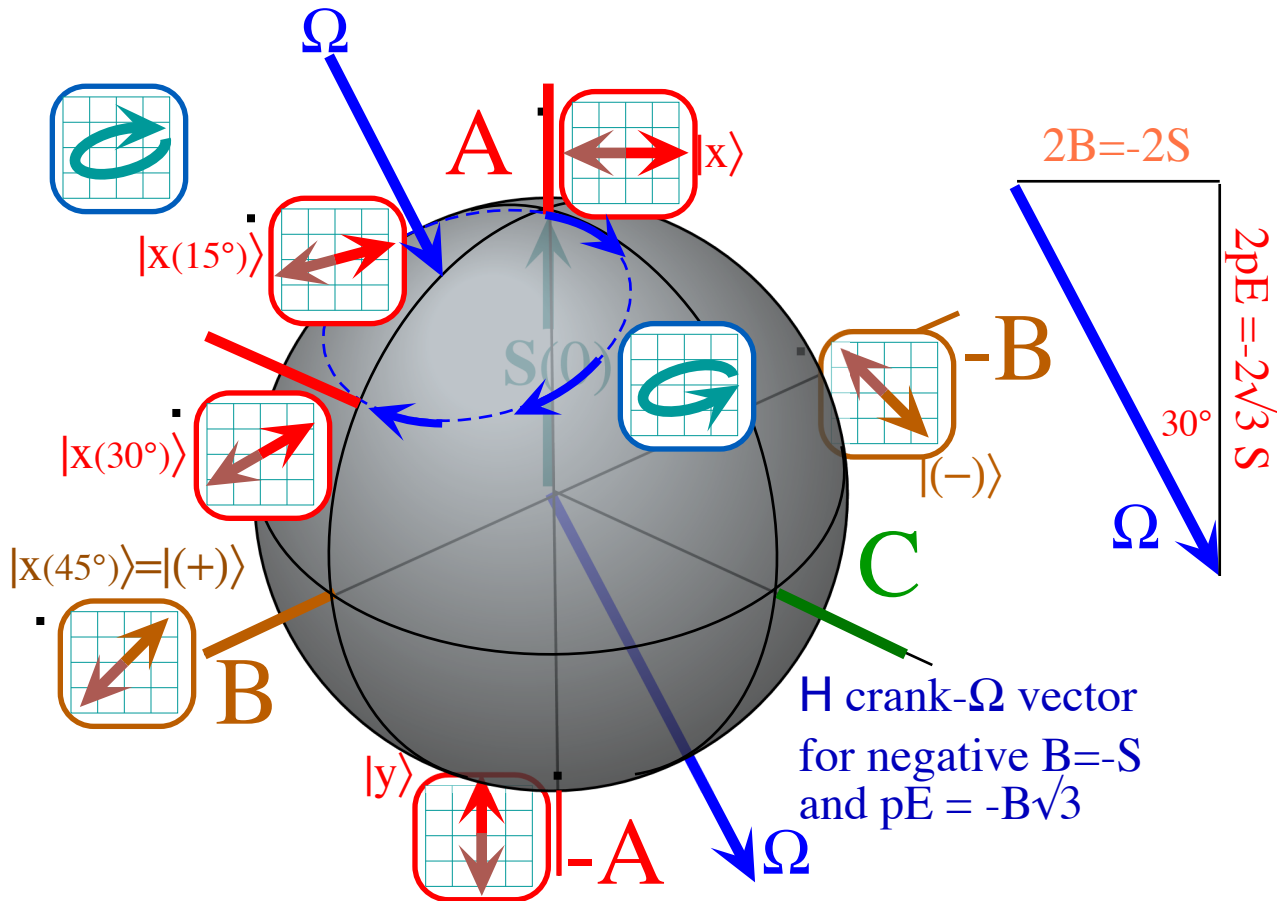


Fig. 10.5.7 Time evolution of a AB -type beat. \mathbf{S} -vector rotates from A to $\beta=60^\circ$ and back to A .

Notice how effectively the symmetry breaking parameter pE quenches resonance when it gets much larger than the coupling or tunneling parameter S . The Ω -vector approaches the A -axis closely. Since the Ω -vector determines the two \mathbf{S} -vectors that represent eigenstates of \mathbf{H} , it is seen that the original A -type base states of x and y polarization are recovered quite closely. These are the eigenstates of the A -Hamiltonian that start the ABC classification in Sec. 10.2a.

$$\mathbf{H}_{c_2^A} = \begin{pmatrix} A & 0 \\ 0 & D \end{pmatrix} \quad (10.2.2h)_{repeated}$$

Crank Ω polar angles (φ, ϑ) versus Spin \mathbf{S} polar angles (α, β)

The azimuth- α and polar- β angles of spin \mathbf{S} of a state $|\psi\rangle$ are set in (10.5.8b). We need azimuth- φ and polar- ϑ angles of crank vectors Ω or $\Theta = \Omega \cdot t$ of a Hamiltonian \mathbf{H} . These are defined below and in Fig. 10.5.8.

$$\mathbf{S}_X = (N/2) \cos \alpha \sin \beta = \text{Re} \psi_1^* \psi_2 \quad \Omega_X = \Omega \cos \varphi \sin \vartheta = 2 \text{Re } H_{21} = 2B \quad (10.5.20a)$$

$$\mathbf{S}_Y = (N/2) \sin \alpha \sin \beta = \text{Im} \psi_1^* \psi_2 \quad \Omega_Y = \Omega \sin \varphi \sin \vartheta = 2 \text{Im } H_{21} = 2C \quad (10.5.20b)$$

$$\mathbf{S}_Z = (N/2) \cos \beta = (\psi_1^* \psi_1 - \psi_2^* \psi_2) / 2 \quad \Omega_Z = \Omega \cos \vartheta = H_{11} - H_{22} = A - D \quad (10.5.20c)$$

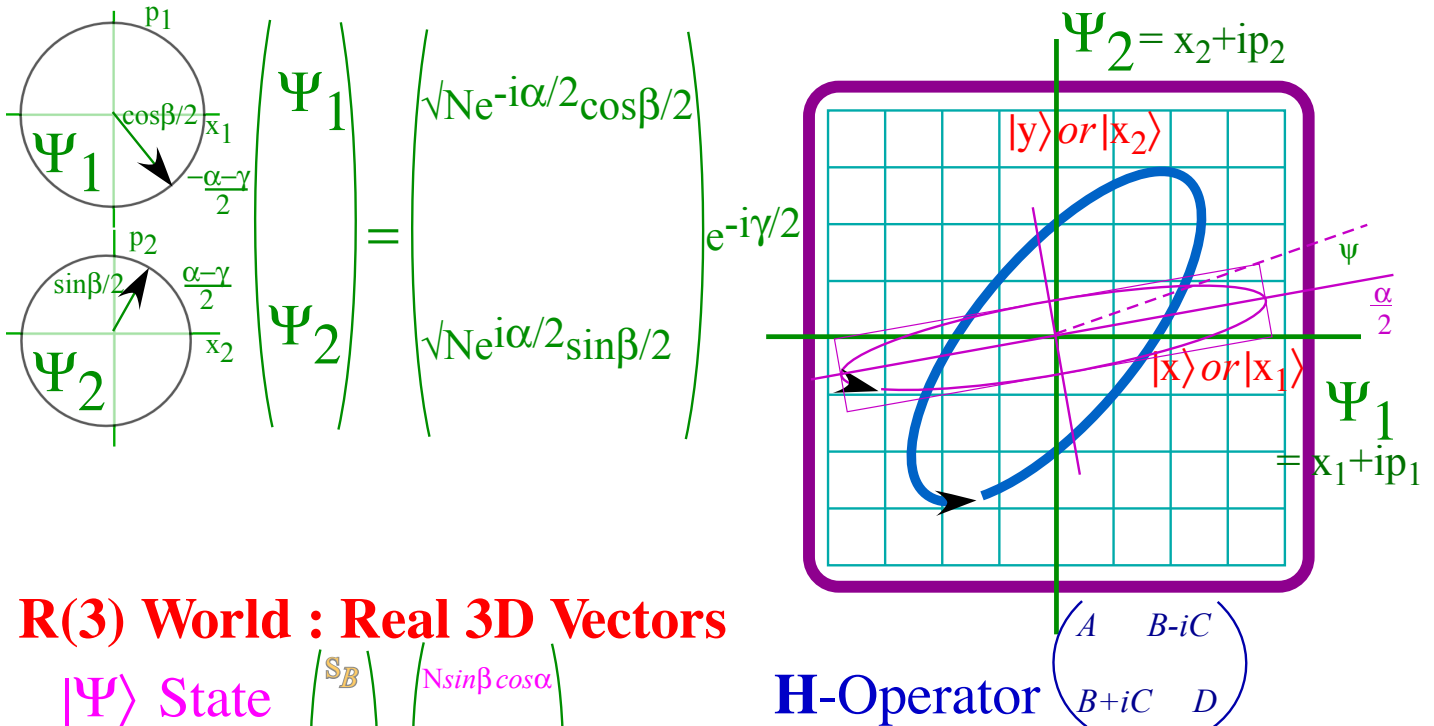
$$\mathbf{S}_0 = (N/2) = (\psi_1^* \psi_1 + \psi_2^* \psi_2) / 2 \quad \Omega_0 = \Omega = H_{11} + H_{22} = A + D \quad (10.5.20d)$$

Since eigenstate \mathbf{S} aligns to Ω , finding $|\epsilon_{hi}\rangle$ or $|\epsilon_{lo}\rangle$ means equating angles: $(\alpha, \beta) = (\varphi, \vartheta)$ or $(\varphi, \vartheta + \pi)$.

This is a very powerful way to analyze and understand eigensolutions of $U(2)$ systems. It will be used later.

U(2) World : Complex 2D Spinors

2-State ket $|\Psi\rangle =$



R(3) World : Real 3D Vectors

$|\Psi\rangle$ State Spin Vector \mathbf{S}

$$\begin{pmatrix} S_B \\ S_C \\ S_A \end{pmatrix} = \begin{pmatrix} N \sin\beta \cos\alpha \\ N \sin\beta \sin\alpha \\ N \cos\beta \end{pmatrix} \frac{1}{2}$$

H-Operator
Angular velocity

$$\mathbf{\Omega} = \begin{pmatrix} \Omega_B \\ \Omega_C \\ \Omega_A \end{pmatrix} = \begin{pmatrix} 2B \\ 2C \\ A-D \end{pmatrix} = \begin{pmatrix} \Omega \sin\vartheta \cos\phi \\ \Omega \sin\vartheta \sin\phi \\ \Omega \cos\vartheta \end{pmatrix}$$

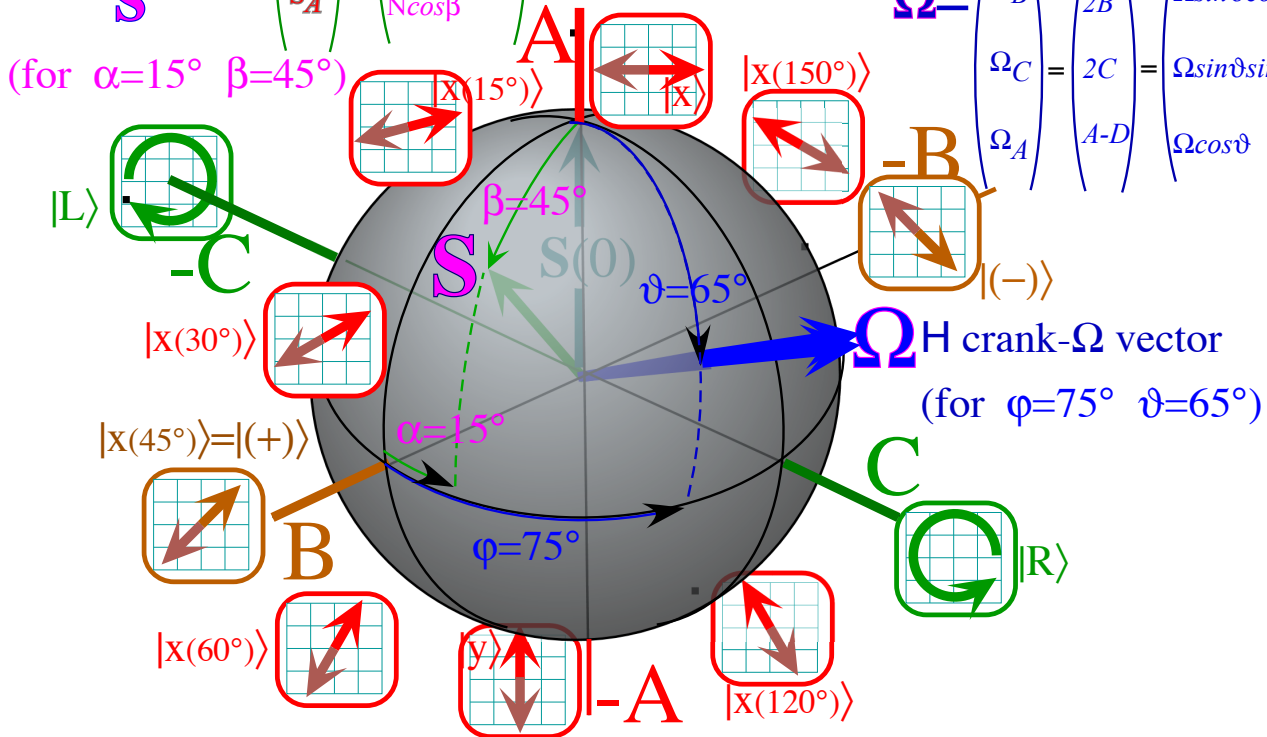


Fig. 10.5.8 Comparison of (a) Complex U(2) spinor picture in (Ψ_1, Ψ_2) -space, With (b) Real R(3) vector picture in (A, B, C) -space.

Hamilton's generalization of $\exp(-i\omega t) = \cos\omega t - i\sin\omega t$: $\exp(-i\sigma t) = \text{What?}$

When Hamilton generalized imaginary numbers to quaternions he had also generalized the famous Theorem of DeMoivre ($e^{-i\alpha} = \cos\alpha - i\sin\alpha$). Engineers use $e^{i\alpha}$ to rotate phase by α in AC theory, and a 2D Planck time phasor $e^{-i\omega t} = \cos\omega t - i\sin\omega t$ of wave theory generalizes to a 3D rotation $e^{-i\Omega\sigma t}$.

An exponential expression for a 2-by-2-polarization rotation matrix was given in (10.2.18).

$$\mathbf{R}(\varphi) = e^{\varphi\mathbf{G}}, \text{ represented by: } \begin{pmatrix} \cos\varphi & -\sin\varphi \\ \sin\varphi & \cos\varphi \end{pmatrix} = e^{\varphi \begin{pmatrix} 0 & -1 \\ 1 & 0 \end{pmatrix}} = e^{-i\varphi \begin{pmatrix} 0 & -i \\ i & 0 \end{pmatrix}} \quad (10.5.21)$$

This is a C- or Y-rotation by φ in (x,y)-space, and φ is half the angle $\beta=2\varphi$ that \mathbf{S} rotates in 3-space.

$$\begin{aligned} \mathbf{R}_C(\varphi) &= e^{-i\varphi\sigma_C} = e^{-i2\varphi\mathbf{S}_C} = \mathbf{1} \cos\varphi - i \sigma_C \sin\varphi \\ &= e^{-i\varphi \begin{pmatrix} 0 & -i \\ i & 0 \end{pmatrix}} = e^{-i2\varphi \begin{pmatrix} 0 & -i \\ i & 0 \end{pmatrix} \frac{1}{2}} = \begin{pmatrix} \cos\varphi & -\sin\varphi \\ \sin\varphi & \cos\varphi \end{pmatrix} = \begin{pmatrix} 1 & 0 \\ 0 & 1 \end{pmatrix} \cos\varphi - i \begin{pmatrix} 0 & -i \\ i & 0 \end{pmatrix} \sin\varphi \end{aligned} \quad (10.5.22)$$

The rotation $e^{-i\varphi\sigma_C}$ breaks down to a sum of a unit operator $\mathbf{1}$ times $\cos(\varphi)$ minus $i\sigma_C$ times $\sin(\varphi)$, a generalization of the DeMoivre exponential: $e^{-i\phi} = \cos\phi - i\sin\phi$. These represent enormous milestones in the history of mathematics, but Hamilton's contribution is particularly powerful as we will see. It is hard to imagine quantum theory without either one of these great developments.

The other two types *A* and *B* of rotations are listed in the $U(2)$ catalog in Fig. 10.4.2. The *A* or Z-type rotation generated by asymmetric-diagonal σ_A is also diagonal but complex.

$$\begin{aligned} \mathbf{R}_A(\theta) &= e^{-i\theta\sigma_A} = e^{-i2\theta\mathbf{S}_A} = \mathbf{1} \cos\theta - i \sigma_A \sin\theta \\ &= e^{-i\theta \begin{pmatrix} 1 & 0 \\ 0 & -1 \end{pmatrix}} = e^{-i2\theta \begin{pmatrix} 1 & 0 \\ 0 & -1 \end{pmatrix} \frac{1}{2}} = \begin{pmatrix} e^{-i\theta} & 0 \\ 0 & e^{i\theta} \end{pmatrix} = \begin{pmatrix} 1 & 0 \\ 0 & 1 \end{pmatrix} \cos\theta - i \begin{pmatrix} 1 & 0 \\ 0 & -1 \end{pmatrix} \sin\theta \end{aligned} \quad (10.5.23)$$

The *B* or X type rotation is complex and non-diagonal. (Check it by doing a σ_B spectral decomposition.)

$$\begin{aligned} \mathbf{R}_B(\chi) &= e^{-i\chi\sigma_B} = e^{-i2\chi\mathbf{S}_B} = \mathbf{1} \cos\chi - i \sigma_B \sin\chi \\ &= e^{-i\chi \begin{pmatrix} 0 & 1 \\ 1 & 0 \end{pmatrix}} = e^{-i2\chi \begin{pmatrix} 0 & 1 \\ 1 & 0 \end{pmatrix} \frac{1}{2}} = \begin{pmatrix} \cos\chi & -i\sin\chi \\ -i\sin\chi & \cos\chi \end{pmatrix} = \begin{pmatrix} 1 & 0 \\ 0 & 1 \end{pmatrix} \cos\chi - i \begin{pmatrix} 0 & 1 \\ 1 & 0 \end{pmatrix} \sin\chi \end{aligned} \quad (10.5.24)$$

The key idea here is that $e^{-i\phi\sigma} = \cos\phi - i\sigma\sin\phi$ works not just for separate $\sigma = \sigma_B, \sigma_C$, or σ_A but for any combination-reflection $\sigma = \sigma_{AB}$ or σ_{ABCD} provided $\sigma^2 = I$. Evolution operator $\mathbf{U} = e^{-i\mathbf{H}t}$ ($\hbar=1$) has Hamiltonian $\mathbf{H} = \sigma \cdot \Omega / 2 = (\Omega/2)\sigma$ defined by crank vector Ω or rotation axis vector $\Theta = \Omega t$ as in (10.5.10).

$$\mathbf{U} = e^{-i\mathbf{H}t} = e^{-i\frac{\Theta}{2} \hat{\Theta} \cdot \sigma} = \mathbf{R}[\Theta] = \cos\frac{\Theta}{2} \mathbf{1} - i \sin\frac{\Theta}{2} \hat{\Theta} \cdot \sigma = e^{-i\frac{1}{2} \Theta \cdot \sigma} = e^{-i\Theta \cdot \mathbf{S}} \quad (10.5.25a)$$

The rotation axis is given by its polar coordinates (φ, ϑ) and angle of turn $\Theta = \sqrt{\Theta_X^2 + \Theta_Y^2 + \Theta_Z^2} = \Omega t$.

$$\Theta = (\Theta_X, \Theta_Y, \Theta_Z) = |\Theta| \cdot (\cos\varphi \sin\vartheta, \sin\varphi \sin\vartheta, \cos\vartheta) = (\Theta_B, \Theta_C, \Theta_A)$$

Representing $\sigma_X = \sigma_B, \sigma_Y = \sigma_C$, and $\sigma_Z = \sigma_A$ by their usual matrices gives a representation of $\mathbf{U} = \mathbf{R}$.

$$\begin{aligned} \mathbf{R}[\Theta] &= \cos\frac{\Theta}{2} \mathbf{1} - i \sigma_X \hat{\Theta}_X \sin\frac{\Theta}{2} - i \sigma_Y \hat{\Theta}_Y \sin\frac{\Theta}{2} - i \sigma_Z \hat{\Theta}_Z \sin\frac{\Theta}{2} \\ &= \cos\frac{\Theta}{2} \begin{pmatrix} 1 & 0 \\ 0 & 1 \end{pmatrix} - i \begin{pmatrix} 0 & 1 \\ 1 & 0 \end{pmatrix} \hat{\Theta}_X \sin\frac{\Theta}{2} - i \begin{pmatrix} 0 & -i \\ i & 0 \end{pmatrix} \hat{\Theta}_Y \sin\frac{\Theta}{2} - i \begin{pmatrix} 1 & 0 \\ 0 & -1 \end{pmatrix} \hat{\Theta}_Z \sin\frac{\Theta}{2} \end{aligned}$$

Unit rotation axis vector $\hat{\Theta} = (\hat{\Theta}_X, \hat{\Theta}_Y, \hat{\Theta}_Z) = (\cos\varphi \sin\vartheta, \sin\varphi \sin\vartheta, \cos\vartheta)$ is defined.

$$\begin{pmatrix} \langle 1 | \mathbf{R}[\Theta] | 1 \rangle & \langle 1 | \mathbf{R}[\Theta] | 2 \rangle \\ \langle 2 | \mathbf{R}[\Theta] | 1 \rangle & \langle 2 | \mathbf{R}[\Theta] | 2 \rangle \end{pmatrix} = \begin{pmatrix} \cos \frac{\Theta}{2} - i \hat{\Theta}_Z \sin \frac{\Theta}{2} & -i \sin \frac{\Theta}{2} (\hat{\Theta}_X - i \hat{\Theta}_Y) \\ -i \sin \frac{\Theta}{2} (\hat{\Theta}_X + i \hat{\Theta}_Y) & \cos \frac{\Theta}{2} + i \hat{\Theta}_Z \sin \frac{\Theta}{2} \end{pmatrix} \quad (10.5.25b)$$

In terms of polar axis angles $[\varphi, \vartheta, \Theta = \Omega \cdot t]$ this expands to a general *SU(2) rotation matrix*.

$$\begin{aligned} \mathbf{R}[\Theta] &= \begin{pmatrix} \cos \frac{\Theta}{2} - i \cos \vartheta \sin \frac{\Theta}{2} & -i \sin \frac{\Theta}{2} (\cos \varphi \sin \vartheta - i \sin \varphi \sin \vartheta) \\ -i \sin \frac{\Theta}{2} (\cos \varphi \sin \vartheta + i \sin \varphi \sin \vartheta) & \cos \frac{\Theta}{2} + i \cos \vartheta \sin \frac{\Theta}{2} \end{pmatrix} \\ &= \mathbf{R}[\varphi \vartheta \Theta] = \begin{pmatrix} \cos \frac{\Theta}{2} - i \cos \vartheta \sin \frac{\Theta}{2} & -i e^{-i\varphi} \sin \vartheta \sin \frac{\Theta}{2} \\ -i e^{i\varphi} \sin \vartheta \sin \frac{\Theta}{2} & \cos \frac{\Theta}{2} + i \cos \vartheta \sin \frac{\Theta}{2} \end{pmatrix} = e^{-i\mathbf{H}t} = e^{-i\Theta \cdot \mathbf{S}} \end{aligned} \quad (10.5.25c)$$

H eigenstates $|\varepsilon_{hi}(\alpha, \beta)\rangle$ or $|\varepsilon_{lo}(\alpha, \beta)\rangle$ have angles (α, β) in (10.5.8) given by (φ, ϑ) or $(\varphi, \vartheta + \pi)$.

Why the 1/2?

The $1/2$ in front of angle Θ is there because $\Theta = \Omega \cdot t$ is the angle of rotation in 3D-**ABC** space in Fig. 10.5.8b. Angle Θ or β is twice the 2D-spinor-space angle φ or $\beta/2$ in Fig. 10.5.8a. Why is this?

One answer is that to transform spinor operator **O** from **O** to $\mathbf{O}' = \mathbf{R} \mathbf{O} \mathbf{R}^\dagger$ by rotation **R** requires *two* **R**'s. For example, $\mathbf{O} = \sigma_Z = \sigma_A$ transformed by $\mathbf{R}_Y = \mathbf{R}_C$ is the following.

$$\begin{aligned} \mathbf{R}_Y(\varphi) \sigma_Z \mathbf{R}_Y(\varphi)^\dagger &= \sigma_X \sin 2\varphi + \sigma_Z \cos 2\varphi \\ \begin{pmatrix} \cos \varphi & -\sin \varphi \\ \sin \varphi & \cos \varphi \end{pmatrix} \begin{pmatrix} 1 & 0 \\ 0 & -1 \end{pmatrix} \begin{pmatrix} \cos \varphi & \sin \varphi \\ -\sin \varphi & \cos \varphi \end{pmatrix} & \\ = \begin{pmatrix} \cos^2 \varphi - \sin^2 \varphi & 2 \sin \varphi \cos \varphi \\ 2 \sin \varphi \cos \varphi & \sin^2 \varphi - \cos^2 \varphi \end{pmatrix} = \begin{pmatrix} \cos 2\varphi & \sin 2\varphi \\ \sin 2\varphi & -\cos 2\varphi \end{pmatrix} = \begin{pmatrix} 0 & 1 \\ 1 & 0 \end{pmatrix} \sin 2\varphi + \begin{pmatrix} 1 & 0 \\ 0 & -1 \end{pmatrix} \cos 2\varphi & \end{aligned} \quad (10.5.26)$$

For angle $2\varphi = \pi/2$, this relates $\sigma_Z = \sigma_A$ to $\sigma_X = \sigma_B$ as is done in (10.3.9). A rotation by $2\varphi = \Theta = \beta$ in **ABC**-operator 3-space $(\sigma_X, \sigma_Y, \sigma_Z)$ is twice the angle φ used for spinor 2-space. Spinor-1/2 factors double in vector 3-space, and spinors have half-angles $\varphi = \beta/2$ so that $\beta = \Theta$ is a real 3D-rotation. Also, recall in (10.3.12) that two mirror planes separated by φ yield rotations by 2φ .

The evolution-rotation-operator $\mathbf{U} = e^{-i\Theta \cdot \sigma/2} = e^{-i\Theta \cdot \mathbf{S}}$ by 3D-angle Θ may be viewed two ways: A 3D rotation by Θ generated by spin *vector* operator $\mathbf{S} = \sigma/2$, or a 2D rotation by $\Theta/2$ generated by a *spinor* operator σ . The $1/2$ -factors have quite deep significance. They are related to electrons having $1/2$ quantum of spin $\mathbf{S} = \sigma/2$. They deserve deep consideration. We shall try again later to explain more about the mysterious $1/2$!

Problems for Chapter 10.

ABCDanonical?

10.1.1. The canonical definition of momentum does not always give $p_j = m dx_j/dt$. (See “Deep Classical..” Chapter 5.3)

- What is the general definition of p_j in terms of a Lagrangian L ? First, what is L in terms of Hamiltonian H ?
- Find L and p_j for the classical ABCD Hamiltonian (10.1.3c).
- Is the Schrodinger-to-Classical-Oscillator analogy correct if there is *explicit* time dependence $A(t)$, $B(t)$,...etc.?

All fall down

10.1.2. The fall-line at any point in a 2D potential $V(x,y)$ is determined by ∇V (or $-\nabla V$, which?)

- Relate acceleration-force vector (10.1.5) for the general potential $V=(1/2)\mathbf{x}\cdot\mathbf{A}\cdot\mathbf{x}$ (10.1.6b) to the gradient ∇V .
- Find eigenvectors and eigenvalues of acceleration matrix \mathbf{A} . Show how eigenvectors relate to V-ellipse axes for: case A: (A=4, D=1, B=0, C=0), case B: (A=D=4, B=-1, C=0), case AB: (A=4, D=1, B=1, C=0). Relate each to a classical normal mode frequency.
- Find eigenvectors and eigenvalues of Hamiltonian matrix \mathbf{H} for: case A: (A=4, D=1, B=0, C=0), case B: (A=D=4, B=-1, C=0), case AB: (A=4, D=1, B=1, C=0). Relate each to a quantum energy or eigenfrequency.

Groupie quaternions

10.1.3 Do the quaternions $\{\mathbf{1}, \mathbf{i}, \mathbf{j}, \mathbf{k}\}$ by themselves make a group? How about Pauli $\{\sigma_I, \sigma_A, \sigma_B, \sigma_C\}$?

- How about the set $\{\mathbf{1}, \mathbf{i}, \mathbf{j}, \mathbf{k}, -\mathbf{1}, -\mathbf{i}, -\mathbf{j}, -\mathbf{k}\}$? Construct a 4x4 multiplication table for $\{\mathbf{1}, \mathbf{i}, \mathbf{j}, \mathbf{k}\}$.
- How about the set $\{\sigma_I, \sigma_A, \sigma_B, \sigma_C, -\sigma_I, -\sigma_A, -\sigma_B, -\sigma_C\}$? Construct a 4x4 multiplication table.
- Show that $\sigma_m \cdot \sigma_n = \delta_{mn}\mathbf{1} + i\epsilon_{mnp} \sigma_p$.

Use the Phase Luke!

10.2.1 Suppose a particle is oscillating at frequency ω according to $x(t) = A \sin(\omega t)$ while experiencing an applied force at the same frequency but ahead in phase angle ϕ according to $F(t) = F \sin(\omega t - \phi)$.

- Does positive ϕ represent a force ahead or behind?
- Sketch a F versus x (Work-cycle) diagram for $\phi = 0, \pi/4, \pi/2, \pi$, and $3\pi/2$.
- Calculate the work F does on x each cycle as a function of ϕ and indicate how it relates to area of F-x plots (b).
- At the moment shown in Fig. 10.2.6, what is the phase angle ϕ between x_1 and x_2 . Who's ahead? How does the phase angle vary with time? How does the energy flow (in the classical model) between the two vary with time?

B versus C

10.3.1 The \mathbf{H} -matrix for the symmetry B , and C was given in the form of the tunneling amplitudes ($B=-S$) plus magnetic Zeeman (dipole) energy shifts (C). As the relative magnitudes of these vary the eigenstates, eigenvalues, and symmetry changes, too.

- Write the $\mathbf{H}(H, B, C=0)$ matrix in a basis that is most appropriate for its (What? B , or C ?) -symmetry and use the lowest order perturbation theory to describe the effect of small C -value. Compare your result to that of the exact avoided crossing eigenvalues for ($B=1, C=0.2$). Describe the set or group of matrix operators that commute with $\mathbf{H}(H, B, C=0)$ and with $\mathbf{H}(H, B=1, C=0.2)$, that is, give both finite "rotation" matrices and their generators.

Sketch eigenstate phasor and polarization diagrams[†] for each case.

Sketch ABC Ω and \mathbf{S} vector diagrams[†] for each case.

- Write the $\mathbf{H}(H, B=0, C)$ matrix in a basis that is most appropriate for its (What? B , or C ?) -symmetry and use the lowest order perturbation theory to describe the effect of small B -value. Compare your result to that of the exact avoided crossing eigenvalues for ($B=0.2, C=1$). Describe the set or group of matrix operators that commute with $\mathbf{H}(H, B=0, C)$ and with $\mathbf{H}(H, B=0.2, C=1)$, that is, give both finite "rotation" matrices and their generators.

Sketch eigenstate phasor and polarization diagrams[†] for each case.

Sketch ABC Ω and \mathbf{S} vector diagrams[†] for each case. [†]See Sec. 10.5.

Commute or else!

10.3.2 Use spectral decompositions to derive the form of the general $U(2)$ matrix that commutes...

- ...with $\sigma_A = \begin{pmatrix} 1 & 0 \\ 0 & -1 \end{pmatrix}$
- ...with $\sigma_B = \begin{pmatrix} 0 & 1 \\ 1 & 0 \end{pmatrix}$
- ...with $\sigma_C = \begin{pmatrix} 0 & -i \\ i & 0 \end{pmatrix}$
- ...with $M = \begin{pmatrix} 4 & 1 \\ 3 & 2 \end{pmatrix}$.

(e to h) Derive the form of the most general $SU(2)$ matrices that commute with each of the above.

Eigenvalues easy as ABCD

10.4.1 The expansion (10.4.5b-c) gives a closed form expression for eigenvalues of a general \mathbf{H}_{ABCD} .

- Verify all parts of (10.4.5).
- Show the eigenvalues so obtained agree with a direct diagonalization of \mathbf{H}_{ABCD} .
- Show that this is a special case of \mathbf{H}_{AB} eigenvalues in (10.3.11).

Ellipses on ellipses

10.4.2 The elliptical eigenstate orbits of Fig. 10.4.1 are seen to correspond to the elliptical equipotential level curves.

- Do they really? How so?
- Work the eigensolutions for Fig. 10.4.1 and plot their ellipses.
- Are the ellipse major axes of orthogonal eigenvectors themselves orthogonal? Why or why not?

Eigenvectors easy as ABCD

10.5.1 The prescription (10.5.20) for finding general U(2) eigenvectors is powerful and important.

- Write it out in detail for the AB-Hamiltonian in Fig. 10.5.7. Give eigenstates easily. (Recall (10.5.8a))
- Show how a polarization ellipse would evolve and fill a rectangle if x-polarization were fed to this \mathbf{H} .
- Do similarly with the Hamiltonian and initial spin shown in Fig. 10.5.8.

Very cross prodots

10.5.2 Using the σ -operator definitions and the Levi-Civita tensor definition

derive the following. (First prove Levi-Civita rule: $\varepsilon_{abc}\varepsilon_{dec} = \delta_{ad}\delta_{be} - \delta_{ae}\delta_{bd}$)

$$(a) \sigma_a \sigma_b = \delta_{ab} + i \sum_c \varepsilon_{abc} \sigma_c \quad (b) \sigma_a \sigma_b \sigma_a = 2\delta_{ab} \sigma_a - \sigma_b \quad (c) (\boldsymbol{\sigma} \cdot \mathbf{A})(\boldsymbol{\sigma} \cdot \mathbf{B}) = (\mathbf{A} \cdot \mathbf{B}) + i(\mathbf{A} \times \mathbf{B}) \cdot \boldsymbol{\sigma}$$

Spinor round

10.5.3 Use spectral decomposition to derive three rotation operators (A-C) and base transforms (d-g).

$$(a) \quad \mathbf{R}(\theta_{xy}) = e^{-i\frac{\theta_{xy}}{2}\sigma_z} = \mathbf{1} \cos \frac{\theta_{xy}}{2} - i\sigma_z \sin \frac{\theta_{xy}}{2} = \begin{pmatrix} e^{-i\theta_{xy}/2} & 0 \\ 0 & e^{i\theta_{xy}/2} \end{pmatrix}$$

$$(b) \quad \mathbf{R}(\theta_{yz}) = e^{-i\frac{\theta_{yz}}{2}\sigma_x} = \mathbf{1} \cos \frac{\theta_{yz}}{2} - i\sigma_x \sin \frac{\theta_{yz}}{2} = \begin{pmatrix} \text{---} & \text{---} \\ \text{---} & \text{---} \end{pmatrix}$$

$$(c) \quad \mathbf{R}(\theta_{zx}) = e^{-i\frac{\theta_{zx}}{2}\sigma_y} = \mathbf{1} \cos \frac{\theta_{zx}}{2} - i\sigma_y \sin \frac{\theta_{zx}}{2} = \begin{pmatrix} \text{---} & \text{---} \\ \text{---} & \text{---} \end{pmatrix}$$

$$(d) \quad \mathbf{R}(\theta_{ab}) \cdot \mathbf{1} \cdot \mathbf{R}^\dagger(\theta_{ab}) = \mathbf{1}$$

$$(e) \quad \mathbf{R}(\theta_{ab}) \cdot \sigma_a \cdot \mathbf{R}^\dagger(\theta_{ab}) = \sigma_a \cos \theta_{ab} + \sigma_b \sin \theta_{ab}$$

$$(f) \quad \mathbf{R}(\theta_{ab}) \cdot \sigma_b \cdot \mathbf{R}^\dagger(\theta_{ab}) = -\sigma_a \sin \theta_{ab} + \sigma_b \cos \theta_{ab}$$

$$(g) \quad \mathbf{R}(\theta_{ab}) \cdot \sigma_c \cdot \mathbf{R}^\dagger(\theta_{ab}) = \sigma_c \quad (\text{Let: } \varepsilon_{abc} = 1)$$

The Lorentz district

10.5.4 Use spectral decomposition to derive three Lorentz operators (A-C) and base transforms (d-f).

$$(a) \quad \mathbf{L}(\theta_{tz}) = e^{\frac{\theta_{tz}}{2}\sigma_z} = \mathbf{1} \cosh \frac{\theta_{tz}}{2} + \sigma_z \sinh \frac{\theta_{tz}}{2} = \begin{pmatrix} e^{\theta_{tz}/2} & 0 \\ 0 & e^{-\theta_{tz}/2} \end{pmatrix}$$

$$(b) \quad \mathbf{L}(\theta_{tx}) = e^{\frac{\theta_{tx}}{2}\sigma_x} = \mathbf{1} \cosh \frac{\theta_{tx}}{2} + \sigma_x \sinh \frac{\theta_{tx}}{2} = \begin{pmatrix} \text{---} & \text{---} \\ \text{---} & \text{---} \end{pmatrix}$$

- (c) $L(\theta_{ty}) = e^{\frac{\theta_{ty}}{2} \sigma_y} = \mathbf{1} \sinh \frac{\theta_{ty}}{2} + \sigma_y \cosh \frac{\theta_{ty}}{2} = \begin{pmatrix} \text{---} & \text{---} \\ \text{---} & \text{---} \end{pmatrix}$
- (d) $L(\theta_{ta}) \cdot \mathbf{1} \cdot L^\dagger(\theta_{ta}) = \mathbf{1} \cosh \theta_{ta} + \sigma_a \sinh \theta_{ta}$
- (e) $L(\theta_{ta}) \cdot \sigma_a \cdot L^\dagger(\theta_{ta}) = \mathbf{1} \sinh \theta_{ta} + \sigma_a \cosh \theta_{ta}$
- (f) $L(\theta_{ta}) \cdot \sigma_c \cdot L^\dagger(\theta_{ta}) = \sigma_c$ (Let: $\epsilon_{abc}=1$)

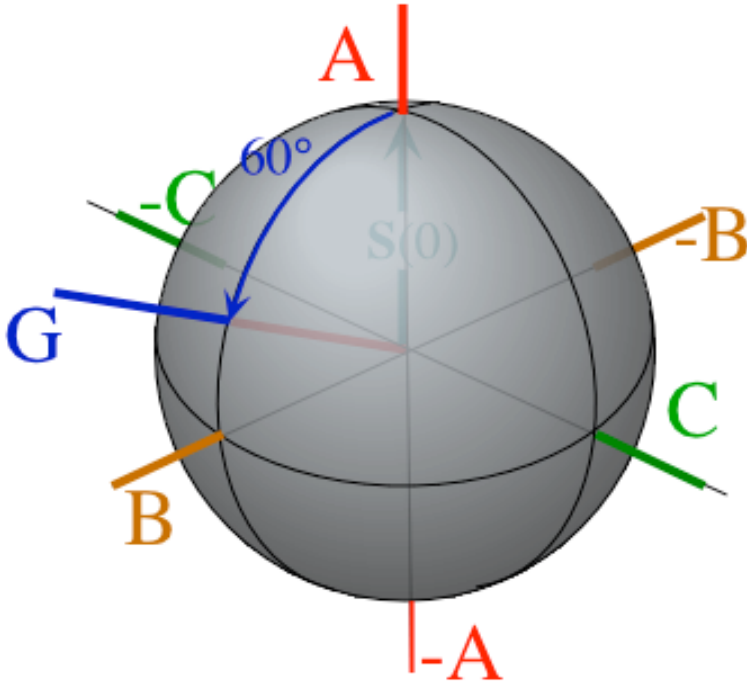


Fig. 1

10.5.5. Suppose an NMR spin system described by Hamiltonian $H = g \mathbf{S} \cdot \mathbf{B} = g/2 \boldsymbol{\sigma} \cdot \mathbf{B}$ is initially in a state

$$|\Psi(0)\rangle = \frac{\sqrt{3}}{2} |\uparrow\rangle + \frac{1}{2} |\downarrow\rangle = \begin{pmatrix} \sqrt{3}/2 \\ 1/2 \end{pmatrix} \tag{5.1}$$

- (a) Write out H and its Schrodinger equation using 2-dimensional matrix notation.
- (b) Write out H and its Bloch equation using 2-dimensional matrix notation.
- (c) Define a set of H that make state (5.1) stationary. What other state(s) are also stationary.
- (d) Find constant Hamiltonian H which will drive state (5.1) thru spin-up $|\uparrow\rangle$ in a given time τ .

$$|\langle \uparrow | \Psi(\tau) \rangle|^2 = 1 \quad \text{but: } |\langle \uparrow | \Psi(t) \rangle|^2 \neq 1 \text{ for } t < \tau \tag{5.2}$$

A number of H satisfy (5.2) but we prefer one which requires the least energy. Explain by describing a set of H . (Hint: Does least energy this also mean least angle of spin vector rotation?)

- (e) Give the eigenkets and energy eigenvalues of the Hamiltonian resulting from (d) in terms of τ and \hbar and sketch an energy level diagram.
- (f) Give a formula for the angular frequency of radiation in terms of τ and \hbar that might be observed as the state (5.1) and Hamiltonian from (d) are allowed to time-evolve.
- (g) Indicate where on Fig. 1 would be the initial spin vector, the driving magnetic B -field, and path followed by spin vector.
- (h) Let this be the analogous optical polarization problem. Show how the polarization E evolves.
- (j) What is the maximum energy or frequency of radiation that can result from (5.1-2) above.

Review Topics & Formulas for Unit 3

<p><i>Fourier Series Coefficients</i></p> $\langle k_m \Psi \rangle = \int_{-L/2}^{L/2} dx \langle k_m x \rangle \langle x \Psi \rangle$ $\langle k_m x \rangle = \frac{e^{-ik_m x}}{\sqrt{L}} = \langle x k_m \rangle^*$	<p><i>Fourier Integral Transform</i></p> $\langle k \Psi \rangle = \int_{-\infty}^{\infty} dx \langle k x \rangle \langle x \Psi \rangle$ <p><i>Kernal</i> : $\langle k x \rangle = \frac{e^{-ikx}}{\sqrt{2\pi}} = \langle x k \rangle^*$</p>	<p><i>Fourier C_N Transformation</i></p> $\langle k_m \Psi \rangle = \sum_{p=0}^{p=N-1} \langle k_m x_p \rangle \langle x_p \Psi \rangle$ $\langle k_m x_p \rangle = \frac{e^{-ik_m x_p}}{\sqrt{N}} = \langle x_p k_m \rangle^*$
<p><i>x-Wavefunction Ψ(x)=</i></p> $\langle x \Psi \rangle = \sum_{m=-\infty}^{m=\infty} \langle x k_m \rangle \langle k_m \Psi \rangle$ <p><i>Ortho – Completeness</i></p> $\sum_{m=0}^{m=\infty} \langle x k_m \rangle \langle k_m x' \rangle = \delta(x - x')$ $\int_{-L/2}^{L/2} dx \langle k_m x \rangle \langle x k_{m'} \rangle = \delta_{m,m'}$ <p><i>Discrete momentum m</i> <i>Continuous position x</i></p>	<p><i>x-Wavefunction Ψ(x)=</i></p> $\langle x \Psi \rangle = \int_{-\infty}^{\infty} dk \langle x k \rangle \langle k \Psi \rangle$ <p><i>Ortho – Completeness</i></p> $\int_{-\infty}^{\infty} dk \langle x k \rangle \langle k x' \rangle = \delta(x - x')$ $\int_{-\infty}^{\infty} dx \langle k x \rangle \langle x k' \rangle = \delta(k - k')$ <p><i>Continuous momentum k</i> <i>Continuous position x</i></p>	<p><i>x-Wavefunction Ψ(x)=</i></p> $\langle x_p \Psi \rangle = \sum_{m=0}^{m=N-1} \langle x_p k_m \rangle \langle k_m \Psi \rangle$ <p><i>Ortho – Completeness</i></p> $\sum_{m=0}^{m=N-1} \langle x_p k_m \rangle \langle k_m x_{p'} \rangle = \delta_{p,p'}$ $\sum_{p=0}^{p=N-1} \langle k_m x_p \rangle \langle x_p k_{m'} \rangle = \delta_{m,m'}$ <p><i>Discrete momentum m</i> <i>Discrete position x_p</i></p>
<p><i>Time Evolution Operator U</i></p> $ \Psi(t)\rangle = \mathbf{U}(t,0) \Psi(0)\rangle$ <p><i>Hamiltonian Generator H</i></p> $i\hbar \frac{\partial}{\partial t} \mathbf{U}(t,0) = \mathbf{H} \mathbf{U}(t,0)$	<p><i>Time Evolution Operator U</i></p> $\mathbf{U}(t,0) = e^{-i t \mathbf{H} / \hbar}$ <p><i>Schrodinger t – Equation</i></p> $i\hbar \frac{\partial}{\partial t} \Psi(t)\rangle = \mathbf{H} \Psi(t)\rangle$	<p><i>U must be Unitary</i></p> $\mathbf{U}^\dagger(t) = \mathbf{U}^{-1}(t) = \mathbf{U}(-t)$ $\left(e^{-i\mathbf{H}t/\hbar} \right)^\dagger = e^{i\mathbf{H}^\dagger t/\hbar} = e^{i\mathbf{H}t/\hbar}$ <p><i>so H is Hermitian H[†] = H</i></p>

Schrodinger time-independent energy eigen equation.

$$\mathbf{H} | \omega_m \rangle = \hbar \omega_m | \omega_m \rangle = \epsilon_m | \omega_m \rangle \tag{9.3.1a}$$

H-eigenvalues use **r**-expansion (9.2.6) of **H** and C₆ symmetry **r^p**-eigenvalues from (8.2.9).

$$\langle k_m | \mathbf{r}^p | k_m \rangle = e^{-ipk_m a} = e^{-ipm2\pi/N} \text{ where: } k_m = m(2\pi/Na)$$

$$\begin{aligned} \langle k_m | \mathbf{H} | k_m \rangle &= H \langle k_m | \mathbf{1} | k_m \rangle + S \langle k_m | \mathbf{r} | k_m \rangle + T \langle k_m | \mathbf{r}^2 | k_m \rangle + U \langle k_m | \mathbf{r}^3 | k_m \rangle + T^* \langle k_m | \mathbf{r}^4 | k_m \rangle + S^* \langle k_m | \mathbf{r}^5 | k_m \rangle \\ &= H + S e^{-ik_m a} + T e^{-i2k_m a} + U e^{-i3k_m a} + T^* e^{i2k_m a} + S^* e^{ik_m a} \end{aligned} \tag{9.3.5a}$$

Bloch dispersion relation. And Bohr limit ($k \ll \pi/a$) approximation. *Band group velocity V_{group}.*

$$\hbar \omega_m = E_m = H - 2|S| \cos(k_m a) = H - 2|S| + |S|(k_m a)^2 + .. \tag{9.3.8}$$

$$V_{group} = \frac{d\omega_m}{dk_m} = 2 \frac{|S|}{\hbar} a \sin(k_m a) \left(\cong 2 \frac{|S|}{\hbar} k_m a^2, \text{ for: } k_m \ll \pi / a \right) \tag{9.3.10}$$

Effective mass M_{eff} inversely proportional to S. $M_{eff}(0) = \hbar^2 / (2|S| a^2)$ (9.3.11a)

Fourier transform of a Gaussian $e^{-(m/\Delta m)^2}$ momentum distribution is a Gaussian $e^{-(\phi/\Delta\phi)^2}$ in coordinate ϕ .

$$\langle m|\Psi\rangle = e^{-(m/\Delta m)^2} \text{ implies: } \langle \phi|\Psi\rangle = e^{-(\phi/\Delta\phi)^2} \tag{9.3.14}$$

The relation between momentum uncertainty Δm and coordinate uncertainty $\Delta\phi$ is a Heisenberg relation.

$$\Delta m/2 = 1/\Delta\phi, \text{ or: } \Delta m \Delta\phi = 2 \tag{9.3.15}$$

Bohr wave quantum speed limits

$$V_{group}^{Bohr} (m \leftrightarrow n) = \frac{\omega_m - \omega_n}{k_m - k_n} = \frac{(m^2 - n^2)h\nu_1}{(m - n)h/L} = (m + n)\frac{L}{\tau_1} = (m + n)V_1 \tag{9.3.16}$$

Predicting fractional revivals: Farey Sum \oplus_F of the rational fractions n_1/d_1 and n_2/d_2

$$t_{12\text{-intersection}} = \frac{n_2 + n_1}{d_2 + d_1} = \frac{n_2}{d_2} \oplus_F \frac{n_1}{d_1} \tag{9.3.18}$$

U(2)-Oscillation and R(3)-Rotation Analogies for 2-Dimension or Spin-1/2 Systems

General U(2) Hamiltonian Matrix	General U(2) State Vector $ \Psi\rangle =$
$\begin{pmatrix} A & B - iC \\ B + iC & D \end{pmatrix} =$	$\begin{pmatrix} \Psi_1 \\ \Psi_2 \end{pmatrix} = \begin{pmatrix} x_1 + i p_1 \\ x_2 + i p_2 \end{pmatrix}$
$\begin{pmatrix} 2\Omega_0 + \Omega_Z & \Omega_X - i\Omega_Y \\ \Omega_X + i\Omega_Y & 2\Omega_0 - \Omega_Z \end{pmatrix} \frac{1}{2}$	$= \sqrt{N} \begin{pmatrix} e^{-i\alpha/2} \cos \beta / 2 \\ e^{i\alpha/2} \sin \beta / 2 \end{pmatrix} e^{-i\frac{\gamma}{2}}$

Asymmetric Diagonal C_2^A	Bilateral (Balanced) C_2^B	Circular, Cyclotron, Curly C_2^C
$\mathbf{H} = \begin{pmatrix} A & 0 \\ 0 & D \end{pmatrix} = \Omega_0 \mathbf{1} + \Omega_A \sigma_A$	$\mathbf{H} = \begin{pmatrix} A & B \\ B & A \end{pmatrix} = \Omega_0 \mathbf{1} + \Omega_B \sigma_B$	$\mathbf{H} = \begin{pmatrix} A & -iC \\ iC & A \end{pmatrix} = \Omega_0 \mathbf{1} + \Omega_C \sigma_C$
$= \frac{A+D}{2} \begin{pmatrix} 1 & 0 \\ 0 & 1 \end{pmatrix} + \frac{A-D}{2} \begin{pmatrix} 1 & 0 \\ 0 & -1 \end{pmatrix}$	$= A \begin{pmatrix} 1 & 0 \\ 0 & 1 \end{pmatrix} + B \begin{pmatrix} 0 & 1 \\ 1 & 0 \end{pmatrix}$	$= A \begin{pmatrix} 1 & 0 \\ 0 & 1 \end{pmatrix} + C \begin{pmatrix} 0 & -i \\ i & 0 \end{pmatrix}$

Hermitian Hamilton-Jordan-Pauli-Jones ABC or XYZ operator basis for U(2) Hamiltonians

A - Type or Z - Spin Op	B - Type or X - Spin Op	C - Type or Y - Spin Op
$\frac{i\mathbf{q}_Z}{2} = \mathbf{J}_Z = \mathbf{S}_Z = \frac{\sigma_Z}{2}$	$\frac{i\mathbf{q}_X}{2} = \mathbf{J}_X = \mathbf{S}_X = \frac{\sigma_X}{2}$	$\frac{i\mathbf{q}_Y}{2} = \mathbf{J}_Y = \mathbf{S}_Y = \frac{\sigma_Y}{2}$
$= \mathbf{S}_A = \begin{pmatrix} 1 & 0 \\ 0 & -1 \end{pmatrix} \frac{1}{2}$	$= \mathbf{S}_B = \begin{pmatrix} 0 & 1 \\ 1 & 0 \end{pmatrix} \frac{1}{2}$	$= \mathbf{S}_C = \begin{pmatrix} 0 & -i \\ i & 0 \end{pmatrix} \frac{1}{2}$

A - Spin Expectation Value	B - Spin Expectation Value	C - Spin Expectation Value
$S_Z = S_A = \langle \Psi \mathbf{S}_Z \Psi \rangle$	$S_X = S_B = \langle \Psi \mathbf{S}_X \Psi \rangle$	$S_Y = S_C = \langle \Psi \mathbf{S}_Y \Psi \rangle$
$= N (p_1^2 + x_1^2 - p_2^2 - x_2^2) / 2$	$= N (x_1 x_2 + p_1 p_2)$	$= N (x_1 p_2 - x_2 p_1)$
$= (N/2) \cos \beta$	$= (N/2) \cos \alpha \sin \beta$	$= (N/2) \sin \alpha \sin \beta$
$= (\Psi_1^* \Psi_1 - \Psi_2^* \Psi_2) / 2$	$= \text{Re } \Psi_1^* \Psi_2$	$= \text{Im } \Psi_1^* \Psi_2$

$U(2)$ Hamiltonian Operator \mathbf{H} $U(2)$ \mathbf{H} in ABC notation

$$\mathbf{H} = \begin{pmatrix} A & B - iC \\ B + iC & D \end{pmatrix}$$

$$\begin{aligned} \mathbf{H} &= \Omega_0 \mathbf{1} + \mathbf{\Omega} \cdot \mathbf{S}, \quad \mathbf{\Omega} \cdot \mathbf{S} = \\ &= \Omega_X \mathbf{S}_X + \Omega_Y \mathbf{S}_Y + \Omega_Z \mathbf{S}_Z \\ &= \Omega_X \frac{\sigma_X}{2} + \Omega_Y \frac{\sigma_Y}{2} + \Omega_Z \frac{\sigma_Z}{2} \end{aligned}$$

$$\begin{aligned} \mathbf{H} &= \Omega_0 \mathbf{1} + \mathbf{\Omega} \cdot \mathbf{S}, \quad \mathbf{\Omega} \cdot \mathbf{S} = \\ &= (A - D) \mathbf{S}_A + 2B \mathbf{S}_B + 2C \mathbf{S}_C \\ &= \frac{A - D}{2} \sigma_Z + B \sigma_X + C \sigma_Y \end{aligned}$$

$$\begin{aligned} \Omega_Z = \Omega_A = H_{11} - H_{22} &= A - D & \Omega_X = \Omega_B = 2\text{Re}H_{21} &= 2B & \Omega_Y = \Omega_C = 2\text{Im}H_{21} &= 2C \\ &= \Omega \cos\vartheta \text{ (H-Crank A-Component)} & &= \Omega \cos\varphi \sin\vartheta \text{ (}\Omega \text{ B-Component)} & &= \Omega \sin\varphi \sin\vartheta \text{ (}\Omega \text{ C-Component)} \end{aligned}$$

Density Operator (Pure 2-state only) $\rho = |\Psi\rangle\langle\Psi| = \begin{pmatrix} \Psi_1 \\ \Psi_2 \end{pmatrix} \otimes \begin{pmatrix} \Psi_1^* & \Psi_2^* \end{pmatrix} = \begin{pmatrix} \Psi_1 \Psi_1^* & \Psi_1 \Psi_2^* \\ \Psi_2 \Psi_1^* & \Psi_2 \Psi_2^* \end{pmatrix}$

$$\begin{pmatrix} \rho_{11} & \rho_{12} \\ \rho_{21} & \rho_{22} \end{pmatrix} = \begin{pmatrix} \Psi_1^* \Psi_1 & \Psi_2^* \Psi_1 \\ \Psi_1^* \Psi_2 & \Psi_2^* \Psi_2 \end{pmatrix} = \rho = \frac{N}{2} \mathbf{1} + S_X \sigma_X + S_Y \sigma_Y + S_Z \sigma_Z = N/2 \mathbf{1} + \mathbf{S} \cdot \boldsymbol{\sigma}$$

Bloch equations. $i\hbar \frac{\partial}{\partial t} \rho = i\hbar \dot{\rho} = \mathbf{H}\rho - \rho\mathbf{H} = [\mathbf{H}, \rho]$ or: $\frac{\partial \mathbf{S}}{\partial t} = \dot{\mathbf{S}} = \mathbf{\Omega} \times \mathbf{S}$

Hamilton-Pauli Identities

$$(\mathbf{A} \cdot \boldsymbol{\sigma})(\mathbf{B} \cdot \boldsymbol{\sigma}) = \mathbf{A} \cdot \mathbf{B} + i(\mathbf{A} \times \mathbf{B}) \cdot \boldsymbol{\sigma}, \quad \sigma_\mu \sigma_\nu = \delta_{\mu\nu} \mathbf{1} + i \epsilon_{\mu\nu\lambda} \sigma_\lambda.$$

$SU(2)$ rotation matrix by rotation axis vector $\Theta = \Omega t$. and Two-state evolution operator

$$\begin{aligned} \mathbf{R}[\Theta] &= \cos\frac{\Theta}{2} \mathbf{1} - i\sigma_X \hat{\Theta}_X \sin\frac{\Theta}{2} - i\sigma_Y \hat{\Theta}_Y \sin\frac{\Theta}{2} - i\sigma_Z \hat{\Theta}_Z \sin\frac{\Theta}{2} \\ \begin{pmatrix} \langle 1 | \mathbf{R}[\Theta] | 1 \rangle & \langle 1 | \mathbf{R}[\Theta] | 2 \rangle \\ \langle 2 | \mathbf{R}[\Theta] | 1 \rangle & \langle 2 | \mathbf{R}[\Theta] | 2 \rangle \end{pmatrix} &= \begin{pmatrix} \cos\frac{\Theta}{2} - i\hat{\Theta}_Z \sin\frac{\Theta}{2} & -i\sin\frac{\Theta}{2}(\hat{\Theta}_X - i\hat{\Theta}_Y) \\ -i\sin\frac{\Theta}{2}(\hat{\Theta}_X + i\hat{\Theta}_Y) & \cos\frac{\Theta}{2} + i\hat{\Theta}_Z \sin\frac{\Theta}{2} \end{pmatrix} \end{aligned} \quad (10.5.25b)$$

The rotation axis is given by its *polar coordinates* (φ, ϑ) and *angle of turn* $\Theta = \sqrt{\Theta_X^2 + \Theta_Y^2 + \Theta_Z^2} = \Omega t$.

$$\Theta = (\Theta_X, \Theta_Y, \Theta_Z) = \Theta (\cos\varphi \sin\vartheta, \sin\varphi \sin\vartheta, \cos\vartheta) = (\Theta_B, \Theta_C, \Theta_A)$$

Unit rotation axis vector $\hat{\Theta} = \bar{\Theta} / |\Theta| = \begin{pmatrix} \hat{\Theta}_X & \hat{\Theta}_Y & \hat{\Theta}_Z \end{pmatrix} = \begin{pmatrix} \cos\varphi \sin\vartheta & \sin\varphi \sin\vartheta & \cos\vartheta \end{pmatrix}$

$$\begin{aligned} \mathbf{R}[\Theta] &= \begin{pmatrix} \cos\frac{\Theta}{2} - i\cos\vartheta \sin\frac{\Theta}{2} & -i\sin\frac{\Theta}{2}(\cos\varphi \sin\vartheta - i\sin\varphi \sin\vartheta) \\ -i\sin\frac{\Theta}{2}(\cos\varphi \sin\vartheta + i\sin\varphi \sin\vartheta) & \cos\frac{\Theta}{2} + i\cos\vartheta \sin\frac{\Theta}{2} \end{pmatrix} \\ &= \mathbf{R}[\varphi\vartheta\Theta] = \begin{pmatrix} \cos\frac{\Theta}{2} - i\cos\vartheta \sin\frac{\Theta}{2} & -ie^{-i\varphi} \sin\vartheta \sin\frac{\Theta}{2} \\ -ie^{i\varphi} \sin\vartheta \sin\frac{\Theta}{2} & \cos\frac{\Theta}{2} + i\cos\vartheta \sin\frac{\Theta}{2} \end{pmatrix} = e^{-i\mathbf{H}t} = e^{-i\mathbf{\Theta} \cdot \mathbf{S}} \end{aligned} \quad (10.5.25c)$$

Hamiltonian generator determines crank rate Ω .

$$\begin{aligned} \Omega_Z = \Omega_A = H_{11} - H_{22} &= A - D & \Omega_X = \Omega_B = 2\text{Re}H_{21} &= 2B & \Omega_Y = \Omega_C = 2\text{Im}H_{21} &= 2C \\ &= \Omega \cos\vartheta \text{ (H-Crank A-Component)} & &= \Omega \cos\varphi \sin\vartheta \text{ (}\Omega \text{ B-Component)} & &= \Omega \sin\varphi \sin\vartheta \text{ (}\Omega \text{ C-Component)} \end{aligned}$$

U(2)-R(3) Two-State and Spin-Vector Summary

Hamiltonian H *Hamiltonian Ω-vector Eigenvectors |ε⟩, |ε'⟩ and Spin expectation S-vector*
Operator & matrix in |1⟩, |2⟩-basis in ABC-space *in |1⟩, |2⟩-space* *in ABC-space*

$$\begin{aligned}
 \mathbf{H} &= \Omega_0 \mathbf{1} + \Omega \cdot \mathbf{S} \\
 &= \frac{(A+D)}{2} \mathbf{1} + (A-D) \mathbf{S}_A \\
 &\quad + 2B \mathbf{S}_B + 2C \mathbf{S}_C \\
 &= \begin{pmatrix} A & B-iC \\ B+iC & D \end{pmatrix}
 \end{aligned}
 \quad
 \bar{\Omega} = \begin{pmatrix} \Omega_A \\ \Omega_B \\ \Omega_C \end{pmatrix} = \begin{pmatrix} A-D \\ 2B \\ 2C \end{pmatrix}$$

$$\begin{aligned}
 |\varepsilon\rangle &= \begin{pmatrix} x_1 + ip_1 \\ x_2 + ip_2 \end{pmatrix} \\
 |\varepsilon'\rangle &= \begin{pmatrix} x'_1 + ip'_1 \\ x'_2 + ip'_2 \end{pmatrix}
 \end{aligned}
 \quad
 \mathbf{S} = \begin{pmatrix} S_A \\ S_B \\ S_C \end{pmatrix} = \begin{pmatrix} \langle \varepsilon | \mathbf{S}_A | \varepsilon \rangle \\ \langle \varepsilon | \mathbf{S}_B | \varepsilon \rangle \\ \langle \varepsilon | \mathbf{S}_C | \varepsilon \rangle \end{pmatrix}$$

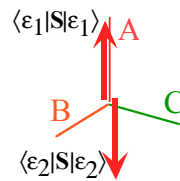
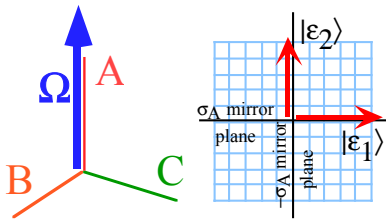
$$= \begin{pmatrix} \frac{x_1^2 + p_1^2 - x_2^2 - p_2^2}{2} \\ x_1 x_2 + p_1 p_2 \\ x_1 p_2 - x_2 p_1 \end{pmatrix}$$

A. Asymmetric – Diagonal

$$\mathbf{H}^A = \frac{(A+D)}{2} \mathbf{1} + (A-D) \mathbf{S}_A = \begin{pmatrix} A & 0 \\ 0 & D \end{pmatrix}$$

$$\bar{\Omega} = \begin{pmatrix} \Omega_A \\ \Omega_B \\ \Omega_C \end{pmatrix} = \begin{pmatrix} A-D \\ 0 \\ 0 \end{pmatrix}$$

$$\begin{aligned}
 |\varepsilon_1\rangle &= \begin{pmatrix} 1 \\ 0 \end{pmatrix} \\
 |\varepsilon_2\rangle &= \begin{pmatrix} 0 \\ 1 \end{pmatrix}
 \end{aligned}
 \quad
 \begin{aligned}
 \langle \varepsilon_1 | \mathbf{S}_A | \varepsilon_1 \rangle &= \begin{pmatrix} 1/2 \\ 0 \\ 0 \end{pmatrix} \\
 \langle \varepsilon_2 | \mathbf{S}_A | \varepsilon_2 \rangle &= \begin{pmatrix} -1/2 \\ 0 \\ 0 \end{pmatrix}
 \end{aligned}$$



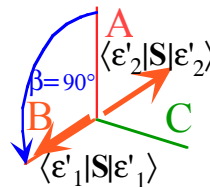
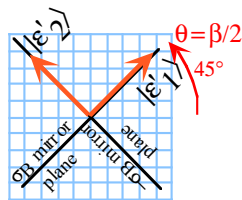
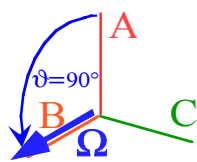
B. Bilateral – Balanced

$$\mathbf{H}^B = A \cdot \mathbf{1} + 2B \mathbf{S}_B = \begin{pmatrix} A & B \\ B & A \end{pmatrix}$$

$$\bar{\Omega} = \begin{pmatrix} \Omega_A \\ \Omega_B \\ \Omega_C \end{pmatrix} = \begin{pmatrix} 0 \\ 2B \\ 0 \end{pmatrix}$$

$$\begin{aligned}
 |\varepsilon'_1\rangle &= \begin{pmatrix} 1/\sqrt{2} \\ 1/\sqrt{2} \end{pmatrix} \\
 |\varepsilon'_2\rangle &= \begin{pmatrix} -1/\sqrt{2} \\ 1/\sqrt{2} \end{pmatrix}
 \end{aligned}
 \quad
 \begin{aligned}
 \langle \varepsilon'_1 | \mathbf{S}_A | \varepsilon'_1 \rangle &= \begin{pmatrix} 0 \\ 1/2 \\ 0 \end{pmatrix} \\
 \langle \varepsilon'_2 | \mathbf{S}_A | \varepsilon'_2 \rangle &= \begin{pmatrix} 0 \\ -1/2 \\ 0 \end{pmatrix}
 \end{aligned}$$

$$S_B = \frac{1}{2} \begin{pmatrix} 0 & 1 \\ 1 & 0 \end{pmatrix} = \frac{1}{2} \sigma_B$$



AB. Asymmetric – Bilateral

$$\mathbf{H}^{AB} = \frac{(A-D)}{2} \mathbf{1} + (A-D)\mathbf{S}_A + 2B\mathbf{S}_B = \begin{pmatrix} A & B \\ B & D \end{pmatrix}$$

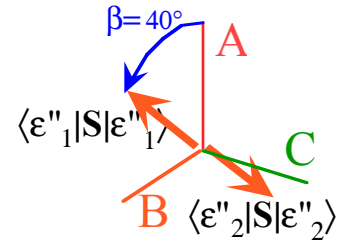
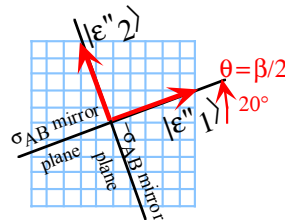
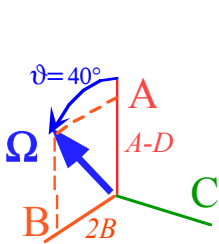
$$\bar{\Omega} = \begin{pmatrix} \Omega_A \\ \Omega_B \\ \Omega_C \end{pmatrix} = \begin{pmatrix} A-D \\ 2B \\ 0 \end{pmatrix}$$

$$|\epsilon_1'\rangle = \begin{pmatrix} \cos \theta \\ \sin \theta \end{pmatrix}$$

$$|\epsilon_2'\rangle = \begin{pmatrix} -\sin \theta \\ \cos \theta \end{pmatrix}$$

$$\begin{pmatrix} \langle \epsilon_1' | \mathbf{S}_A | \epsilon_1' \rangle \\ \langle \epsilon_1' | \mathbf{S}_B | \epsilon_1' \rangle \\ \langle \epsilon_1' | \mathbf{S}_C | \epsilon_1' \rangle \end{pmatrix} = \frac{1}{2} \begin{pmatrix} \cos \beta \\ \sin \beta \\ 0 \end{pmatrix}$$

$$\begin{pmatrix} \langle \epsilon_2' | \mathbf{S}_A | \epsilon_2' \rangle \\ \langle \epsilon_2' | \mathbf{S}_B | \epsilon_2' \rangle \\ \langle \epsilon_2' | \mathbf{S}_C | \epsilon_2' \rangle \end{pmatrix} = \frac{1}{2} \begin{pmatrix} -\cos \beta \\ -\sin \beta \\ 0 \end{pmatrix}$$



C. Circular – Complex

$$\mathbf{H}^C = A \cdot \mathbf{1} + 2C\mathbf{S}_C = \begin{pmatrix} A & -iC \\ iC & A \end{pmatrix}$$

$$\bar{\Omega} = \begin{pmatrix} \Omega_A \\ \Omega_B \\ \Omega_C \end{pmatrix} = \begin{pmatrix} 0 \\ 0 \\ 2C \end{pmatrix}$$

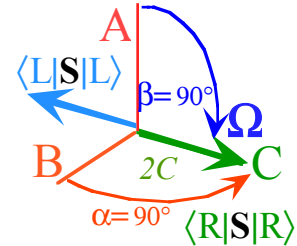
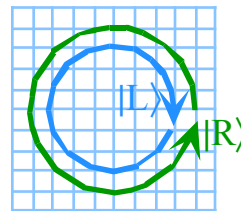
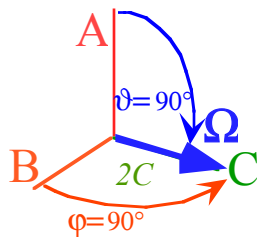
$$|R\rangle = \begin{pmatrix} 1/\sqrt{2} \\ i/\sqrt{2} \end{pmatrix}$$

$$|L\rangle = \begin{pmatrix} 1/\sqrt{2} \\ -i/\sqrt{2} \end{pmatrix}$$

$$\begin{pmatrix} \langle R | \mathbf{S}_A | R \rangle \\ \langle R | \mathbf{S}_B | R \rangle \\ \langle R | \mathbf{S}_C | R \rangle \end{pmatrix} = \begin{pmatrix} 0 \\ 0 \\ 1/2 \end{pmatrix}$$

$$\begin{pmatrix} \langle L | \mathbf{S}_A | L \rangle \\ \langle L | \mathbf{S}_B | L \rangle \\ \langle L | \mathbf{S}_C | L \rangle \end{pmatrix} = \begin{pmatrix} 0 \\ 0 \\ -1/2 \end{pmatrix}$$

$$S_C = \frac{1}{2} \begin{pmatrix} 0 & -i \\ i & 0 \end{pmatrix} = \frac{1}{2} \sigma_C$$



Polar Angle Descriptions of $U(2)$ Hamiltonian \mathbf{H} and its state space $|\epsilon\rangle, |\epsilon'\rangle \dots$

Crank Axis angles $(\varphi, \vartheta, \Omega)$ ($\Omega = \sqrt{\Omega_X^2 + \Omega_Y^2 + \Omega_Z^2}$)

Spin Vector Euler angles (α, β, γ)

$$\mathbf{H} = \Omega_0 \mathbf{1} + \bar{\Omega} \cdot \mathbf{S} = \frac{1}{2} \begin{pmatrix} 2\Omega_0 + \Omega_Z & \Omega_X - i\Omega_Y \\ \Omega_X + i\Omega_Y & 2\Omega_0 - \Omega_Z \end{pmatrix}$$

$$\bar{\Omega} = \begin{pmatrix} \Omega_A \\ \Omega_B \\ \Omega_C \end{pmatrix} = \begin{pmatrix} A-D \\ 2B \\ 2C \end{pmatrix} = \Omega \begin{pmatrix} \cos \vartheta \\ \cos \varphi \sin \vartheta \\ \sin \varphi \sin \vartheta \end{pmatrix}$$

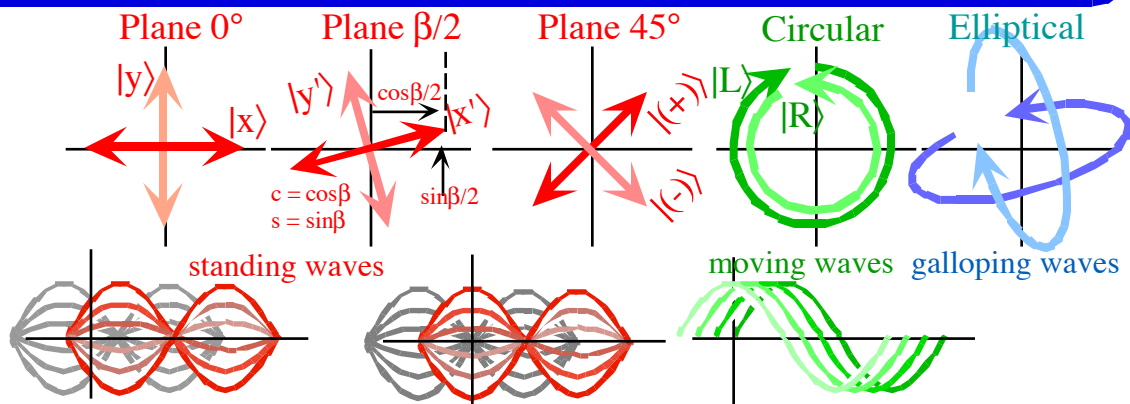
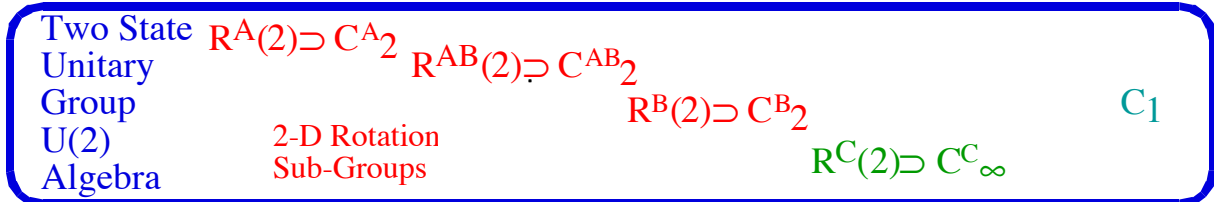
$$|\epsilon\rangle = \begin{pmatrix} e^{-i\alpha/2} \cos \beta / 2 \\ e^{i\alpha/2} \sin \beta / 2 \end{pmatrix} e^{-i\gamma/2}$$

$$|\epsilon'\rangle = \begin{pmatrix} -e^{-i\alpha/2} \sin \beta / 2 \\ e^{i\alpha/2} \cos \beta / 2 \end{pmatrix} e^{-i\gamma/2}$$

$$\mathbf{S} = \begin{pmatrix} S_A \\ S_B \\ S_C \end{pmatrix} = \begin{pmatrix} \langle \epsilon | \mathbf{S}_A | \epsilon \rangle \\ \langle \epsilon | \mathbf{S}_B | \epsilon \rangle \\ \langle \epsilon | \mathbf{S}_C | \epsilon \rangle \end{pmatrix} = \begin{pmatrix} \cos \beta \\ \cos \alpha \sin \beta \\ \sin \alpha \sin \beta \end{pmatrix}$$

Catalog of Two-State Hamiltonians

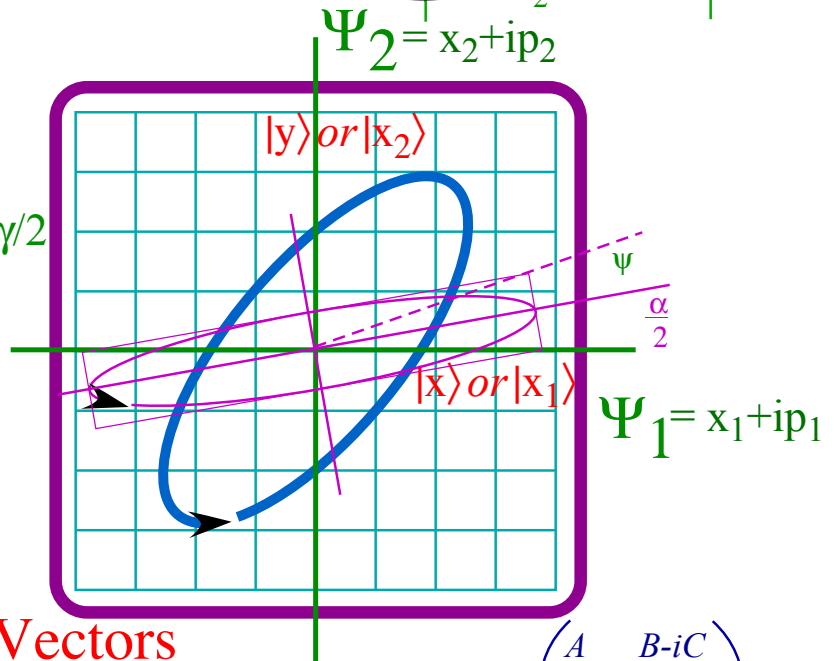
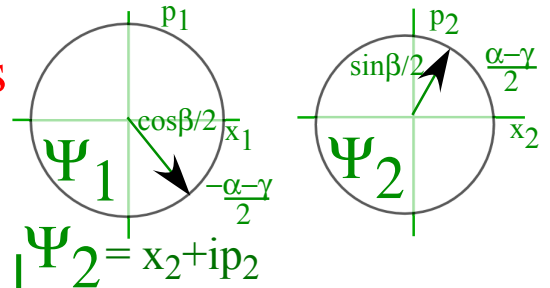
$H = H^\dagger =$	$H_{U(2)} =$ $\begin{pmatrix} A & 0 \\ 0 & A \end{pmatrix}$	$H_{C_2^A} =$ $\begin{pmatrix} A & 0 \\ 0 & D \end{pmatrix}$	$H_{C_2^{AB}} =$ $\begin{pmatrix} A & B \\ B & D \end{pmatrix}$	$H_{C_2^B} =$ $\begin{pmatrix} A & B \\ B & A \end{pmatrix}$	$H_{C_2^C} =$ $\begin{pmatrix} A & -iC \\ iC & A \end{pmatrix}$	$H_{C_1} =$ $\begin{pmatrix} A & B - iC \\ B + iC & D \end{pmatrix}$
Commute with:	$U = \begin{pmatrix} U_{11} & U_{12} \\ U_{21} & U_{22} \end{pmatrix}$	$R(\theta) = \begin{pmatrix} e^{-i\theta} & 0 \\ 0 & e^{i\theta} \end{pmatrix}$	$R(\zeta) = \begin{pmatrix} \cos \zeta & -is \sin \zeta \\ -ic \sin \zeta & \cos \zeta \\ -is \sin \zeta & +ic \sin \zeta \end{pmatrix}$	$R(\chi) = \begin{pmatrix} \cos \chi & -i \sin \chi \\ -i \sin \chi & \cos \chi \end{pmatrix}$	$R(\varphi) = \begin{pmatrix} \cos \varphi & -\sin \varphi \\ \sin \varphi & \cos \varphi \end{pmatrix}$	$\mathbf{1}(\lambda) = e^{i\lambda} \begin{pmatrix} 1 & 0 \\ 0 & 1 \end{pmatrix}$
Generated by:	$e_{11} = \begin{pmatrix} 1 & 0 \\ 0 & 0 \end{pmatrix}$ $e_{12} = \begin{pmatrix} 0 & 1 \\ 0 & 0 \end{pmatrix}$ $e_{21} = \begin{pmatrix} 0 & 0 \\ 1 & 0 \end{pmatrix}$ $e_{22} = \begin{pmatrix} 0 & 0 \\ 0 & 1 \end{pmatrix}$	$G_A = \left. \frac{dR(\theta)}{d\theta} \right _0 = \begin{pmatrix} -i & 0 \\ 0 & i \end{pmatrix}$	$G_{AB} = \left. \frac{dR(\zeta)}{d\zeta} \right _0 = \begin{pmatrix} -ic & -is \\ -is & ic \end{pmatrix}$	$G_B = \left. \frac{dR(\chi)}{d\chi} \right _0 = \begin{pmatrix} 0 & -i \\ -i & 0 \end{pmatrix}$	$G_C = \left. \frac{dR(\varphi)}{d\varphi} \right _0 = \begin{pmatrix} 0 & -1 \\ 1 & 0 \end{pmatrix}$	$G_1 = \left. \frac{dR(\lambda)}{d\lambda} \right _0 = \begin{pmatrix} 1 & 0 \\ 0 & 1 \end{pmatrix}$
Spin Operator:	(all)	$\sigma_A = iG_A = \begin{pmatrix} 1 & 0 \\ 0 & -1 \end{pmatrix}$	$\sigma_{AB} = iG_{AB} = \begin{pmatrix} c & s \\ s & -c \end{pmatrix}$	$\sigma_B = iG_B = \begin{pmatrix} 0 & 1 \\ 1 & 0 \end{pmatrix}$	$\sigma_C = iG_C = \begin{pmatrix} 0 & -i \\ i & 0 \end{pmatrix}$	$\sigma_0 = \begin{pmatrix} 1 & 0 \\ 0 & 1 \end{pmatrix}$
Symmetry:	U(2)	$C_2^A \subset R^A(2)$	$C_2^{AB} \subset R^{AB}(2)$	$C_2^B \subset R^B(2)$	$C_2^C \subset R^C(2)$	C_1
H Eigenkets	(Anyket is an eigenvector)	$ x\rangle, y\rangle$ $\begin{pmatrix} 1 \\ 0 \end{pmatrix}, \begin{pmatrix} 0 \\ 1 \end{pmatrix}$	$ x'\rangle, y'\rangle$ $\begin{pmatrix} \cos \frac{\beta}{2} \\ \sin \frac{\beta}{2} \end{pmatrix}, \begin{pmatrix} -\sin \frac{\beta}{2} \\ \cos \frac{\beta}{2} \end{pmatrix}$	$ +\rangle, -\rangle$ $\frac{1}{\sqrt{2}} \begin{pmatrix} 1 \\ 1 \end{pmatrix}, \frac{1}{\sqrt{2}} \begin{pmatrix} 1 \\ -1 \end{pmatrix}$	$ L\rangle, R\rangle$ $\frac{1}{\sqrt{2}} \begin{pmatrix} 1 \\ -i \end{pmatrix}, \frac{1}{\sqrt{2}} \begin{pmatrix} 1 \\ i \end{pmatrix}$	$ \epsilon\rangle$ Depends on A, B, C, and D



U(2) World : Complex 2D Spinors

2-State ket $|\Psi\rangle =$

$$\begin{pmatrix} \Psi_1 \\ \Psi_2 \end{pmatrix} = \begin{pmatrix} \sqrt{N}e^{-i\alpha/2}\cos\beta/2 \\ \sqrt{N}e^{i\alpha/2}\sin\beta/2 \end{pmatrix} e^{-i\gamma/2}$$



R(3) World : Real 3D Vectors

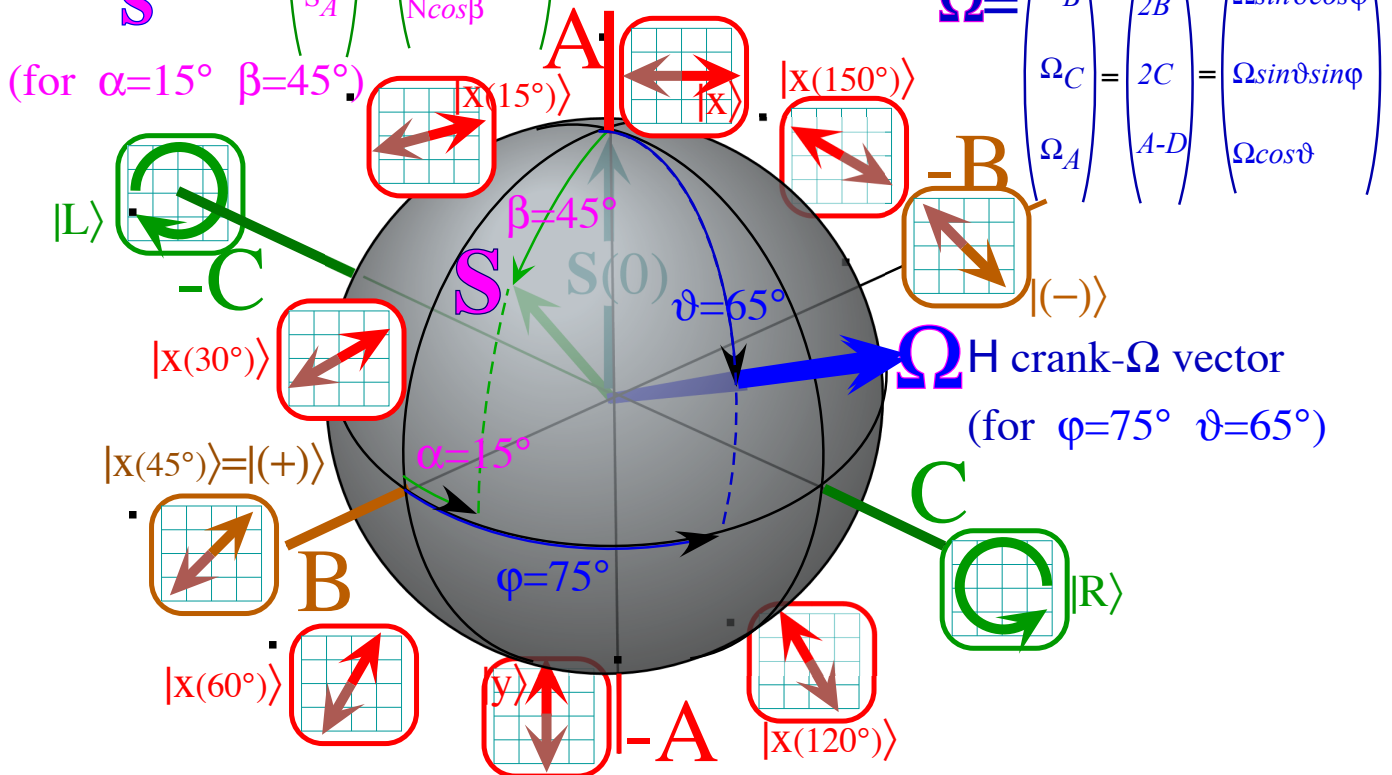
$|\Psi\rangle$ State Spin Vector \mathbf{S}

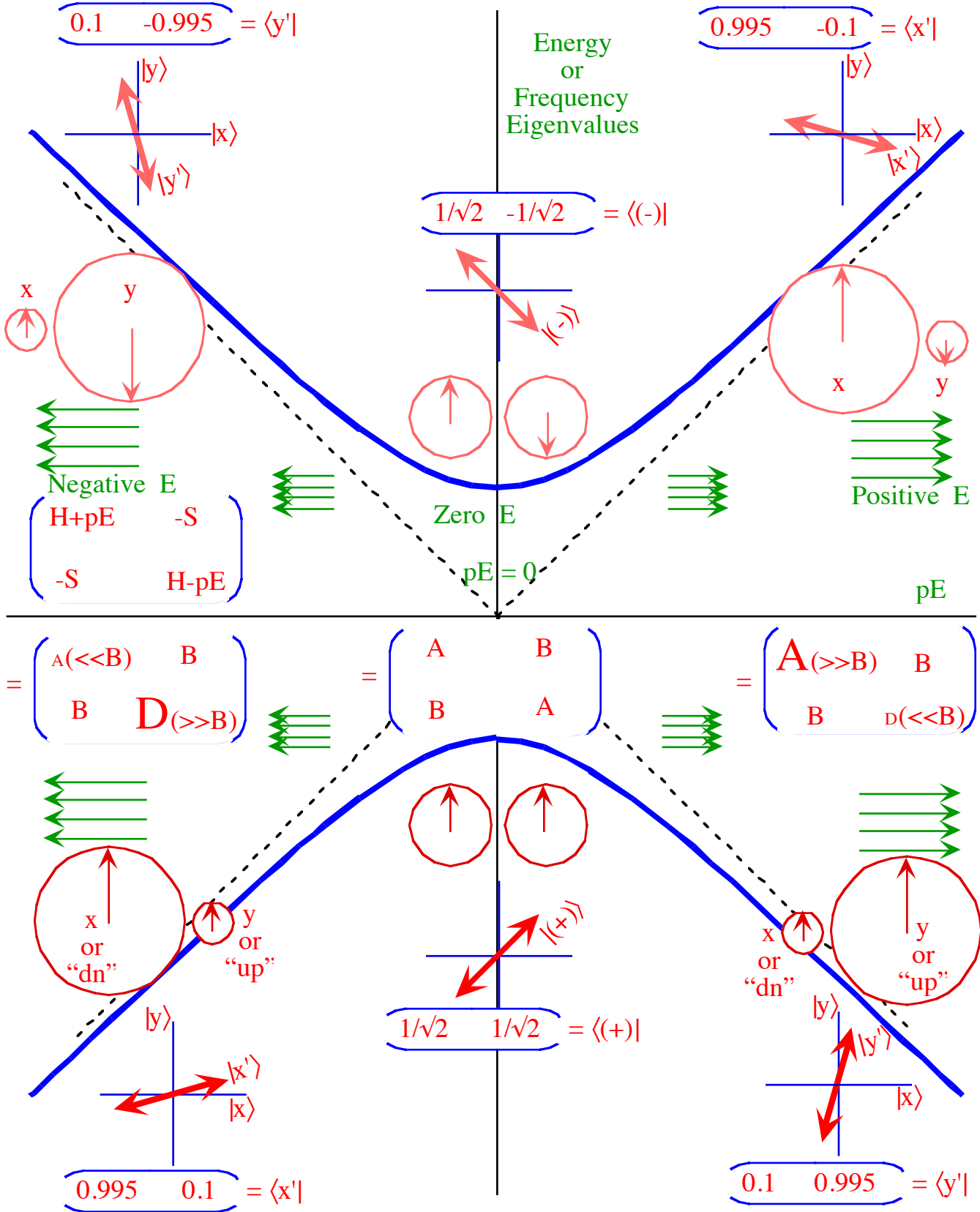
$$\begin{pmatrix} S_B \\ S_C \\ S_A \end{pmatrix} = \begin{pmatrix} N\sin\beta\cos\alpha \\ N\sin\beta\sin\alpha \\ N\cos\beta \end{pmatrix} \frac{1}{2}$$

H-Operator Angular velocity

$$\begin{pmatrix} A & B-iC \\ B+iC & D \end{pmatrix}$$

$$\Omega = \begin{pmatrix} \Omega_B \\ \Omega_C \\ \Omega_A \end{pmatrix} = \begin{pmatrix} 2B \\ 2C \\ A-D \end{pmatrix} = \begin{pmatrix} \Omega\sin\vartheta\cos\phi \\ \Omega\sin\vartheta\sin\phi \\ \Omega\cos\vartheta \end{pmatrix}$$

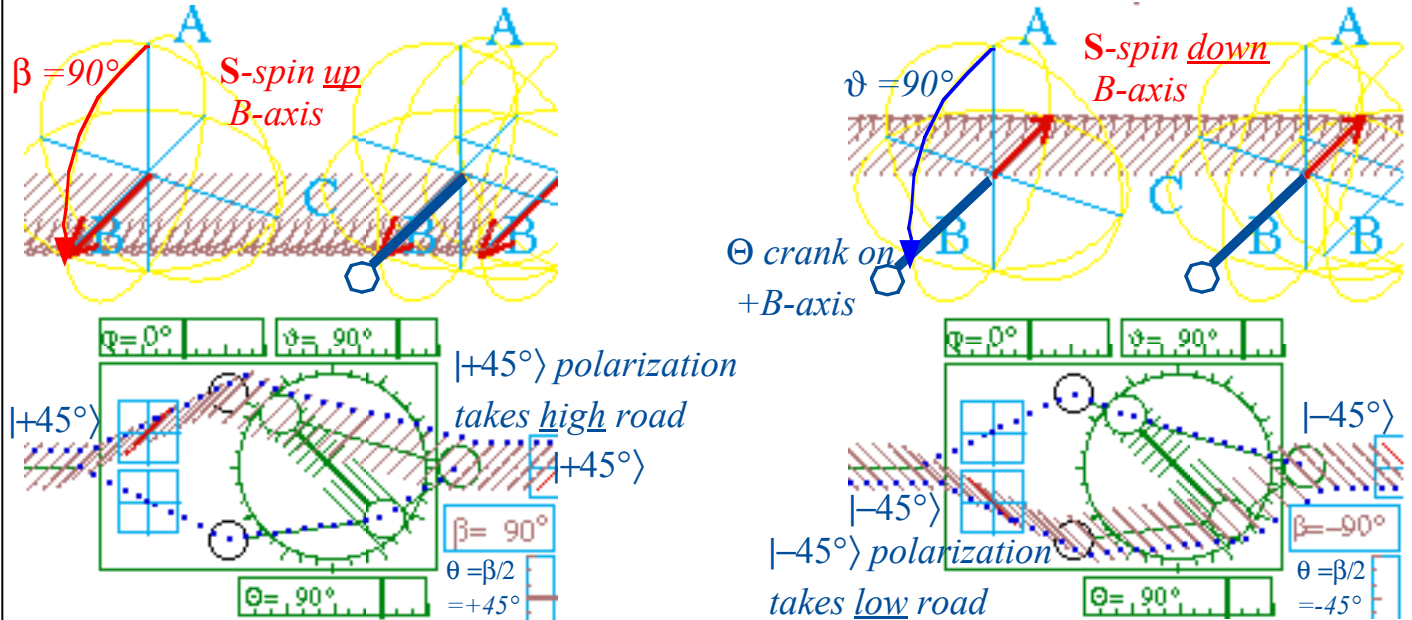




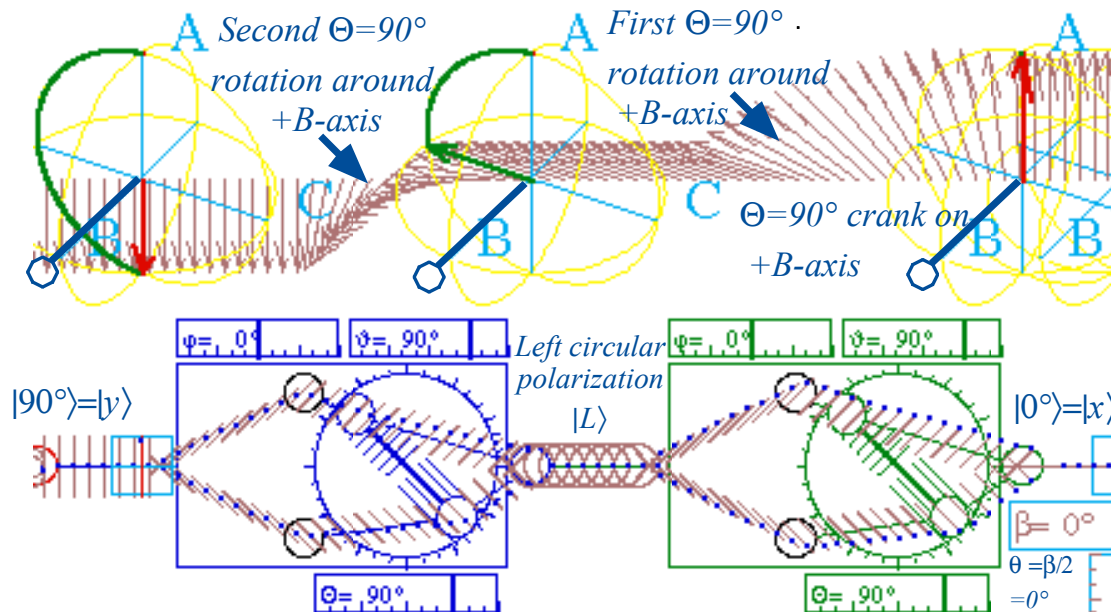
Avoided-crossing Hyperbolas. Eigenvalues and eigenstates of AB-symmetry Stark-effects.

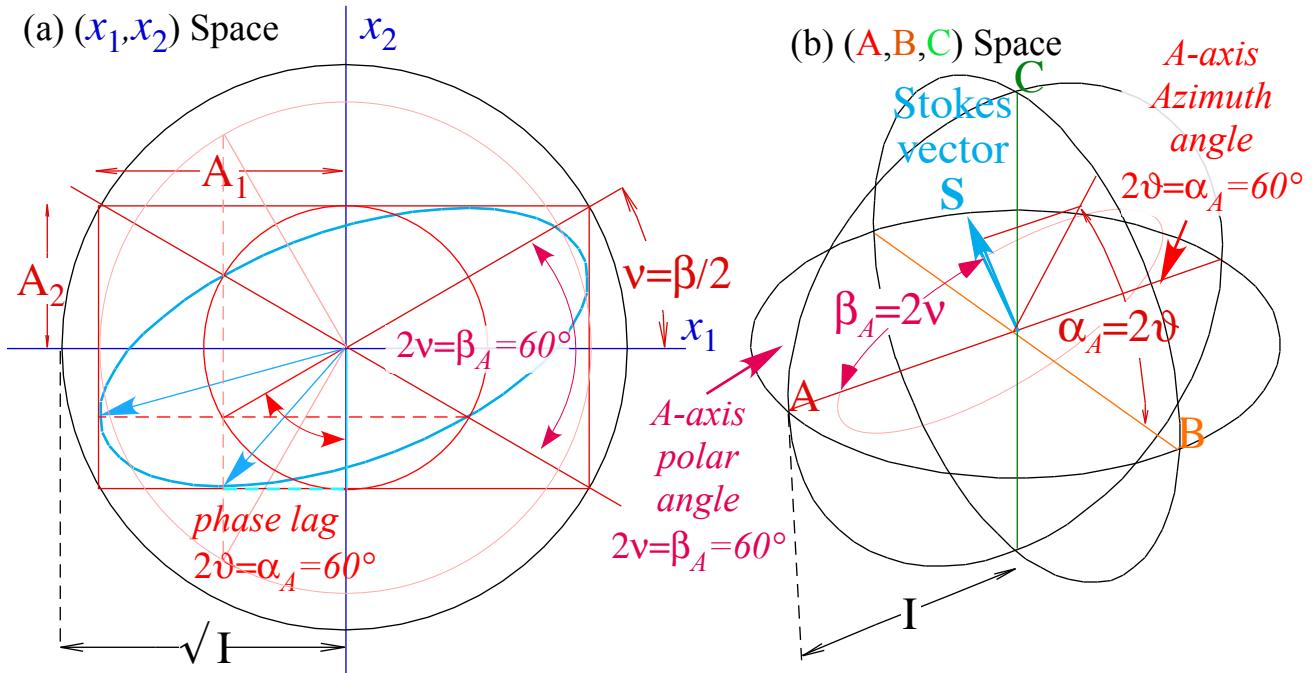
Easy eigensolution and evolution for polarizer-analyzers based on spin-crank alignment

The behavior of spin-1/2 or optical polarization states inside analyzers is easy to understand and calculate using the polar angles (α, β) of the state spin vector \mathbf{S} and the polar angles (φ, ϑ) of the analyzer crank Θ . The first eigenstate (own-state) of the analyzer which flies through the upper path unscathed (except for phase shift) is simply one whose \mathbf{S} angles (α, β) equal the angles (φ, ϑ) of crank Θ , that is, a state whose spin \mathbf{S} lies along analyzer crank Θ , or $\alpha = \varphi$ and $\beta = \vartheta$. The second eigenstate which flies through the lower path is a state whose spin \mathbf{S} lies opposite to the analyzer crank Θ , so $\alpha = \varphi$ and $\beta = \vartheta - \pi$. Below $\vartheta = 90^\circ$ and $\varphi = 0^\circ$ so the eigenstates have spin up-B ($\beta = 90^\circ$ and $\alpha = 0^\circ$) or else spin down-B ($\beta = -90^\circ$ and $\alpha = 0^\circ$).



However, other polarization states such as $|x\rangle$ (spin- \mathbf{S} along the A -axis) are changed by going through the analyzer. Now the $\Theta = 90^\circ$ shift of one path over the other has the effect of rotating the spin vector by $\Theta = 90^\circ$. So the first analyzer takes $|x\rangle$ into $|L\rangle$ (left circular or spin down- C) and another identical analyzer takes $|L\rangle$ into $|y\rangle$ (vertical or spin down- A). Each of these analyzers acts like a *quarter-wave plate*.





Unit 3 Chapter 10 Appendices A-B: Coordinate Analysis of U(2) States

Appendix 10.A. U(2) Angles and Spin Rotation Operators.....	2
(a) Equivalence transformations of rotations	5
(b) Euler equivalence transformations of 3-vectors	5
(c) Euler angle goniometer: Double valued position	6
(d) Axis angle rotation: Double valued operation	11
(1) Combining rotations: U(2) group products	13
(2) Mirror reflections and Hamilton's turns.....	13
(3) Similarity transformation and Hamilton's turns.....	16
(e) Quaternion and spinor algebra (again).....	16
Why rotations are such a big deal	17
Appendix 10.B Spin control and ellipsometry.....	1
(a). Polarization ellipsometry coordinate angles.....	5
(1) Type-A ellipsometry Euler angles	6
(2) Type-C ellipsometry Euler angles	8
(b) Beam evolution of polarization	11
Problems for Appendix 10.A and B	13

Appendix 10.A. $U(2)$ Angles and Spin Rotation Operators

Every $U(2)$ state $|\Psi(\alpha\beta\gamma)\rangle$ can be obtained from an original base state $|1\rangle$ by doing three rotations shown in Fig. 10.A.1, the first by γ around the Z (or A) axes, the second by β around Y (or C) and the third by α around Z again. This “favors” the Z -axis. Equivalent axial choices are discussed in Appendix 10.B.

$$\begin{aligned} |\Psi\rangle &= \mathbf{R}(\alpha\beta\gamma)|1\rangle = \mathbf{R}(\alpha \text{ around } Z) \mathbf{R}(\beta \text{ around } Y) \mathbf{R}(\gamma \text{ around } Z) |1\rangle \\ &= \begin{pmatrix} e^{-i\frac{\alpha}{2}} & 0 \\ 0 & e^{i\frac{\alpha}{2}} \end{pmatrix} \begin{pmatrix} \cos\frac{\beta}{2} & -\sin\frac{\beta}{2} \\ \sin\frac{\beta}{2} & \cos\frac{\beta}{2} \end{pmatrix} \begin{pmatrix} e^{-i\frac{\gamma}{2}} & 0 \\ 0 & e^{i\frac{\gamma}{2}} \end{pmatrix} \begin{pmatrix} 1 \\ 0 \end{pmatrix} \end{aligned}$$

A matrix representation of this gives exactly the original state definition (10.5.8a) with unit norm ($N=1$).

$$\begin{aligned} \mathbf{R}(\alpha\beta\gamma)|1\rangle &= \mathbf{R}(\alpha \ 00) \mathbf{R}(0\beta \ 0) \mathbf{R}(00\gamma) |1\rangle = |\Psi\rangle \\ &= \begin{pmatrix} e^{-i\frac{\alpha+\gamma}{2}} \cos\frac{\beta}{2} & -e^{-i\frac{\alpha-\gamma}{2}} \sin\frac{\beta}{2} \\ e^{i\frac{\alpha-\gamma}{2}} \sin\frac{\beta}{2} & e^{i\frac{\alpha+\gamma}{2}} \cos\frac{\beta}{2} \end{pmatrix} \begin{pmatrix} 1 \\ 0 \end{pmatrix} = \begin{pmatrix} e^{-i\frac{\alpha}{2}} \cos\frac{\beta}{2} \\ e^{i\frac{\alpha}{2}} \sin\frac{\beta}{2} \end{pmatrix} e^{-i\frac{\gamma}{2}} \end{aligned} \quad (10.A.1a)$$

The resulting *Euler* ($\alpha\beta\gamma$)-angle matrix is simpler in form and construction than the Θ -axis matrix (10.5.25c) using $[\varphi, \vartheta, \Theta]$ angles. Do not confuse the two kinds of angles! We use parentheses () around Euler angles as in $\mathbf{R}(\alpha\beta\gamma)$ while square braces [] are used when a rotation is labeled $\mathbf{R}[\varphi, \vartheta, \Omega t = \Theta]$ by axis-angles. It is important to relate the two. A Hamilton expansion of $\mathbf{R}(\alpha\beta\gamma)$ yields its Θ -axis.

$$\begin{aligned} \mathbf{R}(\alpha\beta\gamma) &= \begin{pmatrix} e^{-i\frac{\alpha+\gamma}{2}} \cos\frac{\beta}{2} & -e^{-i\frac{\alpha-\gamma}{2}} \sin\frac{\beta}{2} \\ e^{i\frac{\alpha-\gamma}{2}} \sin\frac{\beta}{2} & e^{i\frac{\alpha+\gamma}{2}} \cos\frac{\beta}{2} \end{pmatrix} = \cos\frac{\alpha+\gamma}{2} \cos\frac{\beta}{2} \begin{pmatrix} 1 & 0 \\ 0 & 1 \end{pmatrix} \\ &\quad -i \begin{pmatrix} 0 & 1 \\ 1 & 0 \end{pmatrix} \sin\frac{\gamma-\alpha}{2} \sin\frac{\beta}{2} - i \begin{pmatrix} 0 & -i \\ i & 0 \end{pmatrix} \cos\frac{\gamma-\alpha}{2} \sin\frac{\beta}{2} - i \begin{pmatrix} 1 & 0 \\ 0 & -1 \end{pmatrix} \sin\frac{\alpha+\gamma}{2} \cos\frac{\beta}{2} \end{aligned} \quad (10.A.1b)$$

We equate $\mathbf{R}(\alpha\beta\gamma)$'s expansion term-by-term to the Θ -axis-angle $\mathbf{R}[\varphi, \vartheta, \Theta]$ expansion (10.5.25a-c).

$$\begin{aligned} \mathbf{R}[\hat{\Theta}] &= \begin{pmatrix} \cos\frac{\Theta}{2} - i\hat{\Theta}_Z \sin\frac{\Theta}{2} & -i\sin\frac{\Theta}{2}(\hat{\Theta}_X - i\hat{\Theta}_Y) \\ -i\sin\frac{\Theta}{2}(\hat{\Theta}_X + i\hat{\Theta}_Y) & \cos\frac{\Theta}{2} + i\hat{\Theta}_Z \sin\frac{\Theta}{2} \end{pmatrix} = \cos\frac{\Theta}{2} \begin{pmatrix} 1 & 0 \\ 0 & 1 \end{pmatrix} \\ &\quad -i \begin{pmatrix} 0 & 1 \\ 1 & 0 \end{pmatrix} \hat{\Theta}_X \sin\frac{\Theta}{2} - i \begin{pmatrix} 0 & -i \\ i & 0 \end{pmatrix} \hat{\Theta}_Y \sin\frac{\Theta}{2} - i \begin{pmatrix} 1 & 0 \\ 0 & -1 \end{pmatrix} \hat{\Theta}_Z \sin\frac{\Theta}{2} \end{aligned} \quad (10.5.25a-c)\text{repeated}$$

The Re-Im 4-D phasor coordinates ($x_j = \text{Re}\Psi_j$, $p_j = \text{Im}\Psi_j$) show up in the Euler vs. Axis angle relations.

$$\begin{aligned} x_1 &= \cos[(\gamma+\alpha)/2] \cos\beta/2 = \cos\Theta/2 \\ -p_2 &= \sin[(\gamma-\alpha)/2] \sin\beta/2 = \hat{\Theta}_X \sin\Theta/2 = \cos\varphi \sin\vartheta \sin\Theta/2 \\ x_2 &= \cos[(\gamma-\alpha)/2] \sin\beta/2 = \hat{\Theta}_Y \sin\Theta/2 = \sin\varphi \sin\vartheta \sin\Theta/2 \\ -p_1 &= \sin[(\gamma+\alpha)/2] \cos\beta/2 = \hat{\Theta}_Z \sin\Theta/2 = \cos\vartheta \sin\Theta/2 \end{aligned} \quad (10.A.1c)$$

Solving these relations yields the following Euler angles in terms of axis angles

$$\alpha = \varphi - \pi/2 + T, \quad \beta = 2\sin^{-1}(\sin\Omega/2 \sin\vartheta), \quad \gamma = \pi/2 - \varphi + T, \quad (10.A.1d)$$

where; $T = \tan^{-1}(\tan(\Omega/2) \cos\vartheta)$ while the axis-angles in terms of Euler angles are

$$\varphi = (\alpha - \gamma + \pi)/2, \quad \vartheta = \tan^{-1}[\tan\beta/2 / \sin(\alpha + \gamma)/2], \quad \Omega = 2 \cos^{-1}[\cos\beta/2 \cos(\alpha + \gamma)/2]. \quad (10.A.1e)$$

It is important to understand the practical difference between Euler angles ($\alpha\beta\gamma$) and axis angles $[\varphi, \vartheta, \Theta]$. Euler angles ($\alpha\beta\gamma$) are coordinates of rotated states of position while axis-angles $[\varphi, \vartheta, \Theta]$ are parameters of rotation operators or angular velocity. Euler angles ($\alpha\beta\gamma$) serve as convenient polar coordinates of spin vectors \mathbf{S} (Recall Fig. 10.5.2) and for orbiting or spinning bodies as shown below, while axis angles $[\varphi, \vartheta, \Theta]$ are the polar coordinates and rotation angle of a crank-axis Ω for an operation. Euler angles ($\alpha\beta\gamma$) label the state and density operator of a $U(2)$ system, while axis angles $[\varphi, \vartheta, \Theta]$ label its Hamiltonian and time-evolution operator. Euler ($\alpha\beta\gamma$) tell where \mathbf{S} is; axis $[\varphi, \vartheta, \Omega]$ where it's going.

Fig. 10.A.1 shows explicitly how to construct a general spin state or density operator labeled by Euler ($\alpha\beta\gamma$)-angles by illustrating the sequence of rotations: (1) **Z**-rotation $\mathbf{R}(00\gamma)$ by angle γ , followed by (2) **Y**-rotation $\mathbf{R}(0\beta0)$ by angle β , followed by (3) **Z**-rotation $\mathbf{R}(\alpha00)$ by angle α . The result is a spin vector \mathbf{S} pointing with polar angle β or beta (often labeled by its rhyme sake 'theta') and an azimuthal angle α (often labeled with a 'phi'), in exact agreement with (10.5.8c) and Example 7 in Fig. 10.5.4.

One new 'twist' added here is not found in other treatments of $U(2)$. We interpret the third Euler angle γ and overall phase or gauge factor $e^{-i\gamma/2}$ in (10.A.1a) as a twist of a rigid body attached to the spin \mathbf{S} -vector. Indeed, the first Z-rotation $\mathbf{R}(00\gamma)$ by angle γ twists the spin vector as shown in the upper right hand γ -part of Fig. 10.A.1. This means that the overall phase, which got canceled out of the 3D-density - spin-operator formulas involving $\Psi^*\Psi$ quantities, is still present if we consider a 3D spin-body instead of just a spin vector. Twisting a spin vector by γ does nothing if it's just a line, but a solid vector body actually "feels" a twist by γ . Nuclear, molecular and atomic spin rotations all have a twist angle.

A note of caution is in order with respect to exponential operator notation. Axis angle operations were given in (10.5.15) using a single exponential-of-a-sum expression.

$$\mathbf{R}[\vec{\Theta}] = e^{-i\vec{\Theta}\cdot\mathbf{S}} = e^{-i(\Theta_x\mathbf{S}_x + \Theta_y\mathbf{S}_y + \Theta_z\mathbf{S}_z)} = e^{-i\Theta(\hat{\Theta}_x\mathbf{S}_x + \hat{\Theta}_y\mathbf{S}_y + \hat{\Theta}_z\mathbf{S}_z)} \quad (10.A.2a)$$

Euler angle operation (10.A.1a) is a product of three separate single exponentials.

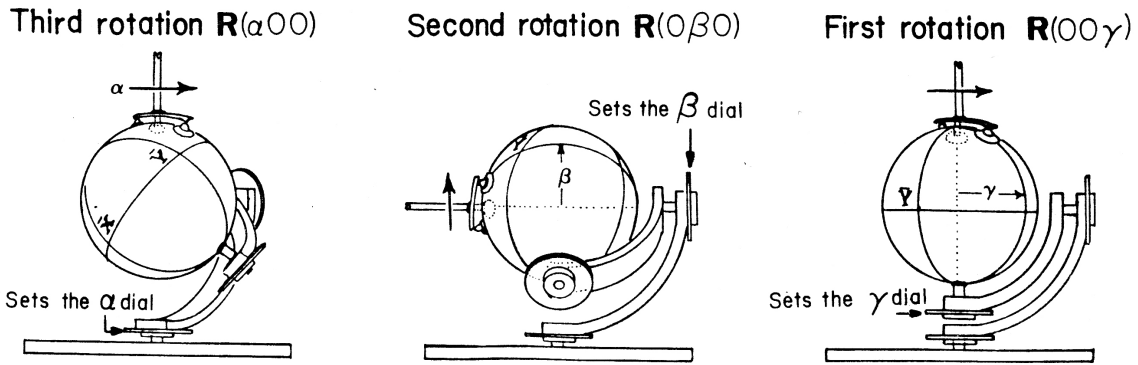
$$\mathbf{R}(\alpha\beta\gamma) = e^{-i\alpha\mathbf{S}_z} e^{-i\beta\mathbf{S}_y} e^{-i\gamma\mathbf{S}_z} \quad (10.A.2b)$$

Unless operators \mathbf{A} and \mathbf{B} commute, you cannot combine $e^{i\mathbf{A}} e^{i\mathbf{B}}$ into $e^{i(\mathbf{A}+\mathbf{B})}$ nor can you factor $e^{i(\mathbf{A}+\mathbf{B})}$.

In rare cases (and this is one of them) where two operators commute with their commutator you can write

$$e^{\mathbf{A}} e^{\mathbf{B}} e^{-[\mathbf{A},\mathbf{B}]} = e^{(\mathbf{A}+\mathbf{B})} = e^{\mathbf{B}} e^{\mathbf{A}} e^{[\mathbf{A},\mathbf{B}]} \quad \text{if: } [\mathbf{A}, [\mathbf{A}, \mathbf{B}]] = 0 = [\mathbf{A}, [\mathbf{A}, \mathbf{B}]] \quad (10.A.3)$$

This is the first part of what is known as the *Baker-Campbell-Hausdorff theorem*.



Sequence $R(\alpha 0 0)R(0 \beta 0)R(0 0 \gamma)$ sets Euler Angle position state $|\alpha \beta \gamma\rangle$
 using Z-rotation $R(\alpha 0 0)$ following Y-rotation $R(0 \beta 0)$ following Z-rotation $R(0 0 \gamma) = R(\gamma 0 0)$

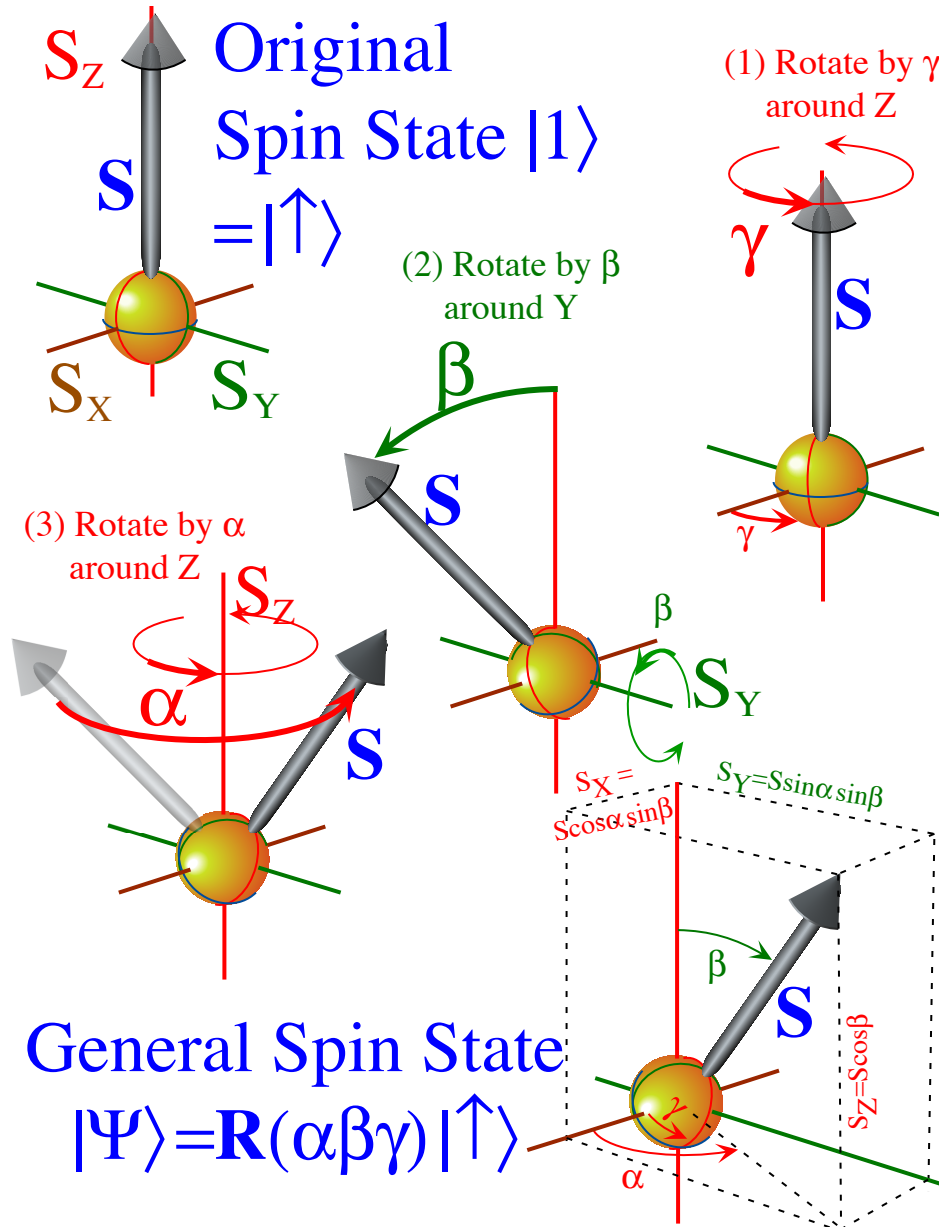


Fig. 10.A.1 The operational definition of Euler $(\alpha \beta \gamma)$ -angle coordinates applied to a spin-state.

(a) Equivalence transformations of rotations

Another way to factor the axis-angle expression (10.A.2a) is to find a transformation \mathbf{T} that builds the rotation $\mathbf{R}[\varphi, \vartheta, \Theta]$ by Θ about an axis Θ at polar angle (φ, ϑ) out of a Z -axis twist rotation $e^{-i\Theta\mathbf{S}_Z}$.

$$\mathbf{R}[\varphi, \vartheta, \Theta] = \mathbf{T} e^{-i\Theta\mathbf{S}_Z} \mathbf{T}^\dagger \quad (10.A.4)$$

The desired transformation \mathbf{T} is just the Euler operation $\mathbf{R}(\varphi\vartheta 0)$ such as was diagrammed in Fig. 10.A.1, only we leave off the twist γ since it would just cancel out. Effectively, we take the Θ -axis from polar-angle location $[\varphi, \vartheta]$ to the Z -axis with an inverse Euler-op $\mathbf{T}^\dagger = \mathbf{R}^\dagger(\varphi\vartheta 0)$, then do the Z -twist $e^{-i\Theta\mathbf{S}_Z}$, and finally, return the axis to its original (φ, ϑ) -position with the Euler rotation (*sans* twist) $\mathbf{T} = \mathbf{R}(\varphi\vartheta 0)$.

$$\mathbf{R}[\varphi, \vartheta, \Theta] = \mathbf{R}(\varphi\vartheta 0) e^{-i\Theta\mathbf{S}_Z} \mathbf{R}^\dagger(\varphi\vartheta 0) = \mathbf{R}(\varphi\vartheta 0) \mathbf{R}(00\Theta) \mathbf{R}^\dagger(\varphi\vartheta 0) \quad (10.A.5a)$$

Expanding the Euler rotations using (10.A.2b) gives (Note: $\mathbf{R}^\dagger(0\vartheta 0) = \mathbf{R}(0-\vartheta 0)$ and $\mathbf{R}^\dagger\mathbf{S}^\dagger = (\mathbf{S}\mathbf{R})^\dagger$)

$$\mathbf{R}[\varphi, \vartheta, \Theta] = \mathbf{R}(\varphi 0 0) \mathbf{R}(0\vartheta 0) \mathbf{R}(00\Theta) \mathbf{R}(0-\vartheta 0) \mathbf{R}(-\varphi 0 0) \quad (10.A.5b)$$

$$\mathbf{R}[\varphi, \vartheta, \Theta] = e^{-i\varphi\mathbf{S}_Z} e^{-i\vartheta\mathbf{S}_Y} e^{-i\Theta\mathbf{S}_Z} e^{+i\vartheta\mathbf{S}_Y} e^{+i\varphi\mathbf{S}_Z} \quad (10.A.5c)$$

So axis-defined $\mathbf{R}[\varphi, \vartheta, \Theta]$ factors into five monomial exponentials instead of three factors found in the much simpler Euler rotation $\mathbf{R}(\alpha\beta\gamma)$. (Check that this gives the desired 2-by-2 matrix (10.5.25c).) The expression of rotations in terms of just a Y and two Z rotations keeps the matrix arithmetic to a minimum since generally the Z -rotations are diagonal and the Y -rotations, while not diagonal, are generally real. This is very important when we deal with big 201-by-201 spin-100 matrices! But, it helps even with medium-sized 3-by-3, 4-by-4, and 5-by-5 spin-1, spin-3/2, and spin-2 matrices seen later on.

It is important to understand the transformation (10.A.4) as a simple $\mathbf{R}(\varphi\vartheta 0)$ -rotation of an operator's crank-vector Θ . The magic-vector of an operator like a rotation \mathbf{R} or a Hamiltonian \mathbf{H} or a time evolution operator \mathbf{U} gets transformed just like the spin vector \mathbf{S} in Fig. 10.A.1, which, after all, is the magic vector of the spin-state density operator ρ . Such a transformation $\mathbf{R}' = \mathbf{T} \mathbf{R} \mathbf{T}^\dagger$ is called a *similarity* or *equivalence transformation* because the resulting rotation \mathbf{R}' must be similar or equivalent to the original \mathbf{R} . In particular, it must have the same trace, determinant, eigenvalues, etc., which means it must rotate by the same angle Θ as the original. So, the crank vector has the same $\Theta = |\Theta|$ length as the original, but, it will be in a different direction $\Theta' = \mathbf{R} \cdot \Theta$. Let's see how to quickly calculate a 3-by-3 direction-cosine R -matrix.

(b) Euler equivalence transformations of 3-vectors

The 3-by-3 transformation matrix $R(\alpha\beta\gamma)$ describing an Euler rotation of real 3-vectors is a little more complicated than the 2-by-2 spinor matrix (10.A.1), but simpler than the axis-angle matrix $R[\varphi\vartheta\Theta]$ you will derive later. The triple product rotation $\mathbf{R}(\alpha\beta\gamma)$ made 3-by-3 rotation matrices is

$$\begin{aligned} \langle R(\alpha\beta\gamma) \rangle &= \langle R(\alpha 0 0) \rangle \quad \langle R(0\beta 0) \rangle \quad \langle R(00\gamma) \rangle \\ &= \begin{pmatrix} \cos\alpha & -\sin\alpha & 0 \\ \sin\alpha & \cos\alpha & 0 \\ 0 & 0 & 1 \end{pmatrix} \begin{pmatrix} \cos\beta & 0 & \sin\beta \\ 0 & 1 & 0 \\ -\sin\beta & 0 & \cos\beta \end{pmatrix} \begin{pmatrix} \cos\gamma & -\sin\gamma & 0 \\ \sin\gamma & \cos\gamma & 0 \\ 0 & 0 & 1 \end{pmatrix} \quad (10.A.6a) \end{aligned}$$

The resulting transformation matrix is

$$\begin{aligned}
 |e_{\bar{X}}\rangle &= R(\alpha\beta\gamma)|e_X\rangle & |e_{\bar{Y}}\rangle &= R(\alpha\beta\gamma)|e_Y\rangle & |e_{\bar{Z}}\rangle &= R(\alpha\beta\gamma)|e_Z\rangle \\
 \langle R(\alpha\beta\gamma) | &= \begin{pmatrix} \langle e_X | \\ \langle e_Y | \\ \langle e_Z | \end{pmatrix} \begin{pmatrix} \cos\alpha \cos\beta \cos\gamma - \sin\alpha \sin\gamma & -\cos\alpha \cos\beta \sin\gamma - \sin\alpha \cos\gamma & \cos\alpha \sin\beta \\ \sin\alpha \cos\beta \cos\gamma + \cos\alpha \sin\gamma & -\sin\alpha \cos\beta \sin\gamma + \cos\alpha \cos\gamma & \sin\alpha \sin\beta \\ -\cos\gamma \sin\beta & \sin\gamma \sin\beta & \cos\beta \end{pmatrix} \quad (10.A.6b)
 \end{aligned}$$

The third column contains the Cartesian components of the $\mathbf{R}(\alpha\beta\gamma)$ -rotated Z -axis which is labeled

$$\hat{e}_Z = |e_{\bar{Z}}\rangle = (\cos\alpha \sin\beta, \sin\alpha \sin\beta, \cos\beta) \quad \text{or:} \quad e_Z = e_X \cos\alpha \sin\beta + e_Y \sin\alpha \sin\beta + e_Z \cos\beta$$

It is the same as the polar coordinate components $(\cos\alpha \sin\beta, \sin\alpha \sin\beta, \cos\beta)$ seen in Fig. 10.A.1 or (10.5.8b). The matrix gives the X, Y, Z -direction cosines $e_X \cdot e_{\bar{X}} = \langle X | \bar{X} \rangle$, $e_X \cdot e_{\bar{Y}} = \langle X | \bar{Y} \rangle$, ...etc. so any vector be quickly transformed passively (Recall Fig. 2.2.2) or actively (Recall Fig. 2.2.3).

(c) Euler angle goniometer: Double valued position

Research laboratories which need to orient crystals or X-ray targets or perform angular scattering experiments of any kind must be equipped with some sort of *goniometer* such as is sketched in Fig. 10.A.1 or Fig. 10.A.2 and photographed there and in Fig. 10.A.3. Theorists, too, would do well to "equip" their minds with such a device since it is a powerful "thought tool" for understanding the $R(3)$ and $SU(2)$ group properties of Euler angles.

Two metal frames labeled x' and x'' , respectively, are used to connect the laboratory or **LAB** frame $\{X, Y, Z\}$ to the body or **BOD** frame $\{\bar{X}, \bar{Y}, \bar{Z}\}$ through a series of three bearings labeled and measured by dials that keep track of the Euler angles $(\alpha\beta\gamma)$. The goniometer shows a number of things immediately.

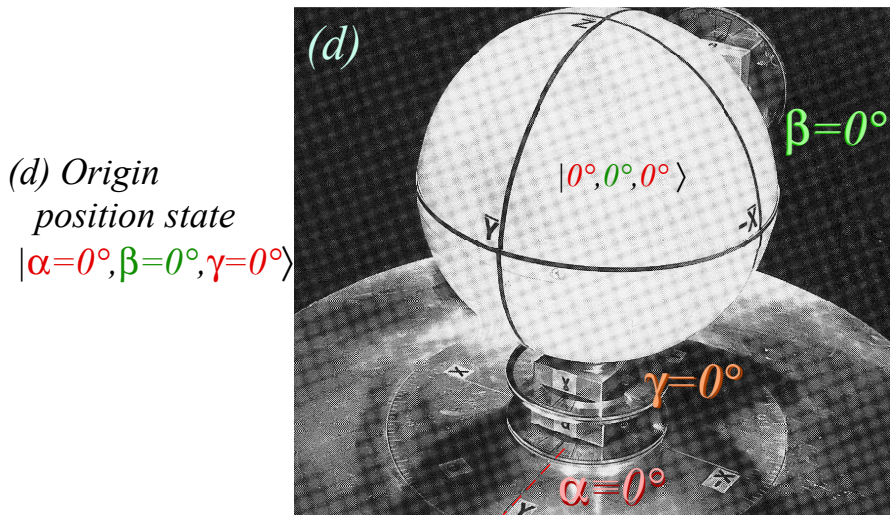
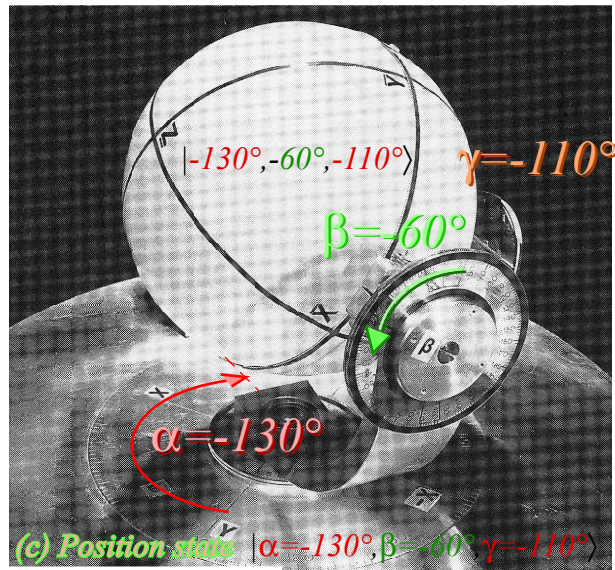
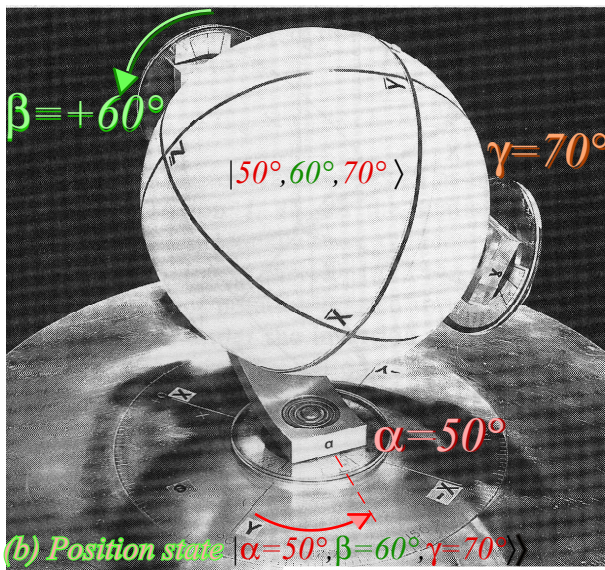
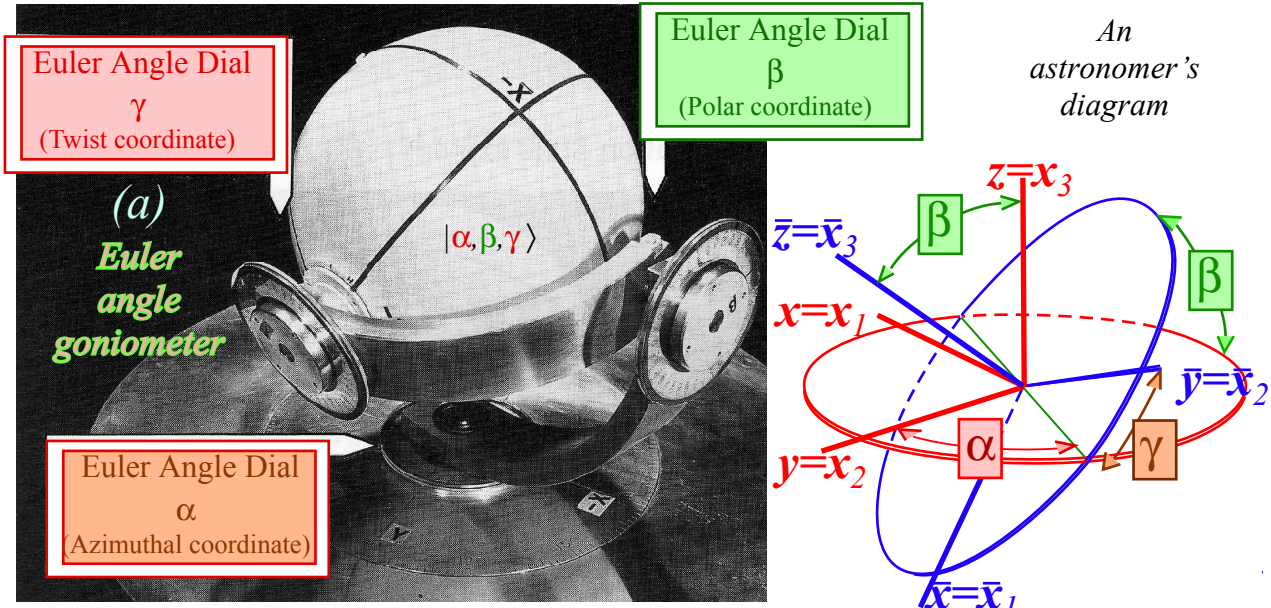
First, it demonstrates clearly that Euler angles are primarily *position coordinates*. While the operator definition given by Fig. 10.A.1 had to be performed in a definite (Z_α) , (Y_β) , and (Z_γ) order, the dials shown in Fig. 10.A.2 are totally independent of each other. You may set them in any order and the same position state will be obtained and exactly the one obtained by operators in Fig. 10.A.1.

Second, the device shows how Euler angles are natural choices for any laboratory or theoretical problem involving 3D rotation. Indeed, $(\alpha\beta\gamma)$ are the same as *yaw* (α), *pitch* (β), and *roll* (γ) used by a pilot of space ship, airplane, or submarine to track the bow or \bar{Z} -axis of the craft body relative to Earth or stars.

Third, the convention used in Fig. 10.A.1-2 makes the first two Euler angles (α and β) into azimuth and polar angles of the body zenith \bar{Z} . This is the appropriate for atomic and molecular physics where the body zenith \bar{Z} is a symmetry axis, radius vector, or other significant body point.

Fourth, it is seen from Fig. 10.A.2 the second two Euler angles (β and γ), more correctly, their minuses ($-\beta$ and $-\gamma$) are also azimuth and polar angles, but for the **LAB** zenith Z relative to the body frame. Note that the last row of matrix (10.A.6b) has exactly the polar coordinate form using $-\beta$ and $-\gamma$ as azimuth and polar angle, respectively. This is sketched in the upper left hand corner of Fig. 10.A.4.

Fig. 10.A.2 Euler angle device relates body frame to lab frame through a succession of frames and dials.



For $\beta=0^\circ$, ball frame holds its position as the α and γ frames swivel by angle ϕ to any state of form $|\alpha=\phi, \beta=0^\circ, \gamma=-\phi^\circ\rangle$ including origin state $|\alpha=0^\circ, \beta=0^\circ, \gamma=0^\circ\rangle$.

Other slightly different conventions exist for Euler angles. Indeed, the first were based on astronomical orientation of planetary orbits and celestial stellar tracks. In this case the zenith of an orbit plane is not a measurable or observable point. The azimuth and polar angle of the orbit zenith is useless. Instead the astronomer records the azimuth of the points where the body rises or sets; the so-called *ascending or descending nodes*. These are located exactly $\pm 90^\circ$, respectively, from the azimuth of the orbital zenith so old Euler definitions measure azimuth α from the $\pm Y$ -axis instead of the X -axis. The astronomer will also record the *orbital inclination* which is the same as β except, possibly, for a \pm -sign.

One should be aware of the fact that Euler angles, and for that matter, any 3D angular coordinates, are intrinsically and fundamentally *double valued*. This is no surprise to us; Fig. 10.5.6 shows that 3D spin vectors went around twice (4π) every time the $U(2)$ spinor rotation went around once (2π). However, a mechanical demonstration of this is shown in Fig. 10.A.5b-c. It is easy to see that two different settings, one with positive β (α, β, γ) and another with negative β ($\pi-\alpha, -\beta, \pi-\gamma$) leave the body in the same lab-relative position. Calculus texts restrict polar angle θ to being positive to avoid dealing with this.

The case of $\beta=0$ (Fig. 10.A.2d) might seem to avoid double valued trouble, but unfortunately, things just get worse there. Then the two remaining α and γ coordinates become *infinite-valued* since the state $(\alpha, 0, \gamma)$ is the same position as $(\alpha-\phi, 0, \gamma+\phi)$ for all ϕ . This worst of all singularities occurs right at the origin of $R(3)$ and $U(2)$ group parameter space namely $(\alpha=0, \beta=0, \gamma=0)$ or, more likely to be found, $(\alpha=\phi, \beta=0, \gamma=-\phi)$. There is another such singularity at $\beta=\pi$, too. The singular ϕ -floppiness is a killer, literally; the singularity at (000) corresponds to gyroscopic *gimbal-lock* so dreaded by pilots who fly acrobatic maneuvers that depended upon gyroscopic instruments.

However, the infinite valued rotational origin is a necessary to allow an arbitrary axis-angle rotation $\mathbf{R}[\varphi, \vartheta, \Theta]$ operator to produce the Euler- $(\alpha\beta\gamma)$ -angle position states

$$\mathbf{R}(\alpha\beta\gamma) |000\rangle = |\alpha\beta\gamma\rangle = \mathbf{R}[\varphi, \vartheta, \Theta] |000\rangle = \mathbf{R}[\varphi, \vartheta, \Theta] |\varphi-\pi/2, 0, \pi/2-\varphi\rangle \quad (10.A.7)$$

according to Euler-axis angle relations (10.A.1). The device which demonstrates this is shown attached to the Euler angle goniometer in Fig. 10.A.3. However, gimbal-lock prevents motion from the original position until the goniometer x'-frame is tucked under the axis-angle crank support at azimuth φ , that is, until the origin is reset from $(\alpha=0, \beta=0, \gamma=0)$ to $(\varphi-\pi/2, 0, \pi/2-\varphi)$. Recall, that an azimuth of α puts the x'-frame at $\alpha-90^\circ$. Then, the continuous rotation by axis angle $\Theta=\Omega\cdot t$ may begin as shown below in in Fig. 10.A.5.

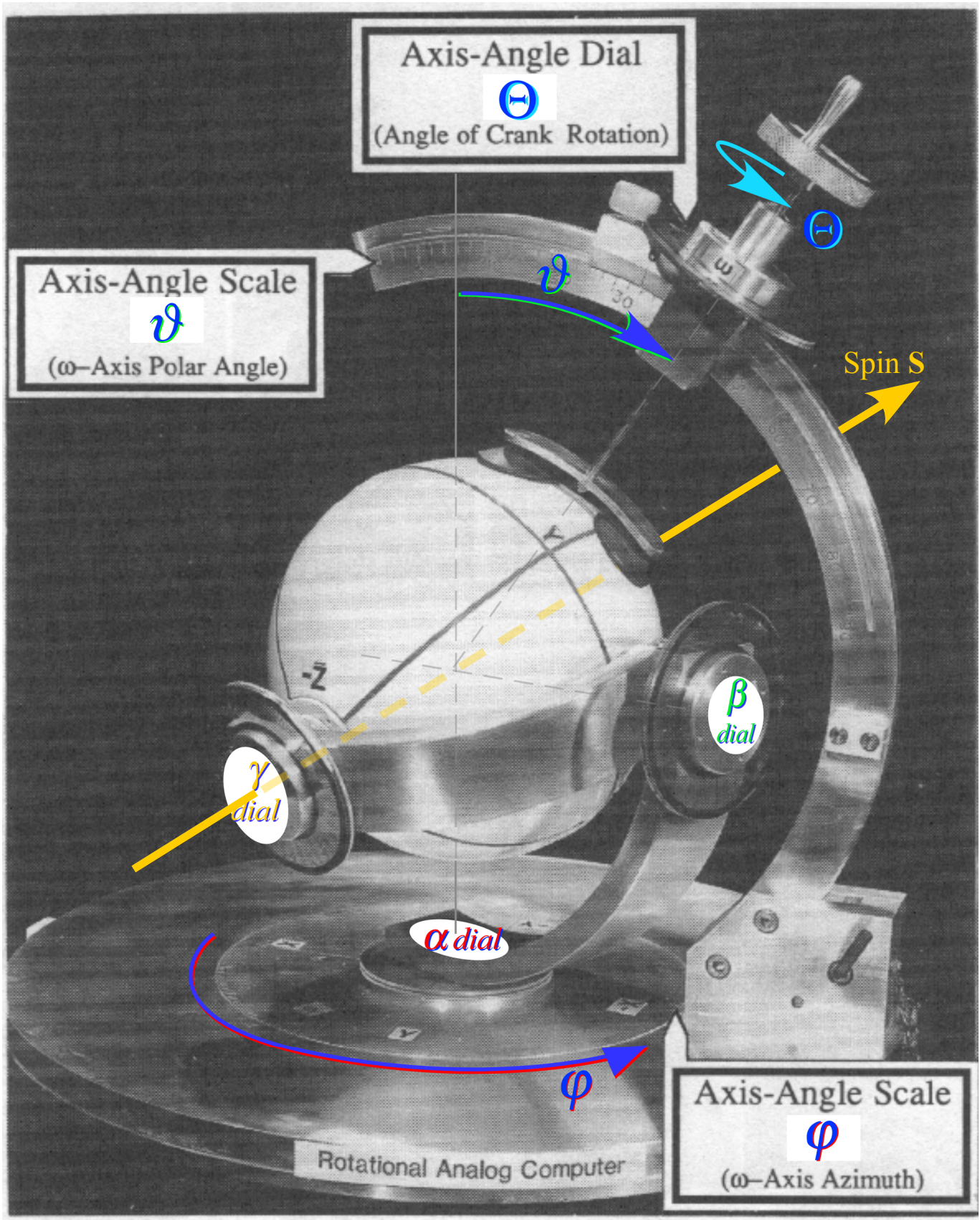


Fig. 10.A.3 Mechanical crank axis angles $[\phi, \vartheta, \Theta]$ operating on sphere having Euler angles (α, β, γ)

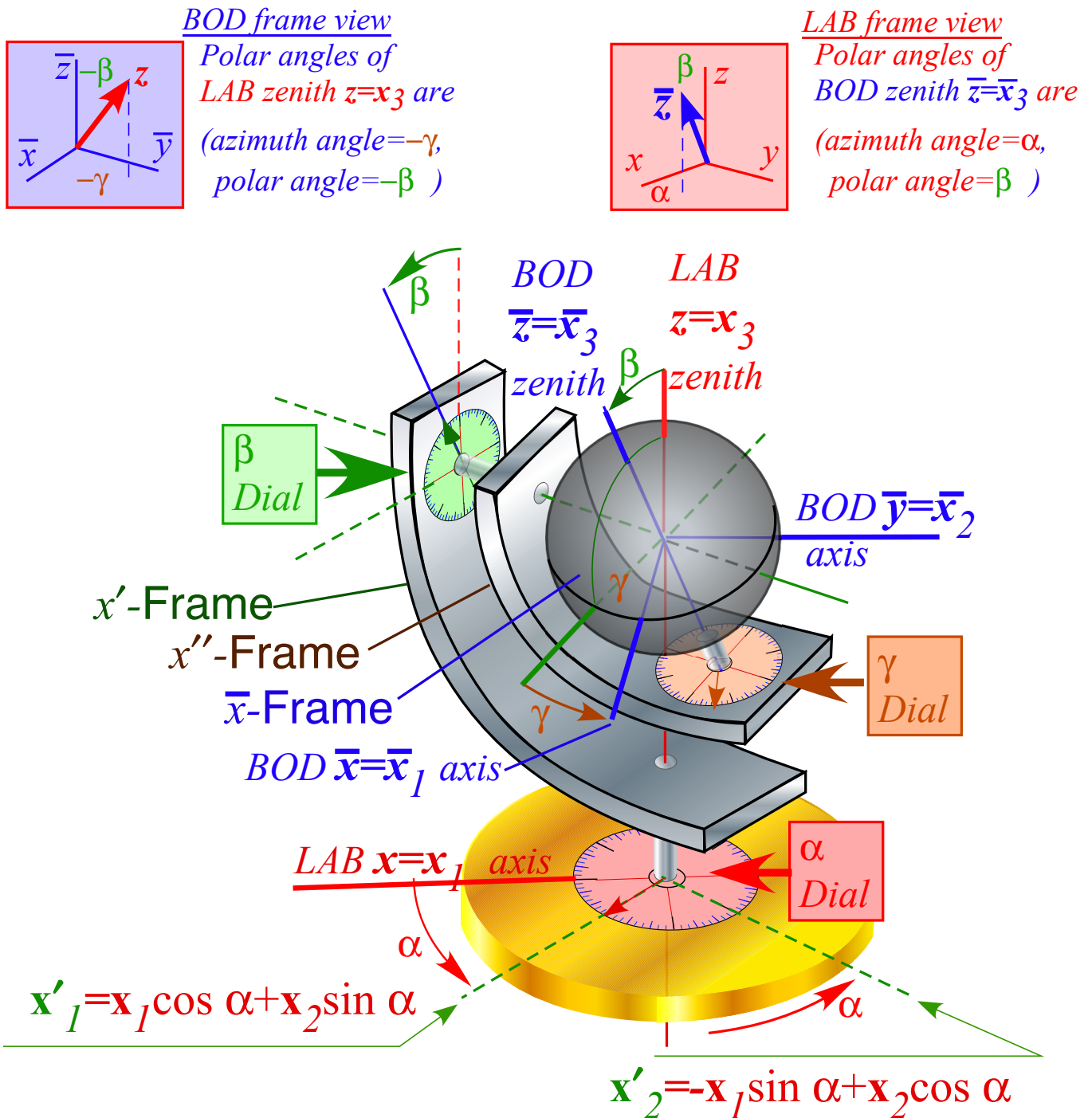


Fig. 10.A.4 Mechanical device demonstrating Euler angles (α, β, γ) as coordinates of a body BOD-frame relative to a “star-fixed” LAB-frame.

LAB-frame view sees BOD- \bar{Z} axis with polar angles of azimuth α and polar angle β .
 BOD-frame view sees LAB-Z axis with polar angles of azimuth $-\gamma$ and polar angle $-\beta$.

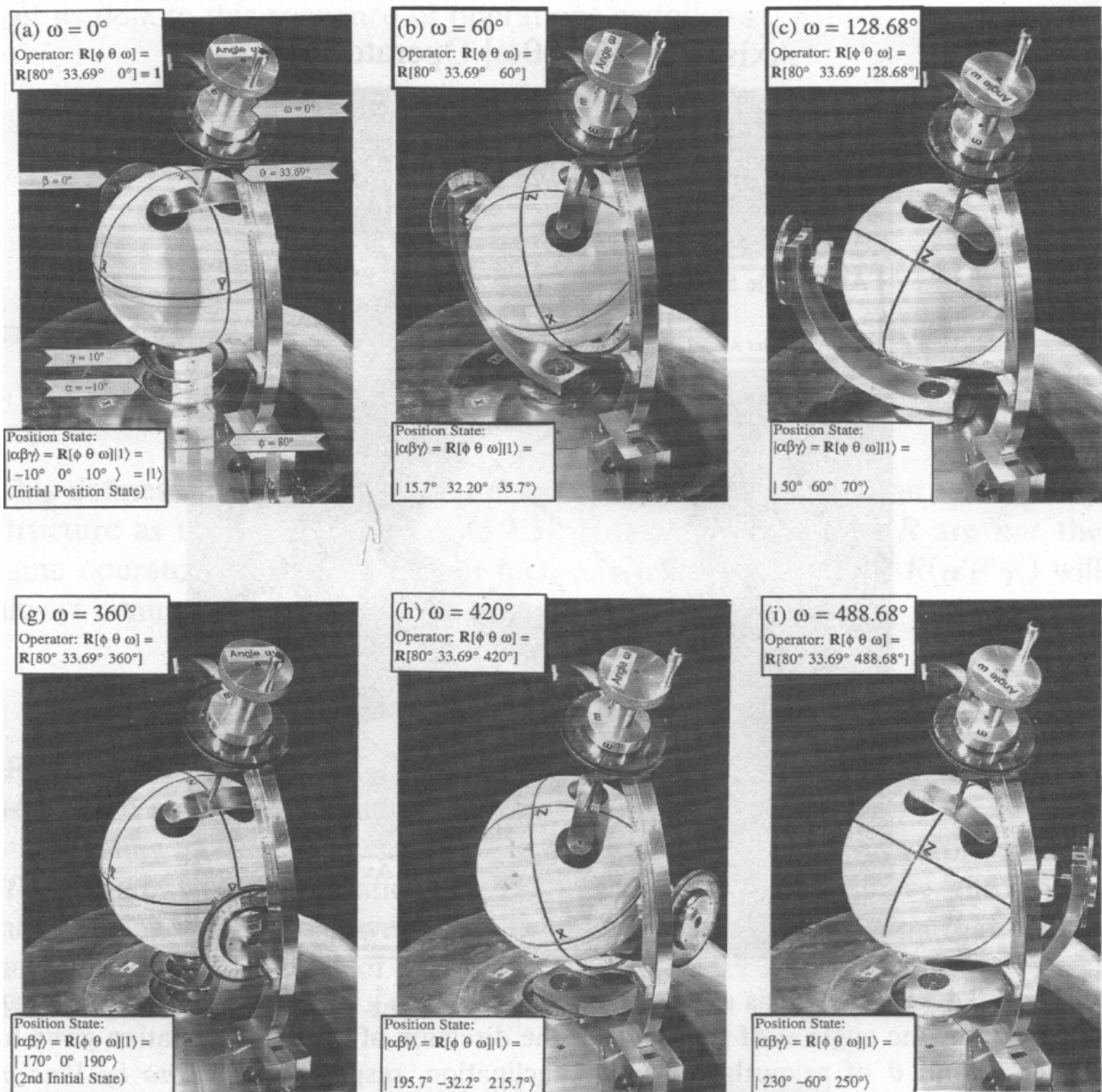


Fig. 10.A.5 Rotational 4π sequence 1st Row: (a) First origin state $\omega=\Theta=0$, (b-f) First position states.

(d) Axis angle rotation: Double valued operation

In Fig. 10.A.5 we attempt to follow an entire 720° or 4π rotation that connects the two positions shown in Fig. 10.A.2(b-c). First use relations (10.A.1) to derive the axis angles $[\varphi=80^\circ, \vartheta=34^\circ, \Theta=129^\circ]$ for the “first” initial Euler position state $(\alpha=50^\circ, \beta=60^\circ, \gamma=70^\circ)$ in Fig. 10.A.5(c) and Fig. 10.A.3(a).

$$R(\alpha=50^\circ, \beta=60^\circ, \gamma=70^\circ) |000\rangle = R[\varphi=80^\circ, \vartheta=34^\circ, \Theta=129^\circ] |000\rangle \quad (10.A.8a)$$

It starts from a "first" origin state in Fig. 10.A.5(a). (Note figure notation: $\phi=\varphi, \theta=\vartheta, \omega=\Theta$)

$$|000\rangle = |\varphi-\pi/2, 0, \pi/2-\varphi\rangle = |\alpha=-10^\circ, \beta=0^\circ, \gamma=10^\circ\rangle = R[\varphi, \vartheta, \Theta=0^\circ] |000\rangle \quad (10.A.8b)$$

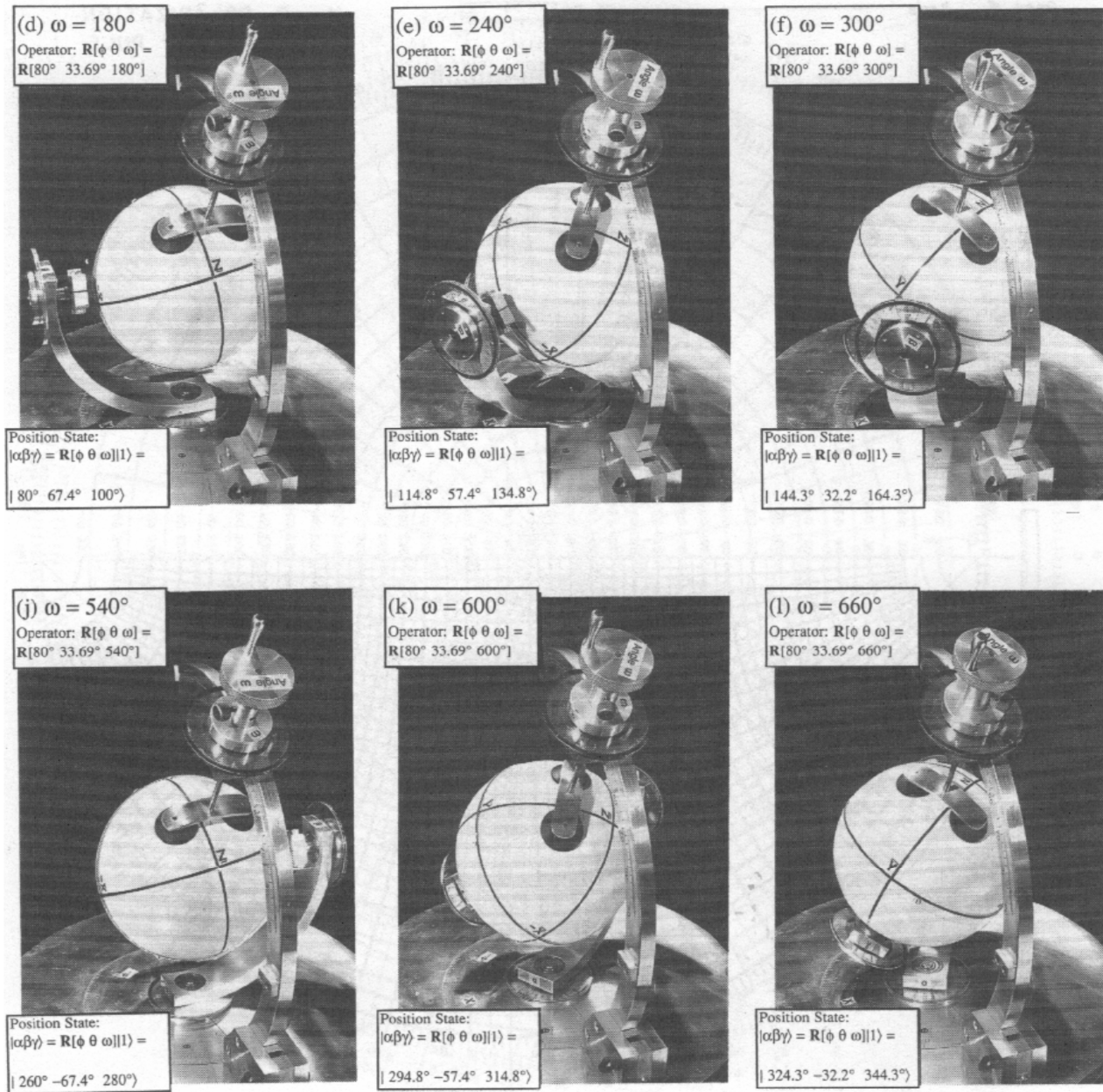


Fig. 10.A.5 2nd Row: (g) 2nd origin state $\omega = \Theta = 2\pi$, (h-l) 2nd negative- β position states.

A 2π rotation (a-g) by $\Theta = \omega = 360^\circ$ gives the "second" origin state in Fig. 10.A.5(g).

$$\mathbf{R}[\varphi=80^\circ, \vartheta=34^\circ, \Theta=360^\circ] |000\rangle = |\alpha=170^\circ, \beta=0^\circ, \gamma=190^\circ\rangle \quad (10.A.8c)$$

The ball "looks" the same in the "second" initial state of Fig. 10.A.5(i) or Fig. 10.A.3(b) as in the "first."

$$\mathbf{R}[\varphi=80^\circ, \vartheta=34^\circ, \Theta=489^\circ] |000\rangle = |\alpha=230^\circ, \beta=-60^\circ, \gamma=250^\circ\rangle \quad (10.A.8c)$$

However, "looks" by classical eyes are deceiving in quantum rotations. In fact, the α, γ -Euler angles and the goniometer x' -frame for each "second" position in figures 10.A.5(g-l) are π -flipped from those above

them in figures 10.A.5(a-f). Also, β is negative. Another "full" 2π rotation (either way) is needed to finish a full-quantum rotation of $0\text{-modulo-}4\pi$ and return apparatus to first initial position in Fig. 10.A.5(c).

There is a double-valued nature of the 3D-space we occupy. It has been noted repeatedly in Chapter 10 comparisons of the real 3-D $R(3)$ spin-vector world *versus* the complex 2-D $U(2)$ spinor world in Fig. 10.5.8. Photon polarization spin-vector \mathbf{S} goes twice (4π) around $R(3)$ space while the polarization \mathbf{E} -vector or Ψ -spinor goes just once around $U(2)$ space in Fig. 10.5.5 and Fig. 10.5.6. Also, spinor reflections only need half the angle of the rotations they accomplish in Fig. 10.3.3. They also provide a more elegant formula and graphical "slide-rule" for rotation group products as we show now.

(1) Combining rotations: $U(2)$ group products

The product of $\mathbf{R}[\Theta'] \mathbf{R}[\Theta]$ of any two rotations is another rotation operator $\mathbf{R}[\Theta'']$ which can be computed using Hamilton's axis-angle expansion. First we multiply the separate expansions.

$$\begin{aligned} \mathbf{R}[\bar{\Theta}'] \mathbf{R}[\bar{\Theta}] &= \left(\cos \frac{\Theta'}{2} \mathbf{1} - i \sin \frac{\Theta'}{2} \hat{\Theta}' \cdot \boldsymbol{\sigma} \right) \left(\cos \frac{\Theta}{2} \mathbf{1} - i \sin \frac{\Theta}{2} \hat{\Theta} \cdot \boldsymbol{\sigma} \right) \\ &= \cos \frac{\Theta'}{2} \cos \frac{\Theta}{2} \mathbf{1} - i \left[\cos \frac{\Theta'}{2} \sin \frac{\Theta}{2} \hat{\Theta}' + \cos \frac{\Theta}{2} \sin \frac{\Theta'}{2} \hat{\Theta} \right] \cdot \boldsymbol{\sigma} - \sin \frac{\Theta'}{2} \sin \frac{\Theta}{2} (\hat{\Theta}' \cdot \boldsymbol{\sigma})(\hat{\Theta} \cdot \boldsymbol{\sigma}) \end{aligned} \quad (10.A.9)$$

Then the Jordan-Pauli identity (10.5.13) is used to reduce $(\hat{\Theta}' \cdot \boldsymbol{\sigma})(\hat{\Theta} \cdot \boldsymbol{\sigma})$ to $(\hat{\Theta}' \cdot \hat{\Theta}) \mathbf{1} + (\hat{\Theta}' \times \hat{\Theta}) \cdot \boldsymbol{\sigma}$.

$$\begin{aligned} \mathbf{R}[\bar{\Theta}'] \mathbf{R}[\bar{\Theta}] &= \left(\cos \frac{\Theta''}{2} \right) \mathbf{1} - i \left[\sin \frac{\Theta''}{2} \hat{\Theta}'' \right] \cdot \boldsymbol{\sigma} = \mathbf{R}[\Theta''] \\ &= \left(\cos \frac{\Theta'}{2} \cos \frac{\Theta}{2} - \sin \frac{\Theta'}{2} \sin \frac{\Theta}{2} \hat{\Theta}' \cdot \hat{\Theta} \right) \mathbf{1} - i \left[\cos \frac{\Theta'}{2} \sin \frac{\Theta}{2} \hat{\Theta}' + \cos \frac{\Theta}{2} \sin \frac{\Theta'}{2} \hat{\Theta} + \sin \frac{\Theta'}{2} \sin \frac{\Theta}{2} \hat{\Theta}' \times \hat{\Theta} \right] \cdot \boldsymbol{\sigma} \end{aligned} \quad (10.A.10a)$$

It is straightforward to solve for the new product angle Θ'' and axis unit vector $\hat{\Theta}''$ of crank Θ'' .

$$\begin{aligned} \left(\cos \frac{\Theta''}{2} \right) &= \left(\cos \frac{\Theta'}{2} \cos \frac{\Theta}{2} - \sin \frac{\Theta'}{2} \sin \frac{\Theta}{2} \hat{\Theta}' \cdot \hat{\Theta} \right) \\ \left[\sin \frac{\Theta''}{2} \hat{\Theta}'' \right] &= \left[\cos \frac{\Theta'}{2} \sin \frac{\Theta}{2} \hat{\Theta}' + \cos \frac{\Theta}{2} \sin \frac{\Theta'}{2} \hat{\Theta} + \sin \frac{\Theta'}{2} \sin \frac{\Theta}{2} \hat{\Theta}' \times \hat{\Theta} \right] \end{aligned} \quad (10.A.10b)$$

This is the $U(2)$ group product formula. Now a simple way to visualize this product is done with mirrors!.

(2) Mirror reflections and Hamilton's turns

In Section 10.3b we noted that *mirror reflection* operations are more fundamental than rotations and are done by real Pauli matrices such as σ_A and σ_B or their combination σ_ϕ below. Recall Fig. 10.3.3

$$\sigma_A = \begin{pmatrix} 1 & 0 \\ 0 & -1 \end{pmatrix}, \quad \sigma_B = \begin{pmatrix} 0 & 1 \\ 1 & 0 \end{pmatrix}, \quad \sigma_\phi = \begin{pmatrix} \cos \phi & \sin \phi \\ \sin \phi & -\cos \phi \end{pmatrix} = \sigma_A \cos \phi + \sigma_B \sin \phi$$

Their action is displayed in Fig. 10.A.6. σ_ϕ reflects through a plane inclined at half-angle $\phi/2$ to the x -axis. The product $\sigma_\phi \sigma_A$ is a rotation $\mathbf{R}[\phi]$ by angle ϕ , while $\sigma_A \sigma_\phi$ is a rotation $\mathbf{R}[-\phi]$ the opposite way ($-\phi$).

$$\begin{aligned} \sigma_\phi \sigma_x &= \begin{pmatrix} \cos\phi & \sin\phi \\ \sin\phi & -\cos\phi \end{pmatrix} \begin{pmatrix} 1 & 0 \\ 0 & -1 \end{pmatrix}, & \sigma_x \sigma_\phi &= \begin{pmatrix} 1 & 0 \\ 0 & -1 \end{pmatrix} \begin{pmatrix} \cos\phi & \sin\phi \\ \sin\phi & -\cos\phi \end{pmatrix} \\ &= \begin{pmatrix} \cos\phi & -\sin\phi \\ \sin\phi & \cos\phi \end{pmatrix} = R[\phi], & &= \begin{pmatrix} \cos\phi & -\sin\phi \\ \sin\phi & \cos\phi \end{pmatrix} = R[-\phi] \end{aligned} \tag{10.A.11}$$

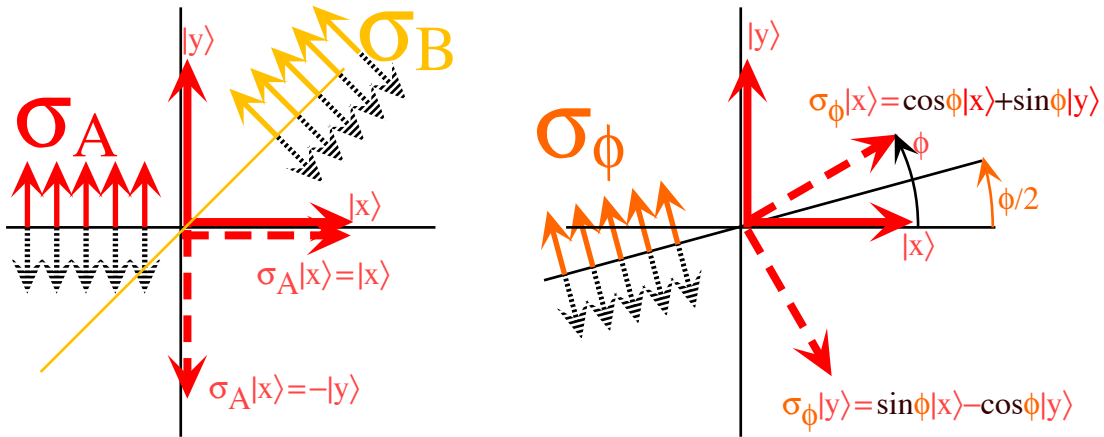


Fig. 10.A.6 Mirror reflections σ_A through xz -plane and σ_ϕ through rotated plane.

Hamilton saw this as a neat way to visualize three-dimensional rotations. Simply install two mirrors so they intersect on a Θ crank vector with half-angle $\Theta/2$ between the first and the second as shown in Fig. 10.A.7. It is like a clothing store mirror which lets you rotate an image of yourself by Θ as you adjust the angle $\Theta/2$ between mirrors. A unit normal vector \mathbf{N}_1 and \mathbf{N}_2 is constructed from each mirror plane and a $\Theta/2$ arc-vector drawn between the first and second plane normals. This arc is called *Hamilton's turn* vector ($\mathbf{N}_1 \rightarrow \mathbf{N}_2$). It is these Hamilton turns that can be "added" like vectors to give $U(2)$ group products!

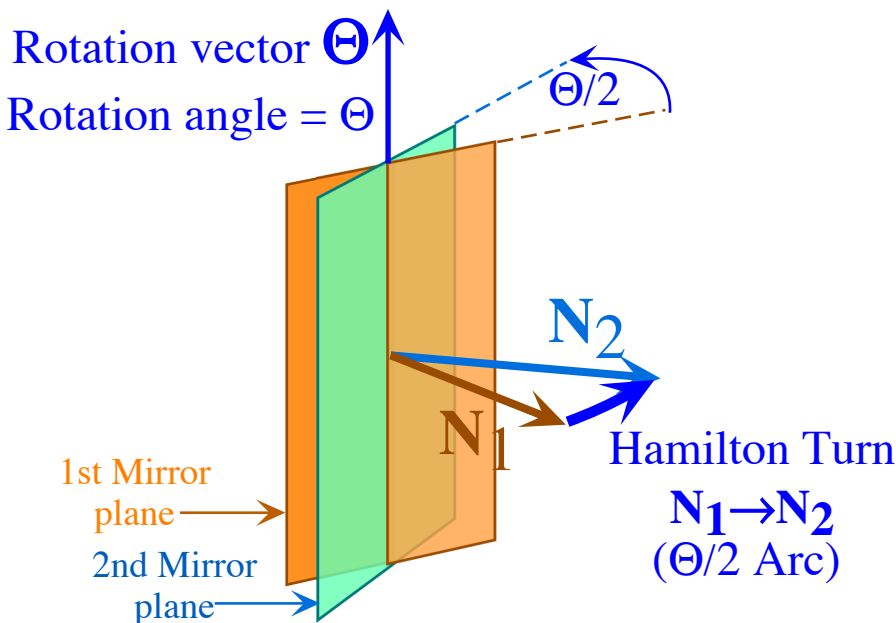


Fig. 10.A.7 Mirror reflection planes, normals, and Hamilton-turn arc vector.

Notice that only the relative angle $\Theta/2$ or $\pi-\Theta/2$ between mirrors is important in defining rotation $\mathbf{R}[\Theta]$; their absolute position is irrelevant. You can swivel the two mirrors anywhere around the Θ -axis. The trick to making products is to swivel the Hamilton turn arc $\mathbf{N}_1 \rightarrow \mathbf{N}_2$ for the first rotation $\mathbf{R}[\Theta]$ around so it meets head-to-tail with the Hamilton turn arc $\mathbf{N}'_1 \rightarrow \mathbf{N}'_2$ of the second rotation as $\mathbf{R}[\Theta']$ as shown in Fig. 10.A.8.

Then the two mirrors associated with \mathbf{N}_2 and \mathbf{N}'_1 lie on top of each other and cancel since two reflections by the same mirror is *no reflection*. That leaves only first mirror (\mathbf{N}_1) and last mirror (\mathbf{N}'_2), and so the resultant Hamilton-turn arc $\mathbf{N}_1 \rightarrow \mathbf{N}'_2$ is the arc of the desired product $\mathbf{R}[\Theta''] = \mathbf{R}[\Theta']\mathbf{R}[\Theta]$.

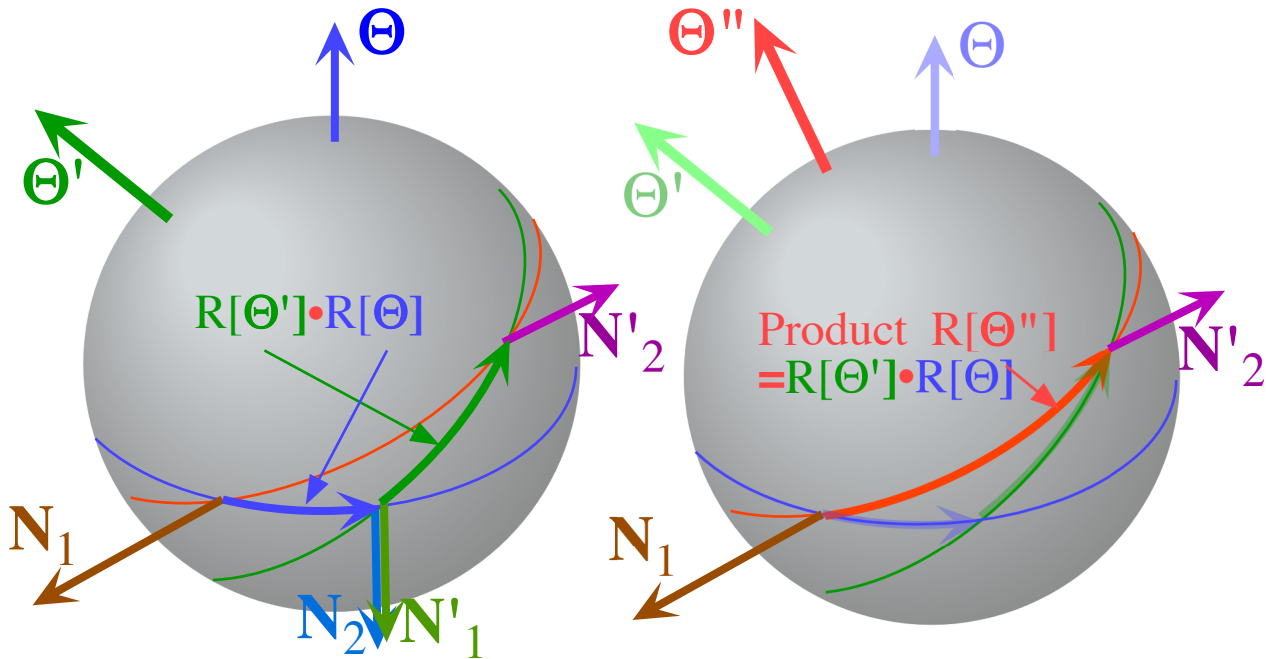


Fig. 10.A.8 Adding Hamilton-turn arcs to compute a U(2) product $\mathbf{R}[\Theta''] = \mathbf{R}[\Theta']\mathbf{R}[\Theta]$.

It is important to note that all Hamilton-turn arcs lie on *great* or *equatorial* circles and slide along the equatorial circles of the rotation axis vector Θ of the rotation $\mathbf{R}[\Theta]$.

Also, note that each Hamilton arc $\Theta/2$, $\Theta'/2$, or $\Theta''/2$ is half of the actual angle Θ , Θ' , or Θ'' of rotation $\mathbf{R}[\Theta]$, $\mathbf{R}[\Theta']$, or $\mathbf{R}[\Theta'']$, respectively. That means that an arc $\Theta/2$ between \mathbf{N}_1 and \mathbf{N}_2 and its supplement angles $(\Theta \pm 2\pi)/2 = \Theta/2 \pm \pi$ between \mathbf{N}_1 and $-\mathbf{N}_2$ represent the same classical rotation by Θ . For classical objects, a rotation by $\Theta \pm 2\pi$ is the same as one by Θ . However, for a quantum spin-1/2 object, the arc pointing from \mathbf{N}_1 to the antipodal normal $-\mathbf{N}_2$ represents a Θ -rotation with an extra π -phase factor $e^{\pm i\pi} = -1$, that is, $-\mathbf{R}[\Theta]$. Recall rotation by 2π of the U(2) polarization state in Fig. 10.5.6 and Fig. 10.5.7 always comes up the same state, but it's π -out of phase. Hamilton's turns account for this.

(3) Similarity transformation and Hamilton's turns

Finally, the Hamilton-turn "vector addition" on a sphere gives different results if the vectors are added in the reverse order to give $\mathbf{R}[\Theta'''] = \mathbf{R}[\Theta]\mathbf{R}[\Theta']$ instead of $\mathbf{R}[\Theta''] = \mathbf{R}[\Theta']\mathbf{R}[\Theta]$. The arc-diagram for

this forms a spherical parallelogram as shown in Fig. 10.A.9. It also shows the effect of a similarity transformation of rotation $R[\Theta''']$ by rotation $R[\Theta]$ to give rotation $R[\Theta''']$.

$$R[\Theta] R[\Theta'''] R[-\Theta] = R[\Theta'''] \quad (10.A.12a) \quad R[-\Theta] R[\Theta'''] R[\Theta] = R[\Theta'''] \quad (10.A.12b)$$

As in (10.A.4), a rotation $R[\Theta]$ of a rotation $R[\Theta''']$ is just that. So everything associated with that rotation $R[\Theta''']$ gets rotated by the full angle Θ around axis Θ . This includes its 'crank vector' Θ and now its Hamilton-turn arc which, in Fig. 10.A.9 gets moved by exactly two $R[\Theta]$ Hamilton-turn arcs into path of the $R[\Theta''']$ turn arc below it, that is, two $R[\Theta]$ Hamilton-turn $\Theta/2$ arcs amount to one whole angle Θ .

Fig. 10.A.9 shows a similarity transformation of rotation $R[\Theta''']$ by rotation $R[\Theta']$ to gives $R[\Theta''']$.

$$R[\Theta'] R[\Theta'''] R[-\Theta'] = R[\Theta'''] \quad (10.A.12c)$$

There are an infinite number of rotations that transform $R[\Theta''']$ into $R[\Theta''']$. Of these, there is one that is by the smallest angle Θ . Can you tell where this one's crank and Hamilton-turn is located in Fig. 10.A.9?

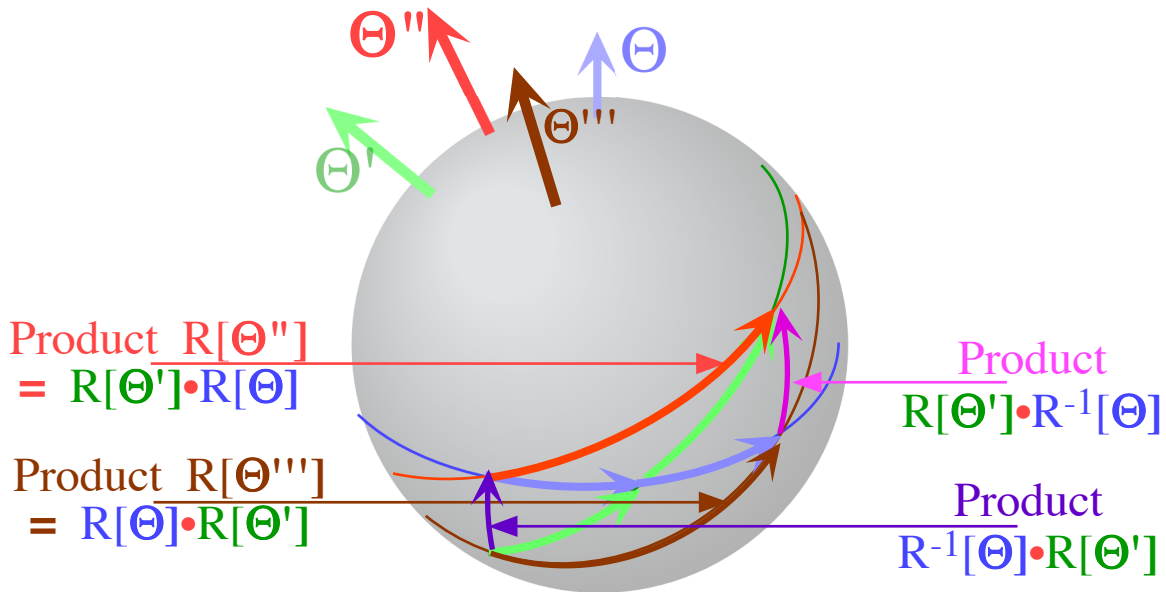


Fig. 10.A.9 Hamilton-turn arc parallelogram with $R[\Theta'''] = R[\Theta']R[\Theta]$ and $R[\Theta'''] = R[\Theta]R[\Theta']$

(e) Quaternion and spinor algebra (again)

Suppose we rotate a spin ket $|\hat{\uparrow}\rangle$ or $|\Psi\rangle$ with an operator like the R above to give a new state

$$|\Psi'\rangle = R |\Psi\rangle$$

and a new density operator

$$\rho' = |\Psi'\rangle\langle\Psi'| = R |\Psi\rangle\langle\Psi| R^\dagger = R \rho R^\dagger \quad (10.A.13a)$$

Use (10.5.5) to write $\rho = N/2 \mathbf{1} + \mathbf{S}\cdot\boldsymbol{\sigma}$ in terms of its \mathbf{S} -vector gives

$$\rho' = R (N/2 \mathbf{1} + \mathbf{S}\cdot\boldsymbol{\sigma}) R^\dagger = (N/2 \mathbf{1} + \mathbf{S}'\cdot\boldsymbol{\sigma}) \quad (10.A.13b)$$

which is just the same \mathbf{S} -vector referred to a rotated spinor basis; in other words an Θ -rotated spin vector.

It is important to remember that R acts only on the $U(2)$ operators ($\sigma_x, \sigma_y, \sigma_z$) and pays no attention to the scalar component $N/2$ or the components of the \mathbf{S} -vector. But, the effect is the same as it would be applying the 3-by-3 matrix transformation R to the \mathbf{S} -vector and leaving the spinor σ 's alone.

$$\rho' = R (N/2 \mathbf{1} + \mathbf{S}\cdot\boldsymbol{\sigma}) R^\dagger = (N/2 \mathbf{1} + \mathbf{S}'\cdot\boldsymbol{\sigma}), \text{ where: } S'_m = R_{mn}S_n \quad (10.A.13c)$$

We will derive the 3-by-3 R-matrix by considering each unit base operator ($\sigma_X, \sigma_Y, \sigma_Z$) in turn. This involves Hamilton's original algebra of quaternions ($\mathbf{q}_X, \mathbf{q}_Y, \mathbf{q}_Z$) = ($-i\sigma_X, -i\sigma_Y, -i\sigma_Z$) which satisfies cyclic multiplication rules below along with the negative squares: $\mathbf{q}_X \mathbf{q}_X = \mathbf{q}_Y \mathbf{q}_Y = \mathbf{q}_Z \mathbf{q}_Z = -\mathbf{1}$, .

$$\mathbf{q}_X \mathbf{q}_Y = \mathbf{q}_Z = - \mathbf{q}_Y \mathbf{q}_Z , \quad \mathbf{q}_Z \mathbf{q}_X = \mathbf{q}_Y = - \mathbf{q}_X \mathbf{q}_Z , \quad \mathbf{q}_Y \mathbf{q}_Z = \mathbf{q}_X = - \mathbf{q}_Z \mathbf{q}_Y . \quad (10.A.14a)$$

These are summarized using the δ_{UV} and $\epsilon_{\lambda UV}$ -tensors (Recall $\epsilon_{\lambda UV}...$ in Appendix 3.A)

$$\mathbf{q}_\mu \mathbf{q}_\nu = -\delta_{\mu\nu} \mathbf{1} + \epsilon_{\mu\nu\lambda} \mathbf{q}_\lambda \quad \text{or:} \quad \sigma_\mu \sigma_\nu = \delta_{\mu\nu} \mathbf{1} + i \epsilon_{\mu\nu\lambda} \sigma_\lambda \quad (10.A.14b)$$

Here, we've written the multiplication rules for Pauli's " σ_μ -quaternions" as well as Hamilton's $\mathbf{q}_\mu = -i\sigma_\mu$.

\bullet	$\mathbf{1}$	\mathbf{q}_X	\mathbf{q}_Y	\mathbf{q}_Z	,	\bullet	$\mathbf{1}$	σ_X	σ_Y	σ_Z	,	σ_X	σ_Y	σ_Z	,	σ_X	σ_Y	σ_Z	$\mathbf{1}$	$i\sigma_Z$	$-i\sigma_Y$	$i\sigma_X$	$\mathbf{1}$	$i\sigma_Y$	$-i\sigma_X$	$\mathbf{1}$				
$\mathbf{1}$	$\mathbf{1}$	\mathbf{q}_X	\mathbf{q}_Y	\mathbf{q}_Z	,	$\mathbf{1}$	$\mathbf{1}$	σ_X	σ_Y	σ_Z	,	σ_X	σ_X	$\mathbf{1}$	$i\sigma_Z$	$-i\sigma_Y$	$i\sigma_X$	$\mathbf{1}$	σ_X	σ_Y	$-i\sigma_Z$	$\mathbf{1}$	$i\sigma_Y$	$-i\sigma_X$	$\mathbf{1}$	σ_Y	σ_Z	$i\sigma_Y$	$-i\sigma_X$	$\mathbf{1}$
\mathbf{q}_X	\mathbf{q}_X	-1	\mathbf{q}_Z	$-\mathbf{q}_Y$,	σ_X	σ_X	$\mathbf{1}$	$i\sigma_Z$	$-i\sigma_Y$,	σ_X	σ_X	$\mathbf{1}$	$i\sigma_Z$	$-i\sigma_Y$	$i\sigma_X$	$\mathbf{1}$	σ_X	σ_Y	$-i\sigma_Z$	$\mathbf{1}$	$i\sigma_Y$	$-i\sigma_X$	$\mathbf{1}$	σ_Y	σ_Z	$i\sigma_Y$	$-i\sigma_X$	$\mathbf{1}$
\mathbf{q}_Y	\mathbf{q}_Y	$-\mathbf{q}_Z$	-1	\mathbf{q}_X	,	σ_Y	σ_Y	$-i\sigma_Z$	$\mathbf{1}$	$i\sigma_X$,	σ_Y	σ_Y	$-i\sigma_Z$	$\mathbf{1}$	$i\sigma_X$	$\mathbf{1}$	σ_Y	σ_Z	$i\sigma_Y$	$-i\sigma_X$	$\mathbf{1}$	$i\sigma_Y$	$-i\sigma_X$	$\mathbf{1}$	σ_Z	σ_Z	$i\sigma_Y$	$-i\sigma_X$	$\mathbf{1}$
\mathbf{q}_Z	\mathbf{q}_Z	\mathbf{q}_Y	$-\mathbf{q}_X$	-1	,	σ_Z	σ_Z	$i\sigma_Y$	$-i\sigma_X$	$\mathbf{1}$,	σ_Z	σ_Z	$i\sigma_Y$	$-i\sigma_X$	$\mathbf{1}$	$\mathbf{1}$	σ_Z	σ_Z	$i\sigma_Y$	$-i\sigma_X$	$\mathbf{1}$	$i\sigma_Y$	$-i\sigma_X$	$\mathbf{1}$	σ_Z	σ_Z	$i\sigma_Y$	$-i\sigma_X$	$\mathbf{1}$

Also, we need *commutation rules* for Pauli's operators as well as Jordan's spin-ops: $\mathbf{J}_\mu = \mathbf{S}_\mu = \sigma_\mu/2$.

$$\sigma_\mu \sigma_\nu - \sigma_\nu \sigma_\mu = [\sigma_\mu, \sigma_\nu] = 2i \epsilon_{\mu\nu\lambda} \sigma_\lambda \quad \text{or:} \quad \mathbf{S}_\mu \mathbf{S}_\nu - \mathbf{S}_\nu \mathbf{S}_\mu = [\mathbf{S}_\mu, \mathbf{S}_\nu] = i \epsilon_{\mu\nu\lambda} \mathbf{S}_\lambda \quad (10.A.14d)$$

The latter are the very important *angular momentum commutation relations* which we will apply later.

Now the application of σ -rules to the derivation of the expression for a general rotation $\mathbf{R}[\Theta]$ of an arbitrary unit 3-vector \mathbf{e}_L or unit spinor σ_L is tricky. But, it's something important that every physicist should do at least once in their life! Therefore we leave the following result as an exercise.

$$\begin{aligned} \mathbf{R}[\Theta] \sigma_L \mathbf{R}[\Theta]^\dagger &= \left(\cos \frac{\Theta}{2} \mathbf{1} - i \sin \frac{\Theta}{2} \hat{\Theta}_K \sigma_K \right) \sigma_L \left(\cos \frac{\Theta}{2} \mathbf{1} - i \sin \frac{\Theta}{2} \hat{\Theta}_N \sigma_N \right)^\dagger \\ &= \sigma_L' = \sigma_L \cos \Theta - \epsilon_{LKM} \hat{\Theta}_K \sigma_M \sin \Theta + (1 - \cos \Theta) \hat{\Theta}_L (\hat{\Theta}_N \sigma_N) \end{aligned} \quad (10.A.15a)$$

You should also demonstrate that this is equivalent to the following 3-vector expression.

$$\begin{aligned} \mathbf{e}_L' &= \mathbf{e}_L \cos \Theta - \epsilon_{LKM} \hat{\Theta}_K \mathbf{e}_M \sin \Theta + (1 - \cos \Theta) \hat{\Theta}_L (\hat{\Theta}_N \mathbf{e}_N) \\ &= \mathbf{e}_L \cos \Theta + \hat{\Theta} \times \mathbf{e}_L \sin \Theta + (1 - \cos \Theta) \hat{\Theta} (\hat{\Theta} \bullet \mathbf{e}_L) \end{aligned} \quad (10.A.15b)$$

The 3-vector transformations are a lot more complicated than the 2-spinor ones. But, they do have one simple property; they all use cosines of whole angles Θ of rotation while the 2-space spinor operations all use half-angles $\Theta/2$ or square-root cosines $\cos \Theta/2 = \sqrt{[1/2 + 1/2 \cos \Theta]}$ of the rotation angle.

Why rotations are such a big deal

In Chapters 8 and 9 we introduced the idea of labeling quantum channels or states using rotational symmetry operators $\mathbf{r}, \mathbf{r}^2, \dots$, and then discovered that the Hamiltonian was made of linear combinations of the \mathbf{r}^p 's, as were their projectors which solved the eigenvalue problem. Similar relations apply to 2-state systems. Indeed, all $SU(2)$ operators are related to rotations in some way including the grand time evolution operator $\mathbf{U}(t)$. When you have a hammer; everything's a nail!

Appendix 10.B Spin control and ellipsometry

So far, rotational analysis has been referred to the Z-axis or, as we have re-labeled it, the *A*-axis. This “favors” base states (spin-up-Z, spin-dn-Z) for electrons, (Plane-x, Plane-y) states for photons, and (N-UP, N-DN) for NH₃ shown in Fig. 10.5.1. It favors an *A*-symmetry (asymmetric-diagonal) Hamiltonian in the *U*(2) catalog of Fig. 10.4.2 which begins with *A*-type base states introduced in Section 10.2(a).

In fact, any axis may be a home base. Three choices *A*, *B*, and *C* (or *Z*, *X*, and *Y*) belong to obvious symmetries. A Hamiltonian near one has archetypical physics. One should be able to quickly relate them.

To begin this, recall the Z-axis or *A*-type Euler angle ($\alpha\beta\gamma$) definition from (10.A.1).

$$|\Psi\rangle = \mathbf{R}(\alpha\beta\gamma)|1\rangle = \mathbf{R}(\alpha\ 00) \mathbf{R}(0\beta\ 0) \mathbf{R}(00\gamma)|1\rangle \quad \begin{array}{l} \text{represented} \\ \text{in } A\text{-basis} \\ \text{by} \end{array} \left(\begin{array}{c} e^{-i\frac{\alpha}{2}} \cos \frac{\beta}{2} \\ e^{i\frac{\alpha}{2}} \sin \frac{\beta}{2} \end{array} \right) e^{-i\frac{\gamma}{2}} \quad (10.B.1)$$

Now we define *X* or *B*-type Euler angles (ABG) and *Y* or *C*-type Euler angles (abg). A general state is defined by any and all of the following three sets of Euler angles; one set for each choice *A*, *B*, or *C*.

$$|\Psi\rangle = \mathbf{R}_Z(\alpha)\mathbf{R}_Y(\beta)\mathbf{R}_Z(\gamma)|\uparrow Z\rangle = \mathbf{R}_X(A)\mathbf{R}_Z(B)\mathbf{R}_X(G)|\uparrow X\rangle = \mathbf{R}_Y(a)\mathbf{R}_X(b)\mathbf{R}_Y(g)|\uparrow Y\rangle \quad (10.B.2)$$

A main-axis operator *Z* (for choice-*A*), *X* (for choice-*B*), or *Y* (for choice-*C*) sets overall phase of its particular favored number-1 state $|1\rangle$ of spin-up-*Z*, spin-up-*X*, or spin-up-*Y*, respectively.

$$|\Psi\rangle = \mathbf{R}_Z(\alpha)\mathbf{R}_Y(\beta)|\uparrow Z\rangle e^{-i\gamma/2} = \mathbf{R}_X(A)\mathbf{R}_Z(B)|\uparrow X\rangle e^{-iG/2} = \mathbf{R}_Y(a)\mathbf{R}_X(b)|\uparrow Y\rangle e^{-ig/2} \quad (10.B.3)$$

Each gives a *different* algebraic and numerical representation for the *same* general state $|\Psi\rangle$.

$$\begin{array}{ccc} \begin{array}{l} \text{represented} \\ \text{in } A\text{-basis} \\ \text{by} \end{array} \left(\begin{array}{c} e^{-i\frac{\alpha}{2}} \cos \frac{\beta}{2} \\ e^{i\frac{\alpha}{2}} \sin \frac{\beta}{2} \end{array} \right) e^{-i\frac{\gamma}{2}} & \begin{array}{l} \text{represented} \\ \text{in } B\text{-basis} \\ \text{by} \end{array} \left(\begin{array}{c} e^{-i\frac{A}{2}} \cos \frac{B}{2} \\ e^{i\frac{A}{2}} \sin \frac{B}{2} \end{array} \right) e^{-i\frac{G}{2}} & \begin{array}{l} \text{represented} \\ \text{in } C\text{-basis} \\ \text{by} \end{array} \left(\begin{array}{c} e^{-i\frac{a}{2}} \cos \frac{b}{2} \\ e^{i\frac{a}{2}} \sin \frac{b}{2} \end{array} \right) e^{-i\frac{g}{2}} \\ (10.B.4a) & (10.B.4b) & (10.B.4c) \end{array}$$

Relating the three kinds of Euler angles begins by connecting the two spin-vector "polar angles"

$$(\alpha, \beta) \text{ related to } (a, b) \text{ related to } (A, B) \dots$$

We cyclicly permute the polar coordinates combinations (*cos*_, *sin*_ *sin*_, *sin*_ *cos*_) in (10.5.8c) and solve.

$$\begin{array}{ccc} \underline{A \text{ or } Z\text{-based}} & \underline{C \text{ or } Y\text{-based}} & \underline{B \text{ or } X\text{-based}} \\ S_A = S_Z = \cos \beta & = S_Z = \sin b \cos a & = S_Z = \sin B \sin A \\ S_C = S_Y = \sin \beta \sin \alpha & = S_Y = \cos b & = S_Y = \sin B \cos A \\ S_B = S_X = \sin \beta \cos \alpha & = S_X = \sin b \sin a & = S_X = \cos B \end{array} \quad (10.B.5)$$

Fig. 10.B.1a below shows the three sets of (azimuth, polar) angles in the top-down-Z view. Arcs drawn are great circles except for two straight lines that meet the spin vector at the β, b, B triple intersection that are lesser circles at the base of a cone of constant X-polar angle *B* or constant Y-polar angle *b*, respectively.

The diagram shows ways to solve a common "spin-erection" problem, finding operations that return an arbitrary initial spin vector to one of the three main axes such as spin-up the Z axis, spin-up the

Y axis, or spin-up the X axis. This also suggests ways to classify and control optical polarization for an arbitrary state of elliptical polarization as will be shown a few pages ahead.

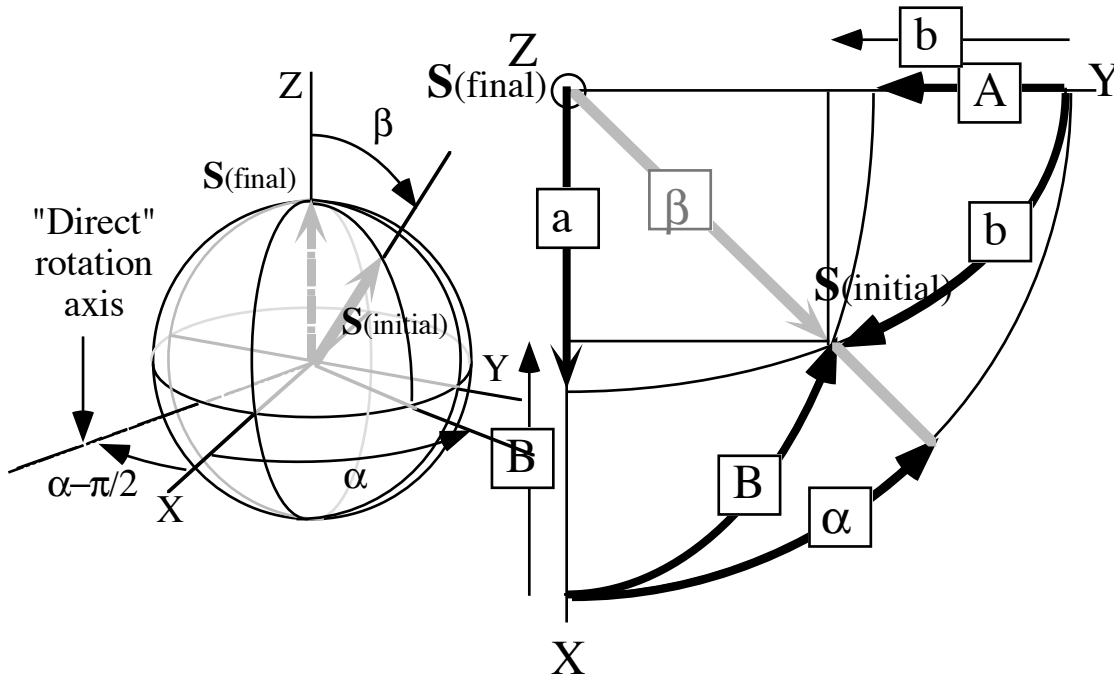


Fig. 10.B.1(a) Map of three different sets of Euler polar angles $(\alpha\beta\gamma)$, (abg) , and (ABG) .

Three examples of ways to relate a state with an arbitrary spin $S(\alpha,\beta)$ to the state of spin-up-Z are sketched below in Fig. 10.B.1. The paths shown are all done using single or double applications of only X and Y generators $G_X = -iJ_X$ and $G_Y = -iJ_Y$ (or, in the first "direct" case, a linear combination of them) to relate the two states.

$$|S\rangle = R_{\text{direct}}[\beta]|\uparrow_z\rangle = R_Y(a)R_X(b-90^\circ)|\uparrow_z\rangle = R_X(A-90^\circ)R_Y(90^\circ-B)|\uparrow_z\rangle$$

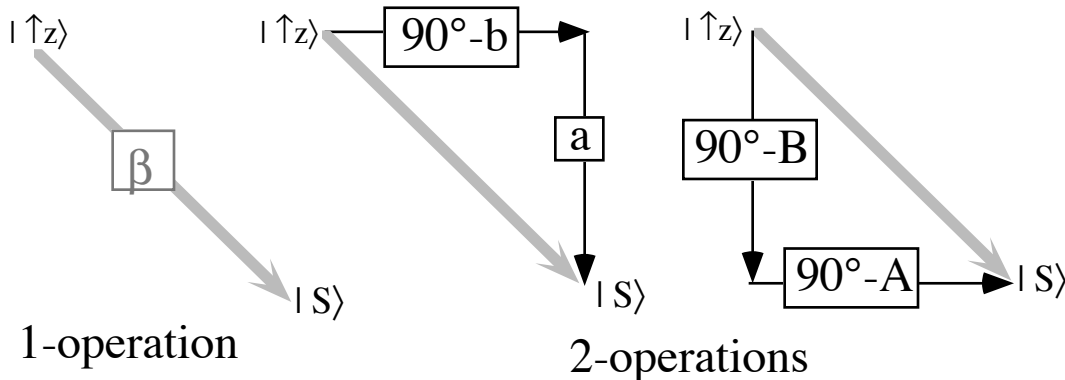


Fig. 10.B.1(b) Map of 1- and 2-op transformations that connect spin-up-Z to an arbitrary spin state.

The "direct" rotation is done using an axis-angle rotation made from a crank vector lying in the X-Y plane with an azimuth of $\alpha - \pi/2$ as shown on the left hand side of Fig. 10.B.1a.

$$\mathbf{R}[\Theta] = \exp^{-i(\Theta \cos(\alpha - \pi/2) \mathbf{J}_X + \Theta \sin(\alpha - \pi/2) \mathbf{J}_Y)}, \text{ where: } \Theta = \beta \quad (10.B.6a)$$

The resulting matrix is found from the axis-angle matrix (10.5.15).

$$\mathbf{R}[\beta \text{ direct}] = \exp^{-i(\beta \sin \alpha \mathbf{J}_X - \Theta \cos \alpha \mathbf{J}_Y)} = \begin{pmatrix} \cos \frac{\beta}{2} & e^{-i\alpha} \sin \frac{\beta}{2} \\ -e^{i\alpha} \sin \frac{\beta}{2} & \cos \frac{\beta}{2} \end{pmatrix} \quad (10.B.6b)$$

We check that the desired transformation "erects" a general spin state (10.A.1a) back to spin-up-Z.

$$\begin{pmatrix} \cos \frac{\beta}{2} & e^{-i\alpha} \sin \frac{\beta}{2} \\ -e^{i\alpha} \sin \frac{\beta}{2} & \cos \frac{\beta}{2} \end{pmatrix} \begin{pmatrix} \cos \frac{\beta}{2} e^{-i\alpha/2} \\ \sin \frac{\beta}{2} e^{i\alpha/2} \end{pmatrix} e^{-i\gamma/2} = \begin{pmatrix} e^{-i\alpha/2} \\ 0 \end{pmatrix} e^{-i\gamma/2} \quad (10.B.6c)$$

Indeed, it does, and it does not change the phase $\phi = -(\alpha + \gamma)/2$ of the first component. This transformation is "twist-free" in the sense of moving a rigid body attached to spin vector \mathbf{S} without changing the γ -dial. The other transformations in Fig. 10.B.1b will affect the overall phase differently. One may set a desired state and its overall phase to a particular value by applying the X and Y rotations three times, following paths like the ones in Fig. 10.B.2. The same can be done by a single operator made up of X , Y , and Z generators such that its crank vector Ω lies in the Z - S bisection plane and has an azimuthal angle measured from the "direct" rotation axis equal to the desired phase. This phase is related to the so-called the "Berry phase" but the geometry behind it goes back to the time of Thales of Miletus around 600 BCE.

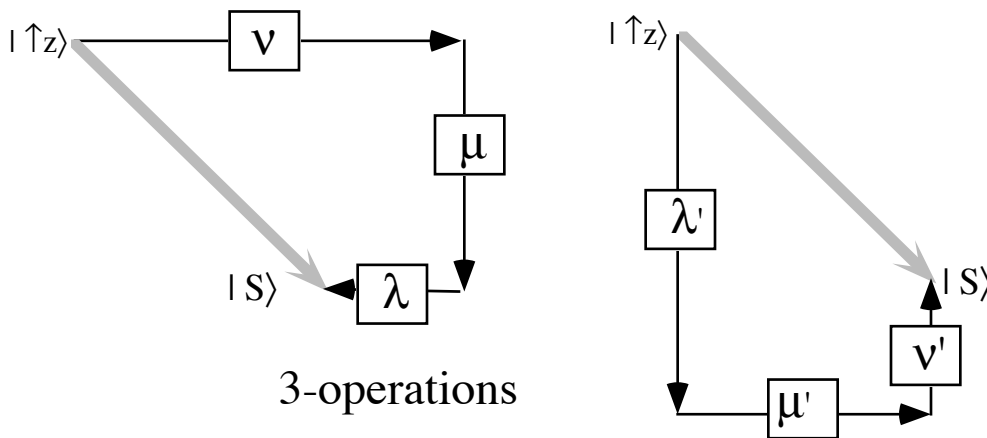


Fig. 10.B.2 Map of 3-op transformations that connect spin-up-Z to an arbitrary spin state and phase.

A multitude of Euler angles may be used singly or together to give various kinds coordinates for photon polarization states. An (over complete) example is shown in Fig. 10.B.3 in which several competing types of angles are drawn at once to characterize the polarization ellipse. Perhaps, the most commonly used set of coordinates are the Faraday tip angle ϕ and elliptical shape angle ψ shown in Fig. 10.B.3a. Twice these angles ($2\phi, 2\psi$) or more precisely ($a=2\phi, b=\pi/2-2\psi$) are Y or C -based polar angles in $R(3)$ space for the resulting spin vector \mathbf{S} . In other words ($a=2\phi, b=\pi/2-2\psi$) are Euler angles (a, b) measured relative to the Y -axis or C -type basis of circular polarization states.

No less useful, however, are a set of coordinates $(2\vartheta, 2\nu)$ based upon the Z -axis or *A-type* basis of x and y plane polarization. These are the standard Euler angles (α, β) introduced previously. Not shown in the Fig. 10.B.3 is a third set of angles based upon the bilaterally symmetric *B-type* basis of $\pm 45^\circ$ plane polarization states or NH_3 eigenstates. All these possible coordinates have varying advantages and disadvantages which depend on what Hamiltonian and physics is being studied.

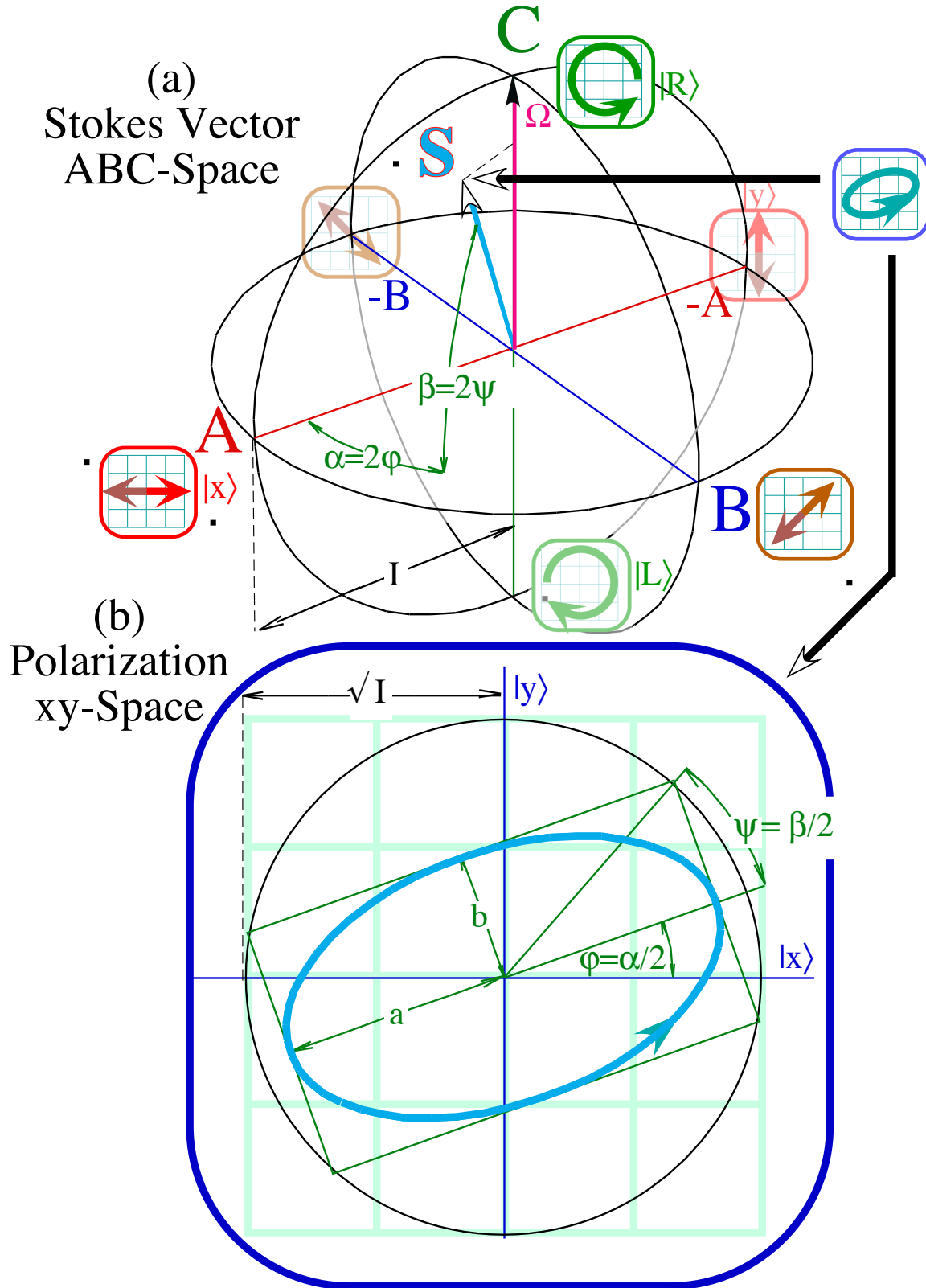


Fig. 10.B.3 Examples of Euler-like coordinates for (a) $U(2)$ polarization ellipse and (b) $R(3)$ spin vector.

(a). Polarization ellipsometry coordinate angles

Optical polarization is analogous to the 2D-harmonic oscillator shown in Section 10.1.

Polarization is usually defined by giving the real x and y electric field amplitudes.

$$\operatorname{Re} E_x = \operatorname{Re} \langle x | \Psi \rangle, \quad \operatorname{Re} E_y = \operatorname{Re} \langle y | \Psi \rangle. \quad (10.B.8)$$

The complex amplitudes $E_x = \langle x | \Psi \rangle$ and $E_y = \langle y | \Psi \rangle$ define the general $U(2)$ polarization state.

$$|\Psi\rangle = |x\rangle\langle x | \Psi \rangle + |y\rangle\langle y | \Psi \rangle \quad (10.B.9)$$

$\operatorname{Re} \langle x | \Psi \rangle$ and $\operatorname{Re} \langle y | \Psi \rangle$ are analogous to oscillator coordinates $x=x_1$ and $y=x_2$ as described by (10.1.1c). For an isotropic oscillator potential $V = k(x^2+y^2)/2$, the general orbit is an ellipse like the one shown in Fig. 10.B.3a. An isotropic oscillator corresponds to the $A=D$ and $B=0=C$ case of $U(2)$ symmetry on the extreme left hand table in the catalog of 2-state symmetry of Fig. 10.4.2. Any ellipse or polarization state is an eigenstate of a Hamiltonian $\mathbf{H}=A\mathbf{1}=D\mathbf{1}$, and any coordinate basis is equally convenient.

However, each lower symmetry case A , AB , B , C , or $U(1)$ in Fig. 10.4.2 has definite eigenstates and coordinates that are most convenient for its analysis. For example, $|\Psi\rangle$ can be written three ways

$$|\Psi\rangle = |x\rangle\langle x | \Psi \rangle + |y\rangle\langle y | \Psi \rangle = |+\rangle\langle + | \Psi \rangle + |-\rangle\langle - | \Psi \rangle = |r\rangle\langle r | \Psi \rangle + |\ell\rangle\langle \ell | \Psi \rangle, \quad (10.B.10)$$

using eigenbasis of A (asymmetric diagonal), B (bilaterally symmetric), or C (circular) Hamiltonians.

The corresponding transformation matrices from plane A -type or (x,y) polarization are as follows.

$$\begin{aligned} \begin{pmatrix} \langle x|x\rangle & \langle x|y\rangle \\ \langle y|x\rangle & \langle y|y\rangle \end{pmatrix} &= \begin{pmatrix} 1 & 0 \\ 0 & 1 \end{pmatrix} & \begin{pmatrix} \langle x|+\rangle & \langle x|-\rangle \\ \langle y|+\rangle & \langle y|-\rangle \end{pmatrix} &= \begin{pmatrix} \frac{1}{\sqrt{2}} & \frac{1}{\sqrt{2}} \\ \frac{1}{\sqrt{2}} & \frac{-1}{\sqrt{2}} \end{pmatrix} & \begin{pmatrix} \langle x|r\rangle & \langle x|\ell\rangle \\ \langle y|r\rangle & \langle y|\ell\rangle \end{pmatrix} &= \begin{pmatrix} \frac{1}{\sqrt{2}} & \frac{1}{\sqrt{2}} \\ \frac{i}{\sqrt{2}} & \frac{-i}{\sqrt{2}} \end{pmatrix} \\ (10.B.11a) & & (10.B.11b) & & (10.B.11c) \end{aligned}$$

These are introduced in Sections 10.2a, b, and c, respectively. An intermediate case labeled AB -type polarization corresponds to plane polarization inclined at angle $\beta/2=\Theta$, as shown in Sec. 10.3 and Fig. 10.1.2ab. AB -transformation can be either a rotation matrix $R(\beta/2)=R[\Theta]$ or a reflection matrix $\sigma(\beta/2)$.

$$\begin{aligned} R\left(\frac{\beta}{2}\right) &= R[\Theta] = \begin{pmatrix} \langle x|x_{AB}\rangle & \langle x|y_{AB}\rangle \\ \langle y|x_{AB}\rangle & \langle y|y_{AB}\rangle \end{pmatrix} & \sigma\left(\frac{\beta}{2}\right) &= \sigma[\Theta] = \begin{pmatrix} \langle x|x_{AB}\rangle & \langle x|\bar{y}_{AB}\rangle \\ \langle y|x_{AB}\rangle & \langle y|\bar{y}_{AB}\rangle \end{pmatrix} \\ &= \begin{pmatrix} \cos\frac{\beta}{2} & -\sin\frac{\beta}{2} \\ \sin\frac{\beta}{2} & \cos\frac{\beta}{2} \end{pmatrix} = \begin{pmatrix} \cos\Theta & -\sin\Theta \\ \sin\Theta & \cos\Theta \end{pmatrix} & & = \begin{pmatrix} \cos\frac{\beta}{2} & \sin\frac{\beta}{2} \\ \sin\frac{\beta}{2} & -\cos\frac{\beta}{2} \end{pmatrix} = \begin{pmatrix} \cos\Theta & \sin\Theta \\ \sin\Theta & -\cos\Theta \end{pmatrix} \\ (10.B.12a) & & & & (10.B.12b) \end{aligned}$$

The only difference is the \pm -sign of the second column. A rotation has a determinate $\det|R|=+1$ while a reflection has $\det|\sigma|=-1$. $\sigma(\beta/2)$ belongs to $U(2)$ but not $SU(2)$. Rotation $R(\beta/2)$ belongs to both.

Unit-determinant or unimodular $SU(2)$ transformations are area or volume-preserving. This is sometimes an advantage, particularly if you are trying to apply $R(\Theta)$ to solid objects in a laboratory! But, light is easier to reflect than to rotate. Transformation (10.B.11b) is a reflection $\sigma[\pi/4]$ through a mirror plane half-way between x and 45° -line. Transformation (10.B.11c) is also a reflection and not in $SU(2)$. From now on we use the following $SU(2)$ C -to- A transformation. Its phase differs from (10.2.23b).

$$\begin{pmatrix} \langle x|R \rangle & \langle x|L \rangle \\ \langle y|R \rangle & \langle y|L \rangle \end{pmatrix} = \begin{pmatrix} \frac{-1}{\sqrt{2}} & \frac{1}{\sqrt{2}} \\ \frac{-i}{\sqrt{2}} & \frac{-i}{\sqrt{2}} \end{pmatrix} \quad (10.B.13)$$

The difference is the sign of the R -column. (This is called a Condon-Shortely phase convention.)

(1) *Type-A ellipsometry Euler angles*

Now we define Euler-angle coordinates (following (10.A.1a)) for A-type linear polarization basis.

$$|\Psi\rangle = (Xe^{-i\vartheta} |x\rangle + Ye^{i\vartheta} |y\rangle)e^{-i\theta} = \sqrt{I}(\cos v e^{-i\vartheta} |x\rangle + \sin v e^{i\vartheta} |y\rangle)e^{-i\theta} \quad (10.B.14a)$$

Here the magnitudes of the E-field components are defined by an A or Z-based Euler polar angle $\beta=2v$.

$$X = \sqrt{I} \cos v = \sqrt{I} \cos \beta/2 = |E_x(\vartheta, v, \theta)| = |\langle x | \Psi \rangle| \quad (10.B.14b)$$

$$Y = \sqrt{I} \sin v = \sqrt{I} \sin \beta/2 = |E_y(\vartheta, v, \theta)| = |\langle y | \Psi \rangle| \quad (10.B.14c)$$

The real E-field components are defined by an A or Z-based Euler azimuthal angle $\alpha/2=\vartheta$ and overall phase angle $\gamma/2 = \theta$. (Note: Do not confuse ϑ or ϕ used below with axis-operator angles defined before.)

$$x_I = \text{Re} E_x(\vartheta, v, \theta) = \text{Re} \langle x | \Psi \rangle = X \cos(\vartheta + \theta) \quad (10.B.14d)$$

$$x_2 = \text{Re} E_y(\vartheta, v, \theta) = \text{Re} \langle y | \Psi \rangle = Y \cos(\vartheta - \theta) \quad (10.B.14e)$$

Coordinates x_I and x_2 trace an ellipse in a horizontal $2X$ -by- $2Y$ box where azimuth $\alpha=2\vartheta$ determines the orientation or shape of the ellipse in the box and overall phase angle $\gamma=2\theta$ ("twist") locates each orbiting point on the ellipse. The enclosing box aspect ratio $X:Y$ is fixed by polar angle $\beta=2v$ in (10.B.14b-c).

Fig. 10.B.4 shows three cases which differ only by the angle $\alpha=2\vartheta$ which has value $\alpha=45^\circ=2(22.5^\circ)$ in the upper Fig. 10.B.4 and increases to $\alpha=90^\circ$ and then $\alpha=180^\circ$ in the successive lower figures. In each case, the box-diagonal angle $\beta/2 = v$ remains fixed at $v = 30^\circ$ or $\beta=60^\circ$.

The Stokes spin \mathbf{S} -vector diagram for each polarization ellipse is drawn in ABC space on the right hand side of the figures. Note that polar angle of the \mathbf{S} -vector remains fixed at $\beta=2v=60^\circ$ with respect to the A-axis, while the azimuth $\alpha=2\vartheta$ rotates from $\alpha=45^\circ$ to $\alpha=90^\circ$ and finally to $\alpha=180^\circ$.

The α -evolution seen in Fig. 10.B.4 is an A -axis rotation similar to that which an A -type (asymmetric-diagonal) Hamiltonian would cause. If the precession rate $\Omega = \dot{\alpha}$ of the \mathbf{S} -vector is much slower than phase angle "orbit" rate $\dot{\gamma}/2 = \dot{\theta}$ around the ellipse, then you can imagine an ellipse changing shape slowly. However, if the precession rate $\Omega = \dot{\alpha}$ becomes a significant fraction of the overall phase rate $\dot{\gamma}/2 = \dot{\theta}$ or actually exceeds it, then each ellipse is not given time to be fully drawn before shape-angle $\alpha=2\vartheta$ changes significantly. Fig. 10.2.2 is an example of such hyper- A -rotation.

In most optical polarization experiments so far, the overall phase rate for optical polarization evolution is hundreds of tera-Hertz and many times that of typical precession rates. However, modern experiments may not be so slow in changing the state of polarization.

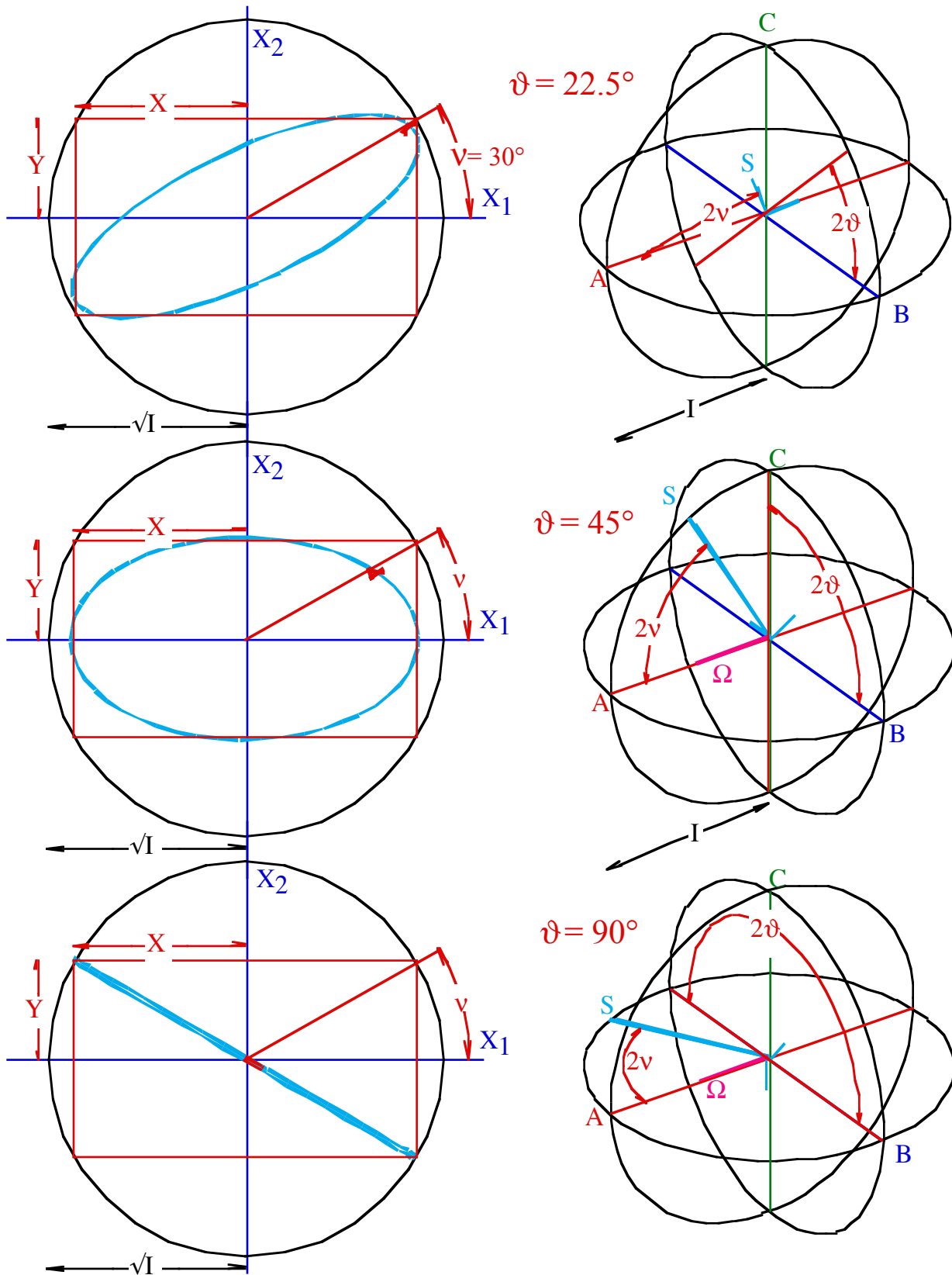


Fig. 10.B.4 A-Type polarization angles ($\alpha=2\vartheta, \beta=2v, \gamma=2\theta$) with rotation to $\alpha=45^\circ, 90^\circ$, and 180° .

(2) *Type-C ellipsometry Euler angles*

Now we define Euler-angle coordinates (following (10.A.1a)) for **C-type** linear polarization basis.

$$|\Psi\rangle = [Re^{-i\varphi}|r\rangle + Le^{i\varphi}|\ell\rangle]e^{-i\Phi} = [Re^{-i\varphi}(|x\rangle+i|y\rangle) + Le^{i\varphi}(|x\rangle-i|y\rangle)]e^{-i\Phi}/\sqrt{2} \quad (10.B.15a)$$

The right and left circular bases $|r\rangle=(|x\rangle+i|y\rangle)/\sqrt{2}$ and $|\ell\rangle=(|x\rangle-i|y\rangle)/\sqrt{2}$ from (10.B.11c) are expanded.

$$\begin{aligned} |\Psi\rangle &= [Re^{-i\varphi} + Le^{i\varphi}]|x\rangle e^{-i\Phi}/\sqrt{2} = [(R+L)\cos\varphi - i(R-L)\sin\varphi]|x\rangle(\cos\Phi - i\sin\Phi)/\sqrt{2} \\ &+ i[Re^{-i\varphi} - Le^{i\varphi}]|y\rangle e^{-i\Phi}/\sqrt{2} + i[(R-L)\cos\varphi - i(R+L)\sin\varphi]|y\rangle(\cos\Phi - i\sin\Phi)/\sqrt{2} \end{aligned}$$

Separating the real and imaginary parts gives a φ -rotation transformation for each part.

$$\begin{aligned} |\Psi\rangle &= [(R+L)\cos\varphi \cos\Phi - (R-L)\sin\varphi \sin\Phi - i(R+L)\sin\varphi \sin\Phi - i(R-L)\sin\varphi \cos\Phi]|x\rangle/\sqrt{2} \\ &+ [(R+L)\sin\varphi \cos\Phi + (R-L)\cos\varphi \sin\Phi + i(R+L)\cos\varphi \cos\Phi - i(R+L)\sin\varphi \sin\Phi]|y\rangle/\sqrt{2} \quad (10.B.15b) \end{aligned}$$

The real E -field (x_1, x_2) -plots in Fig. 10.B.5 are thus given as follows

$$x_1 = \text{Re}E_x(\varphi, \psi, \Phi) = \text{Re}\langle x|\Psi\rangle = (a \cos\Phi)\cos\varphi - (b \sin\Phi)\sin\varphi \quad (10.B.15c)$$

$$x_2 = \text{Re}E_y(\varphi, \psi, \Phi) = \text{Re}\langle y|\Psi\rangle = (a \cos\Phi)\sin\varphi + (b \sin\Phi)\cos\varphi \quad (10.B.15d)$$

where the ellipse semi-major axis a and semi-minor axis b are defined using a new angle ψ .

$$a = (R + L)/\sqrt{2} = \sqrt{I} \cos \psi \quad (10.B.15e)$$

$$b = (R - L)/\sqrt{2} = \sqrt{I} \sin \psi \quad (10.B.15f)$$

The ellipse box aspect ratio $a:b$ is defined by ψ , related below to a **C-based** Euler polar angle $b=\pi/2-2\psi$, just as the $X:Y$ ratio is defined by an **A-based** Euler polar angle $\beta=2\psi$ in (10.B.14b-c). The real E -field components (x_1, x_2) are defined by a **C-based** Euler azimuthal angle $a=2\varphi$ and overall phase angle $g/2=\Phi$. (10.B.15) are analogous to the definition in (10.B.14d-e) by an **A-based** Euler azimuthal angle $\alpha=2\vartheta$ and an overall phase angle $\gamma/2=\theta$. Furthermore, **C-type** evolution or *Faraday rotation* in Fig. 10.B.5 is rotation about the **C-axis** by azimuthal angle $a=2\varphi$, just as **A-type** evolution in Fig. 10.B.4 was **A-axial** rotation by angle $\alpha=2\vartheta$. The latter is called *birefringence*.

Fig. 10.B.5 shows three cases differing only by the angle $a=2\varphi$ which has value $a=30^\circ=2(15^\circ)$ in the upper Fig. 10.B.5 and increases to $a=90^\circ$ and then $a=170^\circ$ in the successive lower figures. In each case, the ellipse-box-diagonal angle $b/2 = \pi/4 - \psi$ remains fixed at $\psi=30^\circ$ or $b=30^\circ$ ($\psi=30^\circ=b$ is just a coincidence!). As we will show, the **C-axial** Euler polar angle of the **S**-vector is $b=\pi/2-2\psi$, in general. The complimentary angle $2\psi=\pi/2-b=b_c$ is a spin polar *elevation* angle or *latitude*, not a polar angle.

As in Fig. 10.B.4, the objects in the real **ABC** **S**-vector 3-space move twice as fast as the ones in the complex $|\Psi\rangle$ -spinor or polarization 2-space. Ellipse rotation by φ is a rotation of the **S**-vector by $a=2\varphi$. The same applies to the overall phase angle Φ which is related by a factor of 2 with the Euler twist or "gauge" angle $g = 2\Phi$ around the **S**-vector axis. Examples of normal ($\Phi \gg \varphi$) and hyper-Faraday rotation ($\Phi \sim \varphi$) are sketched in Fig. 10.2.10 and Fig. 10.2.11, respectively.

*Fig. 10.B.5 C-Type polarization angles ($a=2\varphi, b=\pi/2-2\psi, g=2\Phi$) with C-axial rotation to $a=30^\circ, 90^\circ$, and 170° . Polar angle of **S** from C-axis is fixed at $b=\pi/2-2\psi=30^\circ$.*

To define polar angles of the **S**-vector relative to **A**, **B**, or **C**-axes we can use the transformation relations given by (10.B.5). However, we need to be aware of the base changing transformations behind such shortcuts. For example, suppose we define **C**-axis as our true **Z**-axis of "up" and "down" so that

$$C(\sigma_N) = \begin{pmatrix} \langle r|\sigma_N|r\rangle & \langle r|\sigma_N|\ell\rangle \\ \langle \ell|\sigma_N|r\rangle & \langle \ell|\sigma_N|\ell\rangle \end{pmatrix} \quad (10.B.16)$$

is the following representation of the three Pauli (Hamilton) operators in the **C (circular)** basis $\{|r\rangle, |\ell\rangle\}$.

$$C(\sigma_A) = \begin{pmatrix} 0 & 1 \\ 1 & 0 \end{pmatrix} \quad (10.B.17a) \quad C(\sigma_B) = \begin{pmatrix} 0 & -i \\ i & 0 \end{pmatrix} \quad (10.B.17b) \quad C(\sigma_C) = \begin{pmatrix} 1 & 0 \\ 0 & -1 \end{pmatrix} \quad (10.B.17c)$$

This would be the conventional definition of $(\sigma_X, \sigma_Y, \sigma_Z) = (\sigma_A, \sigma_B, \sigma_C)$ of Pauli operators in that order with the third (σ_Z or σ_C) diagonal. In this text we have had σ_A be the diagonal one. But, in the **A** basis (**Asymmetric diagonal or linear**) σ_A is diagonal. A basis change by (10.B.11c) proves this as shown below.

$$\begin{aligned} L(\sigma_N) &= \begin{pmatrix} \langle x|\sigma_N|x\rangle & \langle x|\sigma_N|y\rangle \\ \langle y|\sigma_N|x\rangle & \langle y|\sigma_N|y\rangle \end{pmatrix} = \begin{pmatrix} \langle x|r\rangle & \langle x|\ell\rangle \\ \langle y|r\rangle & \langle y|\ell\rangle \end{pmatrix} \begin{pmatrix} \langle r|\sigma_N|r\rangle & \langle r|\sigma_N|\ell\rangle \\ \langle \ell|\sigma_N|r\rangle & \langle \ell|\sigma_N|\ell\rangle \end{pmatrix} \begin{pmatrix} \langle r|x\rangle & \langle r|y\rangle \\ \langle \ell|x\rangle & \langle \ell|y\rangle \end{pmatrix} \\ &= T \cdot C(\sigma_N) \cdot T^\dagger = \begin{pmatrix} 1/\sqrt{2} & 1/\sqrt{2} \\ i/\sqrt{2} & -i/\sqrt{2} \end{pmatrix} \begin{pmatrix} \langle r|\sigma_N|r\rangle & \langle r|\sigma_N|\ell\rangle \\ \langle \ell|\sigma_N|r\rangle & \langle \ell|\sigma_N|\ell\rangle \end{pmatrix} \begin{pmatrix} 1/\sqrt{2} & -i/\sqrt{2} \\ 1/\sqrt{2} & i/\sqrt{2} \end{pmatrix} \end{aligned} \quad (10.B.18)$$

The following is the representation of the three operators in the **A (linear)** basis $\{|x\rangle, |y\rangle\}$.

$$L(\sigma_A) = \begin{pmatrix} 1 & 0 \\ 0 & -1 \end{pmatrix} \quad (10.B.19a) \quad L(\sigma_B) = \begin{pmatrix} 0 & 1 \\ 1 & 0 \end{pmatrix} \quad (10.B.19b) \quad L(\sigma_C) = \begin{pmatrix} 0 & -i \\ i & 0 \end{pmatrix} \quad (10.B.19c)$$

This has been the conventional representation for this text, so far. Relative to (10.B.17) it is a cyclic reordering $A \rightarrow B \rightarrow C \rightarrow A$, that is, a 120° rotation around the $[111]$ axis in ABC -space.

σ_N -expectation values are basis-independent (provided the right representations are used for both the states and the operator!) Consider first the linear **A-representations** using (10.B.19) and (10.B.14).

$$\langle \Psi | \sigma_A | \Psi \rangle = \begin{pmatrix} X e^{-i\vartheta} & Y e^{i\vartheta} \end{pmatrix}^* \begin{pmatrix} 1 & 0 \\ 0 & -1 \end{pmatrix} \begin{pmatrix} X e^{-i\vartheta} \\ Y e^{i\vartheta} \end{pmatrix} = X^2 - Y^2 \quad (10.B.20a)$$

$$\langle \Psi | \sigma_B | \Psi \rangle = \begin{pmatrix} X e^{-i\vartheta} & Y e^{i\vartheta} \end{pmatrix}^* \begin{pmatrix} 0 & 1 \\ 1 & 0 \end{pmatrix} \begin{pmatrix} X e^{-i\vartheta} \\ Y e^{i\vartheta} \end{pmatrix} = 2XY \cos 2\vartheta \quad (10.B.20a)$$

$$\langle \Psi | \sigma_C | \Psi \rangle = \begin{pmatrix} X e^{-i\vartheta} & Y e^{i\vartheta} \end{pmatrix}^* \begin{pmatrix} 0 & -i \\ i & 0 \end{pmatrix} \begin{pmatrix} X e^{-i\vartheta} \\ Y e^{i\vartheta} \end{pmatrix} = 2XY \sin 2\vartheta \quad (10.B.20b)$$

Now do the same values in the circular **C-representations** using (10.B.17) and (10.B.15).

$$\langle \Psi | \sigma_A | \Psi \rangle = \begin{pmatrix} R e^{-i\varphi} & L e^{i\varphi} \end{pmatrix}^* \begin{pmatrix} 0 & 1 \\ 1 & 0 \end{pmatrix} \begin{pmatrix} R e^{-i\varphi} \\ L e^{i\varphi} \end{pmatrix} = 2RL \cos 2\varphi = (a^2 - b^2) \cos 2\varphi \quad (10.B.21a)$$

$$\langle \Psi | \sigma_B | \Psi \rangle = \begin{pmatrix} R e^{-i\varphi} & L e^{i\varphi} \end{pmatrix}^* \begin{pmatrix} 0 & -i \\ i & 0 \end{pmatrix} \begin{pmatrix} R e^{-i\varphi} \\ L e^{i\varphi} \end{pmatrix} = 2RL \sin 2\varphi = (a^2 - b^2) \sin 2\varphi \quad (10.B.21b)$$

$$\langle \Psi | \sigma_C | \Psi \rangle = \begin{pmatrix} \text{Re}^{-i\varphi} & L e^{i\varphi} \end{pmatrix}^* \begin{pmatrix} 1 & 0 \\ 0 & -1 \end{pmatrix} \begin{pmatrix} \text{Re}^{-i\varphi} \\ L e^{i\varphi} \end{pmatrix} = R^2 - L^2 = 2ab \quad (10.B.21c)$$

Equating A -defined and C -defined S -vector components $S_N = \langle \Psi | \sigma_N | \Psi \rangle$ relates A -based and C -based Euler angles. Use A -definitions (10.B.14) and C -definitions (10.B.15) as follows.

S-vector	A	Linear Basis	C	Circular Basis
$\langle \Psi \sigma_A \Psi \rangle =$	$X^2 - Y^2$	$= I \cos 2\vartheta$	$= 2RL \cos 2\varphi =$	$(a^2 - b^2) \cos 2\varphi = I \cos 2\psi \cos 2\varphi$
$\langle \Psi \sigma_B \Psi \rangle =$	$2XY \cos 2\vartheta$	$= I \cos 2\vartheta \sin 2\vartheta$	$= 2RL \sin 2\varphi =$	$(a^2 - b^2) \sin 2\varphi = I \cos 2\psi \sin 2\varphi$ (10.B.22)
$\langle \Psi \sigma_C \Psi \rangle =$	$2XY \sin 2\vartheta$	$= I \sin 2\vartheta \sin 2\vartheta$	$= R^2 - L^2 =$	$2ab = I \sin 2\psi$
$\langle \Psi 1 \Psi \rangle =$	$X^2 + Y^2 =$	I	$= R^2 + L^2 =$	$a^2 + b^2$

First notice how the polar coordinates for the C -basis are defined in the right-most column of (10.B.22). The C -azimuth plane projection is $(I \cos 2\psi \cos 2\varphi, I \cos 2\psi \sin 2\varphi)$ while the main C -axial projection is $I \sin 2\psi$. This is different from the A -basis defined in the middle column of (10.B.22) with A -azimuth plane projection is $(I \sin 2\vartheta \cos 2\vartheta, I \sin 2\vartheta \sin 2\vartheta)$ while the main A -axial projection is $I \cos 2\vartheta$.

For A -bases angle $\beta = 2\vartheta$ is a true polar angle measured from the main A -axis as shown in Fig. 10.B.4. For C -bases angle $b_c = 2\psi$ is an elevation angle or complement $b_c = \pi/2 - b$ of a true polar angle $b = \pi/2 - 2\psi$ measured from the main C -axis as shown in Fig. 10.B.5. This is consistent with (10.B.5) which relates Euler polar angles β , b , and B .

The C -component of the S -vector is an oscillator or "*photon*" *angular momentum* component

$$S_C = I(xp_y - yp_x) = I(x_1p_2 - x_2p_1) = 2ab = R^2 - L^2 \quad (10.B.23)$$

according to fundamental definitions (10.5.8c). Comparing this to (10.B.22) above shows that S_C is proportional to the area πab of the polarization ellipse. This makes the C -axis or Z -axis the important one in angular momentum theory which will be treated in later chapters. Given the importance of $U(2) > R(3)$ isotropy and the quantum theory of angular momentum in atomic and nuclear physics, this probably explains why the Pauli representation (10.B.17) is the most widely accepted convention.

However, for anisotropic condensed matter the A -axis (which we have up to now called the Z -axis) has an important *anisotropy* or *Stark-Splitting* component.

$$S_A = I(x_1^2 + p_1^2 - x_2^2 - p_2^2) = X^2 - Y^2 \quad (10.B.24)$$

Maximum or minimum values of the A -component correspond to pure x or pure y polarization just as maximum or minimum values of the C -component correspond to pure R or pure L polarization. Development of the bilateral or B -component and coordination is left as an exercise.

Transformations which change the bases-of-choice or quantization axis from A to B or C belong to a dual or "external" $U(2)$ group that commutes with the $U(2)$ group from which Hamiltonian and evolution operators are made. Dual symmetry is an important topic which will be introduced in Chapter 15 and applied again in Chapters 24, 25, and 30.

(b) Beam evolution of polarization

Evolution of optical polarization is often a function of distance z along a propagating beam. The evolution is described classically by Maxwell's equations which are second order in position.

$$\nabla^2 \mathbf{E} - \nabla(\nabla \cdot \mathbf{E}) = \frac{1}{c^2} \frac{\partial^2 \mathbf{E}}{\partial t^2} + \frac{1}{c^2 \epsilon_0} \frac{\partial^2 \mathbf{P}}{\partial t^2} \quad \text{where: } \mathbf{P} = \epsilon_0 \tilde{\alpha} \cdot \mathbf{E} \quad (10.B.25)$$

This simplifies if all field \mathbf{E} and polarization vectors \mathbf{P} are in the x - y direction transverse to beam line z . The *polarizability α -tensor* relation is then two-dimensional.

$$\mathbf{P} = \epsilon_0 \tilde{\alpha} \cdot \mathbf{E} \quad \text{becomes: } \frac{1}{\epsilon_0} \begin{pmatrix} P_x \\ P_y \end{pmatrix} = \begin{pmatrix} \alpha_{xx} & \alpha_{xy} \\ \alpha_{yx} & \alpha_{yy} \end{pmatrix} \begin{pmatrix} E_x \\ E_y \end{pmatrix} \quad (10.B.26)$$

Furthermore, we assume single frequency vector amplitudes depend on the z -coordinate only

$$\mathbf{P}(z, t) = \mathbf{P}(z) e^{-i\omega t}, \quad \mathbf{E}(z, t) = \mathbf{E}(z) e^{-i\omega t}$$

Maxwell's equations simplify under the preceding conditions.

$$\frac{\partial^2}{\partial z^2} \begin{pmatrix} \langle x | \phi(z) \rangle \\ \langle y | \phi(z) \rangle \end{pmatrix} = -\frac{\omega^2}{c^2} \begin{pmatrix} 1 + \alpha_{xx} & \alpha_{xy} \\ \alpha_{yx} & 1 + \alpha_{yy} \end{pmatrix} \begin{pmatrix} \langle x | \phi(z) \rangle \\ \langle y | \phi(z) \rangle \end{pmatrix}, \quad (10.B.27a)$$

where the complex polarization field is related to the real E-field.

$$\text{Re} \begin{pmatrix} E_x(z) \\ E_y(z) \end{pmatrix} = \text{Re} \begin{pmatrix} \langle x | \phi(z) \rangle \\ \langle y | \phi(z) \rangle \end{pmatrix} \quad (10.B.27b)$$

The forward propagating wave solutions are used in the simplest beam approximation.

$$\begin{pmatrix} \langle x | \phi(z) \rangle \\ \langle y | \phi(z) \rangle \end{pmatrix} = e^{iz} \begin{pmatrix} k_{xx} & k_{xy} \\ k_{yx} & k_{yy} \end{pmatrix} \begin{pmatrix} \langle x | \phi(0) \rangle \\ \langle y | \phi(0) \rangle \end{pmatrix} \quad (10.B.28a)$$

A *wave-vector matrix* \mathbf{k} is the doubly-positive (++) square root of the *susceptibility tensor* $\chi = 1 + \alpha$.

$$\begin{pmatrix} k_{xx} & k_{xy} \\ k_{yx} & k_{yy} \end{pmatrix} = \frac{\omega}{c} \begin{pmatrix} 1 + \alpha_{xx} & \alpha_{xy} \\ \alpha_{yx} & 1 + \alpha_{yy} \end{pmatrix}_{(+,+)}^{1/2} = \frac{\omega}{c} \left(+\sqrt{\chi_1} \mathbf{P}_{\chi_1} + \sqrt{\chi_2} \mathbf{P}_{\chi_2} \right) \quad (10.B.28b)$$

In the absence of absorption or gain the eigenvalues (χ_1, χ_2) of χ are assumed positive-real while the matrix \mathbf{k} and the projectors \mathbf{P}_{χ_1} and \mathbf{P}_{χ_2} of χ and \mathbf{k} are assumed all to be Hermitian. ($\mathbf{k}^\dagger = \mathbf{k}$)

$$\mathbf{P}_{\chi_1} = \frac{\begin{pmatrix} \chi_{xx} - \chi_2 & \chi_{xy} \\ \chi_{yx} & \chi_{yy} - \chi_2 \end{pmatrix}}{\chi_1 - \chi_2}, \quad \mathbf{P}_{\chi_2} = \frac{\begin{pmatrix} \chi_{xx} - \chi_1 & \chi_{xy} \\ \chi_{yx} & \chi_{yy} - \chi_1 \end{pmatrix}}{\chi_2 - \chi_1} \quad (10.B.28c)$$

In this approximation the spatial z -evolution (10.B.28a) due to $e^{i\mathbf{k}z}$ proceeds quite analogously with the temporal t -evolution due to a Hamiltonian $e^{-i\mathbf{H}t/\hbar}$ discussed previously. One difference is that a positive \mathbf{k} will correspond to a negative or *clockwise* $\Omega = -|\Omega|$ crank motion in ABC -space. (As you move down the beam you are effectively "undoing" time ωt and looking at what has already passed you.) Also, time enters here as a simple overall $e^{-i\omega t}$ phase contribution to give a polarization wave operator $e^{i\mathbf{k}z - i\omega t}$. The opposite moving wave $e^{-i\mathbf{k}z - i\omega t}$ is assumed zero. Interference of counter-propagating waves is studied in the next unit.

Problems for Appendix 10.A and B

Euler Can Canonize

10.A.1 An 2D-oscillator canonical phase state (x_1, p_1, x_2, p_2) and a spin-state $|\alpha, \beta, \gamma\rangle$ are both defined by the Euler angles (α, β, γ) through (10.A.1a-b) as well as by axis angles $[\varphi, \vartheta, \Theta]$ through (10.A.1c). (First, verify all parts of (10.A.1).) If rotation-axis- Θ polar angles $[\varphi, \vartheta]$ are fixed while rotation angle $\Theta = \Omega t$ varies uniformly with time, Euler angles (α, β, γ) and phase point (x_1, p_1, x_2, p_2) trace spin and oscillator trajectories, respectively. Verify this for the following cases by discussing plots requested below.

(a) $[\varphi=0, \vartheta=0]$, (b) $[\varphi=0, \vartheta=\pi/2]$, (c) $[\varphi=\pi/2, \vartheta=\pi/2]$, (d) $[\varphi=0, \vartheta=\pi/4]$, (e) $[\varphi=\pi/2, \vartheta=\pi/4]$.

For each case sketch 2D-paths $-p_1$ vs. x_1 and x_2 vs. x_1 and sketch $\hat{\Theta} \sin\Theta/2$ in a 3D $(-p_2, x_2, -p_1)$ -space which should also have paths for $-p_2$ vs. x_2 and x_2 vs. $-p_1$ etc. Also, indicate the paths followed by the tip of the \mathbf{S} -spin-vector (10.5.8c) in 3D-spin space (S_x, S_y, S_z) and characterize as **A**-type, **B**-type, or **C**-type motion, etc., in each case.

Invariantipodals

10.A.2 When an Euler sphere is rotated from origin $|1\rangle$ state $(0=\alpha=\beta=\gamma)$ to some angles (α, β, γ) , there are always points on the sphere which end up exactly where they were before the rotation. Verify this and express the polar-coordinates (ϕ, θ) of all such invariant points in terms of (α, β, γ) .

Spinor-Vector-Rotor

10.A.3 Prove and develop the result (10.A.15) as described below.

$$\begin{aligned} \mathbf{R}[\hat{\Theta}] \sigma_L \mathbf{R}[\hat{\Theta}]^\dagger &= \left(\cos \frac{\Theta}{2} \mathbf{1} - i \sin \frac{\Theta}{2} \hat{\Theta}_K \sigma_K \right) \sigma_L \left(\cos \frac{\Theta}{2} \mathbf{1} - i \sin \frac{\Theta}{2} \hat{\Theta}_N \sigma_N \right)^\dagger \\ &= \sigma_L' = \sigma_L \cos \Theta - \varepsilon_{LKM} \hat{\Theta}_K \sigma_M \sin \Theta + (1 - \cos \Theta) \hat{\Theta}_L (\hat{\Theta}_N \sigma_N) \end{aligned}$$

(a) Using the σ -product definitions and the Levi-Civita tensor identity

$$\varepsilon_{abc} \varepsilon_{dec} = \delta_{ad} \delta_{be} - \delta_{ae} \delta_{bd} \quad (\text{Prove this, too!})$$

to derive the above result. (Equation (10.A.15))

(b) Check if the above result (Eq. (10.A.15a)) yields Eq. (10.A.15b) and sketch the resulting vectors $\hat{\Theta}$ and \mathbf{e}_L (before rotation) and \mathbf{e}'_L (after rotation) for a rotation of \mathbf{e}_z by $\Theta = 120^\circ$ around an axis with polar angle $\vartheta = 54.7^\circ = \arccos(1/\sqrt{3})$ and azimuthal angle $\varphi = 45^\circ$. (As is conventional, we measure polar angles off the Z (or A) axis and azimuthal angles from the X (or B) axis counter clockwise in the XY (or BC) plane. What semi-famous-name axis is this $\hat{\Theta}$? Give Cartesian coordinates.)

(b) Use the above to write down a general 3-by-3 matrix in terms of axis angles $[\varphi, \vartheta, \Theta]$, and test it using angles in (b).

(c) Derive the Euler angles (α, β, γ) for this rotation matrix.

(d) Compare formulas and numerics for 3-by-3 $R(3)$ matrices to the corresponding 2-by-2 $U(2)$ matrices for the same rotations.

(e) Find 3-by-3 $R(3)$ and 2-by-2 $U(2)$ matrices for rotation \mathbf{R}_y by 90° around Y (or C)-axis.

(f) Do products $\mathbf{R}_y \mathbf{R}[\varphi, \vartheta, \Theta]$ and $\mathbf{R}[\varphi, \vartheta, \Theta] \mathbf{R}_y$ numerically and check with product formula (10.A.10). Describe results.

Spinor-Vector-Rotor Polarized

10.B.1. Suppose a Hamiltonian \mathbf{H} has an Ω -vector pointing along the Θ -vector in a preceding problem 10.A.3b. Here we will let $\hbar=1$, and let $\Theta=\Omega t$ with $\Theta=2\pi/3$ at $t=1$.

- Write down the 2-by-2 Hamiltonian matrix \mathbf{H} .
- Give at least two sets of values for Euler angles which give an eigenstate of \mathbf{H} .
- Write out the corresponding complex $U(2)$ eigenstates of \mathbf{H} obtained using (b) and sketch their polarization ellipse-orbit (the real spinor space picture), $U(2)$ phasor picture, and \mathbf{S} -vectors.
- Describe what happens to the initial \mathbf{A} -state $|\Psi(t=0)\rangle = |x\rangle$ (x-polarization or spin-up) given this Hamiltonian \mathbf{H} . Does $|\Psi(t)\rangle$ ever return 100% to $|x\rangle$?
- Does x-polarization ever get close to y-(-A)-polarization? ...45°-(B)-polarization? ...R-(C)-polarization? How long does it take to get from $|\Psi(t=0)\rangle$ to the closest approach to each?

Spin erection. Does it phase $U(2)$?

10.B.2. The following general problem may certainly become relevant if the mythical quantum computer materializes. It involves erecting an arbitrary state with spin vector \mathbf{S} to the spin-up \mathbf{Z} (or \mathbf{A}) position with a particular overall phase Φ . In each case make the description of your solution as simple as possible as though you needed to explain it to engineers.

- For a state of 0-phase with spin on the \mathbf{X} (or \mathbf{B}), describe a single operator that does the above.
- For a state of 0-phase with spin at β in the \mathbf{XZ} (or \mathbf{AB}) plane, describe a single operator that does the above.

The trouble with ϑ

10.B.3. The polarization angle ϑ defies placement in the $U(2)$ diagram of Fig. 10.B.3. (That is, it's not there!) Is it easier to locate if $\nu=45^\circ=\varphi$? Discuss contact points on XY box. Let a cardboard cut-out ellipse of a given I and ν rotate 360° on the floor in the corner of a room always tangent to two walls. What simple curve does its center describe? Does it change radically as $\nu\rightarrow 0$? (It's a lot easier to answer this using $U(2)$ ellipse geometry than by algebraic machination.)

Strange susceptibility

10.B.4. A solid has an xy-susceptibility tensor $\frac{\omega^2}{c^2}(\mathbf{1} + \vec{\alpha}) = \begin{pmatrix} 1.8 & -0.9 + 0.9i \\ -0.9 - 0.9i & 2.7 \end{pmatrix}$ for a z-beam.

- Derive (φ, ψ) and sketch ellipses for all polarization states whose ellipses go unchanged.
- A circular $|\mathbf{R}\rangle$ -state ($\nu=45^\circ$) enters at $z=0$. Discuss its z -evolution. How far is a " π -pulse" (Half-wave plate or π rotation of \mathbf{S})?

To B or not

10.B.5. A B-axial description applies to NH_3 states or a $\pm 45^\circ$ polarization eigenvector medium. First, write the form of the B-type (bilaterally symmetric) Hamiltonian or xy-susceptibility tensor.

- Given an algebraic description of $U(2)$ bases and $R(3)$ spin vectors using B-type Euler angles (A, B, G) .
- Give a geometric sketch of $U(2)$ ellipses and $R(3)$ spin vectors like Fig. 10.B.4-5 as they might evolve under a B-type Hamiltonian or susceptibility tensor. Start with the case $(\varphi=45^\circ, \psi=30^\circ, \Phi=0^\circ)$ in center of Fig. 10.B.5, convert it to (A, B, G) angles, then sketch result of subsequent $45^\circ, 90^\circ$, and 180° rotations of \mathbf{S} around B-axis.